

## รายงานวิจัยฉบับสมบูรณ์

## แบบจำลองทางคณิตศาสตร์สำหรับคำนวณการ เปลี่ยนแปลงของคลื่นตัวแทน

โดย นายวิญญู รัตนปิติกรณ์

กันยายน 2554

## รายงานวิจัยฉบับสมบูรณ์

## แบบจำลองทางคณิตศาสตร์สำหรับคำนวณการเปลี่ยนแปลง ของคลื่นตัวแทน

นายวิญญู รัตนปิติกรณ์ สาขาวิชาวิศวกรรมโยธา สถาบันเทคโนโลยีนานาชาติสิรินธร มหาวิทยาลัยธรรมศาสตร์

สนับสนุนโดยสำนักงานกองทุนสนับสนุนการวิจัย

(ความเห็นในรายงานนี้เป็นของผู้วิจัย สกว. ไม่จำเป็นต้องเห็นด้วยเสมอไป)

## Acknowledgments

The author is thankful to the Thailand Research Fund for providing the financial support of this study.

Sincere appreciation is expressed to the previous researchers for supplying the valuable experimental results to the public, which enabled him to perform this research.

To his wife, for her patience and understanding.

#### **Abstract**

The representative wave heights of an irregular wave train are the essential required factors for many coastal engineering applications such as the design of coastal structures and the study of beach deformations. This study concentrates on the determination of six common representative wave heights, i.e. the mean wave height  $(H_m)$ , the root-mean-square wave height  $(H_{rms})$ , the average of the highest one-third wave height  $(H_{1/3})$ , the average of the highest one-tenth wave height ( $H_{1/10}$ ), the maximum wave height ( $H_{\rm max}$ ) and the spectral significant wave height  $(H_{mo})$  or the spectral root-mean-square wave height  $(H_{moz})$ . Possibly, because of its importance, many wave models have been proposed during the past decades. The main purpose of the present study is to find out suitable wave models for computing  $H_m$ ,  $H_{rms}$ ,  $H_{1/3}$ ,  $H_{1/10}$ ,  $H_{max}$ , and  $H_{mo}$  based on three simple approaches, i.e. empirical approach, representative wave approach, and conversion approach. This study is divided into 3 main chapters. The first chapter describes the transformation of representative wave heights based on empirical approach. The second chapter describes the development of wave models using representative wave approach. The third chapter describes the transformation of representative wave heights based on the conversion approach. The conversion approach consists of four parts, i.e. the wave models for computing the transformation of  $H_{m0}$  [which can be converted to zeroth moment of wave spectrum  $(m_0)$  through the known constant], the wave models for computing the transformation of  $H_{\it rms}$  , the conversion formulas for converting from  $H_{\it rms}$  to other representative wave heights (i.e.  $H_m$ ,  $H_{1/3}$ ,  $H_{1/10}$ , and  $H_{\rm max}$ ), and the conversion formulas for converting from  $m_0$  to other representative wave heights (i.e.  $H_m$ ,  $H_{rms}$ ,  $H_{1/3}$ ,  $H_{1/10}$ , and  $H_{max}$ ). Hence the conversion model should be constructed based on the best model (or formulas) from each part. Therefore, this study is divided into 6 parts. The following is the abstract of the six parts.

The first part concentrates on empirical approach. The empirical approach is introduced to facilitate engineers for design works and preliminary study of coastal processes. It seems that only Goda (1975 and 2009) proposed empirical formulas for computing the transformation of some representative wave heights from offshore to shoreline. The formulas were proposed for computing the transformation of three common representative wave heights (i.e.  $H_{1/3}$ ,  $H_{\rm max}$ , and  $H_{m0}$ ) on plane beaches. The objectives of this part are to verify the Goda formulas for computing the transformation of  $H_{1/3}$ ,  $H_{\rm max}$ , and  $H_{m0}$  on unbarred beaches and to extend the formulas for computing the transformation of  $H_m$ ,  $H_{mms}$ , and  $H_{1/10}$ . Laboratory data from small-scale and large-scale wave flumes with unbarred beach conditions are used to verify the formulas. The verification shows that the formulas give very good predictions of  $H_{1/3}$  and  $H_{m0}$ , but give fair prediction of  $H_{max}$ . The formulas are rewritten in the form of a general formula. The general form of Goda formulas is recalibrated and extended to compute other representative wave heights (i.e.  $H_m$ ,  $H_{rms}$ , and  $H_{1/10}$ ). The general formula gives very good predictions of  $H_m$ ,  $H_{rms}$ ,  $H_{1/3}$ ,  $H_{1/10}$ ,  $H_{max}$ , and  $H_{m0}$ .

The second part focuses on a model for computing representative wave heights (i.e.  $H_{\it rms}$  ,  $H_{\it 1/3}$  ,  $H_{\it 1/10}$  ,  $H_{\it max}$  , and  $H_{\it rmsz}$  ) by using representative wave approach. Many researchers have pointed out that the use of representative wave approach can give erroneous results in the computation of representative wave height transformation. However, the representative wave approach has a great merit in simple calculation. It will be useful for practical works (especially for the design of coastal structures), if this approach can be used to compute the representative wave heights. Rattanapitikon (2008) showed that the representative wave approach can be used to compute the transformation of  $H_{1/3}$  with good accuracy. Therefore, it may be possible to use the representative wave approach to predict the transformation of other representative wave heights, i.e.  $H_m$ ,  $H_{rms}$ ,  $H_{\rm 1/10}$  ,  $H_{\rm max}$  , and  $H_{\rm rmsz}$  . This part is carried out to investigate the possibility of using the representative wave approach and find out a suitable dissipation model that can be used to compute  $H_m$ ,  $H_{rms}$ ,  $H_{1/3}$ ,  $H_{1/10}$ ,  $H_{max}$ , and  $H_{rmsz}$ . A large amount and wide range of experimental conditions (covering small-scale, large-scale, and field experimental conditions) are used to calibrate and examine the model. The representative wave height transformation is computed from the energy flux conservation law. Various energy dissipation models of regular wave breaking are directly applied to the irregular wave model and test their applicability. It is found that by using an appropriate energy dissipation model with new coefficients, the representative wave approach can be used to compute  $H_m$ ,  $H_{rms}$ ,  $H_{1/3}$ ,  $H_{1/10}$ ,  $H_{max}$ , and  $H_{rmsz}$ .

The objective of the third part is to propose the most suitable dissipation model for computing the transformation of spectral significant wave height ( $H_{m0}$ ). A wide range of experimental conditions (covering small-scale, large-scale, and field experiments) were used to examine the models. Fourteen existing dissipation models, for computing root-mean-square wave heights ( $H_{mns}$ ), were applied to compute  $H_{m0}$ . The coefficients of the models were re-calibrated and the accuracy of the models was compared. It appears that the model of Janssen and Battjes (2007) with new coefficients gives the best overall prediction. The simple model proposed in the present paper was modified by changing the formula of stable wave height in the dissipation model. Comparing with the existing models, the modified model is the simplest one but gives better accuracy than those of existing models.

The fourth part focuses on energy dissipation for computing the transformation of root-mean-square ( $\mathit{rms}$ ) wave height in the surf zone. There are two approaches to describe the  $\mathit{rms}$  wave height, i.e. statistical approach (or wave-by-wave approach) and spectral approach (or energy approach). It has been point out by many researchers that the  $\mathit{rms}$  wave height derived from these two approaches is significantly difference. This difference is expected to cause a significant effect on the estimation of energy dissipation. However, no direct literature has been made to describe clearly the applicability of existing energy dissipation models in simulating statistical-based  $\mathit{rms}$  wave height ( $H_{\mathit{rms}}$ ). This part is undertaken to find out the suitable dissipation models for computing  $H_{\mathit{rms}}$ . Five sources of experimental data are used to examine the accuracy of fifteen existing models. The existing models are recalibration before examination. By using the new calibrated coefficients, four existing models give the overall average errors less than 10%. The models developed based on representative wave concept trend to give better estimation than those of parametric wave concept.

The fifth part is undertaken to find out suitable conversion formulas for computing representative wave heights (i.e. mean, significant, highest one-tenth, and maximum wave heights) from the known commonly used parameters (i.e. root-mean-square wave height, water depth, spectral peak period, and beach slope). Seventeen sets of conversion formulas (including existing and modified formulas) are re-calibrated and their accuracy is compared. A large amount and wide range of experimental conditions from small-scale, large-scale, and field experiments (2,619 cases collected from 10 sources) are used to calibrate and verify the conversion formulas. The examination shows that most of the selected formulas give very good predictions and have similar accuracy. The suitable formulas are recommended based on the consideration of accuracy and simplicity of the formulas.

The sixth part focuses on conversion formulas for estimating statistical-based representative wave heights (i.e.  $H_m$ ,  $H_{rms}$ ,  $H_{1/3}$ , and  $H_{1/10}$ ) from zeroth moment of wave spectrum ( $m_0$ ). The applicability of five sets of existing conversion formulas is examined based on two field experiments of COAST3D project (including 13,430 wave records). The examination shows that the conversion formulas of Forristall (1978) give the best prediction. The formulas of Forristall (1978) are modified by reformulating the shape factor in the formulas. The modified formulas give better estimation than those of existing formulas. Simple empirical formulas are also proposed. The empirical formulas give nearly the same accuracy as those of the modified formulas.

#### บทคัดย่อ

การเปลี่ยนแปลงของคลื่น เป็นตัวการสำคัญที่ทำให้เกิดการกัดเซาะและการทับถมชายฝั่งทะเลและทำ ความเสียหายต่อทรัพย์สินหรือสิ่งก่อสร้างบนฝั่ง โครงการนี้จะเน้นไปที่ส่วนของแบบจำลองคลื่น สำหรับ คำนวณการเปลี่ยนแปลงความสูงคลื่นตัวแทนที่ใช้ทั่วไปในการคำนวณการกัดเซาะชายฝั่งและการ ออกแบบสิ่งก่อสร้างบริเวณชายฝั่ง ใค้แก่ mean wave height ( $H_m$ ), root-mean-square wave height  $(H_{rms})$ , average of the highest one-third wave height  $(H_{1/3})$ , average of the highest one-tenth wave height (  $H_{1/10}$  ), the maximum wave height (  $H_{\max}$  ) ដោះ spectral significant wave height (  $H_{mo}$  ) អេទី០ spectral root-mean-square wave height (  $H_{rmsz}$  ) มีหลายวิธีที่สามารถนำมาใช้ในการจำลองการ เปลี่ยนแปลงความสูงคลื่นตัวแทน [ $H_m$ ,  $H_{rms}$ ,  $H_{1/3}$ ,  $H_{1/10}$ ,  $H_{\max}$ , และ  $H_{mo}$  (หรือ  $H_{rmsz}$ )] การศึกษาครั้งนี้จะสนใจเฉพาะสามวิธีหลัก ที่เหมาะสมในทางปฏิบัติ คือ empirical approach, representative wave approach, และ conversion approach จดประสงค์หลักในการศึกษาครั้งนี้คือ การหา แบบจำลองคลื่นที่เหมาะสมสำหรับแต่ละวิธี การศึกษาโครงการนี้แบ่งออกเป็น 3 บทหลักๆ คือ บทที่ 1 เป็นการคำนวณการเปลี่ยนแปลงความสูงคลื่นตัวแทน โดยวิธี empirical approach บทที่ 2 เป็นการคำนวณ การเปลี่ยนแปลงความสูงคลื่นตัวแทนโดยวิธี representative wave approach และบทที่ 3 เป็นการคำนวณ การเปลี่ยนแปลงความสูงคลื่นตัวแทนโดยวิธี conversion approach ซึ่งเป็นการแปลงค่าจากความสูงคลื่น อ้างอิงตัวหนึ่ง ไปเป็นคลื่นตัวแทนตัวอื่นโดยใช้สมการความสัมพันธ์ระหว่างคลื่นตัวแทน วิธี conversion approachนี้ ประกอบด้วย 2 ส่วนหลักๆคือ แบบจำลองคลื่นสำหรับคำนวณการเปลี่ยนแปลงความสูงคลื่น อ้างอิง ( $H_{\it mo}$  หรือ  $H_{\it rms}$ ) และสมการการแปลงคลื่นตัวแทนสำหรับแปลงค่าจากความสูงคลื่นอ้างอิงตัว หนึ่ง ไปเป็นคลื่นตัวแทนตัวอื่น คังนั้น วิธี conversion approach สามารถแบ่งออกเป็น 4 ส่วน คือ ส่วนที่ 1 เป็นแบบจำลองคลื่นสำหรับคำนวณการเปลี่ยนแปลงความสูงคลื่น  $H_{mo}$  ซึ่งสามารถแปลงเป็น zeroth moment of wave spectrum  $(m_0)$  ส่วนที่ 2 เป็นแบบจำลองคลื่นสำหรับคำนวณการเปลี่ยนแปลงความสูง คลื่น  $m{H}_{ms}$  ส่วนที่ 3 เป็นสมการการแปลงค่าจากความสูงคลื่น  $m{H}_{ms}$  ไปเป็นความสูงคลื่น  $m{H}_{m}$  ,  $m{H}_{1/3}$  ,  $H_{1/10}$  ,  $H_{
m max}$  และ ส่วนที่ 4 เป็นสมการการแปลงค่าจากความสูงคลื่นตัวแทนแบบ spectrum (หรือ  $m_0$ ) ไปเป็นความสูงคลื่น  $H_m$  ,  $H_{rms}$  ,  $H_{1/3}$  ,  $H_{1/10}$  , และ  $H_{
m max}$  แบบจำลองคลื่นโดยวิธี conversion approach จะสร้างจากแบบจำลองที่ดีที่สุดจากทั้ง 4 ส่วน ดังนั้นโครงการนี้สามารถแบ่งการศึกษาออกเป็น 6 ส่วนด้วยกัน บทคัดย่อของทั้ง 6 ส่วนมีดังต่อไปนี้

ส่วนที่ 1 เป็นการคำนวณการเปลี่ยนแปลงความสูงคลื่นตัวแทนโดยวิธี empirical approach ใน ปัจจุบันมีเพียง สมการของ Goda (1975 และ 2009) ที่สามารถคำนวณการเปลี่ยนแปลงความสูงคลื่นของ คลื่นตัวแทนจากนอกฝั่งถึงชายฝั่ง แต่สมการมีข้อจำกัดซึ่งสามารถคำนวณได้เฉพาะ  $H_{1/3}$  ,  $H_{\max}$  , และ  $H_{mo}$  สำหรับชายหาดเรียบที่มีความชั้นคงที่เท่านั้น จุดประสงค์ของการศึกษาส่วนนี้คือ ทดสอบความ ถูกต้องของสมการของ  $\operatorname{Goda}(1975$  และ 2009) ในการคำนวณการเปลี่ยนแปลงความสูงคลื่น  $H_{1/3}$  ,  $H_{\max}$  , และ  $H_{mo}$  สำหรับหาดที่ไม่มีเนินทรายใต้น้ำ และประยุกต์ใช้สูตรในการคำนวณการเปลี่ยนแปลง ความสูงคลื่นตัวแทนตัวอื่น ( $H_m$  ,  $H_{rms}$  , และ  $H_{1/10}$ ) ข้อมูลการทดลองจากรางจำลองคลื่นขนาดเล็ก และใหญ่ถูกนำมาใช้ในการทดสอบความถูกต้องของสมการ การทดสอบพบว่าสมการของ  $\operatorname{Goda}$  ให้ผลดี มากสำหรับ  $H_{1/3}$  และ  $H_{mo}$  แต่ให้ผลไม่ดีนักสำหรับ  $H_{\max}$  สมการของ  $\operatorname{Goda}$  ได้ถูกปรับปรุงให้อยู่ใน รูปทั่วไปรูปแบบเดียวกัน แล้วจึงทำการปรับเทียบค่าคงที่ต่างๆในสมการสำหรับการคำนวณการ เปลี่ยนแปลงความสูงคลื่นตัวแทนทั้งหกตัว การทดสอบพบว่าสมการที่ปรับปรุงขึ้นใหม่ ให้ผลดีมาก สำหรับ  $H_m$  ,  $H_{rms}$  ,  $H_{1/3}$  ,  $H_{1/10}$  ,  $H_{\max}$  , และ  $H_{mo}$ 

ส่วนที่ 2 เป็นการคำนวณการเปลี่ยนแปลงความสูงคลื่นตัวแทน โดยวิธี representative wave approach วิธี representative wave approach มุ่งความสนใจ ไปที่ภาพรวมของคลื่นแตกและคำนวณเฉพาะ การเปลี่ยนแปลงความสูงของคลื่นตัวแทน นักวิจัยหลายท่านเชื่อว่าวิธีนี้ให้ผลการคำนวณที่ไม่ดีนัก ดังนั้นการศึกษานี้ทำขึ้นเพื่อทดสอบหาความเป็น ไปได้ที่จะใช้วิธีนี้ในการคำนวณการเปลี่ยนแปลงของ คลื่นตัวแทน โดยทดลองใช้แบบจำลองการสูญเสียพลังงานหลายๆแบบ ข้อมูลการทดลองจำนวนมาก จากรางจำลองคลื่นขนาดเล็กและใหญ่ และจากสนาม ถูกนำใช้ในการทดสอบความถูกต้องของ แบบจำลอง จากการศึกษาพบว่า เมื่อใช้แบบจำลองการสูญเสียพลังงานที่เหมาะสม วิธี representative wave approach จะให้ผลการคำนวณที่ค่อนข้างดีมากสำหรับ  $H_m$ ,  $H_{mss}$ ,  $H_{1/3}$ ,  $H_{1/10}$ ,  $H_{max}$ , และ  $H_{mssz}$ 

จุดประสงค์ของส่วนที่ 3 คือหาแบบจำลองการสูญเสียพลังงานของคลื่นที่เหมาะสมสำหรับคำนวณ การเปลี่ยนแปลงความสูงคลื่น  $H_{mo}$  แบบจำลองการสูญเสียพลังงานของคลื่นสำหรับคำนวณการ เปลี่ยนแปลงความสูงคลื่น  $H_{mo}$  ที่มีอยู่ 14 แบบจำลอง ได้ถูกนำมาประยุกต์ใช้สำหรับคำนวณ  $H_{mo}$  และ ทำการปรับเทียบค่าสัมประสิทธ์ใหม่ ข้อมูลการทดลองจำนวนมาก จากรางจำลองคลื่นขนาดเล็กและ ใหญ่ และจากสนาม ถูกนำมาใช้ในการปรับเทียบและทดสอบความถูกต้องของแบบจำลอง การทดสอบพบว่า แบบจำลองของ Janssen and Battjes (2007) ให้ผลการคำนวณดีที่สุด ได้มีการพัฒนาแบบจำลองที่เสนอให้ผลการ คำนวณที่ดีที่สุดและง่ายต่อการคำนวณที่สุด

จุดประสงค์ของส่วนที่ 4 คือหาแบบจำลองการสูญเสียพลังงานของคลื่นที่เหมาะสม สำหรับ คำนวณการเปลี่ยนแปลงความสูงคลื่น  $H_{ms}$  แบบจำลองการสูญเสียพลังงานของคลื่นสำหรับคำนวณการ เปลี่ยนแปลงความสูงคลื่น  $H_{ms}$  ที่มีอยู่ 15 แบบจำลอง ได้ถูกนำมาทดสอบและปรับเทียบค่าสัมประสิทธ์ ใหม่ ข้อมูลการทดลองจากรางจำลองคลื่นขนาดเล็กและใหญ่ และจากสนาม ถูกนำมาใช้ในการปรับเทียบ และทดสอบความถูกต้องของแบบจำลอง การทดสอบพบว่ามีแบบจำลองอยู่ 4 แบบจำลอง ที่ให้ผลการ

คำนวณดีมาก แบบจำลองที่พัฒนาจาก representative wave approach มีแนวโน้มที่จะให้ผลการคำนวณ ดีกว่า ที่พัฒนาจาก parametric wave concept

ส่วนที่ 5 เป็นการหาสมการที่เหมาะสมสำหรับการแปลงค่าจากความสูงคลื่น  $H_{ms}$  ไปเป็นความ สูงคลื่น  $H_{m}$ ,  $H_{1/3}$ ,  $H_{1/10}$ , และ  $H_{max}$  สมการการแปลงค่า 17 ชุด ได้ถูกนำมาทดสอบและปรับเทียบ ค่าสัมประสิทธ์ใหม่ ข้อมูลการทดลองจำนวนมาก จากรางจำลองคลื่นขนาดเล็กและใหญ่ และจากสนาม ถูกนำมาใช้ในการปรับเทียบและทดสอบความถูกต้องของแบบจำลอง การทดสอบพบว่าสมการส่วน ใหญ่ให้ผลการคำนวณดีมากและค่อนข้างใกล้เคียงกัน

ส่วนที่ 6 เป็นการหาสมการที่เหมาะสมสำหรับการแปลงค่าจากความสูงคลื่นตัวแทนแบบ spectrum ( $H_{mo}$  หรือ  $H_{msz}$ ) ไปเป็นความสูงคลื่น  $H_{m}$ ,  $H_{ms}$ ,  $H_{1/3}$ , และ  $H_{1/10}$  สมการการแปลงค่า 5 ชุด ได้ถูกนำมาทดสอบและปรับเทียบค่าสัมประสิทธ์ใหม่ ข้อมูลการทดลองจากสนามของโครงการ COAST3D ถูกนำมาใช้ในการปรับเทียบและทดสอบความถูกต้องของแบบจำลอง การทดสอบพบว่า สมการของ Forristall (1978) ให้ผลการคำนวณที่ดีที่สุด แต่ยังให้ผลการคำนวณ  $H_{1/10}$  ไม่ดีนัก ดังนั้นจึง มีการปรับปรุงสมการของ Forristall (1978) ในส่วนของ shape factor การทดสอบพบว่าสมการปรับปรุง ใหม่ให้ผลการคำนวณที่ดีขึ้นโดยเฉพาะในส่วนของ  $H_{1/10}$  ได้มีการพัฒนาสมการอย่างง่ายขึ้นมา จากการ เปรียบเทียบพบว่า สมการอย่างง่ายให้ผลการคำนวณใกล้เคียงกับสมการปรับปรุงใหม่

#### **Executive Summary**

**Project Code:** RSA5180016

**Project Title:** Mathematical Model for Computing Representative Wave Heights Transformation

**Investigator:** Mr. Winyu Rattanapitikon, D.Eng., Assoc. Prof., Civil Engineering Program, Sirindhorn International Institute of Technology, Thammasat University. E-mail Address: winyu@siit.tu.ac.th

**Project Period:** 3 years (15 Sep. 2008 – 14 Sep. 2011)

**Objectives:** The main objective of this study is to find out suitable wave models for computing the transformation of representative wave heights (i.e.  $H_m$ ,  $H_{rms}$ ,  $H_{1/3}$ ,  $H_{1/10}$ ,  $H_{max}$ , and  $H_{mo}$ ) based on three simple approaches, i.e. empirical approach, representative wave approach, and conversion approach.

#### Methodology:

- 1) Collect the published experimental data of representative wave heights under irregular wave actions.
- 2) Collect the existing models or formulas for computing the transformation of representative wave heights ( $H_m$ ,  $H_{rms}$ ,  $H_{1/3}$ ,  $H_{1/10}$ ,  $H_{max}$ , and  $H_{mo}$ ) based on three simple approaches, i.e. empirical approach, representative wave approach, and conversion approach.
- 3) Compare the accuracy of existing models or formulas.
- 4) Modify the existing wave models or develop new wave models.

**Results:** Reliable mathematical models for computing the representative wave heights, i.e.  $H_m$ ,  $H_{rms}$ ,  $H_{1/3}$ ,  $H_{1/10}$ ,  $H_{max}$ , and  $H_{mo}$ . The outputs of this project are as follows:

- 1) Rattanapitikon, W., 2010. Verification of conversion formulas for computing representative wave heights. Ocean Engineering 37, 1554-1563.
- 2) Rattanapitikon, W. and Shibayama, T., 2010. Energy dissipation model for computing transformation of spectral significant wave height. Coastal Engineering Journal, JSCE 52, 305-330.
- 3) Nuntakamol, P. and Rattanapitikon, W., 2011. Conversion formulas for estimating statistical-based representative wave heights from zeroth moment of wave spectrum based on field experiments. Ocean Engineering, **submitted**.
- 4) Nuntakamol, P. and Rattanapitikon, W., 2011. Transformation of mean and highest one-tenth wave heights using representative wave approach. Kasetsart Journal: Natural Science, **submitted**.

**Discussion Conclusion:** Based on a wide range and large amount of published experimental results, reliable models are developed for computing the transformation of representative wave heights ( $H_m$ ,  $H_{rms}$ ,  $H_{1/3}$ ,  $H_{1/10}$ ,  $H_{max}$ , and  $H_{mo}$ ) based on three simple approaches, i.e. empirical approach, representative wave approach, and conversion approach. The accuracy of the present models and some existing models are also compared. The comparisons show that the present models give better agreement than those of existing models.

### **CONTENTS**

	cknowledgments	ii
	bstract	
111		
	xecutive Summary	ix
	ist of Symbols	
хi		
	ist of Figures	
хi		
Li	ist of Tables	XV
1	INTRODUCTION	1
	1.1 General	1
	1.2 Scope and Objective of Study	5
	1.3 Organization of Report	5
2	TRANSFORMATION OF REPRESENTATIVE WAVE HEIGHTS	
	USING EMPIRICAL APPROACH	6
	2.1 Introduction	6
	2.2 Goda Formulas	7
	2.3 Collected Laboratory Data	9
	2.4 Formula Examination	12
	2.5 Formula Modification	14
3	TRANSFORMATION OF REPRESENTATIVE WAVE HEIGHTS	
	USING REPRESENTATIVE WAVE APPROACH	19
	3.1 Introduction	19
	3.2 Collected Experimental Data	20
	3.3 Regular Wave Model	21
	3.4 Irregular Wave Model	23
4	TRANSFORMATION OF REPRESENTATIVE WAVE HEIGHTS	
	USING CONVERSION APPROACH	29
	4.1 Introduction	29
	4.2 Transformation of Spectral-Based Wave Heights	30
	4.3 Transformation of Root-Mean-Square Wave Heights	52
	4.4 Conversion from Root-Mean-Square Wave Height to Other Wave Heights	58
	4.5 Conversion from Spectral-Based Wave Height to Other Wave Heights	76
5	CONCLUSIONS	92
R	EFERENCES	95

	NDIX: PAPER REPRINTS	101
	Verification of conversion formulas for computing representative wave heights Energy dissipation model for computing transformation of spectral significant	101
	wave height	112
List o	of Symbols	
4		
A c	position parameter phase velocity	
	cumulative distribution function	
$C_g$	group velocity	
$D_{\scriptscriptstyle B}$	rate of energy dissipation due wave breaking	
erfc	complementary error function	
E	wave energy density	
$E_s$	stable energy density	
$ER_g$	root-mean-square relative error of the data group	
$ER_{avg}$	average root-mean-square relative error	
$ER_{all}$	overall average error	
f	wave frequency	
f(H)	probability density function of wave height	
F(H)	cumulative distribution function of wave height acceleration due to gravity	
g h	water depth	
H	individual wave height	
$H_{\scriptscriptstyle b}$	wave height at breaking point	
$H_{\scriptscriptstyle m}$	mean wave height	
$H_{\mathrm{max}}$	maximum wave height	
$H_{m0}$	spectral significant wave height	
$H_{{\scriptscriptstyle m0,o}}$	deepwater spectral significant wave height	
$H_{\scriptscriptstyle N}$	wave height with exceedance probability of $1/N$	
$H_{\it rep}$	representative wave height	
$H_{rms}$	root-mean-square wave height	
$H_{rmsz}$	spectral-based root-mean-square wave height	
$H_s$	significant wave height	
$H_{st}$	stable wave height	
$H_{tr}$	transitional wave height	
$H_{_{1/N}}$	average of the highest $1/N$ wave heights	
$H_{1/3}$	highest one third wave height	

100

**OUTPUTS** 

 $H_{1/3,o}$  deepwater significant wave height

 $H_{1/10}$  highest one tenth wave height

 $H_{1/250}$  highest one-250<sup>th</sup> wave height

*k* wave number

 $K_s$  shoaling coefficient

L wavelength

 $L_{o}$  deepwater wavelength

m beach slope

 $m_0$  zeroth moment of wave spectrum

M total number of individual waves

N number of individual waves pdf probability density function

 $Q_b$  fraction of breaking waves

*rms* root-mean-square S(f) wave spectrum

t time

 $T_p$  peak spectral wave period

 $T_{m-1,0}$  spectral mean period

 $T_{1/3}$  significant wave period

x distance in cross-shore direction

 $\eta$  water surface elevation

 $\theta$  mean wave angle

 $\rho$  water density

 $\gamma(a,x)$  lower incomplete Gamma function of variables a and x

 $\Gamma$  stable wave factor

 $\Gamma(a,x)$  upper incomplete Gamma function of variables a and x

 $\kappa$  shape parameter

## **List of Figures**

Figure		Page
2.1	Example of computed and measured representative wave heights	17
	transformation (measured data from Smith and Kraus, 1990, case no.	
	6000).	
2.2		17
	transformation (measured data from Ting, 2001, case no. 1).	
2.3	Example of computed and measured representative wave heights	18
	transformation (measured data from Kraus and Smith, 1994, case no.	
	a0515a).	
2.4	Example of computed and measured representative wave heights	18
	transformation (measured data from Dette et al., 1998, case no.	
	11129601).	
4.1	Examples of measured and computed $H_{m0}$ transformation from models	49
	JB07 and M1 (measured data from small-scale experiments).	
4.2	Examples of measured and computed $H_{m0}$ transformation from models	50
	JB07 and M1 (measured data from large-scale experiments).	
4.3	Examples of measured and computed $H_{m0}$ transformation from models	51
	JB07 and M1 (measured data from field experiments).	
4.4	Relationship between measured S and $\sqrt{m_0}/h$ (measured data from	86
	COAST3D project at Egmond).	
4.5		90
	•	
	$\beta_{1/10}$ (measured data from COAST3D project at Egmond).	

### **List of Tables**

Table		Page
2.1	Collected experimental data for verifying empirical formulas.	9
2.2	The errors ( $ER_g$ and $ER_{avg}$ ) of Goda formulas on computing $H_{1/3}$ , $H_{max}$ ,	13
	and $H_{m0}$ for two groups of experiment scales.	
2.3	Default constants ( $C_1$ - $C_5$ ) of the general form of Goda formulas [Eq.	15
	(2.20)].	
2.4	The errors ( $ER_g$ and $ER_{avg}$ ) of the general form of Goda formulas [Eq.	16
	(2.20)] on computing $H_m$ , $H_{rms}$ , $H_{1/3}$ , $H_{1/10}$ , $H_{max}$ , and $H_{m0}$ for two	
3.1	groups of experiment scales.  Summary of collected experimental data for verifying representative wave	20
3.1	approach.	20
3.2	The calibrated constants of models MD1-MD7 for $H_m$ , $H_{rms}$ , $H_{1/3}$ ,	27
	$H_{1/10}$ , $H_{\rm max}$ , and $H_{\rm rmsz}$ .	
3.3	The errors $ER_g$ of the models MD1-MD7 for computing $H_m$ , $H_{rms}$ ,	28
	$H_{1/3}$ , $H_{1/10}$ , $H_{\text{max}}$ , and $H_{\text{rmsz}}$ .	
4.1	Summary of compiled experimental data on $H_{m0}$ .	32
4.2	Values of constants $a_0$ to $a_7$ for computing $Q_b$ .	36
4.3	The errors $ER_g$ and $ER_{avg}$ of each dissipation model for three groups of	44
	experiment-scales by using the default coefficients (measured data from Table 4.1).	
4.4	The errors $ER_g$ and $ER_{avg}$ of each dissipation model for three groups of	46
	experiment-scales by using the calibrated coefficients (measured data from Table 4.1).	
4.5	Summary of collected experimental data of statistical-based <i>rms</i> wave	53
	heights $(H_{rms})$ .	
4.6	The errors $ER_g$ and $ER_{avg}$ of each dissipation model for computing $H_{rms}$	56
	for three groups of experiment-scales (using default coefficients).	
4.7	The errors $ER_{avg}$ of each dissipation models for computing $H_{rms}$ by using	57
	the calibrated coefficients (measured data from Table 4.5).	
4.8	Default and calibrated constants $K_1$ to $K_8$ of the coefficients $\beta$ for	65
	RS07a-RS07c.	
4.9	Collected experimental data for verifying conversion formulas.	68

4.10	The errors $(ER_{avg} \text{ and } ER_{all})$ of the existing formulas on estimating $H_m$ ,	71
	$H_{1/3}$ , $H_{1/10}$ , and $H_{\rm max}$ from three experiment-scales (using default	
	constants).	
4.11	The average errors ( $ER_{avg}$ and $ER_{all}$ ) of the selected formulas on	73
	estimating $H_m$ , $H_{1/3}$ , $H_{1/10}$ , and $H_{\rm max}$ from three experiment-scales	
	(using calibrated constants).	
4.12	The errors $(ER_g)$ of the selected formulas on estimating $H_m$ , $H_{1/3}$ , $H_{1/10}$ ,	74
	and $H_{\text{max}}$ for small-scale, large-scale, and field experiments (using	
	calibrated constants).	
4.13	Selected experimental data for verifying the selected formulas.	75
4.14	Verification results of the selected formulas on estimating $H_m$ , $H_{1/3}$ ,	75
	$H_{\mathrm{1/10}}$ , and $H_{\mathrm{max}}$ from three experiment-scales (using calibrated	
	constants).	
4.15	Collected experimental data from COAST3D project.	82
4.16	The errors ( $ER$ and $ER_{avg}$ ) of the conversion formulas on estimating $H_m$ ,	83
	$H_{rms}$ , $H_{1/3}$ , and $H_{1/10}$ for all data shown in Table 4.15.	
4.17	Calibrated constants $K_3$ and $K_4$ of the coefficients $\beta$ .	91

#### I. INTRODUCTION

#### 1.1. General

In recent years, utilization of coastal area has steadily been increasing for human activities such as transportation, industry, sports, recreation, and sightseeing. During storms, catastrophic beach erosion can occur in the order of hours, resulting in damage to property and resources along the coast. Consequently, protection of beach and infrastructure along the coast against storm wave attack is a primary concern in the field of coastal engineering. The representative wave heights of an irregular wave train are the essential required factors for many coastal engineering applications such as the design of coastal structures and the study of beach deformation.

There are two basic approaches to describing the representative wave heights, i.e. statistical approach (or wave-by-wave approach) and spectral approach (or energy approach). For the statistical approach, an individual wave in a wave record is determined by a zero crossing definition of wave. A wave is defined between two upward (or downward) crossings of the water surface about the mean water elevation. The wave height (H) of an individual wave is defined as the difference between the highest and lowest water surface elevation between two zero-up-crossings (or zero-down-crossings). The statistical-based representative wave heights [i.e. the mean wave height ( $H_m$ ), the root-mean-square wave height ( $H_{rms}$ ), the average of the highest one-third wave height ( $H_{1/3}$ ), the average of the highest one-tenth wave height ( $H_{1/10}$ ), and the maximum wave height ( $H_{max}$ )] can be determined from the wave heights data of the wave record.

For the spectral approach, the moments of a wave spectrum are important in characterizing the spectrum and are useful in relating the spectral description of wave to the statistical-based wave heights. The representative parameter of the average wave energy is the zeroth moment of wave spectrum  $(m_0)$ , which can be obtained by integrating the wave spectrum [S(f)] in the full range of frequency (f) as:

$$m_0 = \int_0^\infty S(f)df \tag{1.1}$$

The spectral-based representative wave heights can be determined from  $m_0$ . Two commonly used spectral representative wave heights are the spectral significant wave height ( $H_{mo}=4\sqrt{m_0}$ ) and the spectral root-mean-square wave height ( $H_{msz}=\sqrt{8m_0}$ ). The spectral representative wave heights can be converted from one to another (and to  $m_0$ ) through the known constant.

The two wave approaches are both important, and neither one alone is sufficient for successful application of wave height for engineering problems (Goda, 1974). While some formulas in the design of coastal structures are appropriate for statistical-based wave heights, others may be more appropriate for spectral-based wave heights. The statistical-based wave heights should be used in those applications where the effect of individual waves is more important than the average wave energy. Measured ocean wave records are often analysed spectrally by the instrument package. Similarly, modern wave hindcasts are often expressed in terms of spectral-based wave height (or zeroth moment of wave spectrum). The present study focuses on five common used statistical-based representative

wave heights (i.e.  $H_m$ ,  $H_{rms}$ ,  $H_{1/3}$ ,  $H_{1/10}$ , and  $H_{max}$ ) and a spectral-based representative wave height (i.e.  $H_{mo}$  or  $H_{rmsz}$ ).

Wave data are usually available in deepwater but not available in the shallow water at the depths required. The wave height in shallow water can be determined from a wave model. Various governing equations have been used in the wave model to compute wave height transformation, e.g. Navier-Stoke equations, Boussinesq equations, mild slope equations, parabolic equations, and energy flux balance equation. If we apply wave model for computing beach transformation, the wave model should be kept as simple as possible because of the frequent updating of wave field for accounting the variability of mean water surface and the change of bottom profiles. Common equation for computing regular wave height transformation is the energy flux balance equation. It is:

$$\frac{\partial \left(Ec_g \cos \theta\right)}{\partial x} = -D_B \tag{1.2}$$

where E is the wave energy density,  $c_g$  is the group velocity,  $\theta$  is the mean wave angle, and  $D_B$  is the energy dissipation rate due to wave breaking.

Irregular wave breaking is more complex than regular wave breaking. In contrast to regular waves, there is no well-defined breaking position for irregular waves. The higher wave tends to break at the greater distance from the shore. Closer to the shore, more and more waves are breaking, until in the inner surf zone almost all the waves are breaking. Common methods to model the representative wave heights ( $H_m$ ,  $H_{rms}$ ,  $H_{1/3}$ ,  $H_{1/10}$ ,  $H_{max}$ , and  $H_{mo}$ ) of an irregular wave train can be classified into five main approaches, i.e. empirical approach, representative wave approach, conversion approach, probabilistic approach, and spectral approach.

The empirical approach is introduced to facilitate engineers for design works and preliminary study of coastal processes. It seems that only Goda (1975) proposed empirical formulas for computing the transformation of  $H_{1/3}$  and  $H_{\rm max}$  from offshore to shoreline. The formulas for computing the transformation of  $H_{1/3}$  and  $H_{\rm max}$  on plane beaches were derived by fitting dimensionless groups to data determined from his probabilistic model. Recently, Goda (2009) showed that the formula for computing  $H_{1/3}$  is also applicable for computing  $H_{m0}$  on plane beaches. The great benefit of this approach is simplicity and minimal time requirements, which can be determined from a pocket calculator. As the formulas were developed based on wave propagation on plane beaches, they should not be applicable for wave propagation on barred beaches. However, the application of the formulas is doubtful for a beach of varying bathymetry in which the sand bar is not formed in the surf zone. Moreover, as the formulas are crude, they are not expected to have good accuracy.

For the representative wave approach, the formulas of regular waves have been directly applied to irregular waves by using representative waves ( $H_m$ ,  $H_{rms}$ ,  $H_{1/3}$ ,  $H_{1/10}$ ,  $H_{max}$ , and  $H_{mo}$ ). Since the highest wave in irregular wave train tends to break at the greatest distance from shore, the initiation of surf zone of irregular waves tend to occur at greater distance from shore than that of regular waves. Therefore, the use of regular wave model may give considerable errors in the surf zone. However, some researchers found that by using an appropriate energy dissipation model with new coefficients, the representative wave approach can be used to compute  $H_{rms}$  (Rattanapitikon et al., 2003)

and  $H_{1/3}$  (Rattanapitikon, 2008).

The conversion approach is used to convert the representative wave heights from one to another through the known relationships. The root-mean-square-wave height (statistical-based or spectral-based) is usually used as a reference wave height of the conversion because it is the output of many wave models (e.g. the models of Battjes and Janssen, 1978; Thornton and Guza, 1983; Larson, 1995; and Rattanapitikon, 2007). Therefore, the other representative wave heights ( $H_m$ ,  $H_{1/3}$ ,  $H_{1/10}$ , and  $H_{max}$ ) can be determined from the known relationships between the representative wave heights (e.g. the relationships of Longuet-Higgins, 1952; Battjes and Groenendijk, 2000; and Rattanapitikon and Shibayama, 2007).

Wave-by-wave approach considers the propagation of individual waves. The incident individual waves may be determined from the irregular wave records or from probability density function ( pdf) of wave height. These individual waves are then propagated shoreward independently using an appropriate regular wave model, assuming no wave-to-wave interaction. The representative wave heights ( $H_m$ ,  $H_{rms}$ ,  $H_{1/3}$ ,  $H_{1/10}$ ,  $H_{max}$ , and  $H_{mo}$ ) at the required location can be constructed from the simulation results of all individual waves. This method is particularly useful if a detailed wave height distribution is required. However, it requires large computation times. Over the past few decades, many research works have been performed in this approach (e.g. Mase and Iwagaki, 1982; Mizuguchi, 1982; Dally, 1990 and 1992; Kuriyama, 1996; and Goda, 2004). The main difference of those research works is the formulation of regular wave model that used to simulate the propagation of individual wave.

The parametric approach may also be considered as a simplified form of the probabilistic approach. It seeks to reduce the computational effort by describing the energy dissipation rate in term of time-averaged parameter. As this approach relies on the macroscopic features of breaking waves and predicts only the transformation of rootmean-square (rms) wave height, it is suitable when a detail wave height distribution is not needed. The works on this approach can be separated into two classes based on the assumption about the pdf of wave height in the surf zone. The first class assumes that the Rayleigh pdf (or modified Rayleigh pdf) is valid in the surf zone. The average rate of energy dissipation is described by integrating the product of energy dissipation of a single broken wave and the probability of occurrence of breaking waves. Various semi-analytical models have been developed based on this class (e.g. Battjes and Janssen, 1978; Thornton and Guza, 1983; Baldock et al., 1998; and Rattanapitikon and Shibayama, 1998). The significant differences of those models are the formulation of energy dissipation of a single broken wave and the assumption on probability of occurrence of breaking waves. The weak point of this class is the assumption on Rayleigh pdf in the surf zone, because this assumption is not supported by some experiments (Dally, 1990). The second class was proposed, by Larson (1995), to overcome the weakness of the first class. Larson (1995) proposed a semi-analytic model without making any assumptions about the pdf in the surf zone. The average rate of energy dissipation is described by adding up the dissipation of each broken wave component and dividing by the total number of waves (including broken and unbroken waves). The semi-analytic model reproduces macroscopic features of wave height and energy flux transformation, including breaking and reforming, in agreement with the individual wave approach that involves transformation of many individual waves.

Spectral approach assumes that irregular wave trains consist of numerous wave

heights with different frequencies. The distribution of the energy of these wave heights when plotted against the frequency (and direction) is called wave spectrum. In the modeling, the incident spectrum is decomposed into a number of component waves. The propagation of each wave component is computed by using an appropriate regular wave model. The wave spectrum at the required location is obtained by assembling the simulation results from all the wave components by linear superposition. Several models have been proposed based on this approach, differing mainly in the regular wave model used to simulate the propagation of wave components (e.g. Izumiya and Horikawa, 1987; Isobe, 1987; Panchang et al., 1990; and Grassa, 1990). The application of this approach may be restricted when applying in the surf zone, i.e. the component waves in frequency domain do not break, but real waves or individual waves in the time domain do break. To overcome this problem, the energy dissipation model developed based on parametric approach may be incorporated to predict the energy losses due to wave breaking (e.g. Mase and Kirby, 1992; Chawla et al., 1998; and Mase and Kitano, 2000). However, the spectrum approach requires large computation times. It may not be appropriate to incorporate into the beach deformation model.

For computing beach deformation, the wave model should be kept as simple as possible because of the frequent updating of wave field to account for the change of bottom profiles. The present study focuses on empirical approach, representative wave approach and conversion approach, as these appear to be the simple methods. During the last few decades, many theories have been developed and experimental studies, both in laboratory and in the field, have been carried out to draw a clearer picture of wave height transformation. Considerable amount of knowledge on the mechanism of wave has been accumulated so far. However, it has not reached to a satisfactory level. Owing to the complexity of the wave breaking mechanism, full description of the mechanism of the wave breaking has not yet been developed. At the present state of knowledge, clearly any type of energy dissipation model due to wave breaking has to be based on empirical or semi-empirical formulas calibrated with the experimental results. Various wave models have been proposed during the past decades. It is not clear which model is the most suitable for the three wave approaches. Moreover, most of the models were developed with the limited experimental conditions. Therefore, their validity is limited according to the range of experimental conditions, which were employed in the calibration. The evidence is that there are so many models exist.

In the past, we could not develop a model based on a large amount of experimental results covering a wide range of test conditions, because they did not exist. However, at present, the experimental results obtained by many researchers have been accumulated and a large amount of experimental results have become available. It is a good time to develop models based on the large amount and wide range of experimental results.

#### 1.2. Scope and Objective of Study

The scope and objectives of the present study can be described as follows:

- 1. This study focuses mainly on two-dimensional irregular wave models.
- 2. Three simple approaches for computing the transformation of  $H_m$ ,  $H_{rms}$ ,  $H_{1/3}$ ,  $H_{1/10}$ ,  $H_{max}$ , and  $H_{mo}$  (or  $H_{rmsz}$ ) are considered in the present study, i.e. empirical approach, representative wave approach, and conversion approach.
- 3. To review and summarize existing models which were developed based on the three approaches.
- 4. To collect a wide range and large amount of published experimental data on  $H_m$ ,  $H_{rms}$ ,  $H_{1/3}$ ,  $H_{1/10}$ ,  $H_{max}$ , and  $H_{mo}$  for calibration and examination of the models.
- 5. To examine the existing wave models for identifying the suitable models for each approach.
- 6. To modify the existing models or develop new models for the three approaches.

#### 1.3. Organization of Report

The contents of some parts of this report are substantially the same as a series of papers submitted to journals. The report updates and extends some material in the papers. The present report is written in the following stages:

- Chapter 1 is an introduction and gives a statement of problem and objective and scope of study.
- Chapter 2 presents empirical formulas for computing the representative wave heights based on empirical approach.
- Chapter 3 describes the transformation of the representative wave heights based on representative wave approach.
- Chapter 4 presents the models and formulas for computing the representative wave heights based on conversion approach.
- Chapter 5 gives conclusions of the study.
- Appendix presents the paper reprints of this research.

# 2. EMPIRICAL FORMULAS FOR COMPUTING REPRESENTATIVE WAVE HEIGHTS TRANSFORMATION

#### 2.1. Introduction

The representative wave heights  $(H_{rep})$  are the essential required factors for the study of beach deformation and the design of coastal structures. This chapter concentrates on the determination of six common representative wave heights, i.e. the mean wave height  $(H_m)$ , the root-mean-square wave height  $(H_{rms})$ , the significant wave height or highest one-third wave height  $(H_{1/3})$ , the highest one-tenth wave height  $(H_{1/10})$ , the maximum wave height  $(H_{max})$ , and the spectral significant wave height  $(H_{m0})$ . Wave data are usually available in deepwater, but not available in shallow water at the depths required. When waves propagate to the nearshore zone, wave profiles steepen, and eventually waves break. Once the waves start to break, a part of wave energy is dissipated, and wave height decreases towards the shore. Irregular wave breaking is more complex than regular wave breaking. In contrast to regular waves, there is no well-defined breaking position for irregular waves. A higher wave tends to break at a greater distance from the shore. Closer to the shore, more and more waves are breaking, until in the inner surf zone, almost all the waves are breaking. The transformation of representative wave heights  $(H_{ren})$  from offshore to shoreline can be determined from a wave model. Common approaches to model the transformation of  $H_{rep}$  may be classified into four main approaches, i.e. empirical approach, representative wave approach, conversion approach, probabilistic approach, and spectral approach. For convenience, most engineers seem to prefer the simplest approach (which does not give bad accuracy) for practical work. Therefore, the present study focuses on the empirical approach, as this appears to be the simplest approach for computing the representative wave heights in shallow water.

The empirical approach is introduced to facilitate engineers for design works and preliminary study of coastal processes. It seems that only Goda (1975) proposed empirical formulas for computing the transformation of  $H_{1/3}$  and  $H_{\rm max}$  from offshore to shoreline. The formulas for computing the transformation of  $H_{1/3}$  and  $H_{\rm max}$  on plane beaches were derived by fitting dimensionless groups to data determined from his probabilistic model. Recently, Goda (2009) showed that the formula for computing  $H_{1/3}$  is also applicable for computing  $H_{m0}$  on plane beaches. The great benefit of this approach is simplicity and minimal time requirements, which can be determined from a pocket calculator. As the formulas were developed based on wave propagation on plane beaches, they should not be applicable for wave propagation on barred beaches. However, the application of the formulas is doubtful for a beach of varying bathymetry in which the sand bar is not formed in the surf zone. Moreover, as the formulas are crude, they are not expected to have good accuracy.

Although the Goda formulas are widely used, it seems that no literature has verified the formulas on computing the transformation of  $H_{\rm 1/3}$  and  $H_{\rm max}$ , and it is not clear whether the formulas are applicable for computing other representative wave heights. The objectives of the present study are to examine the formulas of Goda (1975 and 2009) for

computing the transformation of  $H_{1/3}$ ,  $H_{\rm max}$ , and  $H_{m0}$  on unbarred beach conditions and to extend the formulas for computing the transformation of  $H_m$ ,  $H_{rms}$ , and  $H_{1/10}$ . Laboratory data of waves propagating on unbarred beaches, from small-scale and large-scale wave flumes, are used to verify the formulas.

This chapter is divided into four main parts. The first part describes the empirical formulas of Goda (1975 and 2009). The second part describes the collected data used to verify the formulas. The third part is the examination of the formulas for computing  $H_{1/3}$ ,  $H_{\max}$ , and  $H_{m0}$ . The fourth part describes the general form of Goda formulas for computing  $H_m$ ,  $H_{rms}$ ,  $H_{1/3}$ ,  $H_{1/10}$ ,  $H_{\max}$ , and  $H_{m0}$ .

#### 2.2. Goda Formulas

Goda (1975) proposed a wave model based on the probabilistic approach. The model deals with unidirectional random waves propagating on plane beaches. In the offshore zone, the probability density function (pdf) of wave height is assumed to follow the Rayleigh distribution. The monochromatic nonlinear theory of Shuto (1974) was used to compute wave shoaling. The breaking criterion of Goda (1970) was applied to determine the gradational breaker of the random waves. Wave breaking was assumed to occur with linearly varying probability of occurrence over a small range of wave heights, resulting in a modified distribution with a gradual cutoff of the distribution around the range of breaker heights. The effect of surf beats on breaking wave heights was taken into account by statistically varying the water depth with addition of surf beat amplitude. The model calculates a gradual evolution of the shape of the pdf of the wave heights from offshore throughout the surf zone, from which various representative wave heights (e.g.  $H_m$ ,  $H_{\rm rms}$  ,  $H_{\rm 1/3}$  ,  $H_{\rm 1/10}$  , and  $H_{\rm 1/250}$  ) can be determined. The maximum wave height ( $H_{\rm max}$ ) is set in the computation as that of the highest one-250<sup>th</sup> wave  $(H_{1/250})$ . Since the model was developed based on the plane beach conditions, the model should be applicable if the beach does not deviate much from a plane beach, and the model should not be applicable when a bar is formed on the beach. The applicability of the model has been verified through comparison with several laboratory tests and field measurement data. By using this model, Goda (1975) computed the propagation of unidirectional random waves on plane beaches and presented a set of design diagrams for the transformation of  $H_{1/3}$  and  $H_{\rm max}$  from the offshore to the shoreline for four beach slopes of 1/10, 1/20, 1/30, and 1/100. To facilitate coastal engineers for design work, empirical formulas for computing  $H_{1/3}$  and  $H_{\text{max}}$  are extracted from the design diagrams. Recently, Goda (2009) showed that the formula for computing  $H_{1/3}$  is also applicable for computing the propagation of  $H_{m0}$  on plane beaches. A summary of Goda formulas for computing  $H_{1/3}$ ,  $H_{max}$ , and  $H_{m0}$ are given below.

$$H_{1/3} = \begin{cases} K_s H_{1/3,o} & \frac{h}{L_o} \ge 0.2\\ \min\{(\beta_0 H_{1/3,o} + \beta_1 h), \beta_{\max} H_{1/3,o}, K_s H_{1/3,o}\} & \frac{h}{L_o} < 0.2 \end{cases}$$
(2.1)

$$H_{\text{max}} = \begin{cases} 1.8K_s H_{1/3,o} & \frac{h}{L_o} \ge 0.2\\ \min\left\{ (\beta_0^* H_{1/3,o} + \beta_1^* h), \beta_{\text{max}}^* H_{1/3,o}, 1.8K_s H_{1/3,o} \right\} & \frac{h}{L_o} < 0.2 \end{cases}$$
(2.2)

$$H_{m0} = \begin{cases} K_s H_{m0,o} & \frac{h}{L_o} \ge 0.2\\ \min\{(\beta_0^{**} H_{m0,o} + \beta_1^{**} h), \beta_{\max}^{**} H_{m0,o}, K_s H_{m0,o}\} & \frac{h}{L_o} < 0.2 \end{cases}$$
(2.3)

where  $K_s$  is the shoaling coefficient,  $H_{1/3,o}$  is the deepwater significant wave height,  $H_{m0,o}$  is the deepwater spectral significant wave height, h is the still water depth, and  $L_o$  is the deepwater wavelength related to the significant wave period  $(T_{1/3})$ . If the significant wave period  $(T_{1/3})$  is not available, Goda (2009) suggested using the spectral mean period  $(T_{m-1,0})$ . The coefficients  $\beta$  have been formulated as follows.

$$\beta_0 = 0.028 \left(\frac{H_{1/3,o}}{L_o}\right)^{-0.38} \exp(20m^{1.5})$$
(2.4)

$$\beta_1 = 0.52 \exp(4.2m) \tag{2.5}$$

$$\beta_{\text{max}} = \max \left\{ 0.92, 0.32 \left( \frac{H_{1/3,o}}{L_o} \right)^{-0.29} \exp(2.4m) \right\}$$
 (2.6)

$$\beta_0^* = 0.052 \left(\frac{H_{1/3,o}}{L_o}\right)^{-0.38} \exp(20m^{1.5})$$
(2.7)

$$\beta_1^* = 0.63 \exp(3.8m) \tag{2.8}$$

$$\beta_{\text{max}}^* = \text{max} \left\{ 1.65, 0.53 \left( \frac{H_{1/3,o}}{L_o} \right)^{-0.29} \exp(2.4m) \right\}$$
 (2.9)

$$\beta_0^{**} = 0.028 \left(\frac{H_{m0,o}}{L_o}\right)^{-0.38} \exp(20m^{1.5})$$
(2.10)

$$\beta_1^{**} = 0.52 \exp(4.2m)$$
 (2.11)

$$\beta_{\text{max}}^{**} = \text{max} \left\{ 0.92, 0.32 \left( \frac{H_{m0,o}}{L_o} \right)^{-0.29} \exp(2.4m) \right\}$$
 (2.12)

where m is the beach slope. The shoaling coefficient ( $K_s$ ) is calculated based on the nonlinear wave theory of Shuto (1974). The nonlinear wave shoaling makes the Goda formulas complicated because the shoaling coefficient has to be solved by a numerical method. Thornton and Guza (1983) noted that the use of nonlinear wave theory to shoal random waves introduces unnecessary numerical complications into the relatively crude model. For convenience of computation, Goda (2009) suggested calculating  $K_s$  with the linear wave theory as:

$$K_s = \left[ \left( 1 + \frac{2kh}{\sinh 2kh} \right) \tanh kh \right]^{-1/2} \tag{2.13}$$

where k is the wave number related to  $T_{1/3}$  or  $T_{m-1,0}$ , which can be determined from the dispersion equation.

For the wave period parameter, Goda (1975 and 2009) proposed to use  $T_{\scriptscriptstyle 1/3}$  or  $T_{\scriptscriptstyle m-1,0}$  for computing the related wave parameters. However, comparing among the wave period parameters, the spectral peak period ( $T_{\scriptscriptstyle p}$ ) is the most commonly used parameter and typically reported for the irregular wave data. It seems to be more convenient to use  $T_{\scriptscriptstyle p}$  in the formulas. In the present study, all wave parameters are based on linear wave theory related to  $T_{\scriptscriptstyle p}$ .

#### 2.3. Collected Laboratory Data

As the Goda formulas were derived from the Goda's (1975) model which deals with the unidirectional waves propagating on plane beaches, the data that are used to examine the formulas should be data from the experiments, which were performed under the same conditions, i.e. unidirectional waves and plane beaches. However, it is expected that the formulas may also be valid for beaches of varying bathymetry in which a bar is not formed in the surf zone. Although, the formulas were derived based on the results from the unidirectional wave model, it could be applied to account for the effect of wave refraction by using the equivalent deepwater wave height concept (for more detail, please see Goda, 2009). Nevertheless, the application of equivalent deepwater wave height concept is restricted to use with  $H_{1/3}$  (Goda, 2000). It is not clear whether the concept is applicable for other representative wave heights or not. However, because of the limitation of the available data, the study of applicability of the equivalent deepwater wave height concept is not included in this study.

Laboratory data of representative wave heights transformation from 6 sources were collected for examination and calibration of the formulas. Only the experiments performed based on unidirectional waves propagating on unbarred beaches are used to verify the Goda formulas. A summary of the collected laboratory data is shown in Table 2.1.

**Table 2.1** Collected experimental data for verifying empirical formulas.

Sources	Measured wave heights	No. of	No. of
		cases	data
Smith and Kraus (1990)	$H_m$ , $H_{rms}$ , $H_{1/3}$ , $H_{max}$	3	24
Smith and Vincent (1992)	$H_{m0}$	4	36
Ting (2001)	$H_{m}, H_{rms}, H_{1/3}, H_{1/10}, H_{max}$	1	7
Kraus and Smith (1994)	$H_{m}, H_{rms}, H_{1/3}, H_{1/10}, H_{max}, H_{m0}$	49	780
Roelvink and Reniers (1995)	$H_{m0}$	25	246
Dette et al. (1998)	$H_{rms}$ , $H_{1/3}$ , $H_{1/10}$ , $H_{max}$ , $H_{m0}$	64	1625

**Table 2.1 (cont.)** Collected experimental data.

Sources	$H_{1/3,o}/L_o$ or	m	Beach	Apparatus
	$H_{m0,o}/L_{o}^{*}$		conditions	
Smith and Kraus (1990)	0.030-0.080	0.033	fixed plane	small-scale
Smith and Vincent (1992)	$0.032 \text{-} 0.064^*$	0.033	fixed plane	small-scale
Ting (2001)	0.022	0.029	fixed plane	small-scale
Kraus and Smith (1994)	0.002-0.066	0.034-0.043	movable	large-scale
Roelvink and Reniers (1995)	0.024-0.040*	0.024-0.025	movable	large-scale
Dette et al. (1998)	0.009-0.021	0.022-0.026	movable	large-scale

The collected data are separated into 2 groups based on the experiment scale, i.e. small-scale and large-scale experiments. The experiments of Smith and Kraus (1990), Smith and Vincent (1992), and Ting (2001) were performed in small-scale wave flumes under fixed bed conditions, whereas the experiments of Kraus and Smith (1994), Roelvink and Reniers (1995), and Dette et al. (1998) were undertaken in large-scale wave flumes under movable bed (sandy bed) conditions. For the movable bed conditions, beach profiles were initially set as equilibrium beach profiles, and the beach conditions were varied in time. The collected data cover a range of deepwater significant wave steepness ( $H_{1/3,o}/L_o$  or  $H_{m0,o}/L_o$ ) from 0.002 to 0.080 and average beach slope (m) from 0.022 to 0.043. A brief description of the experiments is given below.

The experiment of Smith and Kraus (1990) was conducted to investigate the macrofeatures of wave breaking over bars and artificial reefs using a small wave flume of 45.70 m long, 0.46 m wide, and 0.91 m deep. Both regular and irregular waves were employed in this experiment. A total of 12 cases were performed for irregular wave tests. Three irregular wave conditions were generated for three bar configurations as well as for a plane beach. A JONSWAP (Hasselmann et al., 1973) computer signal was generated for spectral width parameter of 3.3 and spectral peak periods of 1.07, 1.56, and 1.75 s with significant wave heights of 0.12, 0.15, and 0.14 m, respectively. Water surface elevations were measured at eight cross-shore locations using resistance-type gages. Only 3 cases of waves on a plane beach were used in this study (cases no. 2000, 6000, and 8000).

The experiment of Smith and Vincent (1992) was conducted to examine the development of double-peaked spectral across the surf zone. The tests were performed in a small-scale wave flume of 45.7 m long, 0.45 m wide, and 0.61 m deep. The bottom of the flume is smooth concrete and rises at a slope of 1:30 from the middle of the flume. Water surface elevations were measured at nine cross-shore locations using resistance-type gages. Twelve cases were investigated, differing in the position and the energy density level of the two peaks. The four most energetic cases (i.e. cases 1, 3, 7, and 9) are available in the thesis of Vink (2001) and are used in this study.

The experiment of Ting (2001) was conducted to study wave and turbulence velocities in a broad-banded irregular wave surf zone. The experiment was performed in a small-scale wave flume, which was 37 m long, 0.91 m wide and 1.22 m deep. A false bottom with 1/35 slope built of marine plywood was installed in the flume to create a plane beach. The irregular waves were developed from the TMA spectrum (Bouws et al., 1985), with a spectral peak period of 2.0 s, a spectral significant wave height of 0.15 m, and spectral width parameter of 3.3. Water surface elevations were measured at seven cross-shore locations using a resistance-type gage.

The SUPERTANK laboratory data collection project (Kraus and Smith, 1994) was conducted to investigate cross-shore hydrodynamic and sediment transport processes. A

76-m-long sandy beach was constructed in a large wave tank of 104 m long, 3.7 m wide, and 4.6 m deep. The wave conditions were designed to balance the need for repetition of wave conditions to move the beach profile toward equilibrium, and development of a variety of conditions for hydrodynamic studies. Wave conditions included both regular and irregular waves. The TMA spectral shape (Bouws et al., 1985) with spectral width parameter of 3.3, 20, and 100 was used to design all irregular wave tests. Most of the experiments were performed with the spectral width parameter of 3.3 and only a few experiments were performed with the spectral width parameter of 100. Sixteen resistancetype gages were used to measure water surface elevations across the shore. The initial beach profile of the first major test was a planar foreshore joining to the subaqueous portion formed in a concave shape of equilibrium beach profile. The beach profiles of other testes were initiated using the final profile configuration of the previous run or modified form of it. The beach profiles cover either barred or unbarred beaches. Fourteen major tests (including 128 cases) were performed under irregular wave actions. Only 49 cases of unbarred beach conditions were used in this study. The collected experiments cover deepwater significant wave steepness ( $H_{1/3,o}/L_o$ ) from 0.002 to 0.066, average beach slope from 0.034 to 0.043 and spectral width parameter of 3.3 and 20.

LIP 11D Delta Flume Experiment (Roelvink and Reniers, 1995) was performed at Delft Hydraulics large-scale wave flume. A 175-m-long sandy beach was constructed in a large wave tank of 233 m long, 5 m wide and 7 m deep. The 2 major tests were performed, i.e., with dune (test no. 1A-1C) and without dune (test no 2A-2C). Each major test consisted of several wave conditions. The duration of each wave condition lasted about 12 to 21 hr. Initial beach profiles of the test no. 1A and 1B are equilibrium Dean-type beaches. The beach profiles of other tests (test no. 1B, 1C, 2B, 2E, and 2C) were initiated using the final profile configuration of the previous test. The fixed measurement set-up consisted of 10 pressure gauges and three wave height meters deployed in the flume to measure the wave transformation. Board banded random waves, JONSWAP spectrum with spectral width parameter of 3.3, were generated. During the run, the sand bar feature grows and becomes more pronounced after sometimes. Only the experiments of unbarred beach conditions are used in this study. The collected experiments include 25 cases of wave and beach conditions, covering deepwater significant wave steepness ( $H_{m0,o}/L_o$ ) from 0.024 to 0.040 and average beach slope from 0.024 to 0.025.

SAFE Project (Dette et al., 1998) was carried out to improve the methods of design and performance assessment of beach nourishment. The SAFE Project consisted of four activities, one of which was to perform experiments in a large-scale wave flume in Hannover, Germany. A 250-m-long sandy beach was constructed in a large wave tank of 300 m long, 5 m wide and 7 m deep. The test program was divided into two major phases. The first phase (test no. A, B, C, and H) was aimed to study the beach deformation of equilibrium profile with different beach slope changes. The equilibrium beach profile was adopted from Bruun's (1954) approach ( $h = 0.12x^{2/3}$ ). In the second phase, the sediment transport behaviors of dunes with and without structural aid were investigated (test no. D, E, F, and G). The TMA spectral shape with spectral width parameter of 3.3 was used to design all irregular wave tests. A total of 27 wave gages was installed over a length of 175 m along one wall of the flume. The collected experiments included 64 cases of unbarred beach conditions, covering deepwater significant wave steepness ( $H_{1/3,o}/L_o$ ) from 0.009 to 0.021 and average beach slope from 0.022 to 0.026.

#### 2.4. Formula Examination

The basic parameter for determination of the overall accuracy of the formulas is the average root-mean-square relative error ( $ER_{avg}$ ), which is defined as:

$$ER_{avg} = \frac{\sum_{n=1}^{m} ER_{gn}}{tn}$$
 (2.14)

where n is the data group number,  $ER_{gn}$  is the root-mean-square relative error of the group no. n, and tn is the total number of data groups. A small value of  $ER_{avg}$  indicates good overall accuracy of the prediction.

The root-mean-square relative error of each data group ( $ER_g$ ) is defined as:

$$ER_{g} = 100 \sqrt{\frac{\sum_{i=1}^{nc} (H_{ci} - H_{mi})^{2}}{\sum_{i=1}^{nc} H_{mi}^{2}}}$$
(2.15)

where i is the wave height number,  $H_{ci}$  is the computed wave height of number i,  $H_{mi}$  is the measured wave height of number i, and nc is the total number of measured wave heights in each data group.

The question of how good a model is, is usually defined in a qualitative ranking (e.g. excellent, very good, good, fair, and poor). As the error of some existing irregular wave models is in the range of 7 to 21% (please see Table 2 of Rattanapitikon, 2007), the qualification of error ranges of an irregular wave model may be classified into five ranges [i.e. excellent ( $ER_g < 5.0\%$ ), very good ( $5.0 \le ER_g < 10.0\%$ ), good ( $10.0 \le ER_g < 15.0\%$ ), fair ( $15.0 \le ER_g < 20.0\%$ ), and poor ( $ER_g \ge 20.0\%$ )].

The laboratory data from 6 sources (see Table 2.1) are used to examine the validity of the formulas. The experiments are separated into 2 groups, i.e. small-scale and large-scale experiments. The small-scale experiments were performed under fixed plane beach conditions, while the large-scale experiments were performed under movable unbarred beach conditions.

The computations of  $H_{rep}$  are carried out with the 6 sources of collected data. The variables required for the examination are  $H_{rep}$ ,  $T_p$ , h, m,  $H_{rep,o}$ ,  $L_o$ ,  $K_s$ , and k. The data of  $H_{rep}$ ,  $T_p$ , h, and m are measured directly from the laboratory. The bottom slope (m) used in the computation is the average bottom slope. The data of  $H_{rep,o}$ ,  $L_o$ ,  $K_s$ , and k are calculated based on linear wave theory related to the spectral peak period  $(T_p)$ . The deepwater representative wave height  $(H_{rep,o})$  is calculated from the wave height at the farthest offshore measurement location.

Errors of Eqs. (2.1) – (2.3) on predicting  $H_{1/3}$ ,  $H_{\rm max}$ , and  $H_{m0}$  for two groups of experiment scales are shown in Table 2.2. The examination results from Table 2.2 can be summarized as follows.

(a) It is common to expect that the crude formula should not give very good accuracy. Surprisingly, the Goda formula [Eq. (2.1)] gives very good predictions of  $H_{1/3}$  for either small-scale or large-scale experiments ( $ER_g = 8.7$  and 8.1%, respectively).

- These errors seem to be able to compete with other complicated wave models. However, the use of  $T_p$  (instead of  $T_{1/3}$  or  $T_{m-1,0}$ ) may cause the coefficients in the formula to change slightly. The accuracy of the predictions may be improved by recalibrating the coefficients in the formula.
- (b) The Goda formula [Eq. (2.2)] gives fair predictions of  $H_{\rm max}$  for both of small-scale and large-scale experiments ( $ER_g=18.8$  and 17.6%, respectively). These errors seem not to be acceptable for practical work. As the errors are too large, the formula for computing  $H_{\rm max}$  may have to be modified before use in practical work.
- (c) For computing  $H_{m0}$ , the Goda formula [Eq. (2.3)] gives very good prediction for small-scale experiments ( $ER_g = 5.3\%$ ) and good prediction for large-scale experiments ( $ER_g = 10.4\%$ ). However, many researchers (e.g. Goda, 1974; Thompson and Vincent, 1985; Battjes and Groenendijk, 2000; and Goda, 2009) showed that  $H_{m0}$  is not equal to  $H_{1/3}$ , especially near the breaking point. The coefficients in the formula of  $H_{m0}$  [Eq. (2.3)] are expected to be different from those of  $H_{1/3}$ . Although, the overall accuracy of  $H_{m0}$  is very good ( $ER_{avg} = 7.8\%$ ), it may be possible to improve the accuracy by recalibrating the coefficients.
- (d) The overall errors ( $ER_{avg}$ ) of the formulas for computing  $H_{1/3}$ ,  $H_{max}$ , and  $H_{m0}$  are 8.4, 18.2, and 7.8%, respectively. The formulas give very good predictions of  $H_{1/3}$  and  $H_{m0}$  but give fair prediction of  $H_{max}$ .

**Table 2.2** The errors ( $ER_g$  and  $ER_{avg}$ ) of Goda formulas on computing  $H_{1/3}$ ,  $H_{max}$ , and  $H_{m0}$  for two groups of experiment scales.

$H_{rep}$	No of	Formulas	E	$ER_g$	
	cases		small- scale	large- scale	
$H_{1/3}$	117	Eq. (2.1)	8.7	8.1	8.4
$H_{ m max}$	117	Eq. (2.2)	18.8	17.6	18.2
$H_{m0}$	142	Eq. (2.3)	5.3	10.4	7.8
$H_{ m max}$	117	Eq. (2.16)	10.1	15.0	12.6

#### 2.5. Formula Modification

It can be seen from Eq. (2.2) that  $H_{\max}$  is a function of  $H_{1/3,o}$ . The formula is proposed based on the assumption that the deepwater maximum wave height  $(H_{\max,o})$  is equal to  $1.8H_{1/3,o}$ . The formula may not be appropriate if  $H_{\max,o} \neq 1.8H_{1/3,o}$ . It seems to be more appropriate if the formula is rewritten in terms of the corresponding representative wave height (i.e.  $H_{\max,o}$ ). Equation (2.2) can be rewritten in terms of  $H_{\max,o}$  by replacing  $H_{1/3,o}$  with  $H_{\max,o}/1.8$ . The modified formula for computing  $H_{\max}$  can be expressed as:

$$H_{\text{max}} = \begin{cases} K_{s} H_{\text{max},o} & \frac{h}{L_{o}} \ge 0.2\\ \min \left\{ (\hat{\beta}_{1} H_{\text{max},o} + \hat{\beta}_{2} h), \hat{\beta}_{3} H_{\text{max},o}, K_{s} H_{\text{max},o} \right\} & \frac{h}{L_{o}} < 0.2 \end{cases}$$
(2.16)

$$\hat{\beta}_1 = 0.036 \left( \frac{H_{\text{max},o}}{L_o} \right)^{-0.38} \exp(20m^{1.5})$$
 (2.17)

$$\hat{\beta}_2 = 0.63 \exp(3.8m) \tag{2.18}$$

$$\hat{\beta}_3 = \max \left\{ 0.92, 0.35 \left( \frac{H_{\text{max},o}}{L_o} \right)^{-0.29} \exp(2.4m) \right\}$$
 (2.19)

Errors of Eq. (2.16) on predicting  $H_{\rm max}$  for two groups of experiment scales are shown in the last row of Table 2.2. It can be seen that the overall error ( $ER_{avg}$ ) of the prediction is reduced significantly from 18.2% to be 12.6%. Therefore, the use of Eq. (2.16) for computing  $H_{\rm max}$  seems to be more suitable than that of Eq. (2.2).

#### 2.5.1. General formula

It can be seen from Eqs. (2.1), (2.3), and (2.16) that the pattern of the formulas is similar. They can be written in general form for computing the representative wave heights ( $H_{rep}$ ) as:

$$H_{rep} = \begin{cases} K_{s} H_{rep,o} & \frac{h}{L_{o}} \ge 0.2\\ \min\{(\alpha_{1} H_{rep,o} + \alpha_{2} h), \alpha_{3} H_{rep,o}, K_{s} H_{rep,o}\} & \frac{h}{L_{o}} < 0.2 \end{cases}$$
(2.20)

$$\alpha_1 = C_1 \left(\frac{H_{rep,o}}{L_o}\right)^{-0.38} \exp(20m^{1.5})$$
 (2.21)

$$\alpha_2 = C_2 \exp(C_3 m) \tag{2.22}$$

$$\alpha_3 = \max \left\{ C_4, C_5 \left( \frac{H_{rep,o}}{L_o} \right)^{-0.29} \exp(2.4m) \right\}$$
 (2.23)

where  $C_1 - C_5$  are constants and  $K_s$  is the linear wave shoaling coefficient which is determined from Eq. (2.13). The proposed values of the constants  $C_1 - C_5$  for computing

 $H_{1/3}$ ,  $H_{\text{max}}$ , and  $H_{m0}$  are shown in Table 2.3. The general form of Goda formulas [Eq. (2.20)] consists of three main parts, i.e. the parts of wave shoaling ( $K_sH_{rep,o}$ ), maximum limit of wave height ( $\alpha_3H_{rep,o}$ ), and wave decay in surf zone ( $\alpha_1H_{rep,o}+\alpha_2h$ ).

**Table 2.3** Default constants  $(C_1 - C_5)$  of the general form of Goda formulas [Eq. (2.20)].

$H_{\it rep}$	$C_1$	$C_2$	$C_3$	$C_4$	$C_5$
$H_{1/3}$	0.028	0.52	4.2	0.92	0.32
$H_{ m max}$	0.036	0.63	3.8	0.92	0.35
$H_{m0}$	0.028	0.52	4.2	0.92	0.32

It should be noted that the Goda formulas were derived from the numerical results of Goda's (1975) model which may give some errors compared with the measured data. Also, the use of  $T_p$  (instead of  $T_{1/3}$  or  $T_{m-1,0}$ ) may cause the coefficients in the formula to change slightly. The predictions may be more accurate if the constants ( $C_1$ - $C_5$ ) are re-calibrated with the measured data. Moreover, because the transformation of other representative wave heights (i.e.  $H_m$ ,  $H_{rms}$  and  $H_{1/10}$ ) are in similar fashion as those of  $H_{1/3}$ ,  $H_{max}$ , and  $H_{m0}$ , it may be possible to extend the general formula [Eq. (2.20)] to compute the other representative wave heights (i.e.  $H_m$ ,  $H_{rms}$  and  $H_{1/10}$ ). The calibration of the  $C_1$ - $C_5$  for computing  $H_m$ ,  $H_{rms}$ ,  $H_{1/3}$ ,  $H_{1/10}$ ,  $H_{max}$ , and  $H_{m0}$  are carried out in the next subsection.

#### 2.5.2. Formula calibration and extension

A calibration of the general formula [Eq. (2.20)] is conducted by gradually adjusting the coefficients ( $C_1$ - $C_5$ ) in the formula until the minimum error ( $ER_{avg}$ ) between measured and computed  $H_{rep}$  is obtained. The optimum values of  $C_1$ - $C_5$  for computing the representative wave heights ( $H_m$ ,  $H_{rms}$ ,  $H_{1/3}$ ,  $H_{1/10}$ ,  $H_{max}$ , and  $H_{m0}$ ) are shown in the third to seventh columns of Table 2.4. The errors of the general formula on simulating the representative wave heights are shown in Table 2.4. The examination results from Table 2.4 can be summarized as follows.

(a) After calibration, the constants  $C_1$  and  $C_2$  in the part of wave decay in surf zone are changed significantly, while the other constants are changed slightly. The overall accuracies of the general formula for computing  $H_{1/3}$ ,  $H_{\rm max}$  and  $H_{m0}$  are improved significantly. The formula gives very good overall predictions of  $H_{1/3}$ ,  $H_{\rm max}$ , and  $H_{m0}$ . The overall errors ( $ER_{avg}$ ) of the general formula for computing  $H_{1/3}$ ,  $H_{\rm max}$ , and  $H_{m0}$  are 7.4, 8.8, and 5.9%, respectively. The general formula gives very good predictions of  $H_{1/3}$ , and  $H_{m0}$  for either small-scale or large-scale experiments, while it gives very good prediction of  $H_{\rm max}$  for only small-scale experiments. The accuracy of  $H_{\rm max}$  for large-scale experiments is much less than the others.

- (b) The general formula gives very good predictions of  $H_m$ ,  $H_{rms}$ , and  $H_{1/10}$  for either small-scale or large-scale experiments. The overall errors ( $ER_{avg}$ ) of the general formula for computing  $H_m$ ,  $H_{rms}$ , and  $H_{1/10}$  are 7.5, 7.5, and 7.3%, respectively. This shows that the general formula can be used for computing  $H_m$ ,  $H_{rms}$ , and  $H_{1/10}$ .
- (c) Overall, the general formula gives very good predictions of  $H_m$ ,  $H_{rms}$ ,  $H_{1/3}$ ,  $H_{1/10}$ ,  $H_{max}$ , and  $H_{m0}$ .

**Table 2.4** The errors ( $ER_g$  and  $ER_{avg}$ ) of the general form of Goda formulas [Eq. (2.20)] on computing  $H_m$ ,  $H_{rms}$ ,  $H_{1/3}$ ,  $H_{1/10}$ ,  $H_{max}$ , and  $H_{m0}$  for two groups of experiment scales.

$H_{rep}$	No of	Calibrated constants				E	$R_g$	$ER_{avg}$	
	cases	$C_1$	$C_2$	$C_3$	$C_4$	$C_5$	small- scale	large- scale	
$H_{\scriptscriptstyle m}$	53	0.017	0.40	4.2	0.86	0.28	6.8	8.2	7.5
$H_{rms}$	117	0.023	0.43	4.2	0.86	0.28	7.8	7.2	7.5
$H_{1/3}$	117	0.049	0.44	4.2	0.86	0.32	7.4	7.4	7.4
$H_{\scriptscriptstyle 1/10}$	114	0.062	0.45	4.2	0.86	0.32	7.0	7.6	7.3
$H_{ m max}$	117	0.076	0.45	4.2	0.86	0.32	6.6	11.0	8.8
$H_{m0}$	142	0.049	0.44	4.2	0.86	0.28	5.7	6.1	5.9

To gain an impression of overall performance of the general formula, the results of Eq. (2.20) are plotted against the measured data. Examples of computed representative wave heights transformation across-shore are shown in Figs. 2.1 to 2.4. Case numbers in Figs. 2.1 to 2.4 are kept to be the same as the originals. It can be seen from Figs. 2.1 to 2.4 that the fluctuation of measured wave heights in large-scale wave flumes is larger than that in small-scale wave flumes. The fluctuation of measured  $H_{\rm max}$  in large-scale wave flumes is the largest. The formula could not predict the fluctuation of wave height profiles. It seems to be impossible to use the simple formula for simulating the fluctuation. However, from the general tendency of computed wave heights from Figs. 2.1 to 2.4, we can judge that the formula gives reasonably well estimations of the transformation of representative wave heights in small-scale and large-scale wave flumes.

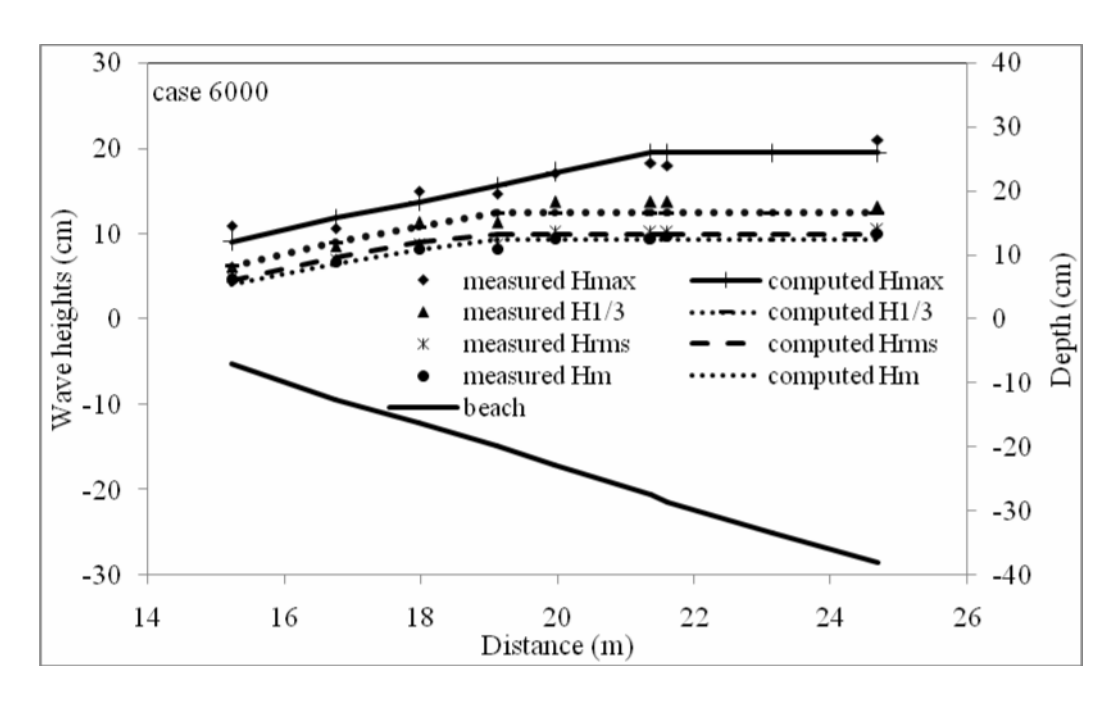


**Fig. 2.1** Example of computed and measured representative wave heights transformation (measured data from Smith and Kraus, 1990, case no. 6000).

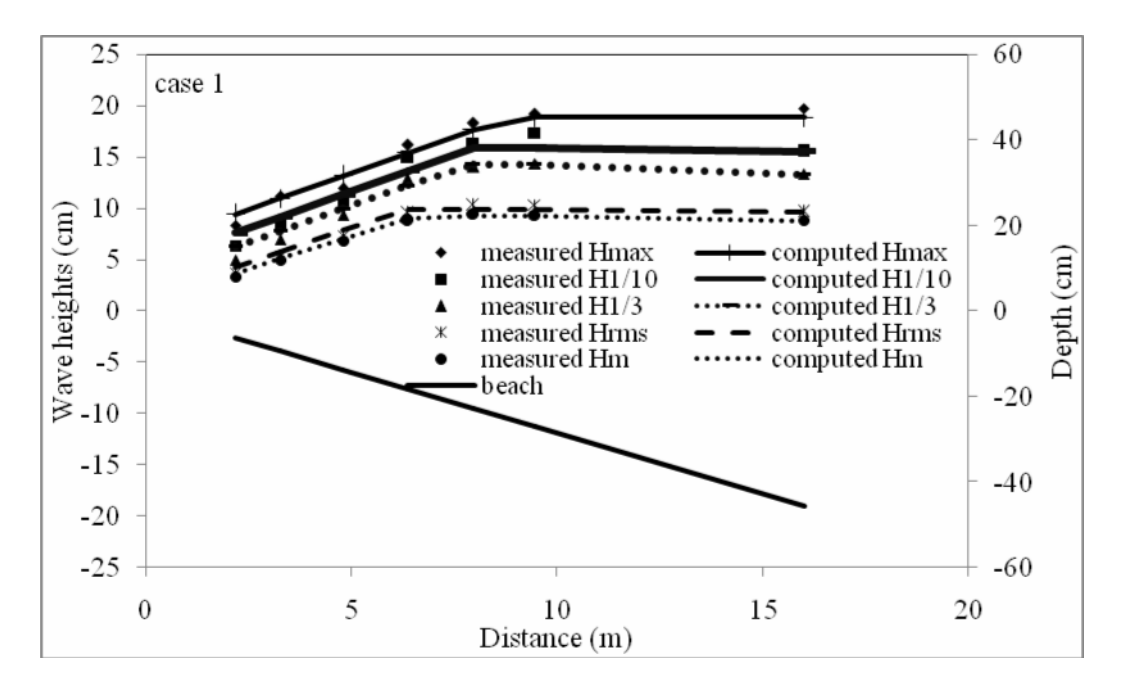


**Fig. 2.2** Example of computed and measured representative wave heights transformation (measured data from Ting, 2001, case no. 1).

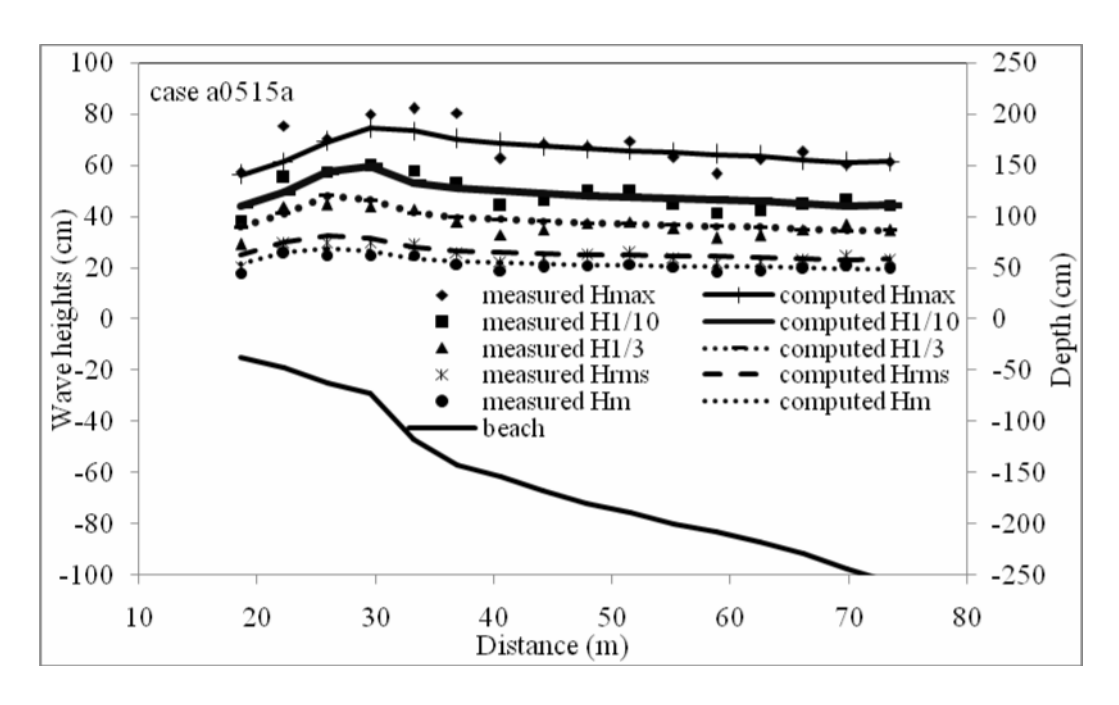


**Fig. 2.3** Example of computed and measured representative wave heights transformation (measured data from Kraus and Smith, 1994, case no. a0515a).

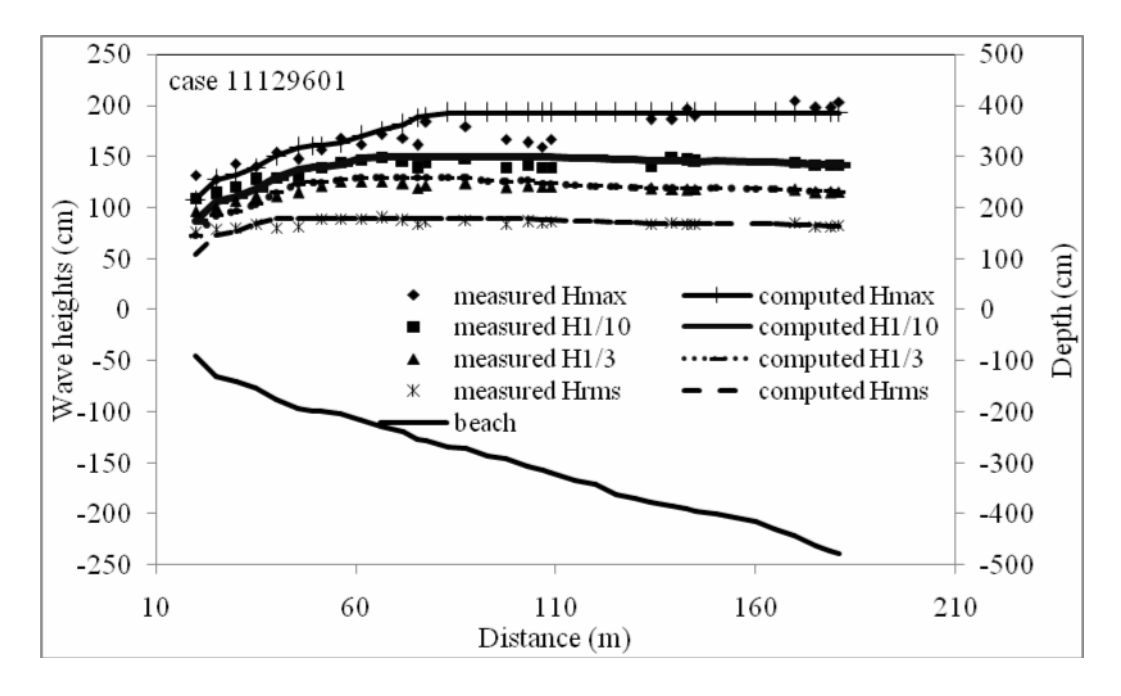


**Fig. 2.4** Example of computed and measured representative wave heights transformation (measured data from Dette et al., 1998, case no. 11129601).

# 3. TRANSFORMATION OF REPRESENTATIVE WAVE HEIGHTS USING REPRESENTATIVE WAVE APPROACH

#### 3.1. Introduction

The present chapter concentrates on the determination of six common representative wave heights, i.e. the mean wave height  $(H_m)$ , the root-mean-square wave height  $(H_{rms})$ , the significant wave height  $(H_{1/3})$ , the highest one-tenth wave height  $(H_{1/10})$ , the maximum wave height ( $H_{\rm max}$ ), and the spectral root-mean-square wave height ( $H_{\rm rmsz}$ ). The representative wave heights are the essential required factors for the study of beach deformation and the design of coastal structures. When waves propagate to the nearshore zone, wave profiles steepen and eventually waves break. Once the waves start to break, a part of wave energy is transformed into turbulence and heat, and wave height decreases towards the shore. Irregular wave breaking is more complex than regular wave breaking. In contrast to regular waves, there is no well-defined breaking position for irregular waves. The higher wave tends to break at the greater distance from the shore. Closer to the shore, more and more waves are breaking, until in the inner surf zone almost all the waves are breaking. Wave data are usually available in deepwater but not available in the shallow water at the depths required. The representative wave heights (  $H_{\rm m}$  ,  $H_{\rm rms}$  ,  $H_{\rm 1/10}$  ,  $H_{\mathrm{max}}$  , and  $H_{\mathrm{msz}}$ ) in shallow water can be determined from a wave height transformation model. Common methods to model the representative wave heights (  $H_{m}$  ,  $H_{rms}$  ,  $H_{1/3}$  ,  $H_{\rm 1/10}$ ,  $H_{\rm max}$ , and  $H_{\rm rmsz}$ ) may be classified into five approaches, i.e. empirical approach, representative wave approach, conversion approach, wave-by-wave approach, and spectral approach. The present chapter concentrates on the representative wave approach.

For the representative wave approach, the regular wave models are directly applied to irregular waves by using the representative wave heights. The approach is easy to understand and also simple to use. However, the characteristics of the irregular waves (e.g. wave height and period) are statistical variability in contrast to regular waves, which has a single height, period, and direction. As the representative wave approach does not consider such variability, the method may possibly contain a large estimation error. It seems that no literature has pointed out that the representative wave approach is applicable in the surf zone. Consequently, engineers have been reluctant to use the representative wave approach. However, the representative wave approach has the merits of easy understanding, simple application and it is not necessary to assume the shape of the pdf of wave heights. It will be useful for some practical work if this approach can be used to compute the representative wave heights in shallow water. Moreover, Rattanapitikon et al. (2003) and Rattanapitikon (2008) reported that the representative wave approach can be used to compute  $H_{rms}$  and  $H_{1/3}$  with very good accuracy. It may also be used to compute other representative wave heights (  $H_{m}$  ,  $H_{1/10}$  ,  $H_{max}$  , and  $H_{rmsz}$  ). The main objective of this study is to investigate the possibility of using the representative wave approach.

This chapter is divided into four main parts. The first part describes the collected data. The second part describes some existing regular wave models. The third part describes modeling of irregular waves using representative wave approach. The fourth part deals with the modification of the selected model.

# 3.2. Collected Experimental Data

Experimental data from 13 sources, including 1729 cases, have been collected for calibration and examination of the models. The experiments cover wide range of wave and bottom topography conditions, including small-scale, large-scale, and field experiments. A summary of the collected experimental data is given in Table 3.1.

 Table 3.1 Summary of collected experimental data for verifying representative wave

approach.

approach.			
Sources	No. of cases	Apparatus	Measured parameters
Smith and Kraus (1990)	12	small-scale	$H_m, H_{rms}, H_{1/3}, H_{max}$
Hurue (1990)	1	small-scale	$H_{1/3}$
Katayama (1991)	2	small-scale	$H_{1/3}$
Smith and Vincent (1992)	4	small-scale	H <sub>rmsz</sub>
Hamilton and Ebersole (2001)	1	small-scale	$H_{rmsz}$
Smith and Seabergh (2001)	11	small-scale	$H_m, H_{1/3}, H_{rmsz}$
Ting (2001)	1	small-scale	$H_{m}, H_{rms}, H_{1/3}, H_{1/10}, H_{max}$
Kraus and Smith (1994)	128	large-scale	$H_{m}, H_{rms}, H_{1/3}, H_{1/10}, H_{max}, H_{rmsz}$
Roelvink and Reniers (1995)	95	large-scale	H <sub>rmsz</sub>
Dette et al. (1989)	138	large-scale	$H_{rms}$ , $H_{1/3}$ , $H_{1/10}$ , $H_{max}$ , $H_{rmsz}$
Thornton and Guza (1986)	4	field	$H_{rms}$
Birkemeier et al. (1997)	745	field	$H_{rmsz}$
Herbers et al. (2006)	587	field	H <sub>rmsz</sub>
Total	1729		

The collected experimental data shown in Table 3.1 are separated into 3 groups based on experiment scale, i.e. small-scale, large-scale, and field experiments. The data cover a range of deepwater wave steepness ( $H_{so}/L_o$ , where  $H_{so}$  is the deepwater significant wave height) from 0.002 to 0.064. The examination of these independent data sources and wide range of experimental conditions are expected to clearly demonstrate the accuracy of the models. A brief description of the experiments is given below.

The experiment of Smith and Kraus (1990) was conducted to investigate the macrofeatures of wave breaking over bars and artificial reefs using a small wave flume of 45.70 m long, 0.46 m wide, and 0.91 m deep. Both regular and irregular waves were employed in this experiment. A total of 12 cases were performed for irregular wave tests. Three irregular wave conditions were generated for three bar configurations as well as for a plane beach. A JONSWAP (Hasselmann et al., 1973) computer signal was generated for spectral width parameter of 3.3 and spectral peak periods of 1.07, 1.56, and 1.75 s with significant wave heights of 0.12, 0.15, and 0.14 m respectively. Water surface elevations were measured at eight cross-shore locations using resistance-type gages.

The experiment of Ting (2001) was conducted to study wave and turbulence velocities in a broad-banded irregular wave surf zone. The experiment was performed in a small-scale wave flume, which was 37 m long, 0.91 m wide and 1.22 m deep. A false

bottom with 1/35 slope built of marine plywood was installed in the flume to create a plane beach. The irregular waves were developed from the TMA spectrum (Bouws et al., 1985), with a spectral peak period of 2.0 s, a spectrally based significant wave height of 0.15 m and spectral width parameter of 3.3. Water surface elevations were measured at seven cross-shore locations using a resistance-type gage.

The SUPERTANK laboratory data collection project (Kraus and Smith, 1994) was conducted to investigate cross-shore hydrodynamic and sediment transport processes from August 5 to September 13, 1992 at Oregon State University, Corvallis, Oregon, USA. A 76-m-long sandy beach was constructed in a large wave tank of 104 m long, 3.7 m wide, and 4.6 m deep. Wave conditions included both regular and irregular waves. In all, 20 major tests were performed, and each major test consisted of several cases. Most of the tests (14 major tests) were performed under the irregular wave actions. The wave conditions were designed to balance the need for repetition of wave conditions to move the beach profile toward equilibrium and development of a variety of conditions for hydrodynamic studies. The TMA spectral shape (Bouws et al., 1985) was used to design all irregular wave tests. The collected experiments for irregular waves included 128 cases of wave and beach conditions (a total of 2047 wave records), covering incident significant wave heights from 0.2 m to 1.0 m, spectral peak periods from 3.0 sec to 10.0 sec, and spectral width parameter between 3.3 (broad-banded) and 100 (narrow-banded). Sixteen resistance-type gages were used to measure water surface elevations across shore.

SAFE Project (Dette et al., 1998) was carried out to improve the methods of design and performance assessment of beach nourishment. The SAFE Project consisted of four activities, one of which was to perform experiments in a large-scale wave flume in Hannover, Germany. A 250-m-long sandy beach was constructed in a large wave tank of 300 m long, 5 m wide and 7 m deep. The test program was divided into two major phases. The first phase (cases A, B, C, and H) was aimed to study the beach deformation of equilibrium profile with different beach slope changes. The equilibrium beach profile was adopted from the Bruun (1954)'s approach ( $h = 0.12x^{2/3}$ ). In the second phase, the sediment transport behaviors of dunes with and without structural aid were investigated (cases D, E, F, and G). The TMA spectral shape (Bouws et al., 1985) was used to design all irregular wave tests. The tests were performed under normal wave conditions ( $H_{so}/L_o$ = 0.010, water depth in the horizontal section = 4.0 m) and storm wave conditions (  $H_{so}/L_{o}$  = 0.018, water depth in the horizontal section = 5.0 m). A total of 27 wave gages was installed over a length of 175 m along one wall of the flume. The collected experiments included 138 cases of wave and beach conditions, covering deepwater wave steepness  $(H_{so}/L_a)$  from 0.010 to 0.018.

# 3.3. Regular Wave Model

Common equation for computing regular wave height transformation across-shore is the energy flux balance equation. It is:

$$\frac{\partial \left(Ec_g \cos \theta\right)}{\partial x} = -D_B \tag{3.1}$$

where E is the wave energy density,  $c_g$  is the group velocity,  $\theta$  is the mean wave angle, x is the distance in cross shore direction, and  $D_B$  is the energy dissipation rate due to wave breaking which is zero outside the surf zone. The energy dissipation rate due to

bottom friction is neglected. In the present study, all variables are based on the linear wave theory. Snell's law is employed to describe wave refraction.

$$\frac{\sin \theta}{c}$$
 = constant (3.2)

where c is the phase velocity.

From the linear wave theory, the wave energy density (E) is equal to  $\rho gH^2/8$ , where H is the wave height. Therefore, Eq. (3.1) can be written in terms of wave height as:

$$\frac{\rho g}{8} \frac{\partial \left(H^2 c_g \cos \theta\right)}{\partial x} = -D_B \tag{3.3}$$

The wave height transformation can be computed from the energy flux balance equation [Eq. (3.3)] by substituting the model of energy dissipation rate ( $D_B$ ) and numerically integrating from offshore to shoreline. In the offshore zone, the energy dissipation rate is set to zero. The main difficulty of Eq. (3.3) is how to formulate the energy dissipation rate caused by the breaking waves. During the past decades, various models have been developed for computing the energy dissipation of regular wave breaking. Widely used concepts for computing energy dissipation rate  $(D_R)$  for regular wave breaking are the bore concept and the stable energy concept.

The bore concept is based on the similarity between the breaking wave and the hydraulic jump. Several models have been proposed based on slightly different assumptions on the conversion from energy dissipation of hydraulic jump to energy dissipation of a breaking wave. Some existing  $D_R$  models, which were developed based on the bore concept, are listed below.

a) Battjes and Janssen (1978): 
$$D_B = 0.47 \frac{\rho g H^2}{4T}$$
 (3.4)

b) Thornton and Guza (1983): 
$$D_B = 0.67 \frac{\rho g H^3}{4Th}$$
 (3.5)

b) Thornton and Guza (1983): 
$$D_B = 0.67 \frac{\rho g H^3}{4Th}$$
 (3.5)  
c) Deigaard et al. (1991):  $D_B = 0.48 \frac{\rho g h H^3}{T(4h^2 - H^2)}$  (3.6)

where h is the water depth, and T is the wave period. The constants in the above models were calibrated by Rattanapitikon et al. (2003) based on a wide range of experimental conditions.

The stable energy concept was introduced by Dally et al. (1985) based on an analysis of the measured breaking wave height on horizontal slope of Horikawa and Kuo (1966). When a breaking wave enters an area with horizontal bed, the breaking continues (the wave height decreases) until some stable wave height is attained. The development of the stable energy concept was based on an observation of stable wave height on horizontal slope. Dally et al. (1985) assumed that the energy dissipation rate was proportional to the difference between the local energy flux per unit depth and the stable energy flux per unit depth. Several models have been proposed on the basis of this concept. The main difference is the formula for computing the stable wave height (for more detail, please see Rattanapitikon et al., 2003). Some existing  $D_B$  models, which were developed based on the stable energy concept, are listed as follows.

a) Dally et al. (1985): 
$$D_B = 0.15 \frac{\rho g c_g}{8h} \left[ H^2 - (0.4h)^2 \right]$$
 (3.7)

b) Rattanapitikon and Shibayama (1998):

$$D_{B} = 0.15 \frac{\rho gc}{8h} \left\{ H^{2} - \left[ h \exp\left(-0.36 - \frac{1.25h}{\sqrt{LH}}\right) \right]^{2} \right\}$$
 (3.8)

c) Rattanapitikon et al. (2003): 
$$D_B = 0.15 \frac{\rho g c_g}{8h} (H^2 - 0.27 H_b^2)$$
 (3.9)

d) Rattanapitikon (2008): 
$$D_B = \frac{\rho g H^2 c_g}{8h} \left[ 0.010 \left( \frac{H_b}{H} \right)^2 - 0.128 \left( \frac{H_b}{H} \right) + 0.226 \right]$$
 (3.10)

in which the breaker height  $H_b$  is determined from the formula of Miche (1944) as:

$$H_b = 0.14L \tanh(kh) \tag{3.11}$$

where L is the local wavelength, and k is the local wave number. The second terms on the right hand side of Eqs. (3.7) to (3.10) are the terms of stable wave height. The energy dissipation will be zero if the wave height is less than the stable wave height.

# 3.4. Irregular Wave Model

For the representative wave approach, the energy flux of the representative wave represents the average energy flux of an irregular wave train. The governing equation (energy flux conservation) of the representative wave ( $H_{rms}$ ) can be derived based on the assumptions of linear wave theory and Rayleigh distribution of wave heights (for more detail, please see e.g. Larson, 1995). Although the crude assumptions of the representative wave approach may not be theoretically justified (mainly because of the nonlinearity of each individual wave), the approach is physical validity (the prediction agrees well with actual measurements). There are many wave models that are successful in using the energy flux conservation of the representative wave ( $H_{rms}$ ) for computing the transformation of  $H_{rms}$  across-shore, e.g. the models of Battjess and Janssen (1978), Thornton and Guza (1983), Larson (1995), Baldock et al. (1998), Ruessink et al. (2003), and Rattanapitikon (2007). If the energy flux conservation of  $H_{rms}$  is valid, the energy flux conservation of  $H_{s}$  should also be valid; because  $H_{rms}$  can be converted to  $H_{s}$  through the known coefficient (i.e.  $H_{s} = 1.42H_{rms}$  for the Rayleigh distribution).

In the present study, for the significant wave representation method, the regular wave model is applied directly to irregular waves by using the significant wave height  $(H_s)$  and the spectral peak period  $(T_p)$ . The spectral peak period is used because it is the most commonly used parameter and typically reported for the irregular wave data. Since the  $D_B$  formulas shown in Sec. 3.3 [Eqs. (3.7) to (3.10)] were developed for regular waves, it is not clear which formula is suitable for the significant wave representation method. Therefore, all of them were used to investigate the possibility of simulating the significant wave height transformation.

Similar to the regular wave model, the irregular wave model based on representative wave approach can be computed from the energy flux conservation as:

$$\frac{\rho g}{8} \frac{\partial \left(H_{rep}^2 c_g \cos \alpha\right)}{\partial x} = -D_B \tag{3.12}$$

where  $H_{rep}$  is the representative wave heights, i.e. mean wave height  $(H_m)$ , root-mean-square wave height  $(H_{rms})$ , significant wave height or highest one-third wave height

 $(H_{1/3})$ , highest one-tenth wave height  $(H_{1/10})$ , maximum wave height  $(H_{max})$ , and spectral root-mean-square wave height  $(H_{max})$ .

Since the highest wave in irregular wave train tends to break at the greatest distance from shore, the initiation of surf zone of irregular waves tend to occur at greater distance from shore than that of regular waves. Therefore, the use of regular wave model may give considerable errors in the surf zone. To overcome this problem, the coefficient of breaker height formula for regular waves may have to be reduced when applying to model irregular waves.

Applying regular wave dissipation models [Eqs. (3.7) - (3.10)] for representative wave height ( $H_{rep}$ ) and spectral peak period ( $T_p$ ), the dissipation models for irregular wave breaking can be expressed as:

model (1): 
$$D_{B} = K_{1} \frac{\rho g H_{rep}^{2}}{4T_{p}}$$
 (3.13)

model (2): 
$$D_{B} = K_{2} \frac{\rho g H_{rep}^{3}}{4T_{n}h}$$
 (3.14)

model (3): 
$$D_{B} = K_{3} \frac{\rho g h H_{rep}^{3}}{T_{p} (4h^{2} - H_{rep}^{2})}$$
 (3.15)

model (4): 
$$D_{B} = K_{4} \frac{\rho g c_{g}}{8h} \left[ H_{rep}^{2} - (K_{5}h)^{2} \right]$$
 (3.16)

model (5): 
$$D_{B} = K_{6} \frac{\rho gc}{8h} \left[ H_{rep}^{2} - \left( K_{7} h \exp \left( -0.36 - 1.25 \frac{h}{\sqrt{LH_{rep}}} \right) \right)^{2} \right]$$
(3.17)

model (6): 
$$D_{B} = K_{8} \frac{\rho g c_{g}}{8h} \left\{ H_{rep}^{2} - \left[ K_{9} L \tanh(kh) \right]^{2} \right\}$$
 (3.18)

model (7): 
$$D_{B} = \frac{\rho g H_{rep}^{2} c_{g}}{8h} \left[ K_{10} \left( \frac{H_{b}}{H_{rep}} \right)^{2} - K_{11} \left( \frac{H_{b}}{H_{rep}} \right) + K_{12} \right]$$
(3.19)

where  $K_1$ - $K_{12}$  are constants. It can be seen from Eqs. (3.7) - (3.10) that the coefficients  $K_1$ - $K_{12}$  for the regular wave models are 0.47, 0.67, 0.48, 0.15, 0.4, 0.15, 1.0, 0.15, 0.073, 0.010, 0.128, and 0.226, respectively. When applying to the irregular wave,  $K_1$ - $K_{12}$  are the adjustable coefficients to allow for the effect of the transformation to irregular waves. Hereafter, Eqs. (3.13) - (3.19) are referred to as MD1, MD2, MD3, MD4, MD5, MD6, and MD7, respectively. The variables  $c_g$ , c, L, and k in the models MD1-MD7 are calculated based on the peak spectral wave period ( $T_p$ ).

When waves propagate toward a shore, the wave profile steepens and then eventually breaks. Once the wave starts to break, energy flux is dissipated to turbulence and causes a decrease in wave energy and wave height towards the shore. Hence, the primary task is to consider the point where the wave starts to break (incipient wave breaking). The incipient wave breaking is used in an effort to provide the starting point to include the energy dissipation rate ( $D_B$ ) in the equation of energy flux conservation. In the present study, the formula of Miche (1944) is selected for inclusion into the irregular wave model. However, the Miche's (1944) formula was developed for regular wave breaking. It

is necessary to modify before applying to irregular wave model. For using in the representative wave approach, the Miche's (1944) formula is modified to be:

$$H_{rep,b} = K_{13}L \tanh(kh) \tag{3.20}$$

where  $K_{13}$  is constant. The energy dissipation ( $D_B$ ) of models MD1-MD7 occur when  $H_{rep} \geq H_{rep,b}$  and is equal to zero when  $H_{rep} < H_{rep,b}$ .

## 3.4.1. Model calibration and examination

The objective of this section is to calibrate and test the applicability of models MD1-MD7. All collected data shown in Table 3.1 are used to calibrate and examine the models. The collected experimental data shown in Table 3.1 are separated into 3 groups based on experiment scale, i.e. small-scale, large-scale, and field experiments. The examination is performed for all collected data shown in Table 3.1. The examination of these independent data sources and wide range of experimental conditions are expected to clearly demonstrate the accuracy of the models.

The basic parameter for determination of the overall accuracy of the model is the average rms relative error ( $ER_{avg}$ ), which is defined as:

$$ER_{avg} = \frac{\sum_{n=1}^{m} ER_{gn}}{tn}$$
(3.21)

where n is the data group number,  $ER_{gn}$  is the rms relative error of the group no. n, and tn is the total number of data group. The small value of  $ER_{avg}$  indicates good overall accuracy of the wave model.

The rms relative error of each data group ( $ER_g$ ) is defined as:

$$ER_{g} = 100 \sqrt{\frac{\sum_{i=1}^{nc} (H_{ci} - H_{mi})^{2}}{\sum_{i=1}^{nc} H_{mi}^{2}}}$$
(3.22)

where i is the wave height number,  $H_{ci}$  is the computed representative wave height of number i,  $H_{mi}$  is the measured representative wave height of number i, and nc is the total number of measured significant wave heights in each data group.

The question of how good a model is usually defined in a qualitative ranking (e.g. excellent, very good, good, fair, and poor). As the error of some existing irregular wave models is in the range of 7 to 21% (please see Table 5 of Rattanapitikon, 2007), the qualification of error ranges of an irregular wave model may be classify into five ranges [i.e. excellent ( $ER_g < 5.0\%$ ), very good ( $5.0 \le ER_g < 10.0\%$ ), good ( $10.0 \le ER_g < 15.0\%$ ), fair ( $15.0 \le ER_g < 20.0\%$ ), and poor ( $ER_g \ge 20.0\%$ )] and the acceptable error should be less than 10.0%.

The transformation of each representative wave height is determined by substituting each dissipation model (MD1 - MD7) into Eq. (3.12) and replacing  $H_{rep}$  by each representative wave height ( $H_m$ ,  $H_{rms}$ ,  $H_{1/3}$ ,  $H_{1/10}$ ,  $H_{max}$ , and  $H_{rmsz}$ ) after that take numerical integration from offshore to shoreline. The energy dissipation is set to be zero in the offshore zone. The incipient wave breaking is computed from Eq. (3.20). The

backward finite difference scheme is used to solve the differential equations. The grid length ( $\Delta x$ ) is set to be equal to the length between the point of measured wave height, except if  $\Delta x > 5$ m,  $\Delta x$  is set to be 5 m. The length steps ( $\Delta x$ ) used in the present study are 0.2 - 1.5 m for small-scale experiments and 2.1 - 5.0 m for large-scale and field experiments.

A calibration of each model is conducted by varying the coefficients ( $K_1$ - $K_{13}$ ) in the model until the minimum error ( $ER_{avg}$ ) between measured and computed representative wave heights is obtained. The optimum values of  $K_1$ - $K_{13}$  are shown in Table 3.2. The errors of models MD1-MD7 on simulating  $H_{rep}$  are shown in Table 3.3. The results from Table 3.3 can be summarized in the following points:

- (a) Overall, the stable energy concept gives a better prediction than the bore concept.
- (b) The accuracy of models for small-scale wave flume in descending order are MD7, MD6, MD4, MD5, MD2, MD3, and MD1.
- (c) The accuracy of models for large-scale wave flume in descending order are MD7, MD6, MD5, MD4, MD2, MD1, and MD3.
- (d) The accuracy of models for field experiment in descending order are MD4, MD6, MD7, MD5, MD3, MD2, and MD1.
- (e) The overall accuracy of the models in descending order are MD7, MD6, MD4, MD5, MD2, MD1, and MD3. The models that can be used for computing the irregular wave height transformation are MD4 to MD7.
- (f) The average error  $ER_{avg}$  of the best model (MD7) is 7.9 %. This number confirms in a quantitative sense the high degree of realism processed by the model. This means that the representative wave approach is acceptable to use for computing the irregular wave height transformation.

**Table 3.2** The calibrated constants of models MD1-MD7 for  $H_m$ ,  $H_{rms}$ ,  $H_{1/3}$ ,  $H_{1/10}$ ,  $H_{\rm max}$ , and  $H_{rmsz}$ .

Models	Constants	$H_{\scriptscriptstyle m}$	$H_{rms}$	$H_{1/3}$	$H_{\scriptscriptstyle 1/10}$	$H_{ m max}$	$H_{rmsz}$
MD1	$K_1$	0.32	0.35	0.35	0.36	0.33	0.27
	<b>K</b> <sub>13</sub>	0.066	0.070	0.097	0.110	0.140	0.058
MD2	$K_2$	0.62	0.60	0.53	0.45	0.44	0.63
	<b>K</b> <sub>13</sub>	0.066	0.070	0.097	0.110	0.140	0.058
MD3	$K_3$	0.67	0.61	0.40	0.38	0.37	0.61
	<i>K</i> <sub>13</sub>	0.066	0.070	0.097	0.110	0.140	0.058
MD4	$K_4$	0.09	0.09	0.09	0.09	0.09	0.09
	$K_5$	0.28	0.31	0.42	0.54	0.51	0.30
	K <sub>13</sub>	0.052	0.055	0.076	0.089	0.095	0.051
MD5	$K_6$	0.09	0.09	0.09	0.09	0.09	0.09
	$K_7$	0.81	0.79	1.04	1.15	1.24	0.75
	<i>K</i> <sub>13</sub>	0.052	0.055	0.076	0.089	0.095	0.051
MD6	$K_8$	0.09	0.09	0.09	0.09	0.09	0.09
	$K_9$	0.052	0.055	0.076	0.089	0.095	0.051
	<i>K</i> <sub>13</sub>	0.052	0.055	0.076	0.089	0.095	0.051
MD7	$K_{10}$	0.095	0.095	0.095	0.095	0.095	0.095
	K <sub>11</sub>	0.263	0.263	0.263	0.263	0.263	0.263
	K <sub>12</sub>	0.179	0.179	0.179	0.179	0.179	0.179
	<b>K</b> <sub>13</sub>	0.052	0.055	0.076	0.089	0.095	0.051

**Table 3.3** The errors  $ER_g$  of the models MD1-MD7 for computing  $H_m$ ,  $H_{rms}$ ,  $H_{1/3}$ ,  $H_{1/10}$ ,  $H_{\rm max}$ , and  $H_{rmsz}$ .

Apparatus	Models	$H_{\scriptscriptstyle m}$	$H_{rms}$	$H_{1/3}$	$H_{1/10}$	$H_{\mathrm{max}}$	$H_{rmsz}$	Avg.
Small-scale	MD1	14.2	15.0	13.5	4.9	18.0	16.4	13.7
	MD2	11.6	11.1	12.2	4.4	16.4	12.2	11.3
	MD3	12.6	11.1	10.0	4.3	32.0	12.0	13.7
	MD4	11.0	11.3	11.6	4.0	12.3	6.3	9.4
	MD5	9.8	11.7	9.9	4.2	10.3	12.1	9.7
	MD6	9.1	9.2	9.1	4.2	10.3	8.4	8.4
	MD7	8.0	7.9	8.2	4.0	9.4	8.8	7.7
Large-scale	MD1	11.3	8.3	8.1	8.5	15.9	11.7	10.6
	MD2	10.3	7.3	6.4	7.4	14.3	10.0	9.3
	MD3	9.6	6.8	6.7	7.7	24.7	9.6	10.8
	MD4	8.3	7.9	7.1	7.3	12.9	7.5	8.5
	MD5	9.6	6.8	5.6	6.5	11.0	8.1	7.9
	MD6	8.4	6.9	5.8	6.7	11.8	7.5	7.8
	MD7	8.2	6.8	5.7	6.4	11.0	6.6	7.5
Field	MD1	-	30.5	-	-	-	17.8	24.1
	MD2	-	29.5	-	-	-	15.5	22.5
	MD3	-	27.5	-	-	-	15.0	21.2
	MD4	-	8.4	-	-	-	9.7	9.1
	MD5	-	17.7	-	-	-	12.1	14.9
	MD6	-	10.4	-	-	-	9.9	10.1
	MD7	-	11.0	-	-	-	9.5	10.3
All-scales	MD1	12.8	17.9	10.8	6.7	16.9	15.3	13.4
	MD2	11.0	16.0	9.3	5.9	15.3	12.5	11.7
	MD3	11.1	15.1	8.4	6.0	28.4	12.2	13.5
	MD4	9.7	9.2	9.4	5.6	12.6	7.8	9.1
	MD5	9.7	12.1	7.7	5.3	10.7	10.8	9.4
	MD6	8.7	8.8	7.5	5.5	11.0	8.6	8.4
	MD7	8.1	8.6	6.9	5.2	10.2	8.3	7.9

# 4. TRANSFORMATION OF REPRESENTATIVE WAVE HEIGHTS USING CONVERSION APPROACH

## 4.1. Introduction

The representative wave heights [e.g. the mean wave height ( $H_m$ ), the root-mean-square wave height ( $H_{rms}$ ), the significant wave height ( $H_{1/10}$ ), the highest one-tenth wave height ( $H_{1/10}$ ), the maximum wave height ( $H_{max}$ ), and the spectral significant wave height ( $H_{m0}$ )] are the essential required factors for the study of beach deformation and the design of coastal structures. The wave heights are usually available in deepwater but not available at the depths required in shallow water. The wave heights in shallow water can be determined from wave models. Common methods to model the representative wave heights transformation may be classified into five main approaches, i.e. wave-by-wave approach, spectral approach, conversion approach, representative wave approach, and empirical approach. This chapter focuses on the conversion approach.

The conversion approach is used to convert the representative wave heights from one to another through the known relationships. The root-mean-square wave height  $(H_{rms})$  is usually used as a reference wave height of the conversion because it is the output of many wave models (e.g. the models of Battjes and Janssen, 1978; Thornton and Guza, 1983; Larson, 1995; and Rattanapitikon, 2007). Therefore, the other representative wave heights can be determined from the known relationships between the representative wave heights (e.g. the relationships of Longuet-Higgins, 1952; Battjes and Groenendijk, 2000; and Rattanapitikon and Shibayama, 2007). Hence, the conversion approach is a combination of wave model for computing  $H_{rms}$  and the relationships between  $H_{rms}$  and other representative wave heights  $(H_m, H_{1/3}, H_{1/10}, \text{ and } H_{\text{max}})$ . However, there are two approaches to describe the root-mean-square (rms) wave height, i.e. statistical approach and spectral approach. Therefore, the rms wave height can be classified according to its definition based to be statistical-based rms wave height ( $H_{rms}$ ) and spectral-based rmswave height  $(H_{rmsz})$ . These two definitions of rms wave height are usually assumed to be equal. However, it was shown by many researchers (e.g. Thompson and Vincent, 1985; and Battjes and Groenendijk, 2000) that the rms wave heights derived from the two definitions are significantly difference in the surf zone. Hence the conversion approach consists of four parts, i.e. the wave models for computing the transformation of  $H_{m0}$ [which can be converted to zeroth moment of wave spectrum  $(m_0)$  through the known constant], the wave models for computing the transformation of  $H_{rms}$ , the conversion formulas for converting from  $H_{rms}$  to other representative wave heights (i.e.  $H_m$ ,  $H_{1/3}$ ,  $H_{1/10}$  , and  $H_{
m max}$  ), and the conversion formulas for converting from  $\it m_0$  to other representative wave heights (i.e.  $H_m$ ,  $H_{rms}$ ,  $H_{1/3}$ ,  $H_{1/10}$ , and  $H_{max}$ ). Hence the conversion model should be constructed based on the best model (or formulas) from each part.

During the past decades, various wave models have been proposed for computing  $H_{rms}$  and  $H_{rmsz}$  (or  $H_{m0}$ ) and several formulas have been proposed to convert from  $H_{rms}$  to other representative wave heights and to convert from  $H_{m0}$  (or  $m_0$ ) to other representative wave heights. It is not clear which wave model and conversion formulas are

the most suitable for computing the representative wave heights (i.e.  $H_m$ ,  $H_{rms}$ ,  $H_{1/3}$ ,  $H_{1/10}$ ,  $H_{max}$ , and  $H_{m0}$ . The main objective of this chapter is to find out the suitable wave models and conversion formulas that predict well for a wide range of experimental conditions.

This chapter is divided into four main parts. The first part describes the wave models for computing the transformation of  $H_{m0}$  which can be converted to  $H_{rmsz}$  (or  $m_0$ ) through the known constant. The second part describes the wave models for computing the transformation of  $H_{rms}$ . The third part describes the conversion formulas for converting from  $H_{rms}$  to  $H_m$ ,  $H_{1/3}$ ,  $H_{1/10}$ , and  $H_{max}$ . The fourth part describes the conversion formulas for converting from  $m_0$  to  $m_0$  to  $m_0$ ,  $m_0$ ,

# 4.2. Transformation of Spectral-Based Wave Heights

Representative wave heights are the essential required factors for many coastal engineering applications such as the design of coastal structures and the study of beach deformations. Among various representative wave heights, the significant wave height ( $H_s$ ) is most frequently used in the field of coastal engineering (Goda, 2000). There are two main methods to describe the significant wave height, i.e. statistical analysis (or individual wave analysis) and spectral analysis. The statistical-based significant wave height ( $H_{1/3}$ ) is defined as the average height of the highest one-third of the individual waves in a record, while the spectral significant wave height ( $H_{m0}$ ) is defined as four times of square root of zero moment of wave spectrum ( $H_{m0} = 4.0 \sqrt{m_0}$ ). These two definitions of significant wave height are equal if the wave height distribution obeys a Rayleigh distribution.

In deepwater, the measured wave heights from different oceans have been found to closely conform to the Rayleigh distribution (Demerbilek and Vincent, 2006). The relationship  $H_{1/3} = H_{m0} = 4.0 \sqrt{m_0}$  can be derived based on the assumption of a Rayleigh distribution. The relationship has been confirmed by many wave observation data taken throughout the world (Goda, 2000). However, the proportional constants are smaller than those derived from the Rayleigh distribution, e.g. the ratio  $H_{1/3} / \sqrt{m_0}$  is approximately 3.8 instead of 4.0 (Goda, 1979). When waves propagate in shallow water, their profiles steepen and they eventually break. The process of wave breaking becomes relevant in shallow water, causing the wave height distribution to deviate from the Rayleigh distribution. Several researchers stated that the wave height distribution deviated considerably from the Rayleigh distribution (e.g. Klopman, 1996; Battjes and Groenendijk, 2000; and Mendez et al., 2004). This causes the statistical based wave height to differ from the corresponding spectral based wave height.

The two significant wave heights are both important, and neither one alone is sufficient for successful application of wave height for engineering problems (Goda, 1974). While some formulas in the coastal works are appropriate for  $H_{1/3}$ , others may be more appropriate for  $H_{m0}$ . The spectral wave heights ( $H_{m0}$ ) should be used in those applications where the effect of average wave energy is more important than the individual waves.

The wave heights are usually available in deepwater (from measurements or wave hindcasts) but not available at the required depths in shallow water. The wave height at

desired depth can be determined from a wave model. During the past few decades, many wave models have been proposed but most of them are for computing the root-mean-square wave heights ( $H_{rms}$ ), not for  $H_{m0}$ . However, measured ocean wave records are often analyzed spectrally by the instrument package and expressed in terms of  $H_{m0}$ . Similarly, modern wave hindcasts are often expressed in terms of  $H_{m0}$ . It seems to be convenient for engineers to have a wave height transformation model for computing the transformation of  $H_{m0}$  directly. Therefore, the present study concentrates on a wave height transformation model for computing the transformation model for computing the transformation of  $H_{m0}$ .

In this section, the transformation of  $H_{m0}$  is computed from the energy flux conservation equation. The main difficulty of modeling the wave height transformation is how to formulate the rate of dissipation due to wave breaking. Various dissipation models have been proposed by many researchers but most of them were proposed for computing  $H_{rms}$ . Therefore, the existing dissipation models have to be converted to be expressed in terms of  $H_{m0}$  before applying to compute the transformation of  $H_{m0}$ . Similar to the significant wave height, the root-mean-square wave height can be classified according to its definition based to be statistical-based root-mean-square wave height  $(H_{rms})$  and spectral-based root-mean-square wave height ( $H_{msz} = \sqrt{8m_0}$ ). If an energy dissipation model is proposed in terms of  $H_{rms}$ , it seems to be difficult to convert the model to be expressed in terms of  $H_{m0}$ . However, if an energy dissipation model is proposed in terms of  $H_{rmsz}$ , it can be converted to be expressed in terms of  $H_{m0}$  easily (because  $H_{m0} = \sqrt{2}H_{rmsz}$ ). Unfortunately, most existing models were developed without regard for the difference between  $H_{rms}$  and  $H_{rmsz}$ . Moreover, it is not clear which model is the most suitable one for computing  $H_{m0}$ . The main objectives of this section are to apply the existing dissipation models of root-mean-square wave height to compute the transformation of  $H_{m0}$  and to find out the most suitable model for computing  $H_{m0}$ .

## 4.2.1. Compiled experimental data

Experimental data on  $H_{m0}$  transformation from 8 sources, including 1,713 cases, have been compiled to examine the models. A summary of the compiled experimental data is given in Table 4.1. The experiments cover a wide range of wave and beach conditions, including small- and large-scale laboratory and field experiments. The experiments of Smith and Vincent (1992), Hamilton and Ebersole (2001), and Smith and Seabergh (2001) were performed under fixed bed conditions, while the others were performed under moveable bed (sandy beach) conditions. Only the data in the nearshore zone (excluding swash zone) are considered in this study. The data cover a range of deepwater wave steepness ( $H_{m0,0}/L_0$ ) from 0.001 to 0.069.

Table 4.1 Summary of compiled experimental data on  $H_{m0}$ .

Sources	No. of	No. of	Apparatus	Deepwater
	cases	data		wave steepness
		points		$(H_{m0,0}/L_0)$
Smith and Vincent (1992)	4	36	small-scale	0.032-0.064
Hamilton and Ebersole (2001)	1	10	small-scale	0.023
Smith and Seabergh (2001)	15	180	small-scale	0.007-0.069
SUPERTANK project	128	2,047	large-scale	0.002-0.064
LIP IID project	95	923	large-scale	0.005-0.039
SAFE project	138	3,557	large-scale	0.009-0.021
DELILAH project	745	5,049	field	0.001-0.036
DUCK94 project	587	6,104	field	0.001-0.041
Total	1,713	17,906		0.001-0.069

A brief summary of the compiled data is provided below.

The experiment of Smith and Vincent (1992) was conducted to investigate shoaling and decay of multiple wave trains using a small wave flume of 45.7 m long, 0.45 m wide, and 0.9 m deep. The bottom of the flume is smooth concrete and rises at a slope of 1:30 from the middle of the flume. Twelve double-peaked spectra were generated by superimposing two spectra of the TMA type (Bouws et al., 1985) with a spectral width parameter of 20. The cases include two double-peak wave period combinations ( $T_p = 2.5 \text{ s/}1.25 \text{ s}$  and 2.5 s/1.75 s) with two total wave heights ( $H_{m0} = 15.2 \text{ cm}$  and 9.2 cm). The four most energetic cases (i.e. cases 1, 3, 7, and 9) and the dominant peak periods were used in the present study. Water surface elevations were measured at nine cross-shore locations using electrical-resistance gages. The significant wave heights were determined from water surface elevations in the frequency band 0.1 to 2.5 Hz.

The experiment of Hamilton and Ebersole (2001) was conducted to establish uniform longshore currents in a wave basin, which has dimensions of 30 m cross-shore, 50 m longshore, and 1.4 m deep. A concrete beach with 1/30 slope has a cross-shore dimension of 21 m and a longshore dimension of 31 m. The irregular waves were developed from the TMA spectrum (Bouws et al., 1985), with a significant wave height of 0.21 m, spectral peak period of 2.5 s, direction 10°, and spectral width parameter of 3.3. Water surface elevations were measured at ten cross-shore locations using capacitance-type wave gages and four other wave gages were fixed in the longshore direction near the wave generators. The significant wave heights were analyzed based on a lower cut-off frequency of 0.2 Hz.

The experiment of Smith and Seabergh (2001) was conducted to study the effect of ebb current on wave shoaling and breaking in an idealized inlet. The experiment was performed in a wave basin, which has dimensions of 99 m long, 46 m wide, and 0.6 m deep. The physical model included an offshore equilibrium slope, an elliptical ebb shoal located seaward of the inlet, rubble jetties, and a flat entrance channel. The tests were performed under the conditions of regular and irregular waves and with and without currents. Only irregular waves with no current conditions (in total 15 cases) are considered in this study. The irregular waves were developed from the TMA spectrum (Bouws et al., 1985), with significant wave heights from 0.018 to 0.079 m, wave periods from 0.7 to 1.7 s, spectral width parameter of 3.3, and incident wave direction perpendicular to the shore. Water surface elevations were measured at eleven cross-shore locations using capacitance-type gages. The significant wave heights were analyzed over the entire collected water surface elevations.

The SUPERTANK laboratory data collection project (Kraus and Smith, 1994) was conducted to investigate cross-shore hydrodynamic and sediment transport processes from August 5 to September 13, 1992 at Oregon State University, Corvallis, Oregon, USA. A 76-m-long sandy beach was constructed in a large wave tank of 104 m long, 3.7 m wide, and 4.6 m deep. Wave conditions included both regular and irregular waves. In all, 20 major tests were performed, and each major test consisted of several cases. Most of the tests (14 major tests) were performed under the irregular wave actions. The wave conditions were designed to balance the need for repetition of wave conditions to move the beach profile toward equilibrium and development of a variety of conditions for hydrodynamic studies. The TMA spectral shape (Bouws et al., 1985) was used to design all irregular wave tests. The compiled experiments for irregular waves included 128 cases of wave and beach conditions, covering incident significant wave heights from 0.2 m to 1.0 m, spectral peak periods from 3.0 sec to 10.0 sec, and spectral width parameter between 3.3 (broad-banded) and 100 (narrow-banded). Sixteen resistance-type gages were used to measure water surface elevations across shore. A 10-Hz, fifth-order anti-aliasing Bessel filter was applied to eliminate noise and avoid aliasing. The wave spectral analysis was performed on total, low-pass, and high-pass signals. The data from the total signals were used in this study.

LIP 11D Delta Flume Experiment (Roelvink and Reniers, 1995) was performed at Delft Hydraulics large-scale wave flume. A 175-m-long sandy beach was constructed in a large wave tank of 233 m long, 5 m wide and 7 m deep. The two major tests were performed, i.e., with dune (test no. 1A-1C) and without dune (test no 2A-2C). Each major test consisted of several wave conditions. The duration of each wave condition lasted about 12 to 21 hr. Initial beach profiles of tests no. 1A and 2A are equilibrium Dean-type beaches. The beach profiles of other tests (test no. 1B, 1C, 2B, 2E, and 2C) were initiated using the final profile configuration of the previous test. Broad banded random waves, JONSWAP spectrum (Hasselmann et al., 1973) with spectral width parameter of 3.3, were generated. During the run, the sand bar feature grows and becomes more pronounced after some time. Ten fixed wave gages were deployed in the flume to measure water surface elevations. To avoid aliasing, each signal was filtered by analog filter at 5 Hz before analyzing. The compiled experiments included 95 cases of wave and beach conditions, covering incident significant wave heights from 0.6 m to 1.4 m, spectral peak periods from 5 sec to 8 sec, and water level from 4.1 m to 4.6 m.

The SAFE Project (Dette et al., 1998) was carried out to improve the methods of design and performance assessment of beach nourishment. The SAFE Project consisted of four activities, one of which was to perform experiments in a large-scale wave flume in Hannover, Germany. A 250-m-long sandy beach was constructed in a large wave tank of 300 m long, 5 m wide and 7 m deep. The test program was divided into two major phases. The first phase (cases A, B, C, and H) was aimed to study the beach deformation of equilibrium profile with different beach slope changes. The equilibrium beach profile was adopted from Bruun's (1954) approach. In the second phase, the sediment transport behaviors of dunes with and without structural aid were investigated (cases D, E, F, and G). The TMA spectral shape (Bouws et al., 1985) was used to design all irregular wave tests. The tests were performed under normal wave conditions and storm wave conditions. A total of 27 wave gages was installed over a length of 175 m along one wall of the flume. The records from all gages were checked for plausibility before analysis. The compiled experiments included 138 cases of wave and beach conditions, covering incident significant wave heights from 0.65 m to 1.20 m, mean wave period of 5.5 sec, and water level from 4.0 m to 5.0 m.

DELILAH Project (Birkemeier et al., 1997) was conducted on the barred beach in Duck, North Carolina, USA in October 1990. The objective of the project is to improve fundamental understanding and modeling of surf zone physics. The experiment emphasized surf zone hydrodynamics in the presence of a changing barred bathymetry. Nine pressure gauges were installed to measure the nearshore wave heights across-shore and one of them was in the swash zone. Tidal elevations were measured at the FRF pier. The significant wave heights were determined from water surface elevations in the frequency band 0.04 to 0.4 Hz. The measured wave heights are available at http://dksrv.usace.army.mi/jg/del90dir. The data of wave heights and water depths measured during Oct 2-21, 1990 are available. The wave heights and water depths data are available at approximately every 34 min. A total of 776 sets of measured wave heights and water depths are available on the data server. A data set that has only a few points of measurements is not suitable to use for verifying the models. A total of 745 data sets are considered in this study. The incident waves (at the most offshore-ward position) cover the range of significant wave height from 0.4 m to 0.7 m, wave period from 3.4 s to 13.5 s, and direction from -36° to 2° (counter-clockwise from shore normal).

DUCK94 Project (Herbers et al., 2006) was conducted on the barred beach in Duck, North Carolina, USA during Aug - Oct 1994. The project objective is the same as that of DELILAH. The experiment emphasized surf zone hydrodynamics, sediment transport and morphological evolution. Thirteen pressure gauges were installed to measure the nearshore wave heights across-shore and one of them was in the swash zone. Tidal elevations were measured at the FRF pier. The significant wave heights were determined from water surface elevations in the frequency band 0.05 to 0.25 Hz. The measured wave heights, and water depths are available at http://dksrv.usace.army.mi/jg/dk94dir. The wave heights and water depths at every 3 h that were measured during Aug 15 – Oct 31, 1994 are used in the present study. Excluding the data sets that have only a few points of measurements, a total of 587 data sets are considered in the present study. The incident waves (at the most offshore-ward position) cover the range of significant wave height from 0.2 m to 2.6 m, wave period from 4.4 s to 11.4 s, and direction from -56° to 71° (counter-clockwise from shore normal).

## 4.2.2. Model development

When waves propagate to the nearshore zone, wave profiles steepen and eventually waves break. Once the waves start to break, a part of wave energy is transformed into turbulence and heat, and wave height decreases towards the shore. In the present study, wave height transformation is computed from the energy flux conservation equation. It is:  $\frac{\partial \left(Ec_g\cos\theta\right)}{\partial x} = -D_B$ 

$$\frac{\partial \left(Ec_g \cos \theta\right)}{\partial x} = -D_B \tag{4.1}$$

where E is the wave energy density,  $c_{\rm g}$  is the group velocity,  $\theta$  is the mean wave angle, x is the distance in cross shore direction, and  $D_B$  is the energy dissipation rate due to wave breaking which is zero outside the surf zone. The energy dissipation rate due to bottom friction is neglected. In the present study, all variables are based on the linear wave theory and the Snell's law is employed to describe wave refraction as:

$$\frac{\sin \theta}{c}$$
 = constant (4.2)

where c is the phase velocity.

For the spectral analysis, the moments of a wave spectrum are important in characterizing the spectrum and useful in relating the spectral description of waves to the significant wave height. The representative value of the total wave energy is the zero moment of wave spectrum  $(m_0)$ , which can be obtained by integrating the wave spectrum (S(f)) in the full range of frequency (f). The integral is, by definition of the wave spectrum, equal to the variance of the surface elevation (Goda, 2000). Therefore, the zero moment of the spectrum  $(m_0)$  can be expressed as:

$$m_0 = \int_0^\infty S(f)df = \frac{1}{t_n} \int_0^{t_n} \eta^2 dt$$
 (4.3)

where  $\eta$  is the water surface elevation, t is time, and  $t_n$  is the total time of the wave record.

The zero moment  $(m_0)$  can be related to the significant wave height by considering the total energy density of a wave record. From linear wave theory, the total energy density is twice the potential energy density, which can be written in terms of the surface elevation as:

$$E = 2E_p = \frac{2}{t_n} \int_0^{t_n} \frac{\rho g \, \eta^2}{2} dt = \rho g m_0 \tag{4.4}$$

where  $E_p$  is the potential energy density,  $\rho$  is the water density, and g is the acceleration due to gravity.

As the spectral significant wave height  $(H_{m0})$  is defined as  $H_{m0} = 4\sqrt{m_0}$ , the total energy density of a wave record [Eq. (4.4)] can be written in terms of  $H_{m0}$  as:

$$E = \frac{1}{16} \rho g H_{m0}^2 \tag{4.5}$$

Substituting Eq. (4.5) into Eq. (4.1), the governing equation for computing the transformation of  $H_{m0}$  can be written as:

$$\frac{\rho g}{16} \frac{\partial \left(H_{m0}^2 c_g \cos \theta\right)}{\partial x} = -D_B \tag{4.6}$$

The transformation of  $H_{m0}$  can be computed from the energy flux balance equation [Eq. (4.6)] by substituting the formula of the energy dissipation rate ( $D_B$ ) and numerically integrating from offshore to shoreline. In the offshore zone, the energy dissipation rate is set to zero. The difficulty of the energy flux conservation approach is how to formulate the energy dissipation rate caused by the breaking waves. Various dissipation models have been proposed but most of them were proposed in terms of  $H_{rms}$ . The selected existing dissipation models are described as the following.

## 4.2.2.1. Existing energy dissipation models

The first attempt at examination is to collect the existing dissipation models for computing  $H_{rms}$ . Because of the complexity of the wave breaking mechanism, most of the energy dissipation models were developed based on the empirical or semi-empirical approach calibrated with the measured data. Brief reviews of some selected existing dissipation models are described below.

(a) Battjes and Janssen (1978), hereafter referred to as BJ78, proposed to compute  $D_B$  by multiplying the fraction of irregular breaking waves ( $Q_b$ ) by the energy dissipation of a single broken wave. The energy dissipation of a broken wave is described by the bore analogy and assuming that all broken waves have a height equal to breaking wave height ( $H_b$ ). The model was proposed as:

$$D_B = K_1 Q_b \frac{\rho g H_b^2}{4T_p} \tag{4.7}$$

where  $T_p$  is the spectral peak period and  $K_1$  is the adjustable coefficient. The proposed value of  $K_1$  is 1.0. The fraction of breaking waves ( $Q_b$ ) was derived based on the assumption that the probability density function (pdf) of wave heights could be modeled with a Rayleigh distribution truncated at the breaking wave height ( $H_b$ ) and all broken waves have a height equal to the breaking wave height. The result is:

$$\frac{1 - Q_b}{-\ln Q_b} = \left(\frac{H_{rms}}{H_b}\right)^2 \tag{4.8}$$

in which the breaking wave height ( $H_b$ ) is determined from the formula of Miche (1944) with additional coefficient 0.91 as:

$$H_b = K_2 L \tanh(0.91kh) \tag{4.9}$$

where L is the wavelength related to  $T_p$ , k is the wave number, h is the mean water depth,  $K_2$  is the adjustable coefficient. The proposed value of  $K_2$  is 0.14. The  $D_B$  model of BJ78 has been used successfully in many applications (e.g. Abadie et al., 2006; Johnson, 2006; and Oliveira, 2007). As Eq. (4.8) is an implicit equation, it has to be solved for  $Q_b$  by an iteration technique, or by a 1-D look-up table (Southgate and Nairn, 1993). It can be also determined from the polynomial equation as:

$$Q_{b} = \sum_{n=0}^{7} a_{n} \left( \frac{H_{rms}}{H_{b}} \right)^{n}$$
 (4.10)

where  $a_n$  is the constant of  $n^{th}$  term. A multiple regression analysis is used to determine the constants  $a_0$  to  $a_7$ . The correlation coefficient ( $R^2$ ) of Eq. (4.10) is very close to 1 (0.99999999). The values of constants  $a_0$  to  $a_7$  are shown in Table 4.2.

**Table 4.2** Values of constants  $a_0$  to  $a_7$  for computing  $Q_b$ .

Constants	Values
$a_0$	0.2317072
$a_{1}$	-3.6095814
$a_2$	22.5948312
$a_3$	-72.5367918
$a_4$	126.8704405
$a_5$	-120.5676384
$a_6$	60.7419815
$a_7$	-12.7250603

Equation (4.10) is applicable for  $0.25 < H_{rms}/H_b < 1.0$ . For  $H_{rms}/H_b \le 0.25$ , the value of  $Q_b$  is very small and can be set at zero. The value of  $Q_b$  is set to be 1.0 when  $H_{rms}/H_b \ge 1.0$ . As Eqs. (4.8) and (4.10) give almost identical results ( $R^2 = 0.999999999$ ), for convenience, Eq. (4.10) is used in this study.

(b) Thornton and Guza (1983), hereafter referred to as TG83, proposed to compute  $D_B$  by integrating from 0 to  $\infty$  the product of the dissipation for a single broken wave and the pdf of the breaking wave height. The energy dissipation of a single broken wave is described by their bore model which is slightly different from the bore model of BJ78. The pdf of breaking wave height is expressed as a weighting of the Rayleigh distribution. By introducing two forms of the weighting, two models of  $D_B$  were proposed. After calibrating with small-scale experimental data, the models were proposed to be:

Model 1 (hereafter referred to as TG83a):

$$D_{B} = K_{3} \frac{3\sqrt{\pi}}{4} \left(\frac{H_{rms}}{H_{b}h}\right)^{4} \frac{\rho g H_{rms}^{3}}{4T_{p}h}$$
(4.11)

in which

$$H_b = K_4 h \tag{4.12}$$

Model 2 (hereafter referred to as TG83b):

$$D_{B} = K_{5} \frac{3\sqrt{\pi}}{4} \left(\frac{H_{rms}}{H_{b}}\right)^{2} \left\{ 1 - \frac{1}{\left[1 + \left(H_{rms}/H_{b}\right)^{2}\right]^{2.5}} \right\} \frac{\rho g H_{rms}^{3}}{4T_{p}h}$$
(4.13)

in which 
$$H_b = K_6 h \tag{4.14}$$

where  $K_3$  to  $K_6$  are the adjustable coefficients. The proposed values of  $K_3$  to  $K_6$  are 0.51, 0.42, 0.51 and 0.42, respectively.

(c) Battjes and Stive (1985), hereafter referred to as BS85, used the same energy dissipation model as that of BJ78.

$$D_B = K_\gamma Q_b \frac{\rho g H_b^2}{4T_p} \tag{4.15}$$

where  $K_7$  is the adjustable coefficient. The proposed value of  $K_7$  is 1.0. They modified the model of BJ78 by recalibrating the additional coefficient in the breaker height formula [Eq. (4.9)]. The coefficient was related to the deepwater wave steepness  $\left(H_{rms,0}/L_0\right)$ . After calibration with small-scale and field experiments, the breaker height formula was modified to be:

$$H_b = K_8 L \tanh \left\{ \left[ 0.57 + 0.45 \tanh \left( 33 \frac{H_{rms,0}}{L_0} \right) \right] kh \right\}$$
 (4.16)

where  $H_{rms,0}$  is the deepwater root-mean-square wave height,  $L_0$  is the deepwater wavelength, and  $K_8$  is the adjustable coefficient. The proposed value of  $K_8$  is 0.14. Hence, the model of BS85 is similar to that of BJ78 except for the formula of  $H_b$ .

(d) Southgate and Nairn (1993), hereafter referred to as SN93, modified the model of BJ78 by changing the expression of energy dissipation of a breaker height from the bore model of BJ78 to be the bore model of TG83 as:

$$D_{B} = K_{9} Q_{b} \frac{\rho g H_{b}^{3}}{4 T_{n} h} \tag{4.17}$$

where  $K_9$  is the adjustable coefficient. The proposed value of  $K_9$  is 1.0. The fraction of breaking waves  $Q_b$  is determined from Eq. (4.8). The breaker height ( $H_b$ ) is determined from the formula of Nairn (1990) as:

$$H_b = K_{10}h \left[ 0.39 + 0.56 \tanh \left( 33 \frac{H_{rms,0}}{L_0} \right) \right]$$
 (4.18)

where  $K_{10}$  is the adjustable coefficient. The proposed value of  $K_{10}$  is 1.0. Hence, the model of SN93 is similar to that of BJ78 except for the formulas of energy dissipation of a single breaker height and  $H_b$ .

(e) Baldock et al. (1998), hereafter referred to as BHV98, proposed to compute  $D_B$  by integrating from  $H_b$  to  $\infty$  the product of the energy dissipation for a broken wave and the pdf of wave heights. The energy dissipation of a broken wave is described by the bore model of BJ78. The pdf of wave heights inside the surf zone was assumed to be the Rayleigh distribution. The result is:

$$D_{B} = \begin{cases} K_{11} \exp\left[-\left(\frac{H_{b}}{H_{rms}}\right)^{2}\right] \frac{\rho g\left(H_{b}^{2} + H_{rms}^{2}\right)}{4T_{p}} & for \quad H_{rms} < H_{b} \\ K_{11} \exp\left[-1\right] \frac{2\rho gH_{b}^{2}}{4T_{p}} & for \quad H_{rms} \ge H_{b} \end{cases}$$

$$(4.19)$$

where  $K_{11}$  is the adjustable coefficient. The proposed value of  $K_{11}$  is 1.0. The breaker height  $(H_b)$  is determined from the formula of Nairn (1990) as:

$$H_b = K_{12}h \left[ 0.39 + 0.56 \tanh \left( 33 \frac{H_{rms,0}}{L_0} \right) \right]$$
 (4.20)

where  $K_{12}$  is the adjustable coefficient. The proposed value of  $K_{12}$  is 1.0.

(f) Rattanapitikon and Shibayama (1998), hereafter referred to as RS98, modified the model of BJ78 by changing the expression of energy dissipation of a single broken wave from the bore concept to the stable energy concept as:

$$D_{B} = K_{13}Q_{b} \frac{c\rho g}{8h} \left[ H_{rms}^{2} - \left( h \exp(-0.58 - 2.0 \frac{h}{\sqrt{LH_{rms}}}) \right)^{2} \right]$$
(4.21)

where  $K_{13}$  is the adjustable coefficient and the fraction of breaking wave  $(Q_b)$  is computed from Eq. (4.8). The proposed value of  $K_{13}$  is 0.10. The breaking wave height  $(H_b)$  is computed by using the breaking criteria of Goda (1970) as:

$$H_b = K_{14} L_o \left\{ 1 - \exp \left[ -1.5 \frac{\pi h}{L_o} \left( 1 + 15 m^{4/3} \right) \right] \right\}$$
 (4.22)

where m is the average bottom slope and  $K_{14}$  is the adjustable coefficient. The proposed value of  $K_{14}$  is 0.10.

(g) Ruessink et al. (2003), hereafter referred to as RWS03, used the same energy dissipation model as that of BHV98 [Eq. (4.19)] but a different breaker height formula. The breaker height formula of BJ78 [Eq. (4.9)] is modified by relating the additional coefficient with the terms kh. After calibration with field experiments, the model was proposed to be:

$$D_{B} = \begin{cases} K_{15} \exp\left[-\left(\frac{H_{b}}{H_{rms}}\right)^{2}\right] \frac{\rho g\left(H_{b}^{2} + H_{rms}^{2}\right)}{4T_{p}} & for \quad H_{rms} < H_{b} \\ K_{15} \exp\left[-1\right] \frac{2\rho gH_{b}^{2}}{4T_{p}} & for \quad H_{rms} \ge H_{b} \end{cases}$$

$$(4.23)$$

in which

$$H_b = K_{16}L \tanh[(0.86kh + 0.33)kh]$$
 (4.24)

where  $K_{15}$  and  $K_{16}$  are the adjustable coefficients. The proposed values of  $K_{15}$  and  $K_{16}$  are 1.0 and 0.14, respectively.

(h) Rattanapitikon et al. (2003), hereafter referred to as RKS03, developed an energy dissipation model based on the representative wave approach. They applied the dissipation model for regular waves for computing the energy dissipation of irregular waves. It was found that the stable energy concept of Dally et al. (1985) can be used to describe the energy dissipation of irregular wave breaking. After calibration with laboratory and field experiments, the model was proposed to be:

$$D_{B} = K_{17} \frac{\rho g c_{g}}{8h} \left[ H_{rms}^{2} - \left( 0.42 H_{b} \right)^{2} \right]$$
 (4.25)

where  $K_{17}$  is the adjustable coefficient. The proposed value of  $K_{17}$  is 0.12. The value of  $D_B$  is set to be zero when  $H_{rms} \le 0.42 H_b$  and the breaker height ( $H_b$ ) is computed by using the breaking criteria of Miche (1944) as:

$$H_b = K_{18}L \tanh(kh) \tag{4.26}$$

where  $K_{18}$  is the adjustable coefficient. The proposed value of  $K_{18}$  is 0.14.

(i) Rattanapitikon (2007), hereafter referred to as R07, modified six existing models by changing the breaker height formulas in the dissipation models. A total of 42 possible models were considered in the study. Considering accuracy, variance of errors, and simplicity of the possible models, the following model was recommended.

$$D_{B} = K_{19} \frac{\rho g c_{g}}{8h} \left[ H_{rms}^{2} - (0.47 H_{b})^{2} \right]$$
 (4.27)

where  $K_{19}$  is the adjustable coefficient. The proposed value of  $K_{19}$  is 0.07. The value of  $D_B$  is set to be zero when  $H_{rms} \le 0.47 H_b$  and the breaker height  $(H_b)$  is computed by modifying the breaking criteria of BJ78 as

$$H_b = K_{20}L \tanh(0.68kh) \tag{4.28}$$

where  $K_{20}$  is the adjustable coefficient. The proposed value of  $K_{20}$  is 0.14. Hence, the model of R07 is similar to that of RKS03 except for the formula of  $H_b$ .

(j) Alsina and Baldock (2007), hereafter referred to as AB07, modified the model of BHV98 by changing the energy dissipation of a broken wave from the bore model of BJ78 to be the bore model of TG83. The correction is introduced to prevent a shoreline singularity that can develop in shallow water. They proposed an alternative dissipation model as:

$$D_{B} = K_{21} \frac{\rho g H_{rms}^{3}}{4 T_{p} h} \left\{ \left[ \left( \frac{H_{b}}{H_{rms}} \right)^{3} + \frac{3}{2} \frac{H_{b}}{H_{rms}} \right] \exp \left[ -\left( \frac{H_{b}}{H_{rms}} \right)^{2} \right] + \frac{3}{4} \sqrt{\pi} \left[ 1 - erf \left( \frac{H_{b}}{H_{rms}} \right) \right] \right\}$$
(4.29)

where *erf* is the error function and  $K_{21}$  is the adjustable coefficient. The proposed value of  $K_{21}$  is 1.0. The breaking wave height ( $H_b$ ) is determined from the formula of BS85 as:

$$H_b = K_{22}L \tanh \left\{ \left[ 0.57 + 0.45 \tanh \left( 33 \frac{H_{rms,0}}{L_0} \right) \right] kh \right\}$$
 (4.30)

where  $K_{22}$  is the adjustable coefficient. The proposed value of  $K_{22}$  is 0.14.

(k) Janssen and Battjes (2007), hereafter referred to as JB07, derived the same dissipation model as that of AB07 (independently of the study of AB07). The main difference between JB07 and AB07 is the breaker height formula. Their dissipation model can be summarized as:

$$D_{B} = K_{23} \frac{\rho g H_{rms}^{3}}{4 T_{p} h} \left\{ \left[ \left( \frac{H_{b}}{H_{rms}} \right)^{3} + \frac{3}{2} \frac{H_{b}}{H_{rms}} \right] \exp \left[ -\left( \frac{H_{b}}{H_{rms}} \right)^{2} \right] + \frac{3}{4} \sqrt{\pi} \left[ 1 - erf \left( \frac{H_{b}}{H_{rms}} \right) \right] \right\}$$
(4.31)

where  $K_{23}$  is the adjustable coefficient. The proposed value of  $K_{23}$  is 1.0. The breaking wave height ( $H_b$ ) is determined from the formula of Nairn (1990) as:

$$H_b = K_{24} h \left[ 0.39 + 0.56 \tanh \left( 33 \frac{H_{rms,0}}{L_0} \right) \right]$$
 (4.32)

where  $K_{24}$  is the adjustable coefficient. The proposed value of  $K_{24}$  is 1.0.

(1) Rattanapitikon and Sawanggun (2008), hereafter referred to as RS08, modified the model of BJ78 by changing the expression of fraction of breaking waves. In contrast to the common derivation, the fraction of breaking waves was not derived from the assumed *pdf* of wave heights, but derived directly from the measured wave heights. After calibration, the model can be expressed as:

$$D_{B} = K_{25} \frac{\rho g H_{b}^{2}}{4T} \left[ 2.096 \left( \frac{H_{rms}}{H_{b}} \right)^{2} - 1.601 \left( \frac{H_{rms}}{H_{b}} \right) + 0.293 \right] \quad \text{for} \quad \frac{H_{rms}}{H_{b}} > 0.46 \quad (4.33)$$

where  $K_{25}$  is the adjustable coefficient. The proposed value of  $K_{25}$  is 1.0. The value of  $D_B$  is set to be zero when  $H_{rms}/H_b \le 0.46$  and the breaking wave height  $(H_b)$  is determined from the formula of BS85 as:

$$H_b = K_{26}L \tanh \left\{ \left[ 0.57 + 0.45 \tanh \left( 33 \frac{H_{rms,0}}{L_0} \right) \right] kh \right\}$$
 (4.34)

where  $K_{26}$  is the adjustable coefficient. The proposed value of  $K_{26}$  is 0.14.

(m) Apotsos et al. (2008), hereafter referred to as AREG08, modified six existing dissipation models by recalibrating the coefficient in the breaker height formulas incorporated in the dissipation models. The coefficient was related to the deepwater

wave height  $(H_{rms,0})$ . The comparison showed that the model TG83b [Eq. (4.13)] with new breaker height formula gives the smallest error. The modified model was proposed to be:

$$D_{B} = K_{27} \frac{3\sqrt{\pi}}{4} \left(\frac{H_{rms}}{H_{b}}\right)^{2} \left\{ 1 - \frac{1}{\left[1 + \left(H_{rms}/H_{b}\right)^{2}\right]^{2.5}} \right\} \frac{\rho g H_{rms}^{3}}{4T_{p}h}$$
(4.35)

$$H_b = K_{28}[0.18 + 0.40 \tanh(0.9H_{rms,0})]h \tag{4.36}$$

where  $K_{27}$  and  $K_{28}$  are the adjustable coefficients. The proposed values of  $K_{27}$  and  $K_{28}$  are 1.0 and 1.0, respectively.

## 4.2.2.2. Model analysis

The development of the existing dissipation models may be classified into two approaches, i.e. parametric wave approach and stable energy approach. The parametric wave approach seeks to reduce the computational effort by describing the energy dissipation rate in terms of time-averaged parameter. Its description is reduced to a single representative wave height, period, and direction. As this approach relies on the macroscopic features of breaking waves and predicts only the transformation of root-mean-square (rms) wave height, it is suitable when a detail wave height distribution is not needed. The approach assumes that the Rayleigh pdf (or modified Rayleigh pdf) is valid in the surf zone. The average rate of energy dissipation is described by integrating the product of energy dissipation of a single broken wave and the probability of occurrence of breaking waves. Most of the selected models (except RKS03 and R07) were developed based on this approach. The models were developed based on the work of BJ78. The significant differences of those models are the assumption on probability of occurrence of breaking waves, the formulation of energy dissipation of a single broken wave, and the breaker height formula. The models may be grouped into three groups based on the assumed probability of occurrence of breaking waves. The first group (BJ78, BS85, SN93, RS98, and RS08) describes the pdf of wave heights in the surf zone through a sharp cutoff Rayleigh distribution, truncated at a breaker height  $(H_h)$  at which all waves are assumed to break and have heights equal to the breaker height. The second group (TG83a, TG83b, and AREG08) describes the probability of occurrence of breaking waves through a weighted Rayleigh distribution. The third group (BHV98, RWS03, AB07, and JB07) describes the pdf of wave heights in the surf zone through a complete Rayleigh distribution and the wave heights which are greater than a breaker height  $(H_h)$  are considered as broken waves.

The stable energy concept was introduced by Dally et al. (1985) for computing the energy dissipation rate due to regular wave breaking. The model was developed based on the measured breaking wave height on the horizontal bed. When a breaking wave enters an area with a horizontal bed, the breaking continues (the wave height decreases) until some stable wave height is attained. The development of the stable energy concept was based on an observation of stable wave height on horizontal slopes. Dally et al. (1985) assumed that the energy dissipation rate was proportional to the difference between the local energy flux per unit depth and the stable energy flux per unit depth. The energy dissipation will be zero if the wave height is less than the stable wave height. The model seems to be widely used for computing regular wave height transformation. For irregular waves, RKS03 and

R07 showed that the stable energy concept is applicable for computing the transformation of  $H_{rms}$ . The approach has the merits of easy understanding, simple application and it is not necessary to assume the shape of the pdf of wave heights. The stable wave heights of the RKS03 and R07 were proposed in terms of breaker heights. The model of RKS03 used the breaker height formula of Miche (1944), while the model of R07 used the breaker height formula of BJ78. It is known that the process of wave breaking in shallow water is influenced by the incident wave steepness and bottom slope. However, the effect of beach slope is not included in the stable energy models. The effect of beach slope may be included in the models by changing the breaker height formula from Miche (1944) or BJ78 to be the other breaker height formula which includes the effect of beach slope.

These two approaches rely on the macroscopic features of breaking waves and predict only the transformation of  $H_{rms}$ . The two approaches have different advantages and disadvantages. The advantage of the stable energy approach is that it is able to stop wave breaking over bar-trough or step profiles, while the parametric wave approach gives a continuous dissipation due to wave breaking. However, the parametric approach may not give much error in predicting wave height in the trough region because the values of  $H_{rms}/H_b$  and  $Q_b$  are very small in the trough. The prediction may not be locally precise in the trough region, but generally patterns of wave transformation were reported adequately (Battjes and Janssen, 1978). The advantage of the parametric wave approach is that it is able to compute a fraction of wave breaking (which is useful for computing undertow and suspended sediment concentration), while the fraction of wave breaking cannot be determined from the stable energy approach.

## 4.2.2.3. Model adaptation

As the existing dissipation models (shown in section 4.2.2.1) were proposed in terms of  $H_{rms}$ , the models have to be converted to be expressed in terms  $H_{m0}$  before applying to compute  $H_{m0}$ . By assuming that  $H_{m0} = \sqrt{2}H_{rms}$ , the existing dissipation models are applied for computing the transformation of  $H_{m0}$  by substituting  $H_{rms} = H_{m0}/\sqrt{2}$  into the models (shown in section 4.2.2.1). Then the wave height transformation models can be constructed by substituting the dissipation models into the energy flux balance equation [Eq. (4.6)]. Nevertheless, it is not clear which dissipation model is the most suitable one for computing  $H_{m0}$ . Therefore, all of them were used to examine their applicability on simulating  $H_{m0}$ .

#### 4.2.3. Model examination

The objective of this section is to examine the applicability of the fourteen existing dissipation models in simulating  $H_{m0}$ . The measured  $H_{m0}$  from the compiled experiments (shown in Table 4.1) are used to examine the accuracy of existing models.

The transformation of  $H_{m0}$  is computed by numerical integration of the energy flux balance equation [Eq. (4.6)] with the existing energy dissipation models. A backward finite difference scheme is used to solve the energy flux balance equation [Eq. (4.6)].

The basic parameter for determination of the overall accuracy of a model is the average root-mean-square relative error ( $ER_{avg}$ ), which is defined as:

$$ER_{avg} = \frac{\sum_{j=1}^{m} ER_{gj}}{tn} \tag{4.37}$$

where  $ER_{gj}$  is the root-mean-square relative error of the data group j (the group number), and tn is the total number of groups. The small value of  $ER_{avg}$  indicates good overall accuracy of the model.

The root-mean-square relative error of the data group  $(ER_{o})$  is defined as:

$$ER_{g} = 100 \sqrt{\frac{\sum_{i=1}^{ng} (H_{ci} - H_{mi})^{2}}{\sum_{i=1}^{ng} H_{mi}^{2}}}$$
(4.38)

where i is the wave height number,  $H_{ci}$  is the computed wave height of number i,  $H_{mi}$  is the measured wave height of number i, and ng is the total number of measured wave heights in each data group.

The compiled experiments are separated into three groups according to the experiment scale, i.e. small-scale, large-scale and field experiments. It is expected that a good model should be able to predict well for the three groups of different scale. As the present study concentrates on only the transformation of wave height (excluding wave setup), the measured mean water depth is used in the computation. However, the measured wave set-up is not available for the field data. The water depth including tidal change is used for the field experiments.

Using the default coefficients ( $K_1$ - $K_{28}$ ) in the computations, the errors ( $ER_g$  and  $ER_{avg}$ ) of each dissipation model on predicting  $H_{m0}$  for three groups of experiment-scales have been computed and are shown in Table 4.3. It can be seen from Table 4.3 that the models of R07, RS08, BS85, and AB07 give similar overall accuracy ( $8.0 \le ER_{avg} \le 8.5\%$ ) and give better accuracy than the others. For computing beach deformation, a wave model has to be run many times to account the frequent updating of beach profile. The error from the wave model may be accumulated from time to time. Therefore, for computing the beach deformation, the error of the wave model should be kept as small as possible. Hence, the best model should be selected for incorporating in the beach deformation model. It can be seen from Table 4.3 that there is only one model (model of R07) that gives good predictions for the three groups of experiment-scales. Moreover, the model R07 also gives the best overall prediction ( $ER_{avg} = 8.0 \%$ ). However, because some dissipation models were developed with limited experimental conditions and it is not clear whether the models were developed for statistical-based or spectral-based wave heights, the coefficients in each model may not be the optimal values for computing  $H_{m0}$ . Therefore, the errors in Table 4.3 should not be used to judge the applicability of the existing models. The coefficients in all models should be recalibrated before comparing the applicability of the models.

Each model is calibrated by determining the optimal values of coefficients K which yield the minimum  $ER_{avg}$ . In order to determine the universal coefficients K, all compiled experimental data are used to calibrate the models. Using default coefficients K, wave

height transformation for all experiments have been computed and then the average error  $(ER_{avg})$  of the model has been computed from the measured and computed wave heights. The computations are repeated for various choices of coefficients K, until the minimum error  $(ER_{avg})$  is obtained.

**Table 4.3** The errors  $ER_g$  and  $ER_{avg}$  of each dissipation model for three groups of experiment-scales by using the default coefficients (measured data from Table 4.1).

Models	$D_{\scriptscriptstyle B}$	Default	$ER_g$			$ER_{avg}$
	formulas	coefficients	Small-	Large-	Field	
			scale	scale		
BJ78	Eq. (4.7)	$K_1 = 1.0, K_2 = 0.14$	9.7	10.5	17.7	12.6
TG83a	Eq. (4.11)	$K_3 = 0.51, K_4 = 0.42$	13.1	16.1	11.2	13.4
TG83b	Eq. (4.13)	$K_5 = 0.51, K_6 = 0.42$	11.6	8.1	11.3	10.3
BS85	Eq. (4.15)	$K_7 = 1.0, K_8 = 0.14$	8.3	6.7	10.2	8.4
SN93	Eq. (4.17)	$K_9 = 1.0, K_{10} = 1.0$	9.6	9.4	14.5	11.1
BHV98	Eq. (4.19)	$K_{11} = 1.0, K_{12} = 1.0$	7.9	6.5	13.5	9.3
RS98	Eq. (4.21)	$K_{13} = 0.10, K_{14} = 0.10$	12.4	7.1	10.1	9.9
RWS03	Eq. (4.23)	$K_{15} = 1.0, K_{16} = 0.14$	10.8	7.8	10.0	9.5
RKS03	Eq. (4.25)	$K_{17} = 0.12, \ K_{18} = 0.14$	8.9	8.6	12.9	10.1
R07	Eq. (4.27)	$K_{19} = 0.07, \ K_{20} = 0.14$	7.5	7.2	9.3	8.0
AB07	Eq. (4.29)	$K_{21} = 1.0, \ K_{22} = 0.14$	7.8	7.1	10.5	8.5
JB07	Eq. (4.31)	$K_{23} = 1.0, K_{24} = 1.0$	8.8	7.2	11.1	9.0
RS08	Eq. (4.33)	$K_{25} = 1.0, \ K_{26} = 0.14$	7.9	6.7	10.5	8.3
AREG08	Eq. (4.35)	$K_{27} = 1.0, \ K_{28} = 1.0$	10.3	9.1	12.8	10.7

The calibrated coefficients  $K_1$  to  $K_{28}$  are summarized in the third column of Table 4.4. Using the calibrated coefficients ( $K_1$ - $K_{28}$ ) in the computations, the errors ( $ER_g$  and  $ER_{avg}$ ) of each dissipation model on predicting  $H_{m0}$  for three groups of experiment-scales have been computed and are shown in Table 4.4. The results can be summarized as follows:

- (a) The error ( $ER_g$ ) of the calibrated models is in the range of 5.8 to 15.9%. The model of JB07 gives the best predictions for small-scale and large-scale experiments, while the model of R07 gives the best prediction for field experiments.
- (b) Considering overall accuracy ( $ER_{avg}$ ) of the models, the overall accuracies of the models in descending order are JB07, R07, BS85, RS08, AB07, RKS03, SN93, RWS03, BHV98, RS98, TG83b, AREG08, BJ78, and TG83a. The first five of which give similar accuracy ( $7.8 \le ER_{avg} \le 8.1\%$ ) and give better accuracy than the others. The accuracy of the five models seems to be sufficient for the design of coastal structures. As the model of JB07 gives the best overall prediction ( $ER_{avg} = 7.8\%$ ), it

- seems to be the most suitable one for incorporating in the beach deformation model. Since the model of JB07 was developed based on a full Rayleigh distribution of wave heights (which is the individual wave analysis or statistical analysis), the model should be appropriate for computing the statistical-based wave heights. Moreover, several researchers (e.g. Klopman, 1996; Battjes and Groenendijk, 2000; and Mendez et al., 2004) showed that the Rayleigh distribution is not valid in the surf zone. Surprisingly, the model of JB07 gives the best overall prediction.
- (c) The main difference among the models of TG83a, TG83b, AREG08, AB07, and JB07 is the distribution function of breaking wave heights. As the models of AB07 and JB07 are significantly better than those of TG83a, TG83b and AREG08, it is expected that the key step change and improvement in the parametric models was the adoption of a Rayleight *pdf* for all waves as proposed by Baldock et al. (1998).
- (d) The main difference among the models of BHV98, RWS03, AB07, and JB07 is the energy dissipation of a single broken wave, i.e. BHV98 and RWS03 used the bore model of BJ78, while AB07 and JB07 used the bore model of TG83. The results show that the bore model of TG83 is more suitable to incorporate in the models.
- (e) Comparing among the models developed based on the parametric wave approach (BJ78, TG83a, TG83b, BS85, SN93, BHV98, RS98, RWS03, AB07, JB07, RS08, and AREG08), the model JB07 gives the best overall prediction. The significant differences of those models are the assumption on probability of occurrence of breaking waves, the formulation of energy dissipation of a single broken wave, and the breaker height formula. This indicates that the combination which is proposed by JB07 is the most suitable one for computing the transformation of  $H_{m0}$ .
- (f) Comparing between the models developed based on the stable energy approach (RKS03 and R07), the model R07 gives the better overall prediction than the other. This indicates that the breaker height formula used by R07 is more suitable than the other.
- (g) Either parametric wave approach or stable energy approach can be used to compute the transformation of  $H_{m0}$ . The best model for parametric wave approach is JB07, while the best model for stable energy approach is R07.
- (h) Although the model of JB07 gives the best overall prediction, it does not give good predictions for all experiment-scales. The model gives good predictions for small-scale and large-scale experiments but gives fair prediction for field experiments. Another model, which may be used to incorporate in the beach deformation model, is the model of R07. The model gives the second best overall prediction ( $ER_{avg} = 8.0\%$ ) and gives good predictions for all experiment-scales. Moreover, the model of R07 is much simpler than that of JB07.

**Table 4.4** The errors  $ER_g$  and  $ER_{avg}$  of each dissipation model for three groups of experiment-scales by using the calibrated coefficients (measured data from Table 4.1).

Models	$D_{\scriptscriptstyle B}$	Calibrated	$ER_g$			$ER_{avg}$
	formulas	coefficients	Small-	Large-	Field	
			scale	scale		
BJ78	Eq. (4.7)	$K_1 = 0.92, K_2 = 0.12$	13.1	7.9	12.7	11.2
TG83a	Eq. (4.11)	$K_3 = 0.52, K_4 = 0.45$	11.0	15.9	12.4	13.1
TG83b	Eq. (4.13)	$K_5 = 0.42, \ K_6 = 0.41$	10.5	7.9	12.2	10.2
BS85	Eq. (4.15)	$K_7 = 0.75, K_8 = 0.13$	7.6	6.1	10.4	8.0
SN93	Eq. (4.17)	$K_9 = 1.4, \ K_{10} = 0.95$	7.5	7.1	11.5	8.7
BHV98	Eq. (4.19)	$K_{11} = 0.88, \ K_{12} = 0.97$	7.7	6.5	13.3	9.2
RS98	Eq. (4.21)	$K_{13} = 0.10, K_{14} = 0.10$	12.4	7.1	10.1	9.9
RWS03	Eq. (4.23)	$K_{15} = 1.0, \ K_{16} = 0.15$	9.1	7.9	10.3	9.1
RKS03	Eq. (4.25)	$K_{17} = 0.07, \ K_{18} = 0.11$	9.3	7.2	9.5	8.7
R07	Eq. (4.27)	$K_{19} = 0.07, \ K_{20} = 0.14$	7.5	7.2	9.3	8.0
AB07	Eq. (4.29)	$K_{21} = 0.86, \ K_{22} = 0.13$	7.8	6.4	10.2	8.1
JB07	Eq. (4.31)	$K_{23} = 0.70, \ K_{24} = 0.83$	6.9	5.8	10.8	7.8
RS08	Eq. (4.33)	$K_{25} = 0.75, \ K_{26} = 0.13$	7.6	6.2	10.4	8.1
AREG08	Eq. (4.35)	$K_{27} = 0.80, \ K_{28} = 0.90$	10.7	8.6	12.2	10.5
M1	Eq. (4.42)	$K_{29} = 0.27$	6.7	7.2	9.2	7.7
M2	Eq. (4.43)	$K_{30} = 0.75$	24.2	8.6	13.7	15.5

#### 4.2.4. Model modification

Because of the simplicity and good predictions for all experiment-scales of R07's model, the model was selected to modify for better accuracy. The model of R07 can be written in general form as

$$D_B = 0.07 \frac{\rho g c_g}{8h} \left[ 0.5 H_{m0}^2 - H_{st}^2 \right]$$
 (4.39)

where  $H_{st}$  is the stable wave height.

The model of R07 was developed based on the stable energy wave concept. The concept was firstly introduced by Dally et al. (1985) for computing energy dissipation of regular wave breaking. The energy dissipation is assumed to be proportional to the difference between the local energy flux and the stable energy flux. Based on a wide range of experimental conditions, Rattanapitikon et al. (2003) showed that the following stable wave height formulas could also be used for computing the energy dissipation of regular wave breaking.

(a) Dally et al. (1985): 
$$H_{st} = 0.4h$$
 (4.40)

(b) Rattanapitikon and Shibayama (1998): 
$$H_{st} = h \exp\left(-0.36 - 1.25 \frac{h}{\sqrt{LH}}\right)$$
 (4.41)

It is expected that the accuracy of the R07's model [Eq. (4.39)] could be improved by using the suitable  $H_{st}$  formula, and the formula for regular wave breaking may be applicable for irregular wave breaking. In this section, an attempt has been made to modify the model of R07 by changing the terms of stable wave height.

Substituting Eqs. (4.40) and (4.41) into Eq. (4.39), the two modified energy dissipation models for computing  $H_{m0}$  (hereafter referred to as M1 and M2, respectively) can be expressed as

M1: 
$$D_B = 0.07 \frac{\rho g c_g}{8h} \left[ 0.5 H_{m0}^2 - (K_{29}h)^2 \right]$$
 (4.42)

M2: 
$$D_B = 0.07 \frac{\rho g c_g}{8h} \left[ 0.5 H_{m0}^2 - \left( K_{30} h \exp \left( -0.36 - 1.25 \frac{2^{1/4} h}{\sqrt{L H_{m0}}} \right) \right)^2 \right]$$
 (4.43)

where  $K_{29} - K_{30}$  are the adjustable coefficients.

The calibration of the two modified dissipation models is performed by using the measured data shown in Table 4.1. The calibrations are conducted by gradually adjusting the coefficients until the minimum error ( $ER_{avg}$ ) of each model is obtained. The calibrated coefficients of M1 and M2 and the errors ( $ER_g$  and  $ER_{avg}$ ) for three groups of experiment-scales are shown in the last two rows of Table 4.4. The results can be summarized as follows:

- (a) Comparing between the two modified models, the model M1 is much better than the model M2. The model M2 gives too much errors and it should not be used for computing  $H_{m0}$ .
- (b) Comparing among the models developed based on the stable energy approach (RKS03, R07, M1, and M2), the model M1 gives the best overall prediction. This indicates that the stable wave height formula of Dally et al. (1985) is the most suitable one for computing the transformation of  $H_{m0}$ .
- (c) Comparing with the existing models, the model M1 is the simplest model. Because of the simplicity of M1, it is expected that this model will give less accuracy than the others. Surprisingly, the result shows that the simplest model gives the best overall prediction. It should be noted that the stable wave height in the model M1 is proportional to the breaker height formula of TG83 [Eq. (4.12)]. Attempts have been made to modify the model M1 by using other breaker height formulas [Eqs. (4.9), (4.16), (4.18), (4.22), (4.24), and (4.36)]. However, it was found that no model gives better prediction than that of M1.
- (d) Comparing between the best existing model (JB07) and the model M1, the model M1 gives slightly better overall prediction than that of JB07. The model of M1 gives the best predictions for small-scale and field experiments, while the model of JB07 gives the best prediction for large-scale experiments. Moreover, the model M1 gives good predictions for all experiment-scales while the model JB07 does not. Considering the complexity of the models, the model M1 is much simpler than that of JB07. As the simple model gives slightly better accuracy than the more complicated model, it may not necessary to use the complicated model to compute the transformation of  $H_{m0}$ .
- (e) In the present study, the most suitable model is selected based on accuracy and simplicity of the models. Considering the accuracy of the models, the models M1, JB07, R07, BS85, RS08, and AB07 give nearly the same accuracy  $(7.7 \le ER_{avg} \le 8.1)$

and give better accuracy than the others. Considering the simplicity of the 6 models, the formula of model M1 is the simplest one. Therefore, the model M1 is judged to be the most suitable model. Substituting the calibrated coefficients into the model M1, the recommended model can be written as

$$\frac{\rho g}{16} \frac{\partial \left(H_{m0}^2 c_g \cos \theta\right)}{\partial x} = -0.07 \frac{\rho g c_g}{8h} \left[0.5 H_{m0}^2 - \left(0.27h\right)^2\right]$$
(4.44)

The greatest asset of the model M1 is its simplicity and ease of application, i.e. the transformation of  $H_{m0}$  from offshore to shoreline can be computed by using only one equation [Eq. (4.44)]. The model can be converted to compute the transformation of spectral-based root-mean-square wave height ( $H_{rmsz}$ ) by substituting  $H_{m0} = \sqrt{2}H_{rmsz}$  into Eq. (4.44). The result is

$$\frac{\rho g}{8} \frac{\partial \left(H_{rmsz}^2 c_g \cos \theta\right)}{\partial x} = -0.07 \frac{\rho g c_g}{8h} \left[H_{rmsz}^2 - \left(0.27h\right)^2\right] \tag{4.45}$$

To gain an impression of overall performance of the best model of the two approaches, the results of JB07 and M1 are plotted against the measured data. Examples of computed  $H_{m0}$  transformation across-shore are shown in Figs. 4.1 to 4.3. Case numbers in Figs. 4.1-4.3 are kept to be the same as the originals. Overall, it can be seen that the two models are quite realistic in simulation of the  $H_{m0}$  and have similar accuracy. Because the  $H_{m0}$  is computed by a simple expression of energy flux conservation, the models are limited to use on open coasts away from river mouths and coastal structures. As the swash processes are not included in the models, the models are limited to use in the nearshore zone (excluding swash zone). Furthermore, the major disadvantage of the models is that they do not provide any detail on the behavior of individual waves. For example, all waves are assumed to refract based on the mean wave angle, which is not realistic in the case of broad-banded spectra. The effect of directional spread on wave refraction is presented in the book of Goda (2000). For more accuracy, it is essential to follow individual wave transformation.

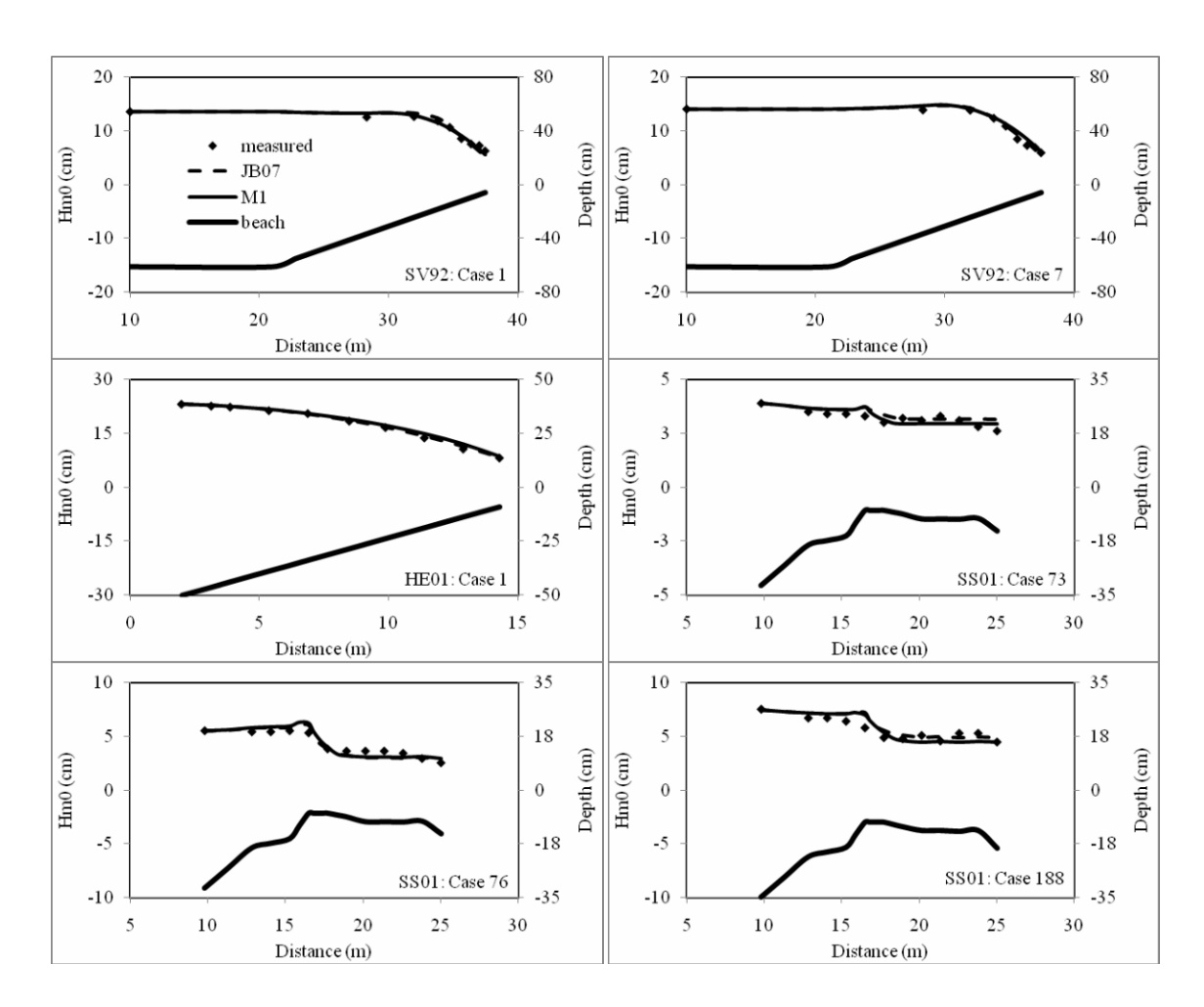


**Fig. 4.1** Examples of measured and computed  $H_{m0}$  transformation from models JB07 and M1 (measured data from small-scale experiments).

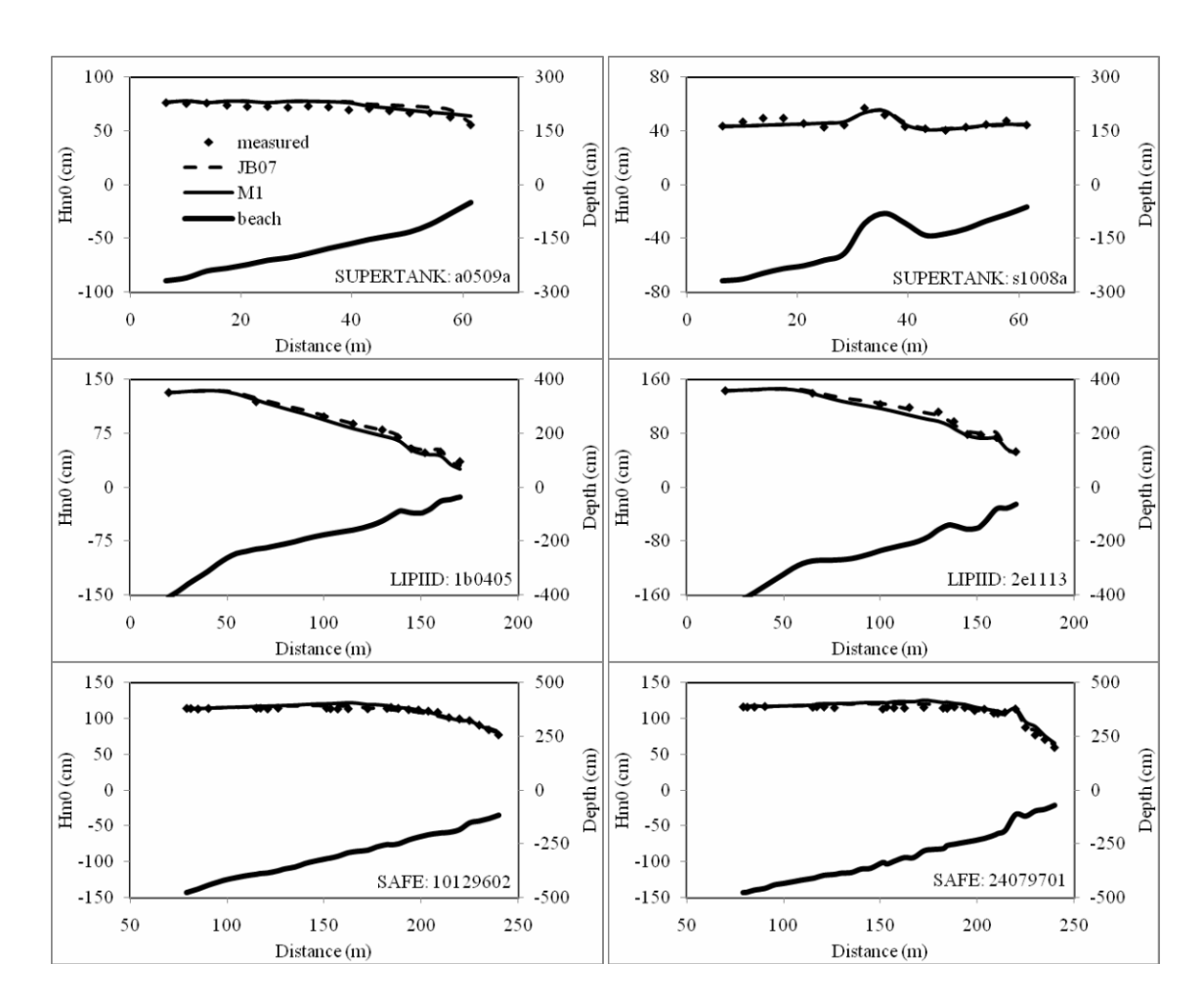


**Fig. 4.2** Examples of measured and computed  $H_{m0}$  transformation from models JB07 and M1 (measured data from large-scale experiments).

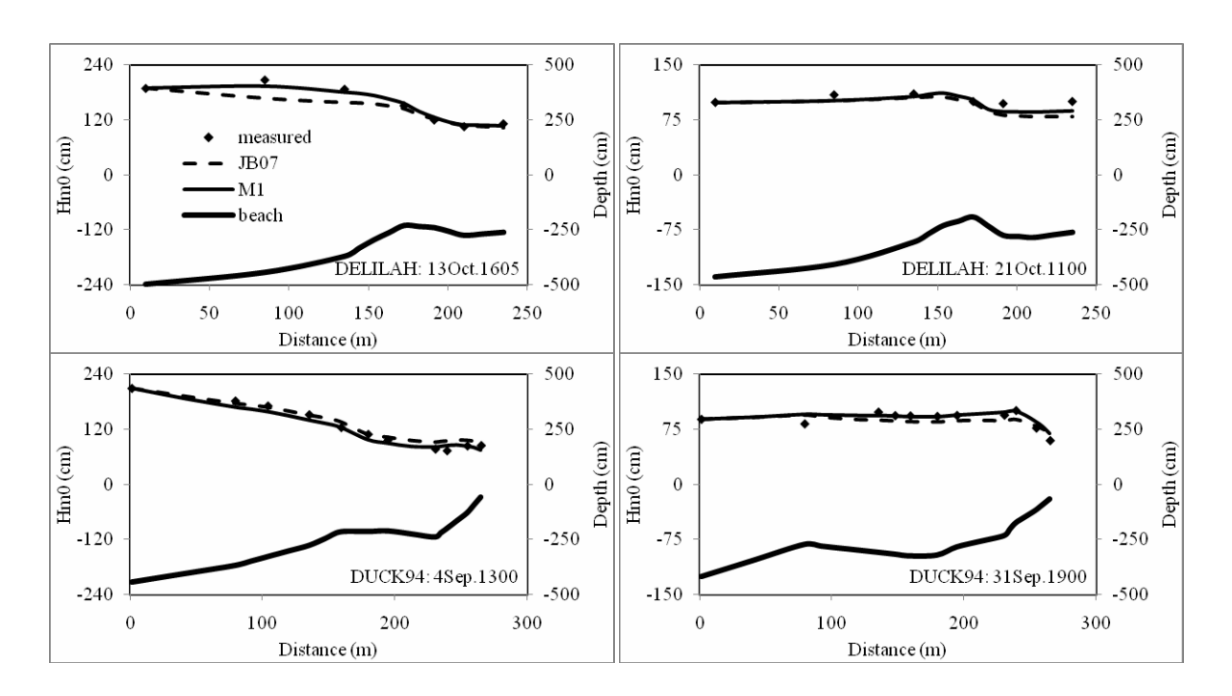


**Fig. 4.3** Examples of measured and computed  $H_{m0}$  transformation from models JB07 and M1 (measured data from field experiments).

## 4.3. Transformation of Root-Mean-Square Wave Heights

The transformation of root-mean-square (rms) wave heights has been a subject of study for decades because of its importance in studying beach deformations and the design of coastal structures. When waves propagate to the nearshore zone, wave profiles steepen and eventually waves break. Once the waves start to break, a part of wave energy is transformed into turbulence and heat, and wave height decreases towards the shore. Irregular wave breaking is more complex than regular wave breaking. In contrast to regular waves, there is no well-defined breaking position for irregular waves. The higher wave tends to break at the greater distance from the shore. Closer to the shore, more and more waves are breaking, until in the inner surf zone almost all the waves are breaking. Thus, the energy dissipation of irregular waves occurs over a considerably greater area than that of regular waves with the same strength. There are several concepts to model the wave height transformation or energy dissipation. For computing beach deformation, the wave model should be kept as simple as possible because of the frequent updating of wave field to account for the change of bottom profiles. Therefore, the present study focuses on the macroscopic features of breaking waves by describing the energy dissipation rate in terms of time-averaged parameter and predicts only the transformation of root-meansquare (rms) wave height. In the present study, wave height transformation is computed from the energy flux conservation law [Eq. (4.1)].

There are two approaches to analyze irregular wave record, i.e. statistical approach and spectral approach. The average energy density based on the two approached can be expressed as:

$$E = \frac{1}{8} \rho g H_{rms}^2 \tag{4.46}$$

$$E = \frac{1}{8} \rho g H_{rmsz}^2 \tag{4.47}$$

where  $\rho$  is the water density, g is the gravity acceleration,  $H_{rms}$  is the statistical-based rms wave height,  $H_{rmsz} = \sqrt{8m_0}$  is the spectral-based rms wave height, and  $m_0$  is the zeroth moment of wave spectrum. There are two definitions of the rms wave height ( $H_{rms}$  and  $H_{rmsz}$ ). The two definitions of rms wave height are usually assumed to be equal. However, it was shown by many researchers (e.g. Thompson and Vincent, 1985; Hughes and Borgman 1987; and Battjes and Groenendijk, 2000) that the rms wave heights derived from the two definitions are significantly difference, especially near the breaking point. It is importance for engineers to understand what definition of rms wave height they are using in the model and which model is suitable in computing  $H_{rms}$  or  $H_{rmsz}$ .

The rms wave height transformation can be computed from the energy flux balance equation [Eq. (4.1)] by substituting the formula of the energy dissipation rate ( $D_B$ ) and numerically integrating from offshore to shoreline. The difficulty of the energy flux conservation approach is how to formulate the energy dissipation rate caused by the breaking waves. During the past decades, various energy dissipation models have been proposed for computing rms wave height in the surf zone. However, most of the models were developed with the regardlessness on the difference between  $H_{rms}$  and  $H_{rmsz}$ . Therefore, the coefficients in the models may not be the optimal values for computing  $H_{rms}$  or  $H_{rmsz}$ . Rattanapitikon and Shibayama (2010) presented the applicable of 14 existing dissipation models on simulating spectral significant wave height (which can be

converted to  $H_{\it rmsz}$  through the known constant). However, no direct literature has been described clearly the applicable of existing models on simulating  $H_{\it rms}$ . Therefore, this section was carried out to recalibrate some existing energy dissipation models and find out the suitable models, which can be used to compute  $H_{\it rms}$  for a wide range of experimental conditions.

## 4.3.1. Collected experimental data

Experimental data of  $H_{rms}$  from 5 sources have been collected to examination of the models. The collected experiments cover a wide range of wave and bottom topography conditions. The experimental data include small-scale, large-scale, and field experiments. Summary of the collected experimental results are shown in Table 4.5.

**Table 4.5** Summary of collected experimental data of statistical-based rms wave heights  $(H_{rms})$ .

Sources	No. of	No. of	Beach	Apparatus
	Cases	Data	Condition	
		Points		
Smith and Kraus (1990)	plane and	12	96 plane and	
	12	90	barred beach	small-scale
Ting (2001)	1	7	plane beach	small-scale
Kraus and Smith (1994):	128	2223	sandy beach	large-scale
SUPERTANK project	120	2223	Sandy Deach	large-scale
Dette et al. (1998):	138	138 3561 sandy beac	sandy beach	large-scale
MAST III – SAFE project	130	3301	sandy beach	large-scale
Thornton and Guza (1986)	4	60	sandy beach	field
Total	283	5947		

The experiment of Smith and Kraus (1990) was conducted to investigate the macrofeatures of wave breaking over bars and artificial reefs using a small wave flume of 45.70 m long, 0.46 m wide, and 0.91 m deep. Both regular and irregular waves were employed in this experiment. A total of 12 cases were performed for irregular wave tests. Three irregular wave conditions were generated for three bar configurations as well as for a plane beach. A JONSWAP (Hasselmann et al., 1973) computer signal was generated for spectral width parameter of 3.3 and spectral peak periods of 1.07, 1.56, and 1.75 s with significant wave heights of 0.12, 0.15, and 0.14 m, respectively. Water surface elevations were measured at eight cross-shore locations using resistance-type gages.

The experiment of Ting (2001) was conducted to study wave and turbulence velocities in a broad-banded irregular wave surf zone. The experiment was performed in a small-scale wave flume, which was 37 m long, 0.91 m wide and 1.22 m deep. A false bottom with 1/35 slope built of marine plywood was installed in the flume to create a plane beach. The irregular waves were developed from the TMA spectrum (Bouws et al., 1985), with a spectral peak period of 2.0 s, a spectrally based significant wave height of 0.15 m and spectral width parameter of 3.3. Water surface elevations were measured at seven cross-shore locations using a resistance-type gage.

The SUPERTANK laboratory data collection project (Kraus and Smith, 1994) was conducted to investigate cross-shore hydrodynamic and sediment transport processes from August 5 to September 13, 1992 at Oregon State University, Corvallis, Oregon, USA. A 76-m-long sandy beach was constructed in a large wave tank of 104 m long, 3.7 m wide, and 4.6 m deep. Wave conditions included both regular and irregular waves. In all, 20 major tests were performed, and each major test consisted of several cases. Most of the tests (14 major tests) were performed under the irregular wave actions. The wave conditions were designed to balance the need for repetition of wave conditions to move the beach profile toward equilibrium and development of a variety of conditions for hydrodynamic studies. The TMA spectral shape (Bouws et al., 1985) was used to design all irregular wave tests. The collected experiments for irregular waves included 128 cases of wave and beach conditions (a total of 2047 wave records), covering incident significant wave heights from 0.2 m to 1.0 m, spectral peak periods from 3.0 sec to 10.0 sec, and spectral width parameter between 3.3 (broad-banded) and 100 (narrow-banded). Sixteen resistance-type gages were used to measure water surface elevations across shore.

SAFE Project (Dette et al., 1998) was carried out to improve the methods of design and performance assessment of beach nourishment. The SAFE Project consisted of four activities, one of which was to perform experiments in a large-scale wave flume in Hannover, Germany. A 250-m-long sandy beach was constructed in a large wave tank of 300 m long, 5 m wide and 7 m deep. The test program was divided into two major phases. The first phase (cases A, B, C, and H) was aimed to study the beach deformation of equilibrium profile with different beach slope changes. The equilibrium beach profile was adopted from the Bruun (1954)'s approach ( $h = 0.12x^{2/3}$ ). In the second phase, the sediment transport behaviors of dunes with and without structural aid were investigated (cases D, E, F, and G). The TMA spectral shape (Bouws et al., 1985) was used to design all irregular wave tests. The tests were performed under normal wave conditions ( $H_{so}/L_o$ = 0.010, water depth in the horizontal section = 4.0 m) and storm wave conditions ( $H_{so}/L_o$  = 0.018, water depth in the horizontal section = 5.0 m). A total of 27 wave gages was installed over a length of 175 m along one wall of the flume. The collected experiments included 138 cases of wave and beach conditions, covering deepwater wave steepness  $(H_{so}/L_a)$  from 0.010 to 0.018.

The experiment of Thornton and Guza (1986) was conducted on a beach with nearly straight and parallel depth contours at Leadbetter Beach, Santa Barbara, California, USA, to measure longshore currents, waves, and beach profiles, during the period January 30 to February 23, 1980.

## 4.3.2. Existing energy dissipation models

During the past decades, various energy dissipation models have been developed based on the parametric approach and the representative wave approach. Because of the complexity of the wave breaking mechanism, most of the energy dissipation models were developed based on the empirical or semi-empirical approach calibrated with the measured *rms* wave height.

Brief reviews of 14 existing dissipation models are described in Sec. 4.2.2.1. The additional one is summarized below:

(a) Rattanapitikon and Shibayama (2010) examined 14 existing dissipation models on simulating spectral significant wave height. The comparison shows that the models of

JB07 and R07 give very good predictions on  $H_{m0}$ . The model of R07 was modified by changing the stable wave height from the term of breaker height to be the term of water depth. As the modified model is similar to that of Dally et al. (1985), it may be also considered as the modified model of Dally et al. (1985). Comparing with the existing models, the modified model is the simplest one but gives the best accuracy. The modified model can be expressed in terms of root-mean-square wave height as:

$$D_B = K_{31} \frac{\rho g c_g}{8h} \left[ H_{rms}^2 - (K_{32}h)^2 \right]$$
 (4.48)

where  $K_{31}$  and  $K_{32}$  are the adjustable coefficients. The proposed values of  $K_{31}$  and  $K_{32}$  are 0.07 and 0.27, respectively. Equation (4.48) is hereafter referred to as MD85. It should be noted that originally Eq. (4.48) is used for computing  $H_{rmsz}$  (not for computing  $H_{rms}$ ).

## 4.3.3. Examination of existing models

The objective of this section is to examine the applicability of the 15 existing dissipation models on simulating  $H_{rms}$ . The measured  $H_{rms}$  from the collected experiments (shown in Table 4.5) are used to examine the existing models.

The *rms* wave height transformation is computed by numerical integration of the energy flux balance equation [Eq. (4.1)] with the energy dissipation rate of the existing models [Eqs. (4.7), (4.11), (4.13), (4.15), (4.17), (4.19), (4.21), (4.23), (4.25), (4.27), (4.29), (4.31), (4.33), (4.35), and (4.48)]. A backward finite difference scheme is used to solve the energy flux balance equation [Eq. (4.1)].

The collected experiments are separated into three groups according to the experiment scale, i.e. small-scale, large-scale, and field experiments. It is expected that a good model should be able to predict well for the three groups of experiment scale. Therefore, the average error  $(ER_{avg})$  from the three groups of experiment scale are used as a main criteria to verify the models.

Using the default coefficients ( $K_1 - K_{28}$ ,  $K_{31}$ , and  $K_{32}$ ) in the computations, the errors ( $ER_g$  and  $ER_{avg}$ ) of each dissipation model on predicting  $H_{rms}$  for three groups of experiment scale have been computed and shown in Table 4.6. It can be seen from Table 4.6 the model of RKS03 gives the best prediction on estimating  $H_{rms}$ . Because most models were developed with the regardlessness on the difference between  $H_{rms}$  and  $H_{rmsz}$ , the coefficients in the models may not be the optimal values for computing both of  $H_{rms}$  and  $H_{rmsz}$ . Therefore, the errors in Table 4.6 should not be used to judge the applicability of the models. The coefficients in all models should be recalibrated before verifying the applicability of the models.

**Table 4.6** The errors  $ER_g$  and  $ER_{avg}$  of each dissipation model for computing  $H_{rms}$  for

three groups of experiment-scales (using default coefficients).

Model	Default coefficients			$ER_{avg}$	
		Small scale	Large scale	Field	
BJ78	$K_1 = 1.0, K_2 = 0.14$	9.3	6.6	26.4	14.1
TG83a	$K_3 = 0.51, K_4 = 0.42$	35.1	18.4	12.8	22.1
TG83b	$K_5 = 0.51, K_6 = 0.42$	28.0	10.4	17.4	18.6
BS85	$K_7 = 1.0, K_8 = 0.14$	8.6	9.8	14.7	11.0
SN93	$K_9 = 1.0, K_{10} = 1.0$	13.1	7.6	26.7	15.8
BHV98	$K_{11} = 1.0, K_{12} = 1.0$	12.5	10.8	16.1	13.1
RS98	$K_{13} = 0.10, K_{14} = 0.10$	11.7	7.9	14.3	11.3
RWS03	$K_{15} = 1.0, K_{16} = 0.14$	14.1	10.8	17.3	14.1
RKS03	$K_{17} = 0.12, K_{18} = 0.14$	9.7	7.7	9.8	9.1
R07	$K_{19} = 0.07, \ K_{20} = 0.14$	9.6	8.8	9.2	9.2
AB07	$K_{21} = 1.0, K_{22} = 0.14$	7.6	8.1	17.4	11.0
JB07	$K_{23} = 1.0, K_{24} = 1.0$	9.7	8.9	15.0	11.2
RS08	$K_{25} = 1.0, K_{26} = 0.14$	8.5	9.5	12.9	10.3
AREG08	$K_{27} = 1.0, K_{28} = 1.0$	30.9	9.9	18.6	19.8
MD85	$K_{31} = 0.07, K_{32} = 0.27$	10.8	9.0	8.8	9.5

## 4.3.4. Model calibration and comparison

All collected data shown in Table 4.5 are used to calibrate the coefficients  $(K_1 - K_{30})$ . The calibrations are conducted by gradually adjusting the coefficients  $K_1 - K_{28}$ ,  $K_{31}$ , and  $K_{32}$  until the minimum error  $(ER_{avg})$  of each model is obtained. The optimum values of  $K_1 - K_{28}$ ,  $K_{31}$ , and  $K_{32}$  are shown in the second column of Table 4.7.

Using the calibrated coefficients in the computations, the errors ( $ER_g$  and  $ER_{avg}$ ) of each dissipation model for three groups of experiment scale have been computed and shown in Table 4.7. The results can be summarized as follows:

- (a) Most of existing models (except TG83a) give very good prediction ( $ER_{avg} < 10.0\%$ ) for large-scale experiments.
- (b) Eight existing models (BJ78, BS85, RS98, RKS03, R07, AB07, JB07, and RS08) give very good prediction ( $ER_{avg} < 10.0\%$ ) for small-scale experiments.
- (c) Four existing models (BHV98, RWS03, R07, and MD85) give very good prediction ( $ER_{avg} < 10.0\%$ ) for field experiments.
- (d) The overall accuracy of models for computing  $H_{rms}$  in descending order are the models of R07, RKS03, MD85, BS85, RS08, BHV98, AB07, RS98, JB07, RWS03, SN93, BJ78, TG83b, AREG08, and TG83a.

- (e) The top four models that give very good prediction on  $H_{rms}$  are the models of R07, RKS03, MD85, and BS85 ( $8.8 \le ER_{avg} \le 9.7 \%$ ).
- (f) The models developed based on representative wave concept trends to give better estimation than those of parametric wave concept.

**Table 4.7** The errors  $ER_{avg}$  of each dissipation models for computing  $H_{rms}$  by using the

calibrated coefficients (measured data from Table 4.5).

Models	Colibrated apofficients	· · · · · · · · · · · · · · · · · · ·	Apparatus		$ER_{avg}$
Models	Calibrated coefficients	Small scale	Large scale	Field	Livavg
BJ78	$K_1 = 1.19, K_2 = 0.15$	8.8	6.8	26.0	13.9
TG83a	$K_3 = 0.51, K_4 = 0.47$	31.2	16.6	15.9	21.2
TG83	$K_5 = 0.10, K_6 = 0.29$	11.0	6.4	25.6	14.3
BS85	$K_7 = 1.37, K_8 = 0.16$	8.1	9.0	11.9	9.7
SN93	$K_9 = 1.57, K_{10} = 1.15$	12.1	8.5	18.5	13.1
BHV98	$K_{11} = 2.06, \ K_{12} = 1.41$	13.0	8.5	8.8	10.1
RS98	$K_{13} = 0.13, K_{14} = 0.12$	8.6	6.9	16.8	10.8
RWS03	$K_{15} = 1.96, \ K_{16} = 0.20$	15.0	9.9	9.3	11.4
RKS03	$K_{17} = 0.09, K_{18} = 0.13$	9.3	7.0	10.2	8.8
R07	$K_{19} = 0.09, \ K_{20} = 0.16$	9.8	7.7	8.8	8.8
AB07	$K_{21} = 1.03, \ K_{22} = 0.15$	6.8	7.3	17.9	10.7
JB07	$K_{23} = 0.98, K_{24} = 0.99$	9.5	8.9	15.2	11.2
RS08	$K_{25} = 1.09, \ K_{26} = 0.15$	8.3	8.3	13.4	10.0
AREG08	$K_{27} = 0.10, \ K_{28} = 0.51$	10.5	6.5	26.1	14.4
MD85	$K_{31} = 0.09, \ K_{32} = 0.31$	11.3	7.9	8.4	9.2

# 4.4. Conversion from Root-Mean-Square Wave Height to Other Representative Wave Heights

The representative wave heights [e.g. mean wave height ( $H_m$ ), root-mean-square wave height ( $H_{rms}$ ), significant wave height ( $H_{1/3}$ ), highest one-tenth wave height ( $H_{1/10}$ ), and maximum wave height ( $H_{max}$ )] are the essential required factors for the study of coastal processes and the design of coastal structures. The wave heights are usually available in deepwater but not available at the depths required in shallow water. The wave heights in shallow water can be determined from a wave transformation model or phase-resolving wave model. However, the output of many existing wave models (e.g. see Rattanapitikon, 2007) is the root-mean-square wave height ( $H_{rms}$ ). Thus, it is necessary to know conversion formulas for converting from  $H_{rms}$  to other representative wave heights. The present study concentrates on the conversion formulas for converting from common parameters obtained from the wave models [i.e.  $H_{rms}$ , water depth (h), spectral peak period ( $T_p$ ), and beach slope (m)] to be other representative wave heights (i.e.  $H_m$ ,  $H_{1/3}$ ,  $H_{1/10}$ , and  $H_{max}$ ).

In deepwater, the probability density function (pdf) of measured wave heights from different oceans have been found to closely obey the Rayleigh distribution (Demerbilek and Vincent, 2006). Widely accepted conversion formulas are derived based on the assumption of the Rayleigh distribution of wave heights. The representative wave heights can all be converted one to another through the known proportional coefficients.

When waves propagate to shallow water, wave profiles steepen and eventually waves break. The higher waves tend to break at a greater distance from the shore. Closer to the shore, more and more waves are breaking, until in the inner surf zone almost all the waves break. Investigations of shallow-water wave records from several studies indicate the wave heights distribution deviates slightly from the Rayleigh distribution and the conversion formulas derived from the Rayleigh distribution are acceptable (e.g. Goodknight and Russell, 1963; Goda, 1974; and Thornton and Guza, 1983). However, some researchers have pointed out that the wave heights deviate considerably from the Rayleigh distribution (e.g. Dally, 1990; Battjes and Groenendijk, 2000; and Mendez et al., 2004); consequently, the conversion formulas derived from the Rayleigh distribution may not be valid in shallow water. It is expected that the deviation of wave heights from the Rayleigh distribution is mainly caused by the wave breaking.

Several conversion formulas have been proposed for computing the representative wave heights, e.g. the formulas of Longuet-Higgins (1952), Glukhovskiy (1966), Klopman (1996), Battjes and Groenendijk, (2000), and Rattanapitikon and Shibayama (2007). Most of them were developed based on an empirical or semi-empirical approach calibrated with experimental data. To make an empirical formula reliable, it has to be calibrated with a large amount and wide range of experimental conditions. However, most of the existing formulas were developed with limited experimental conditions. Therefore, their coefficients may not be the optimal values for a wide range of experimental conditions and their validity may be limited according to the range of experimental conditions that were employed in calibration or verification. It is not clear which formulas are suitable for computing the representative wave heights from offshore to shoreline. No direct study has been made to describe clearly the accuracy of existing conversion formulas on the estimation of  $H_m$ ,  $H_{1/3}$ ,  $H_{1/10}$ , and  $H_{\rm max}$  for a wide range of experimental conditions. This makes engineers and scientists hesitant in using those conversion formulas. The

objective of this study is to find out the suitable conversion formulas that predict well for a wide range of experimental conditions.

This section is divided into three main parts. The first part is a brief review of selected existing and modified formulas for computing the representative wave heights (i.e.  $H_m$ ,  $H_{1/3}$ ,  $H_{1/10}$ , and  $H_{\rm max}$ ) from the known  $H_{\rm rms}$ . The second part presents the collected data for verifying the conversion formulas. The third part describes the verification of the selected conversion formulas.

#### 4.4.1. Selected conversion formulas

Two approaches have been used to derive the conversion formulas for computing representative wave heights. The first approach derives the formulas by curve fitting between the representative wave heights and the breaker height parameters. The second approach derives the formulas from the selected pdf of wave heights. Various conversion formulas have been proposed, some of which are expressed in terms of uncommon output parameters from most of the existing wave models (e.g. spectral bandwidth and wave nonlinearity parameters), e.g. the distributions of Naess (1985), Hughes and Borgman (1987), Mori and Janssen (2006), and Tayfun and Fedele (2007). Including more related parameters is expected to make the pdf more accurate. However, it may not be suitable to incorporate with most of the existing wave models because such parameters are not available from the wave models. Therefore, this study concentrates on only the formulas which are expressed in terms of common parameters obtained from the wave models, i.e.  $H_{rms}$ , h,  $T_p$ , and m. Brief reviews of selected existing and modified formulas for computing  $H_m$ ,  $H_{1/3}$ ,  $H_{1/10}$ , and  $H_{max}$  are presented below.

a) Longuet-Higgins (1952), hereafter referred to as LH52, demonstrated that the Rayleigh distribution is applicable to the wave heights in the sea. The validity of the distribution for deepwater waves has been confirmed by many researchers, even though the bandwidth may not always be narrow-banded (Demerbilek and Vincent, 2006). The cumulative distribution function (cdf) and the probability density function (pdf) of the Rayleigh distribution can be expressed as:

$$F(H) = 1 - \exp\left[-\left(\frac{H}{H_{rms}}\right)^{2}\right] \tag{4.49}$$

$$f(H) = \frac{dF(H)}{dH} = \frac{2H}{H_{rms}^2} \exp\left[-\left(\frac{H}{H_{rms}}\right)^2\right]$$
(4.50)

where F(H) is the cumulative distribution function (cdf) of wave height (H), f(H) is the probability density function (pdf) of wave height (H), and  $H_{rms}$  is the root-mean-square (rms) wave height, which is defined as:

$$H_{rms} = \sqrt{\frac{\sum H^2}{M}} \tag{4.51}$$

where M is the total number of individual waves identified by the zero-crossing method. The conversion formulas are obtained by manipulation of the pdf of wave heights. The average of the highest 1/N wave heights  $(H_{1/N})$  is defined as:

$$H_{1/N} = N \int_{H_N}^{\infty} Hf(H)dH \tag{4.52}$$

where N is the number of individual waves, and  $H_N$  is the wave height with exceedance probability of 1/N which can be obtained from the cdf as:

$$P(H > H_N) = \frac{1}{N} = 1 - F(H_N) = \exp\left[-\left(\frac{H_N}{H_{rms}}\right)^2\right]$$
 (4.53)

where P is the probability of occurrence. Manipulation of Eq. (4.53) yields,

$$H_N = (\ln N)^{1/2} H_{rms} \tag{4.54}$$

Substituting f(H) from Eq. (4.50) and  $H_N$  from Eq. (4.54) into Eq. (4.52), and taking integration, the result is

$$H_{1/N} = \left[ \sqrt{\ln N} + \frac{N\sqrt{\pi}}{2} erfc\left(\sqrt{\ln N}\right) \right] H_{rms}$$
 (4.55)

where erfc(x) is the complementary error function of variable x. The representative wave heights (i.e.  $H_m$ ,  $H_{1/3}$ , and  $H_{1/10}$ ) can be determined by substituting N equal to 1, 3, and 10, respectively into Eq. (4.55). The maximum wave height is affected by the total number of waves in a record (M) which varies from one sample to another. The probability distribution of  $H_{max}$  in general depends on the sample size and the parent distribution from which the sample was obtained. Longuet-Higgins (1952) proposed a cumulative distribution function of  $H_{max}$  by considering that the cumulative probability of  $H_{max}$  is equal to the total probability of all M waves being less than  $H_{max}$ . The result is

$$F_1(H_{\text{max}}) = [F(H_{\text{max}})]^M$$
 (4.56)

where  $F_1(H_{\rm max})$  is the cumulative distribution function of  $H_{\rm max}$ , and  $F(H_{\rm max})$  is the cumulative distribution function of H at  $H=H_{\rm max}$ . Equation (4.56) is valid if  $H_{\rm max}$  of all M waves are independently and identically distributed. Substituting Eq. (4.49) at  $H=H_{\rm max}$  into Eq. (4.56), the cumulative distribution function of  $H_{\rm max}$  is expressed as:

$$F_1(H_{\text{max}}) = \left\{ 1 - \exp \left[ -\left(\frac{H_{\text{max}}}{H_{rms}}\right)^2 \right] \right\}^M$$
 (4.57)

The arithmetic mean (expected value) is usually used as an approximation of  $H_{\rm max}$ . Based on Eq. (4.57), approximated formula for computing the arithmetic mean of  $H_{\rm max}$  is expressed as:

$$H_{\text{max}} = E(H_{\text{max}}) = \left[\int_{0}^{\infty} H_{\text{max}} f_{1}(H_{\text{max}}) dH_{\text{max}}\right] \approx \left(\sqrt{\ln M} + \frac{0.5772}{2\sqrt{\ln M}}\right) H_{rms}$$
(4.58)

where  $E(H_{\text{max}})$  is the expected value of  $H_{\text{max}}$ , and  $f_1(H_{\text{max}})$  is the pdf of  $H_{\text{max}}$ . From the known  $H_{rms}$  and M, the representative wave heights  $H_{1/N}$  are determined from Eq. (4.55) and  $H_{\text{max}}$  is determined from Eq. (4.58).

b) Glukhovskiy (1966), hereafter referred to as G66, proposed a two parameter Weibull distribution to describe the wave height distribution in shallow water. The influence of depth-limited wave breaking is taken into account by including a function of  $H_m/h$  into

the two parameters. However, the mean wave height  $(H_m)$  is not a common output from most existing wave models. Klopman (1996) suggested replacing  $H_m/h$  with  $0.7H_{rms}/h$ . The cdf and pdf of G66 can be written in terms of  $H_{rms}$  as:

$$F(H) = 1 - \exp\left[-A\left(\frac{H}{H_{rms}}\right)^{\kappa}\right]$$
 (4.59)

$$f(H) = \frac{A \kappa H^{\kappa - 1}}{H_{rms}^{\kappa}} \exp \left[ -A \left( \frac{H}{H_{rms}} \right)^{\kappa} \right]$$
 (4.60)

where A and  $\kappa$  are the position and shape parameters, respectively, which can be determined from the following empirical formulas.

$$A = \left(1 + \frac{1}{\sqrt{2\pi}} \frac{C_2 H_{rms}}{h}\right)^{-1} \tag{4.61}$$

$$\kappa = \frac{C_1}{1 - C_2 H_{rms} / h} \tag{4.62}$$

where  $C_1$  and  $C_2$  are the constants. The proposed values of  $C_1$  and  $C_2$  are 2.0 and 0.7, respectively. It should be noted that when the ratio of  $H_{rms}/h$  gets small (deep water), then A approaches 1,  $\kappa$  approaches 2, and the G66 (Weibull) distribution reverts to Rayleigh. The wave height with exceedance probability of 1/N ( $H_N$ ) and the average of the highest 1/N wave heights ( $H_{1/N}$ ) are obtained by manipulation of the probability function (similar procedure as that of LH52). The results are

$$H_N = \left(\frac{\ln N}{A}\right)^{1/\kappa} H_{rms} \tag{4.63}$$

$$H_{1/N} = \frac{N}{A^{1/\kappa}} \Gamma \left[ \frac{1}{\kappa} + 1, \ln N \right] H_{rms}$$
 (4.64)

where  $\Gamma(a,x)$  is the upper incomplete Gamma function of variables a and x. For computing the maximum wave height ( $H_{\rm max}$ ), following the same procedures as that of LH52, the cdf of  $H_{\rm max}$  can be written as:

$$F_{1}(H_{\text{max}}) = \left\{ 1 - \exp \left[ -A \left( \frac{H_{\text{max}}}{H_{\text{rms}}} \right)^{\kappa} \right] \right\}^{M}$$
(4.65)

Based on Eq. (4.65), an approximated formula for computing the expected value of  $H_{\text{max}}$  is expressed as:

$$H_{\text{max}} \approx \frac{1}{A^{1/\kappa}} \left( \left( \ln M \right)^{1/\kappa} + \frac{0.5772 \left( \ln M \right)^{1/\kappa - 1}}{\kappa} \right) H_{rms}$$
 (4.66)

From the known  $H_{rms}$ , h, and M, the representative wave heights  $H_{1/N}$  are determined from Eq. (4.64) and  $H_{max}$  is determined from Eq. (4.66), in which the parameters A and  $\kappa$  are determined from Eqs. (4.61) and (4.62), respectively. It was pointed out by Klopman (1996) that the distribution of G66 is not consistent, i.e. the first moment of the distribution is not equal to  $H_m$  (if the distribution is expressed in terms of  $H_m$ ) or the second moment of the distribution is not equal to  $H_{rms}^2$  (if the distribution is expressed in

terms of  $H_{\it rms}$ ). However, the distribution of G66 has often been mentioned but it seems that no literature shows its applicability on estimating the representative wave heights. It may be worthwhile to examine its applicability on estimating the representative wave heights.

c) Klopman (1996), hereafter referred to as K96, used the same probability function as that of G66 and consequently the same conversion formulas for computing  $H_{1/N}$  and  $H_{\text{max}}$  [Eqs. (4.64) and (4.66), respectively]. He modified the distribution of G66 by reformulating the position and shape parameters (A and  $\kappa$ ) to assure consistency of the distribution. The parameters A and  $\kappa$  of K96 are determined from the following formulas.

$$A = \left[\Gamma\left(\frac{2}{\kappa} + 1\right)\right]^{\kappa/2} \tag{4.67}$$

$$\kappa = \frac{C_3}{1 - C_4 H_{\text{rms}} / h} \tag{4.68}$$

where  $\Gamma(x)$  is the Gamma function of variable x, and  $C_3$  and  $C_4$  are the constants. The proposed values of  $C_3$  and  $C_4$  are 2.0 and 0.7, respectively. From the known  $H_{rms}$ , h, and M, the representative wave heights  $H_{1/N}$  can be determined from Eq. (4.64) and  $H_{max}$  can be determined from Eq. (4.66), in which the parameters A and  $\kappa$  are determined from Eqs. (4.67) and (4.68), respectively.

d) Battjes and Groenendijk (2000), hereafter referred to as BG00, proposed a composite Weibull wave height distribution to describe the wave height distribution on shallow foreshore. The distribution consists of a Weibull distribution with exponent of 2.0 for the lower wave heights and a Weibull with exponent of 3.6 for the higher wave heights. The two Weibull distributions are matched at the transitional wave height ( $H_{tr}$ ). The cumulative distribution function and the probability density function are described as:

$$F(H) = \begin{cases} 1 - \exp\left[-\left(\frac{H}{H_1}\right)^{C_5}\right] & \text{for } H < H_{tr} \\ 1 - \exp\left[-\left(\frac{H}{H_2}\right)^{C_6}\right] & \text{for } H \ge H_{tr} \end{cases}$$

$$(4.69)$$

$$f(H) = \begin{cases} \frac{C_5 H^{C_5 - 1}}{H_1^{C_5}} \exp\left[-\left(\frac{H}{H_1}\right)^{C_5}\right] & for \quad H < H_{tr} \\ \frac{C_6 H^{C_6 - 1}}{H_2^{C_6}} \exp\left[-\left(\frac{H}{H_2}\right)^{C_6}\right] & for \quad H \ge H_{tr} \end{cases}$$
(4.70)

where  $C_5$  and  $C_6$  are the constants,  $H_1$  and  $H_2$  are the scale parameters, and  $H_{tr}$  is the transitional wave height. The proposed values of  $C_5$  and  $C_6$  are 2.0 and 3.6, respectively. The transitional wave height  $(H_{tr})$  is determined from the following empirical formula.

$$H_{tr} = (0.35 + 5.8m)h \tag{4.71}$$

where m is the beach slope. At the transitional wave height, the wave height distribution abruptly changes its shape. This change in shape is ascribed to wave breaking. Therefore,

 $H_{tr}$  can be considered as a kind of depth-limited breaking or breaker height ( $H_b$ ). For convenience in the calculation, all wave heights are normalized with  $H_{rms}$  as:

$$\widetilde{H}_{x} = \frac{H_{x}}{H_{rms}} \tag{4.72}$$

where  $\tilde{H}_x$  is the normalized characteristic wave height. The normalized transitional wave height  $(\tilde{H}_t)$  can be determined from

$$\widetilde{H}_{tr} = \frac{C_7 H_{tr}}{H_{rms}} \tag{4.73}$$

where  $C_7$  is the constant. The proposed value of  $C_7$  is 1.0. The normalized scale parameters  $\tilde{H}_1$  and  $\tilde{H}_2$  are determined by solving the following 2 equations simultaneously.

$$\tilde{H}_2 = \tilde{H}_{tr} \left( \frac{\tilde{H}_1}{\tilde{H}_{tr}} \right)^{C_5/C_6} \tag{4.74}$$

$$1 = \sqrt{\widetilde{H}_1^2 \gamma \left[ \frac{2}{C_5} + 1, \left( \frac{\widetilde{H}_{tr}}{\widetilde{H}_1} \right)^{C_5} \right] + \widetilde{H}_2^2 \Gamma \left[ \frac{2}{C_6} + 1, \left( \frac{\widetilde{H}_{tr}}{\widetilde{H}_2} \right)^{C_6} \right]}$$
(4.75)

where  $\gamma(a,x)$  is the lower incomplete Gamma function of variables a and x. After manipulation of the probability function (for more detail, please see Groenendijk, 1998), the normalized  $H_N$  and  $H_{1/N}$  are expressed as:

$$\widetilde{H}_{N} = \frac{H_{N}}{H_{rms}} = \begin{cases} \widetilde{H}_{1} [\ln N]^{1/C_{5}} & for \quad \widetilde{H}_{N} < \widetilde{H}_{rr} \\ \widetilde{H}_{2} [\ln N]^{1/C_{6}} & for \quad \widetilde{H}_{N} \ge \widetilde{H}_{rr} \end{cases}$$
(4.76)

$$\frac{H_{rms}}{H_{rms}} = \begin{bmatrix} H_{2}[\ln N] & \text{for } H_{N} \geq H_{tr} \\ N\tilde{H}_{1} \left[ \Gamma \left[ \frac{1}{C_{5}} + 1, \ln N \right] - \Gamma \left[ \frac{1}{C_{5}} + 1, \left( \frac{\tilde{H}_{tr}}{\tilde{H}_{1}} \right)^{C_{5}} \right] \right] + N\tilde{H}_{2}\Gamma \left[ \frac{1}{C_{6}} + 1, \left( \frac{\tilde{H}_{tr}}{\tilde{H}_{2}} \right)^{C_{6}} \right] & \text{for } \tilde{H}_{N} < \tilde{H}_{tr} \\ N\tilde{H}_{2}\Gamma \left[ \frac{1}{C_{6}} + 1, \ln N \right] & \text{for } \tilde{H}_{N} \geq \tilde{H}_{tr} 
\end{cases}$$

$$(4.77)$$

Unlike LH52, Battjes and Groenendijk (2000) did not use the probability function of  $H_{\rm max}$  for computing  $H_{\rm max}$ . They determined the highest wave height in a wave record of total number of waves M (or maximum wave height,  $H_{\rm max}$ ) from the formula of  $H_N$  [Eq. (4.76)]. Substituting N=M into Eq. (4.76), the formula for computing the maximum wave height ( $H_{\rm max}$ ) can be expressed as:

$$\widetilde{H}_{M} = \frac{H_{\text{max}}}{H_{rms}} = \begin{cases} \widetilde{H}_{1} \left[ \ln M \right]^{1/C_{5}} & for \quad \widetilde{H}_{M} < \widetilde{H}_{tr} \\ \widetilde{H}_{2} \left[ \ln M \right]^{1/C_{6}} & for \quad \widetilde{H}_{M} \ge \widetilde{H}_{tr} \end{cases}$$

$$(4.78)$$

All conceivable normalized characteristic wave heights are a function of  $\widetilde{H}_{tr}$  only. From the known  $H_{rms}$ , h, m, and M, the normalized transitional wave height ( $\widetilde{H}_{tr}$ ) is determined from Eq. (4.73) and the normalized scale parameters  $\widetilde{H}_1$  and  $\widetilde{H}_2$  are determined from Eqs. (4.74) and (4.75) simultaneously. Once  $\widetilde{H}_1$  and  $\widetilde{H}_2$  have been determined,  $H_{1/N}$  can be determined from Eq. (4.77) and  $H_{max}$  can be determined from

Eq. (4.78). It should be noted that the disadvantage of BG00 is the complexity of the formulas.

e) Elfrink et al. (2006), hereafter referred to as EHR06, used the same probability function as that of G66 and K96 and, consequently, the same conversion formulas for computing  $H_{1/N}$  and  $H_{max}$  [Eqs. (4.64) and (4.66), respectively]. They modified the distribution of K96 by reformulating the shape parameter ( $\kappa$ ). The proposed formula for computing the parameter  $\kappa$  of EHR06 is expressed as:

$$\kappa = C_8 \left[ \tanh \left( \frac{C_9 H_{rms}}{h} \right) - \left( \frac{C_9 H_{rms}}{h} \right)^2 \right]^2 + C_{10}$$
 (4.79)

where  $C_8$  -  $C_{10}$  are the constants. The proposed values of  $C_8$  -  $C_{10}$  are 15.5, 1.0, and 2.03, respectively. From the known  $H_{rms}$ , h, and M, the representative wave heights  $H_{1/N}$  are determined from Eq. (4.64) and  $H_{max}$  is determined from Eq. (4.66), in which the parameters A and  $\kappa$  are determined from Eqs. (4.67) and (4.79), respectively.

f) Rattanapitikon and Shibayama (2007), hereafter referred to as RS07, modified the conversion formulas of LH52 by empirically incorporating the effect of wave breaking into the formulas. The proportional coefficients ( $\beta$ ) in the formulas of LH52 were fitted with three dimensionless parameters ( $H_{rms}/h$ ,  $H_{rms}/H_{tr}$ , and  $H_{rms}/H_b$ ); consequently, three conversion formulas (hereafter referred to as RS07a, RS07b, and RS07c, respectively) were proposed. The general formulas for computing  $H_{1/N}$  and  $H_{max}$  of RS07a-RS07c are expressed as:

$$H_{1/N} = \beta_{1/N} H_{rms} \tag{4.80}$$

$$H_{\text{max}} = \beta_{\text{max}} \left( \sqrt{\ln M} + \frac{0.5772}{2\sqrt{\ln M}} \right) H_{rms}$$
 (4.81)

where  $\beta$  is the proportional coefficient, and subscripts 1/N and max represent the coefficients for  $H_{1/N}$  and  $H_{\max}$ , respectively. The proportional coefficients  $\beta$  for RS07a-RS07c are determined from the following empirical formulas.

RS07a: 
$$\beta = \begin{cases} K_{1} & \text{for } \frac{H_{rms}}{h} \leq K_{3} \\ K_{1} + \frac{(K_{2} - K_{1})}{(K_{4} - K_{3})} \left( \frac{H_{rms}}{h} - K_{3} \right) & \text{for } K_{3} < \frac{H_{rms}}{h} < K_{4} \\ K_{2} & \text{for } \frac{H_{rms}}{h} \geq K_{4} \end{cases}$$

$$K_{1} + \frac{(K_{2} - K_{1})}{(K_{6} - K_{5})} \left( \frac{H_{rms}}{H_{tr}} - K_{5} \right) & \text{for } K_{5} < \frac{H_{rms}}{H_{tr}} < K_{6} \\ K_{2} & \text{for } \frac{H_{rms}}{H_{tr}} \geq K_{6} \end{cases}$$

$$(4.82)$$

$$K_{2} + \frac{(K_{2} - K_{1})}{(K_{6} - K_{5})} \left( \frac{H_{rms}}{H_{tr}} - K_{5} \right) & \text{for } K_{5} < \frac{H_{rms}}{H_{tr}} < K_{6} \\ K_{2} & \text{for } \frac{H_{rms}}{H_{tr}} \geq K_{6} \end{cases}$$

RS07c: 
$$\beta = \begin{cases} K_{1} & for \quad \frac{H_{rms}}{H_{b}} \leq K_{7} \\ K_{1} + \frac{(K_{2} - K_{1})}{(K_{8} - K_{7})} \left( \frac{H_{rms}}{H_{b}} - K_{7} \right) & for \quad K_{7} < \frac{H_{rms}}{H_{b}} < K_{8} \\ K_{2} & for \quad \frac{H_{rms}}{H_{b}} \geq K_{8} \end{cases}$$
(4.84)

where  $K_1$ - $K_8$  are the constants. The proposed values of  $K_1$ - $K_8$  for coefficients  $\beta$  are shown in the third to sixth columns of Table 4.8. The breaker height ( $H_b$ ) is determined from the breaking criteria of Goda (1970) as:

$$H_b = 0.1L_o \left\{ 1 - \exp\left[ -1.5 \frac{\pi h}{L_o} \left( 1 + 15 m^{4/3} \right) \right] \right\}$$
 (4.85)

where  $L_o$  is the deepwater wavelength related to the spectral peak period  $(T_p)$ . The coefficient 0.1 is used according to Rattanapitikon and Shibayama (1998). From the known  $H_{rms}$ , h,  $T_p$ , m, and M, the representative wave heights  $H_{1/N}$  are determined from Eq. (4.80) and  $H_{max}$  is determined from Eq. (4.81), in which the coefficients  $\beta$  for RS07a, RS07b, and RS07c are determined from Eqs. (4.82), (4.83), and (4.84), respectively.

**Table 4.8** Default and calibrated constants  $K_1$  to  $K_8$  of the coefficients  $\beta$  for RS07a-RS07c.

Formulas	Constants	Defaul	t consta	nts		Calibrated constants				
		$oldsymbol{eta_1}$	$oldsymbol{eta_{1/3}}$	$oldsymbol{eta_{1/10}}$	$eta_{ ext{max}}$	$eta_1$	$oldsymbol{eta_{1/3}}$	$oldsymbol{eta_{1/10}}$	$oldsymbol{eta_{ ext{max}}}$	
RS07a	$K_1$	0.87	1.43	1.81	0.97	0.89	1.41	1.75	1.00	
	$K_2$	0.92	1.36	1.58	0.69	0.92	1.34	1.56	0.69	
	$K_3$	0.10	0.10	0.10	0.10	0.06	0.06	0.06	0.06	
	$K_4$	0.52	0.52	0.52	0.52	0.50	0.50	0.50	0.50	
RS07b	$K_1$	0.87	1.43	1.81	0.97	0.89	1.41	1.75	1.00	
	$K_2$	0.92	1.36	1.58	0.69	0.92	1.34	1.56	0.69	
	$K_5$	0.25	0.25	0.25	0.25	0.15	0.15	0.15	0.15	
	$K_6$	0.95	0.95	0.95	0.95	1.00	1.00	1.00	1.00	
RS07c	$K_1$	0.87	1.43	1.81	0.97	0.89	1.41	1.75	1.0	
	$K_2$	0.92	1.36	1.58	0.69	0.92	1.34	1.56	0.69	
	$K_7$	0.43	0.43	0.43	0.43	0.25	0.25	0.25	0.25	
	$K_8$	1.00	1.00	1.00	1.00	1.00	1.00	1.00	1.00	

g) You (2009), hereafter referred to as Y09, proposed using modified Rayleigh and Weibull distributions to describe the distribution of wave orbital velocity amplitudes. As wave height and orbital velocity amplitude have a certain relationship, the distribution of the orbital velocity may also be applicable for describing the wave height distribution. The cumulative distribution functions of the modified Rayleigh distribution (hereafter referred

to as Y09a) and the Weibull distribution (hereafter referred to as Y09b) can be rewritten in a general form as:

$$F(H) = 1 - \exp\left[-A\left(\frac{H}{H_{rms}}\right)^{\kappa}\right]$$
 (4.86)

The cdf of Y09 [Eq. (4.86)] is the same as that of G66. The difference is the terms of parameters A and  $\kappa$  which are set to be constants as:

Y09a: 
$$A = C_{11}$$
 (4.87)

$$\kappa = 2 \tag{4.88}$$

Y09b: 
$$A = 1$$
 (4.89)

$$\kappa = C_{12} \tag{4.90}$$

where  $C_{11}$  and  $C_{12}$  are the constants. The proposed values of  $C_{11}$  and  $C_{12}$  are 1.09 and 2.15, respectively. As the cdf of Y09 is the same as that of G66, the representative wave heights can be determined from the same equations as of G66. From the known  $H_{rms}$  and M, the representative wave heights  $H_{1/N}$  can be determined from Eq. (4.64) and  $H_{max}$  can be determined from Eq. (4.66), in which the parameters A and  $\kappa$  are determined from Eqs. (4.87) and (4.88) for Y09a and from Eqs. (4.89) and (4.90) for Y09b. It should be noted that the distributions of Y09 are not consistent. The second moment of the distributions are not equal to  $H_{rms}^2$ . However, You (2009) showed that the distributions give better accuracy than that of LH52. It may be worthwhile to examine their applicability on predicting the representative wave heights.

h) As wave breaking may cause the wave height distribution to deviate from the Rayleigh distribution, the variable that may affect the distribution in the shallow water is the terms of depth-limited wave breaking or breaker height. There are three breaker parameters which were used by the previous researchers, i.e. h,  $H_{tr}$  [Eq. (4.71)], and  $H_{b}$  [Eq. (4.85)]. Using the suitable breaker parameters in the conversion formulas is expected to give better accuracy. The modification is carried out by changing the breaker parameters in the conversion formulas. Modified K96 formulas (hereafter referred to as MK96) are performed by changing the breaker parameters in the formula of  $\kappa$ . Replacing h in Eq. (4.68) by  $H_{tr}$  and  $H_{b}$ , respectively, the modified  $\kappa$  can be expressed as:

MK96a: 
$$\kappa = \frac{C_{13}}{1 - C_{14}H_{rms}/H_{tr}}$$
 (4.91)

MK96b: 
$$\kappa = \frac{C_{15}}{1 - C_{16}H_{rms}/H_{b}}$$
 (4.92)

where  $C_{13}$  -  $C_{16}$  are the constants which can be determined from formula calibration. The representative wave heights ( $H_{1/N}$ ) are determined from Eq. (4.64) and maximum wave height ( $H_{max}$ ) is determined from Eq. (4.66), in which the parameter A is determined from Eq. (4.67) and the parameters  $\kappa$  for MK96a and MK96b are determined from Eqs. (4.91) and (4.92), respectively.

i) For similar reasons, modified BG00 formulas (hereafter referred to as MBG00) are performed by changing the breaker parameters in the formula of  $\tilde{H}_{tr}$ . Replacing  $H_{tr}$  in Eq. (4.73) by h and  $H_{b}$ , respectively, the modified  $\tilde{H}_{tr}$  can be expressed as:

MBG00a: 
$$\widetilde{H}_{tr} = \frac{C_{17}h}{H_{rms}}$$
 (4.93)

MBG00b: 
$$\widetilde{H}_{tr} = \frac{C_{18}H_b}{H_{rms}}$$
 (4.94)

where  $C_{17}$  and  $C_{18}$  are the constants which can be determined from formula calibration. The representative wave heights  $H_{1/N}$  and  $H_{max}$  are determined from Eqs. (4.77) and (4.78), respectively, in which the parameters  $\tilde{H}_1$  and  $\tilde{H}_2$  are determined from Eqs. (4.74) and (4.75) simultaneously and  $\tilde{H}_{tr}$  for MBG00a and MBG00b are determined from Eqs. (4.93) and (4.94), respectively.

j) As in item h), modified EHR06 formulas (hereafter referred to as MEHR06) are performed by changing the breaker parameters in the formula of  $\kappa$ . Replacing h in Eq. (4.79) by  $H_{tr}$  and  $H_{b}$ , respectively, the modified  $\kappa$  can be expressed as:

MEHR06a: 
$$\kappa = C_{19} \left[ \tanh \left( \frac{C_{20} H_{rms}}{H_{tr}} \right) - \left( \frac{C_{20} H_{rms}}{H_{tr}} \right)^{2} \right]^{2} + C_{21}$$
 (4.95)

MEHR06a: 
$$\kappa = C_{22} \left[ \tanh \left( \frac{C_{23} H_{rms}}{H_b} \right) - \left( \frac{C_{23} H_{rms}}{H_b} \right)^2 \right]^2 + C_{24}$$
 (4.96)

where  $C_{19}$  -  $C_{24}$  are the constants which can be determined from formula calibration. The representative wave heights  $H_{1/N}$  are determined from Eq. (4.64) and  $H_{\text{max}}$  is determined from Eq. (4.66), in which the parameter A is determined from Eq. (4.67) and the parameters  $\kappa$  for MEHR06a and MEHR06b are determined from Eqs. (4.95) and (4.96), respectively.

k) As the distribution of Y09 is not consistent, it should be modified for consistency. The modified Y09 is performed by reformulating the position and shape parameters (A and  $\kappa$ ). As the probability function of Y09 is the same as that of K96, the position parameter (A) can be determined from Eq. (4.67) while the shape parameter ( $\kappa$ ) is set to be a constant as:

$$\kappa = C_{25} \tag{4.97}$$

where  $C_{25}$  is the constant which can be determined from formula calibration. The representative wave heights  $H_{1/N}$  can be determined from Eq. (4.64) and  $H_{\text{max}}$  can be determined from Eq. (4.66), in which the parameters A and  $\kappa$  are determined from Eqs. (4.67) and (4.97), respectively.

#### 4.4.2. Collected experimental data

The experimental data of representative wave heights (i.e.  $H_m$ ,  $H_{rms}$ ,  $H_{1/3}$ ,  $H_{1/10}$ , and  $H_{max}$ ) from 10 sources (covering 2,619 cases and 19,776 wave records) have been collected for examination of the formulas. The data cover the wave heights in either the offshore zone or surf zone. The collected experiments are separated into 3 groups based on the experiment-scale, i.e. small-scale, large-scale, and field experiments. The small-scale

experiments were conducted under fixed beach conditions whereas the large-scale and field experiments were carried out under movable (sandy) beach conditions. The experiments cover a variety of beach conditions and cover a range of deepwater rms wave steepness ( $H_{rmso}/L_o$ ) from 0.0002 to 0.059. A summary of the collected laboratory data is given in Table 4.9. Some of the data sources are the same as those used by Rattanapitikon and Shibayama (2007). The additional data are from the LIP11D project (Roelvink and Reniers, 1995), SAFE project (Dette et al. 1998), Long (1991), and COAST3D project (Soulsby, 1998).

**Table 4.9** Collected experimental data for verifying conversion formulas.

Sources	Apparatus	Measured wave heights
Smith and Kraus (1990)	small-scale	$H_m$ , $H_{rms}$ , $H_{1/3}$ , $H_{max}$
Ting (2001)	small-scale	$H_m$ , $H_{rms}$ , $H_{1/3}$ , $H_{1/10}$ , $H_{max}$
Ting (2002)	small-scale	$H_{m}, H_{rms}, H_{1/3}, H_{1/10}, H_{max}$
Kraus and Smith (1994):	large-scale	$H_{m}, H_{rms}, H_{1/3}, H_{1/10}, H_{max}$
SUPERTANK project		
Roelvink and Reniers, (1995):	large-scale	$H_{rms}$ , $H_{1/3}$ , $H_{1/10}$ , $H_{max}$
LIP11D Project		
Dette et al. (1998):	large-scale	$H_{rms}$ , $H_{1/3}$ , $H_{1/10}$ , $H_{ m max}$
SAFE project		
Goodknight and Russell (1963)	field	$H_{m}, H_{rms}, H_{1/3}, H_{1/10}, H_{max}$
Long (1991)	field	$H_{m}, H_{rms}, H_{1/3}, H_{1/10}, H_{max}$
Ruessink (1999):	field	$H_m, H_{rms}, H_{1/3}, H_{1/10}$
COAST3D Project at Egmond		
Whitehouse and Sutherland (2001):	field	$H_{m}, H_{rms}, H_{1/3}, H_{1/10}, H_{max}$
COAST3D Project at Teigmond		

Table 4.9 (cont.) Collected experimental data.

Sources	No of	No of	M*	$H_{rmso}/L_{o}$
	cases	points		771130 7
Smith and Kraus (1990)	12	96	500	0.021-0.059
Ting (2001)	1	7	186-207	0.016
Ting (2002)	1	7	154-162	0.015
Kraus and Smith (1994):	128	2,048	152-2,046	0.001-0.046
SUPERTANK project				
Roelvink and Reniers, (1995):	87	170	461-892	0.001-0.029
LIP11D Project				
Dette et al. (1998):	138	3,557	182	0.001-0.020
SAFE project				
Goodknight and Russell (1963)	4	80	95-319	0.011-0.025
Long (1991)	11	11	972-1,693	0.002-0.024
Ruessink (1999):	977	6,480	-	0.002-0.030
COAST3D Project at Egmond				
Whitehouse and Sutherland (2001):	1,260	7,320	132-340	0.0002-0.028
COAST3D Project at Teigmond				
Total	2,619	19,776	95-2,046	0.0002-0.059

<sup>\*</sup> for computing H<sub>max</sub>

A brief summary of the additional data is provided below.

LIP 11D Delta Flume Experiment (Roelvink and Reniers, 1995) was performed at Delft Hydraulics large-scale wave flume. A 175-m-long sandy beach was constructed in a large wave tank of 233 m long, 5 m wide and 7 m deep. The 2 major tests were performed, i.e., with dune (test no. 1A-1C) and without dune (test no 2A-2C). Each major test consisted of several wave conditions. The duration of each wave condition lasted about 12 to 21 hr. Initial beach profiles of the test no. 1A and 2A are equilibrium Dean-type beaches  $(h = A_s x^{2/3})$ , where  $A_s$  is the sediment scale parameter and x is the horizontal distance directed offshore). The beach profiles of other tests (test no. 1B, 1C, 2B, 2E, and 2C) were initiated using the final profile configuration of the previous test. Broad banded random waves, JONSWAP spectrum with spectral width parameter of 3.3, were generated. During the run, the sand bar feature grows and becomes more pronounced after some time. Ten fixed wave gages and one moveable wave gage were deployed in the flume to measure the wave transformation. Only the representative wave heights data from the moveable wave gage are available and are used in this study.

SAFE Project (Dette et al., 1998) was carried out to improve the methods of design and performance assessment of beach nourishment. The SAFE Project consisted of four activities, one of which was to perform experiments in a large-scale wave flume in Hannover, Germany. A 250-m-long sandy beach was constructed in a large wave tank of 300 m long, 5 m wide and 7 m deep. The test program was divided into two major phases. The first phase (test no. A, B, C, and H) was intended to study the beach deformation of equilibrium profile with different beach slope changes. The equilibrium beach profile was adopted from Bruun's (1954) approach. In the second phase, the sediment transport behaviors of dunes with and without structural aid were investigated (test no. D, E, F, and G). The TMA spectral shape with spectral width parameter of 3.3 was used to design all irregular wave tests. A total of 27 wave gages were installed over a length of 175 m along one wall of the flume.

Long (1991) analyzed the measured data which were taken from the measurements archive of CERC's FRF in Duck, NC. Test data were time series from a Waverider buoy near 8-m-depth contour about 1 km offshore. Active depth-induced wave breaking happens at this depth only during extreme conditions. This depth is considered either to be intermediate or shallow for all wind waves of interest. Diversity of wave climate was established by selecting cases classified by energy level as well as broad and narrow energy spread in frequency. Eleven test cases were selected for analysis (from September 1986 to February 1987). The selected cases cover a sequence of measurements before, during, and after a large storm.

COAST3D project is a collaborative project co-funded by the European Commission's MAST-III program and national resources, running from October 1996 to March 2001 (Soulsby, 1998). The project was carried out to improve understanding of the coastal processes on non-uniform (3D) coasts. Two field experiments were performed at Egmond-aan-Zee (Ruessink, 1999) and at Teignmouth (Whitehouse and Sutherland, 2001). The data are available online at

"http://www.hrwallingford.co.uk/projects/COAST3D/". A brief summary of the two sites is given below.

The Egmond site is located in the central part of the Dutch North Sea coast. The site was dominated by two well-developed shore-parallel bars intersected by rip channels. Two field experiments were executed, a pilot experiment in spring 1998 and main experiments (A and B) in autumn 1998. Contrary to the pilot campaign, the main experiment witnessed severe conditions. Large waves, strong wind and water level rises due to storm surges were present, resulting in considerable morphologic change (e.g. bar movement, lowering of bar

crests and the presence of rip channels). The experiments were divided into 3 cases, i.e. pre-storm (pilot experiment), storm (main-A experiment), and post storm (main-B experiment). A large variety of instruments, such as pressure sensors, wave buoys and current meters, were deployed at many stations in the study area. Only the stations which have the representative wave heights data are used in this study, i.e. stations 1a, 1b, 1c, 1d, 2, 7a, 7b, 7c, 7d, and 7e for pilot experiment; stations 1a, 1b, 1c, 1d, 2, 7a, 7b, and 7e for main-A experiment; and stations 1a, 1b, 1c, 1d, 2, 7b, 7d, and 7e for main-B experiment.

The Teigmond site is located on the south coast of Devon, UK. The wave climate was mainly characterized by small, short period wind-driven waves. The nature of the coastline was irregular and three-dimensional (3D), with a rocky headland, nearshore banks, and an estuary mouth all adjacent to the beach with its sea defenses (e.g. groins and seawalls). Two field experiments were executed, a pilot experiment (in March 1999) and a main experiment (during October to November 1999). A large variety of instruments, such as pressure sensors, wave buoys and current meters, was deployed at many stations in the study area. Only the stations which are not located close to the structures or river and have the representative wave heights data are used in this study, i.e. stations 15, 18, 22, and 25 for the pilot experiment and stations 3a, 4, 6, 9, 10, 15, 18, 25, 28, 32, and 33 for the main experiment.

# 4.4.3. Examination of existing conversion formulas

The objective of this section is to examine the applicability of the ten sets of existing conversion formulas (presented in section 4.4.1) on estimating  $H_m$ ,  $H_{1/3}$ ,  $H_{1/10}$ , and  $H_{\rm max}$  from the known  $H_{\rm rms}$ . The measured representative wave heights from 10 sources (covering 2,619 cases) of published experimental results (shown in Table 4.9) are used to calibrate and verify the existing formulas. The basic parameter for measuring the accuracy of a formula is the *rms* relative error ( $ER_{\sigma}$ ) which is defined as:

$$ER_{g} = 100 \sqrt{\frac{\sum_{i=1}^{n_{g}} (H_{cr,i} - H_{mr,i})^{2}}{\sum_{i=1}^{n_{g}} H_{mr,i}^{2}}}$$
(4.98)

where  $H_{cr}$  is the computed representative wave height,  $H_{mr}$  is the measured representative wave height, and  $n_g$  is the total number of representative wave heights in each data group.

To measure a performance of a wave height transformation model, some researchers (e.g. Van Rijn et al., 2003; and Grasmeijer and Ruessink, 2003) excluded the effect of measurement error by adding the measurement error ( $\Delta H_{mr}$ ) to the discrepancy term (i.e.  $|H_{cr}-H_{mr}|-\Delta H_{mr}$ ) in the equation for computing error of the model. The measurement error ( $\Delta H_{mr}$ ) may cause an effect on model comparison. However, the present study concentrates on conversion formulas, in which the computed representative wave height ( $H_{cr}$ ) is determined from the measured  $H_{rms}$ . Since the measured  $H_{rms}$  is determined from the same wave record as the measured representative wave heights ( $H_{mr}$ ), the measurement error of  $H_{rms}$  and  $H_{mr}$  should be in the same proportion. Therefore, the

measurement error may not affect the formula comparisons. Hence, the measurement error  $(\Delta H_{mr})$  is not included in Eq. (4.98).

The collected experiments are separated into three groups according to the experiment scale (i.e. small-scale, large-scale, and field experiments), and four representative wave heights (i.e.  $H_m$ ,  $H_{1/3}$ ,  $H_{1/10}$ , and  $H_{\rm max}$ ) are considered in this study. It is expected that a good formula should be able to predict well for all experiment-scales and all representative wave heights. Therefore, the average error from three experiment-scales ( $ER_{avg}$ ) is used to examine the accuracy of the formulas on estimating each representative wave height, and the overall average error from three experiment-scales and four representative wave heights ( $ER_{all}$ ) is used examine the overall accuracy of the formulas. The average error ( $ER_{avg}$ ) and overall average error ( $ER_{all}$ ) are defined as:

$$ER_{avg} = \frac{\sum_{j=1}^{3} ER_{g,j}}{3}$$
 (4.99)

$$ER_{all} = \frac{\sum_{k=1}^{4} ER_{avg,k}}{4}$$
 (4.100)

#### 4.4.3.1. Examination of existing formulas using default constants

The examinations of the formulas of  $H_{1/N}$  and  $H_{max}$  are carried out by using the measured representative wave heights (i.e.  $H_{rms}$ ,  $H_m$ ,  $H_{1/3}$ ,  $H_{1/10}$ , and  $H_{max}$ ) shown in Table 4.9. From the measured  $H_{rms}$ , the other representative wave heights ( $H_m$ ,  $H_{1/3}$ , and  $H_{1/10}$ , and  $H_{max}$ ) are computed by using the formulas of  $H_{1/N}$  and  $H_{max}$ . Using the default constants ( $C_1 - C_{12}$  and  $K_1 - K_8$ ) in the computations, the errors ( $ER_{avg}$  and  $ER_{all}$ ) of existing formulas for computing  $H_m$ ,  $H_{1/3}$ ,  $H_{1/10}$ , and  $H_{max}$  are shown in Table 4.10.

**Table 4.10** The errors ( $ER_{avg}$  and  $ER_{all}$ ) of the existing formulas on estimating  $H_m$ ,  $H_{1/3}$ ,  $H_{1/10}$ , and  $H_{max}$  from three experiment-scales (using default constants).

Formulas	Default		$ER_{avg}$			
	constants	$H_m$	$H_{1/3}$	$H_{1/10}$	$H_{max}$	
LH52	-	3.2	5.0	11.8	24.8	11.2
G66	$C_1 = 2.0, \ C_2 = 0.7$	2.9	3.7	4.8	11.5	5.7
K96	$C_3 = 2.0, C_4 = 0.7$	3.3	3.4	4.6	11.7	5.7
BG00	$C_5 = 2.0, C_6 = 3.6, C_7 = 1.0$	2.7	3.7	6.4	11.6	6.1
EHR06	$C_8 = 15.5, C_9 = 1.0, C_{10} = 2.03$	3.1	3.9	5.5	15.2	6.9
RS07a	from Table 4.8	2.7	3.6	5.5	10.9	5.7
RS07b	from Table 4.8	2.7	3.6	5.3	12.0	5.9
RS07c	from Table 4.8	2.8	3.7	6.3	10.1	5.7
Y09a	$C_{11} = 1.09$	6.5	3.7	8.0	21.2	9.9
Y09b	$C_{12} = 2.15$	3.3	3.7	8.1	19.8	8.7

It can be seen from Table 4.10 that the formulas of G66, K96, RS07a, and RS07c give the same overall accuracy and give better prediction than the others. The overall accuracy of the formulas in descending order are the formulas of G66, K96, RS07a, RS07c, RS07b, BG00, EHR06, Y09b, Y09a, and LH53. Since most formulas were developed based on a limited range of experimental conditions, the constants in the formulas may not be the optimal values for a wide range of experimental conditions. Therefore, the errors in Table 4.10 should not be used to judge the applicability of the formulas. The constants in all formulas were recalibrated to minimize errors and the applicability of the formulas was then reassessed as shown in the following sections.

#### 4.4.3.2. Calibration of selected formulas

The objective of this section is to calibrate the constants in the selected conversion formulas presented in section 4.4.1 based on a large amount and wide range of experimental conditions. Most of measured data shown in Table 4.9 (except eight wave conditions from eight data sources) are used to calibrate the constants. The calibrations are conducted by gradually adjusting the constants until the minimum overall error ( $ER_{all}$ ) of the formulas is obtained. The optimum values of  $K_1 - K_8$  are shown in the last four columns of Table 4.8, while the optimum values of  $C_1 - C_{25}$  are shown in the second column of Table 4.11. Using the calibrated constants in the computations of  $H_m$ ,  $H_{1/3}$ ,  $H_{1/10}$ , and  $H_{max}$  for three experimental scales, the average errors ( $ER_{avg}$  and  $ER_{all}$ ) of the formulas are shown in Table 4.11, and the errors  $ER_g$  are shown in Table 4.12. The results can be summarized as follows:

- (a) After calibrations, the constants in most existing formulas (except EHR06) have to be changed slightly. However, the use of calibrated constants in the formulas is expected to be more reliable than those of default constants because they are recalibrated with a larger amount and wider range of experimental conditions.
- (b) The overall accuracy of the formulas in descending order are the formulas of RS07c, RS07a, MBG00b, MBG00a, RS07b, MEHR06b, EHR06, G66, MK96b, BG00, K96, MEHR06a, MK96a, MY09, Y09b, Y09a, and LH52. The formulas of RS07c give the best prediction ( $ER_{all} = 5.1\%$ ), while the formulas of LH52 give the worst prediction ( $ER_{all} = 11.1\%$ ). This shows that the distribution of wave heights deviates considerably from the Rayleigh distribution. However, the use of LH52 seems to be acceptable for computing  $H_m$  and  $H_{1/3}$ .
- (c) It can be seen from Table 4.12 that the formulas of LH52, Y09a, Y09b, and MY09 give poor predictions ( $ER_g > 20.0\%$ ) on estimating  $H_{\rm max}$  for small-scale experiments. Only the formula of LH52 gives poor prediction on estimating  $H_{\rm max}$  for large-scale experiments.
- (d) The selected formulas can be separated into two groups, i.e. with breaker parameters (the formulas of G66, K96, BG00, EHR06, RS07a, RS07b, RS07c, MK96a, MK96b, MBG00a, MBG00b, MEHR06a, and MEHR06b), and without breaker parameters (the formulas of LH52, Y09a, Y09b, and MY09). As expected, the formulas with breaker parameters give better accuracy than those without breaker parameters. The overall errors ( $ER_{all}$ ) of the formulas with breaker parameters are in the range of 5.1-5.9%

- while the others are in the range of 7.2-11.1%. This means that the effect of wave breaking is significant and the formulas with breaker parameters are superior.
- (e) Comparing among the formulas with breaker parameters, it can be seen from Tables 4.11 and 4.12 that no formula gives significantly better results than the others.
- (f) The accuracy of all formulas with the breaker parameters is very good  $(5.1 \le ER_{all} \le 5.9\%)$  and seems to be acceptable for the design of coastal structures. It should be noted that, in practical work, the representative wave heights are determined from the selected conversion formulas based on the output  $(H_{rms})$  from the selected wave model. As the average errors of some existing wave models on predicting  $H_{rms}$  are in the range of 8.1-11.4% (Rattanapitikon, 2007), the errors of predicting other representative wave heights should be larger than those shown in Tables 4.11 and 4.12.
- (g) Considering the complexity of the formulas with breaker parameters, the formulas of RS07a are the simplest ones while the formulas of MBG00b are the most complex ones. Considering accuracy and simplicity of the all formulas, the formulas of R07a seem to be the most attractive ones for general applications.

**Table 4.11** The average errors ( $ER_{avg}$  and  $ER_{all}$ ) of the selected formulas on estimating  $H_m$ ,  $H_{1/3}$ ,  $H_{1/10}$ , and  $H_{max}$  from three experiment-scales (using calibrated constants).

	1/10 / Illax 1	1				
Formulas	Calibrated		E	$R_{avg}$		$ER_{all}$
	constants	$H_m$	$H_{1/3}$	$H_{1/10}$	$H_{max}$	
LH52	-	3.2	5.0	11.8	24.6	11.1
G66	$C_1 = 2.0, C_2 = 0.64$	2.7	3.4	4.6	11.8	5.6
K96	$C_3 = 2.0, C_4 = 0.66$	3.2	3.2	4.5	11.8	5.7
BG00	$C_5 = 2.2, C_6 = 3.3, C_7 = 1.0$	2.6	3.3	4.9	11.9	5.7
EHR06	$C_8 = 31, C_9 = 0.53, C_{10} = 2.0$	3.2	3.2	4.7	11.2	5.6
RS07a	from Table 4.8	2.5	3.1	4.4	10.7	5.2
RS07b	from Table 4.8	2.4	3.2	4.5	12.0	5.5
RS07c	from Table 4.8	2.4	3.1	4.5	10.2	5.1
Y09a	$C_{11} = 1.12$	7.7	4.1	7.1	20.1	9.8
Y09b	$C_{12} = 2.41$	3.2	4.4	5.7	16.3	7.4
MK96a	$C_{13} = 2.0, C_{14} = 0.32$	3.1	3.4	4.6	12.8	5.9
MK96b	$C_{15} = 2.0, C_{16} = 0.32$	3.2	3.3	4.4	11.6	5.6
MBG00a	$C_5 = 2.2, C_6 = 3.4, C_{17} = 0.49$	2.7	3.1	5.1	10.7	5.4
MBG00b	$C_5 = 2.2, C_6 = 3.5, C_{18} = 1.1$	2.6	3.1	5.0	10.4	5.3
MEHR06a	$C_{19} = 28, \ C_{20} = 0.27, \ C_{21} = 2.0$	3.0	3.4	4.7	12.4	5.9
MEHR06b	$C_{22} = 34$ , $C_{23} = 0.23$ , $C_{24} = 2.0$	3.2	3.2	4.6	11.1	5.5
MY09	$C_{25} = 2.6$	3.2	3.7	5.7	16.0	7.2

**Table 4.12** The errors  $(ER_g)$  of the selected formulas on estimating  $H_m$ ,  $H_{1/3}$ ,  $H_{1/10}$ , and  $H_{max}$  for small-scale, large-scale, and field experiments (using calibrated constants).

Formulas		Smal	ll-scale			Larg	e-scale			F	ield	
	$H_m$	$H_{1/3}$	$H_{1/10}$	$H_{max}$	$H_m$	$H_{1/3}$	$H_{1/10}$	$H_{max}$	$H_m$	$H_{1/3}$	$H_{1/10}$	$H_{max}$
LH52	4.5	7.9	15.3	43.2	2.3	3.7	10.8	20.7	2.9	3.4	9.4	9.9
G66	2.3	3.7	4.3	16.2	3.9	3.8	5.2	9.8	2.1	2.7	4.1	9.5
K96	2.8	3.7	4.3	16.2	4.4	3.5	5.2	9.9	2.3	2.5	4.1	9.5
BG00	2.4	4.6	4.9	12.6	3.3	2.5	5.1	10.0	2.2	2.7	4.7	13.0
EHR06	2.6	3.4	4.6	14.8	4.4	3.6	5.1	9.3	2.5	2.7	4.4	9.5
RS07a	2.2	4.1	4.1	11.9	3.1	3.0	5.1	10.0	2.0	2.3	4.0	10.1
RS07b	2.3	4.3	4.3	14.1	2.9	2.9	4.9	9.7	2.0	2.4	4.2	12.2
RS07c	2.2	4.1	4.3	10.4	3.0	2.9	5.0	9.6	2.0	2.4	4.1	10.7
Y09a	9.5	3.8	9.3	35.5	5.8	4.8	6.8	16.1	7.9	3.7	5.2	8.8
Y09b	4.4	3.7	5.3	22.9	2.3	5.2	6.4	12.8	2.9	4.2	5.3	13.2
MK96a	2.5	3.8	4.4	18.3	3.9	3.4	4.9	9.6	2.7	3.0	4.4	10.4
MK96b	2.7	3.6	4.1	14.8	4.5	3.5	5.1	9.8	2.5	2.7	4.2	10.2
MBG00a	2.4	4.2	5.1	10.5	3.6	2.6	5.3	10.4	2.0	2.4	4.8	11.2
MBG00b	2.3	4.3	4.9	9.3	3.4	2.5	5.1	10.3	2.0	2.5	4.8	11.7
MEHR06a	2.4	3.6	4.6	17.6	3.8	3.4	4.8	9.1	2.8	3.1	4.6	10.6
MEHR06b	2.6	3.4	4.4	14.1	4.4	3.5	5.0	9.3	2.6	2.8	4.4	10.0
MY09	2.0	4.3	5.5	20.9	5.0	4.0	6.4	12.9	2.6	2.8	5.2	14.1

#### 4.4.3.3. Verification of selected formulas

Eight wave conditions from eight sources (which have more than one case each) are used to verify the conversion formulas. The first case from each data source is selected for verifying the formulas. The experimental conditions of the selected data are shown in Table 4.13. Using the calibrated constants in the computations of  $H_m$ ,  $H_{1/3}$ ,  $H_{1/10}$ , and  $H_{\text{max}}$  for three experiment-scales, the average errors ( $ER_{avg}$  and  $ER_{all}$ ) of the formulas are shown in Table 4.14. The results can be summarized as follows:

- (a) The overall accuracy of the formulas in descending order are the formulas of MBG00b, RS07c, MBG00a, RS07a, MEHR06b, EHR06, G66, BG00, MK96b, K96, MEHR06a, RS07b, MK96a, MY09, Y09b, Y09a, and LH52. The formulas of MBG00b give the best prediction ( $ER_{all} = 5.2\%$ ), while the formulas of LH52 give the worst prediction ( $ER_{all} = 10.2\%$ ).
- (b) The errors in the verification are slightly different from that in the calibration. This is because the number of data that were used in the calibration and verification are different. However, the results of verification are overall similar to that of calibration, i.e. the use of LH52 is acceptable for computing  $H_m$  and  $H_{1/3}$ ; the effect of wave breaking is significant and the formulas with breaker parameters are superior; and the formulas with breaker parameters give very good predictions and have similar accuracy.

**Table 4.13** Selected experimental data for verifying the selected formulas.

Sources	Case	No of	M*	$H_{\it rmso}/L_{\!o}$
	No	points		
Smith and Kraus (1990)	R2000	8	500	0.059
Kraus and Smith (1994):	A0509A	16	354-376	0.043
SUPERTANK project				
Roelvink and Reniers, (1995):	1A0203	2	828-891	0.018
LIP11D Project				
Dette et al. (1998):	06129601	21	182	0.007
SAFE project				
Goodknight and Russell (1963)	Audrey	14	95-319	0.011-0.021
Long (1991)	140986a	1	1,693	0.003
Ruessink (1999):	05064	9	_	0.006
COAST3D Project at Egmond				
Whitehouse and Sutherland (2001):	12500	1	_	0.0003
COAST3D Project at Teigmond				
Total		72	95-1,693	0.0003-0.059

<sup>\*</sup> for computing H<sub>max</sub>

**Table 4.14** Verification results of the selected formulas on estimating  $H_m$ ,  $H_{1/3}$ ,  $H_{1/10}$ , and  $H_{\rm max}$  from three experiment-scales (using calibrated constants).

Formulas	Calibrated		E	$ER_{avg}$		
	constants	$H_m$	$H_{1/3}$	$H_{1/10}$	$H_{max}$	
LH52	-	3.1	4.2	6.8	26.7	10.2
G66	$C_1 = 2.0, C_2 = 0.64$	2.7	3.4	6.3	13.7	6.5
K96	$C_3 = 2.0, C_4 = 0.66$	3.1	3.3	6.2	13.7	6.6
BG00	$C_5 = 2.2, C_6 = 3.3, C_7 = 1.0$	2.5	3.2	6.1	14.2	6.5
EHR06	$C_8 = 31, C_9 = 0.53, C_{10} = 2.0$	3.2	3.3	6.1	12.9	6.4
RS07a	from Table 4.8	2.4	3.4	6.6	12.7	6.3
RS07b	from Table 4.8	2.6	3.6	7.2	14.8	7.0
RS07c	from Table 4.8	2.6	3.4	6.8	10.0	5.7
Y09a	$C_{11} = 1.12$	7.0	5.2	6.6	21.6	10.1
Y09b	$C_{12} = 2.41$	3.1	5.5	8.9	16.8	8.6
MK96a	$C_{13} = 2.0, C_{14} = 0.32$	3.1	3.6	6.8	14.9	7.1
MK96b	$C_{15} = 2.0, C_{16} = 0.32$	3.7	3.5	6.9	12.0	6.5
MBG00a	$C_5 = 2.2, C_6 = 3.4, C_{17} = 0.49$	2.3	3.0	5.2	12.4	5.7
MBG00b	$C_5 = 2.2, C_6 = 3.5, C_{18} = 1.1$	2.5	2.8	5.3	10.4	5.2
MEHR06a	$C_{19} = 28, \ C_{20} = 0.27, \ C_{21} = 2.0$	3.1	3.6	6.8	14.6	7.0
MEHR06b	$C_{22} = 34$ , $C_{23} = 0.23$ , $C_{24} = 2.0$	3.8	3.5	6.7	11.2	6.3
MY09	$C_{25} = 2.6$	4.0	4.6	8.7	16.4	8.4

# 4.5. Conversion from Spectral-Based Wave Height to Other Representative Wave Heights

Representative wave height is one of the most essential required factors for many coastal and ocean engineering applications such as the design of structures and the study of beach deformations. There are two basic approaches to describing wave height parameters, i.e. statistical approach (or wave-by-wave approach) and spectral approach. The two approaches are both important, and neither one alone is sufficient for successful application of wave height for engineering problems (Goda, 1974). While some formulas in coastal and ocean engineering are appropriate for statistical-based wave heights, others may be more appropriate for spectral-based wave heights [related to zeroth moment of wave spectrum  $(m_0)$ ]. The statistical-based wave heights should be used in those applications where the effect of individual waves is more important than the average wave energy. Measured ocean wave records are often analyzed spectrally by an instrument package. Similarly, modern wave hindcasts are often expressed in terms of spectral-based wave height (or  $m_0$ ). The spectral-based wave heights are usually available in deepwater, but not available at the depths required in shallow water. The wave heights in shallow water can be determined from a spectral-based wave model. Hence the output of the wave model is the spectral-based wave height, e.g. spectral significant wave height  $(H_{m0} = 4\sqrt{m_0})$ . However, some formulas in coastal and ocean engineering applications are expressed in terms of statistical-based representative wave heights. Therefore, it is necessary to know conversion formulas for converting from  $m_0$  to statistical-based representative wave heights. The present study focuses on conversion formulas for converting from common parameters obtained from the spectral-based wave model [i.e.  $m_0$ , water depth (h), and spectral peak period  $(T_n)$ ] to the four common statistical-based representative wave heights, i.e. mean wave height  $(H_m)$ , root-mean-square wave height  $(H_{rms})$ , average of the highest one-third wave height  $(H_{1/3})$ , and average of the highest one-tenth wave height ( $H_{1/10}$ ).

Conversions formulas are usually derived based on a given probability distribution function of wave heights. Longuet-Higgins (1952) first applied a Rayleigh distribution function to describe the distribution of ocean waves under the conditions of narrow band spectrum and linear Gaussian ocean surface. If the Rayleigh distribution of wave heights is valid, the representative wave heights can be determined from  $\sqrt{m_0}$  through known proportional constants, e.g.  $H_{1/3} = 4\sqrt{m_0}$ . Because of their simplicity, the conversion formulas of Longuet-Higgins (1952) are widely used in practical work. However, based on the analysis of field data for wind-driven waves in deepwater, Goda (1979) found that the proportional constants have to be reduced, e.g.  $H_{1/3} \approx 3.8 \sqrt{m_0}$ . This discrepancy is expected to be caused by the broad band spectrum in the field (Longuet-Higgins, 1980). Moreover, when waves propagate in shallow water, the effect of wave breaking may become relevant, causing the wave height distribution to deviate from the Rayleigh distribution. Nevertheless, it is not clear whether this deviation has a significant effect on the estimation of the representative wave heights or not. Some researchers demonstrated that the wave height distribution deviated slightly from the Rayleigh distribution (e.g. Thornton and Guza, 1983; Goda and Kudaka, 2007; and Risio et al., 2010). On the other hand, several researchers stated that the wave height distribution deviated considerably

from the Rayleigh distribution (e.g. Klopman, 1996; Battjes and Groenendijk, 2000; and Mendez et al., 2004).

Several conversion formulas with depth-limited wave breaking have been proposed for computing the representative wave heights in shallow water. Battjes and Groenendijk, (2000) compared the accuracy of their formulas with those of Longuet-Higgins (1952) and Klopman (1996), and found that their formulas give the best prediction for small-scale laboratory data. The main difference between laboratory and field experiments is the incident wave spectrum. In the laboratory, the incident wave spectrum is usually based on some standard spectra (e.g. TMA and JONSWAP spectra), while the actual wave spectra in the field usually exhibit some deviations from the standard spectra (Goda, 2000). Therefore, it is not clear, whether the formulas developed based on laboratory conditions are applicable in the field or not. The main objective of this study is to examine five sets of existing conversion formulas with field experiments, and find out a suitable set of conversion formulas.

This section is divided into five main parts. The first part is a brief review of selected existing conversion formulas for computing the representative wave heights (i.e.  $H_m$ ,  $H_{rms}$ ,  $H_{1/3}$ , and  $H_{1/10}$ ) from the common parameters obtained from a spectral-based wave model (i.e.  $m_0$ , h, and  $T_p$ ). The second part is a brief review of the experiments of COAST3D project which are used to examine the conversion formulas. The third part is examination of the existing conversion formulas. The fourth part describes the modification of the best set of existing conversion formulas. The last part presents empirical formulas for computing the representative wave heights.

#### 4.5.1. Existing formulas

For the statistical approach, an individual wave in a wave record is determined by a zero crossing definition of wave. A wave is defined between two upward (or downward) crossings of the water surface about the mean water elevation. The wave height (H) of an individual wave is defined as the difference between the highest and lowest water surface elevation between two zero-up-crossings (or zero-down-crossings). The statistical-based representative wave heights (i.e.  $H_m$ ,  $H_{rms}$ ,  $H_{1/3}$ , and  $H_{1/10}$ ) can be determined from the wave heights data of the wave record.

For the spectral approach, the moments of a wave spectrum are important in characterizing the spectrum and are useful in relating the spectral description of wave to the statistical-based wave heights. The representative parameter of the average wave energy is the zeroth moment of wave spectrum  $(m_0)$ , which can be obtained by integrating the wave spectrum [S(f)] in the full range of frequency (f) as:

$$m_0 = \int_0^\infty S(f)df \tag{4.101}$$

Conversion formulas for computing the statistical-based representative wave heights from the known  $m_0$  can be derived from a given probability density function (pdf) of wave heights. Various pdfs of wave heights have been proposed, some of them are expressed in terms of uncommon output parameters, which are not available from some existing spectral-based wave models (e.g. spectral bandwidth, spectral shape, and wave nonlinearity parameters), e.g. the distributions of Naess (1985), Tayfun and Fedele (2007), Vandever et al. (2008), and Petrova and Soares (2011). Including more related parameters

is expected to make the pdf more accurate. However, it may not be suitable to incorporate them with some spectral-based wave models because such parameters are not available from the wave models. Therefore, this study concentrates on only pdfs which are expressed in terms of common parameters obtained from the spectral-based wave model, i.e.  $m_0$ , h, and  $T_p$ . Brief reviews of the selected existing conversion formulas are described below.

a) Longuet-Higgins (1952), hereafter referred to as LH52, demonstrated that a Rayleigh distribution is applicable to the wave heights in the sea. The Rayleigh distribution is derived based on the assumption that ocean surface elevations follow a linear Gaussian distribution, and the wave energy is concentrated in a narrow band of frequencies. The cumulative distribution function (cdf) of Rayleigh is expressed as:

$$F(H) = 1 - \exp\left[-\left(\frac{H}{\sqrt{8m_0}}\right)^2\right]$$
 (4.102)

where H is the individual wave height, and F(H) is the cdf of H. Longuet-Higgins (1952) derived the conversion formulas based on this cdf.

The root-mean-square wave height can be calculated from the second moment of the *pdf* as:

$$H_{rms} = \sqrt{\int_{0}^{\infty} H^{2} f(H) dH} = \sqrt{\Gamma(\frac{2}{2} + 1)} \sqrt{8m_{0}} = \sqrt{8m_{0}}$$
 (4.103)

where f(H) = dF(H)/dH is the pdf of H, and  $\Gamma(x)$  is the Gamma function of variable x. The formula for computing the average of the highest 1/N wave heights is obtained by manipulation of the pdf of wave heights. The result is:

$$H_{1/N} = N \int_{H_N}^{\infty} Hf(H)dH = N\Gamma \left[ \frac{1}{2} + 1, \ln N \right] \sqrt{8m_0}$$
 (4.104)

where  $H_{1/N}$  the average of the highest 1/N wave heights, N is the number of individual waves,  $H_N$  is the wave height with exceedance probability of 1/N, and  $\Gamma(a,x)$  is the upper incomplete Gamma function of variables a and x. The representative wave heights (i.e.  $H_m$ ,  $H_{1/3}$ , and  $H_{1/10}$ ) can be determined by substituting N equal to 1, 3, and 10, respectively into Eq. (4.104). It can be seen that the conversion formulas of LH52 consists of two main formulas, i.e. the formulas for computing  $H_{rms}$  and  $H_{1/N}$ . From the known  $\sqrt{m_0}$ , the root-mean-square wave height ( $H_{rms}$ ) is determined from Eq. (4.103), and other representative wave heights ( $H_{1/N}$ ) are determined from Eq. (4.104). Substituting N equal to 1, 3, and 10, respectively into Eq. (4.104), yields  $H_m = 2.51\sqrt{m_0}$ ,  $H_{1/3} = 4.00\sqrt{m_0}$ , and  $H_{1/10} = 5.09\sqrt{m_0}$ .

b) Forristall (1978), hereafter referred to as F78, analyzed deepwater wave data recorded during hurricanes in the Gulf of Mexico, and suggested that wave height distribution fits well with the following Weibull distribution.

$$F(H) = 1 - \exp\left[-\left(\frac{H}{2.724\sqrt{m_0}}\right)^{2.126}\right]$$
 (4.105)

Following the same procedures as that of LH52, the formulas for computing  $H_{rms}$  and  $H_{1/N}$  can be derived to be:

$$H_{rms} = \sqrt{2.724^2 m_0 \Gamma(\frac{2}{2.126} + 1)} = 2.689 \sqrt{m_0}$$
 (4.106)

$$H_{1/N} = N2.724\sqrt{m_0}\Gamma \left[\frac{1}{2.126} + 1, \ln(N)\right]$$
 (4.107)

From the known  $\sqrt{m_0}$ , the root-mean-square wave height ( $H_{rms}$ ) is determined from Eq. (4.106), and the other representative wave heights ( $H_{1/N}$ ) are determined from Eq. (4.107). Substituting N equal to 1, 3, and 10, respectively into Eq. (4.107), yields  $H_m = 2.41 \sqrt{m_0}$ ,  $H_{1/3} = 3.77 \sqrt{m_0}$ , and  $H_{1/10} = 4.73 \sqrt{m_0}$ .

c) Klopman (1996), hereafter referred to as K96, used the same probability function as that of Glukhovskiy (1966). He modified the distribution of Glukhovskiy (1966) by reformulating the position and shape parameters. The relationship between  $H_{rms}$  and  $m_0$  was assumed to be the same as that of LH52 [Eq. (4.103)]. The following Weibull distribution is used to describe the wave height distribution.

$$F(H) = 1 - \exp\left[-A\left(\frac{H}{\sqrt{8m_0}}\right)^{\kappa}\right] \tag{4.108}$$

where A is the position parameter, and  $\kappa$  is the shape parameter. The influence of depth-limited wave breaking is taken into account by including a function of  $H_{rms}/h$  (or  $\sqrt{m_0}/h$ ) into the shape parameter as:

$$\kappa = \frac{2}{1 - 1.98\sqrt{m_0}/h} \tag{4.109}$$

where h is the water depth. To assure consistency, the second moment of the pdf has to be equal to  $H_{mns}^2$ . This yields the position parameter (A) as:

$$A = \left[\Gamma\left(\frac{2}{\kappa} + 1\right)\right]^{\kappa/2} \tag{4.110}$$

Similar to the derivation of LH52, the formula for computing the average of the highest 1/N wave heights ( $H_{1/N}$ ) is obtained by manipulation of the pdf of wave heights. The formula for computing  $H_{1/N}$  can be derived to be:

$$H_{1/N} = N \int_{H_N}^{\infty} Hf(H) dH = \frac{N}{A^{1/\kappa}} \Gamma \left[ \frac{1}{\kappa} + 1, \ln N \right] \sqrt{8m_0}$$
 (4.111)

From the known  $\sqrt{m_0}$  and h, the root-mean-square wave height  $(H_{rms})$  is determined from Eq. (4.103), and the other representative wave heights  $(H_{1/N})$  are determined from Eq. (4.111), in which the parameters  $\kappa$  and A are determined from Eqs. (4.109) and (4.110), respectively. It should be noted that the Rayleigh distribution is considered as a

special case of the Weibull distribution. If the parameter  $\kappa$  is equal to 2, the formulas of K96 will become the same as those of LH52.

d) Battjes and Groenendijk (2000), hereafter referred to as BG00, proposed a composite Weibull wave height distribution to describe the wave height distribution on shallow foreshore. The distribution consists of a Weibull distribution with exponent of 2.0 for the lower wave heights and a Weibull distribution with exponent of 3.6 for the higher wave heights. The two Weibull distributions are matched at the transitional wave height ( $H_{tr}$ ). The cdf is expressed as:

$$F(H) = \begin{cases} 1 - \exp\left[-\left(\frac{H}{H_1}\right)^2\right] & \text{for } H < H_{tr} \\ 1 - \exp\left[-\left(\frac{H}{H_2}\right)^{3.6}\right] & \text{for } H \ge H_{tr} \end{cases}$$

$$(4.112)$$

where  $H_1$  and  $H_2$  are the scale parameters. The transitional wave height  $(H_{tr})$  is determined from the following empirical formula.

$$H_{tr} = (0.35 + 5.8m)h (4.113)$$

where m is the beach slope. For convenience in the calculations, all wave heights are normalized with  $H_{rms}$  as:

$$\widetilde{H}_{x} = \frac{H_{x}}{H_{rms}} \tag{4.114}$$

where  $\tilde{H}_x$  is the normalized characteristic wave height. The root-mean-square wave height  $(H_{rms})$  is proposed as a function of  $m_0$  and h as:

$$H_{ms} = \left(2.69 + 3.24 \frac{\sqrt{m_0}}{h}\right) \sqrt{m_0} \tag{4.115}$$

The normalized scale parameters  $\tilde{H}_1$  and  $\tilde{H}_2$  are determined by solving the following 2 equations simultaneously.

$$\tilde{H}_2 = \tilde{H}_{tr} \left( \frac{\tilde{H}_1}{\tilde{H}_{tr}} \right)^{2/3.6} \tag{4.116}$$

$$1 = \sqrt{\widetilde{H}_{1}^{2} \gamma \left[ 2, \left( \frac{\widetilde{H}_{tr}}{\widetilde{H}_{1}} \right)^{2} \right] + \widetilde{H}_{2}^{2} \Gamma \left[ 1.556, \left( \frac{\widetilde{H}_{tr}}{\widetilde{H}_{2}} \right)^{3.6} \right]}$$
(4.117)

where  $\gamma(a,x)$  is the lower incomplete Gamma function of variables a and x. After manipulation of the probability function (for more detail, please see Groenendijk, 1998), the normalized  $H_{\scriptscriptstyle N}$  and  $H_{\scriptscriptstyle 1/N}$  are expressed as:

$$\widetilde{H}_{N} = \frac{H_{N}}{H_{rms}} = \begin{cases} \widetilde{H}_{1} [\ln N]^{1/2} & \text{for } \widetilde{H}_{N} < \widetilde{H}_{tr} \\ \widetilde{H}_{2} [\ln N]^{1/3.6} & \text{for } \widetilde{H}_{N} \ge \widetilde{H}_{tr} \end{cases}$$

$$(4.118)$$

$$\frac{H_{1/N}}{H_{rms}} = \begin{cases}
N\widetilde{H}_{1}\left[\Gamma[1.5, \ln N] - \Gamma\left[1.5, \left(\frac{\widetilde{H}_{tr}}{\widetilde{H}_{1}}\right)^{2}\right]\right] + N\widetilde{H}_{2}\Gamma\left[1.278, \left(\frac{\widetilde{H}_{tr}}{\widetilde{H}_{2}}\right)^{3.6}\right] & \text{for } \widetilde{H}_{N} < \widetilde{H}_{tr} \\
N\widetilde{H}_{2}\Gamma[1.278, \ln N] & \text{for } \widetilde{H}_{N} \ge \widetilde{H}_{tr}
\end{cases} \tag{4.119}$$

From the known  $\sqrt{m_0}$ , h, and m, the root-mean-square wave height ( $H_{rms}$ ) is determined from Eq. (4.115), and the normalized scale parameters  $\tilde{H}_1$  and  $\tilde{H}_2$  are determined from Eqs. (4.116) and (4.117) simultaneously. Once  $\tilde{H}_1$  and  $\tilde{H}_2$  have been determined,  $H_{1/N}$  can be determined from Eqs. (4.118) and (4.119).

e) Elfrink et al. (2006), hereafter referred to as EHR06, used the same probability function as that of K96 and, consequently, the same conversion formulas for computing  $H_{rms}$  and  $H_{1/N}$  [Eqs. (4.103) and (4.111), respectively]. They modified the distribution of K96 by reformulating the shape parameter ( $\kappa$ ). The proposed formula for computing the parameter  $\kappa$  of EHR06 is expressed as:

$$\kappa = 15.5 \left[ \tanh \left( \frac{H_{rms}}{h} \right) - \left( \frac{H_{rms}}{h} \right)^2 \right]^2 + 2.03$$
 (4.120)

From the known  $\sqrt{m_0}$  and h, the representative wave heights  $H_{rms}$  and  $H_{1/N}$  are determined from Eqs. (4.103) and (4.111), respectively, in which the parameters  $\kappa$  and A are determined from Eqs. (4.120) and (4.110), respectively.

It can be seen that the existing formulas are derived based on 2 main distribution functions, i.e. Weibull and composite Weibull distributions. The formulas of BG00 are based on a composite Weibull distribution function, while the others (LH52, F78, K96 and EHR06) are based on a Weibull distribution function. Conversion formulas of a composite Weibull distribution are much more complicated than that of a Weibull distribution. With regard to simplicity of the conversion formulas from Weibull distributions, the formulas of LH52 and F78 have equal simplicity and are simpler than those of K96 and EHR06.

### 4.5.2. Collected experimental data

The existing models of wave height distribution (or conversion formulas) are determined by local parameters of wave field and water depth. The models are expected to be valid for slow evolution of wave and bathymetry (Battjes and Groenendijk, 2000), and have a small influence by discharge from river or wave reflection from structures. Therefore, the selected measuring stations should not be located close to structures or a river mouth, and should not have a significant change in wave and bathymetry. The data required for examination of the conversion formulas are  $m_0$ , h,  $T_p$ ,  $H_m$ ,  $H_{rms}$ ,  $H_{1/3}$ , and  $H_{1/10}$ . Two field experiments from COAST3D project (including 2,237 cases and 13,430 wave records) are used to examine the conversion formulas. The experiments cover a range of  $\sqrt{m_0}/h$  from 0.003 to 0.286, and a range of relative depth (h/L) from 0.01 to 0.63. The collected wave data belong to the category of deepwater, intermediate-depth, and shallow water waves. A summary of the experimental data is shown in Table 4.15. A brief summary of the experiments is outlined below.

COAST3D project is a collaborative project co-funded by the European Commission's MAST-III program and national resources (Soulsby, 1998). Two field experiments were performed at two sites, i.e. at Egmond-aan-Zee (Ruessink, 1999) and at Teignmouth (Whitehouse and Sutherland, 2001). The data are available online at "http://www.hrwallingford.co.uk/projects/COAST3D/". A brief summary of the two sites is given below.

The Egmond site is located in the central part of the Dutch North Sea coast. The study area was about 0.5 by 0.5 km near the beach of Egmond. The site was dominated by two well-developed shore-parallel bars intersected by rip channels. Two field campaigns were executed, i.e. a pilot experiment (during April to May 1998), and main experiments (during October to November 1998). The experiments were divided into 3 conditions, i.e. pre-storm (pilot experiment), storm (main-A experiment), and post storm (main-B experiment). For main-A experiment, large waves and water level rises due to storm surges were present, resulting in considerably bathymetric change (e.g. bar movement and the presence of rip channels). A large variety of instruments was deployed at many stations in the study area. The completed data are available at some stations, i.e. stations 1a, 1b, 1c, 1d, 2, 7a, 7b, 7c, 7d, and 7e for pilot experiment; stations 1a, 1b, 1c, 1d, 2, 7a, 7b, and 7e for main-A experiment; and stations 1a, 1b, 1c, 1d, 2, 7b, 7d, and 7e for main-B experiment. Most available stations (except station 2 for main-A experiment) are used in this study. Station 2 was located close to the crest of a sand bar. Because of the consideration changes of waves and sand bar during storms, the data from station 2 for main-A experiment is excluded in the present study.

The Teigmond site is located on the south coast of Devon, UK. The study area was about 1.5 km along the beach by 1.0 km offshore of the beach. The Teign river mount is situated at the southern end of the beach. The beach is protected by groins and seawalls. A leisure pier is situated around the mid-way along the beach. Two field campaigns were executed, i.e. a pilot experiment (in March 1999), and a main experiment (during October to November 1999). During the experiments, bathymetric changes were minor. A large variety of instruments was deployed at many stations in the study area. The data of water depth and representative wave heights are available at some stations, i.e. stations 1, 2, 15, 18, 22, and 25 for the pilot experiment; and stations 1, 2, 3a, 4, 6, 9, 10, 15, 18, 19a, 20a, 25, 28, 29, 32, and 33 for the main experiment. If the stations are located close to the structures or river mouth, the wave spectra may be affected by discharge from the river and wave reflection from the structures. Only the data at the stations which are not located close to the structures or river mouth are used in the present study, i.e. stations 15, 18, 22, and 25 for the pilot experiment; and stations 3a, 4, 6, 9, 10, 15, 18, 25, 28, 32, and 33 for the main experiment.

**Table 4.15** Collected experimental data from COAST3D project.

Sites	No of	No of	$\sqrt{m_0} / h$	h/L
	cases	records	<b>V</b> 0	
Egmond	977	6,110	0.010-0.286	0.01-0.31
Teigmond	1,260	7,320	0.003-0.110	0.01-0.63
Total	2,237	13,430	0.003-0.286	0.01-0.63

# 4.5.3. Examination of existing formulas

The basic parameter for measuring the accuracy of the conversion formulas is the root-mean-square relative error (*ER*) which is defined as:

$$ER = 100 \sqrt{\frac{\sum_{i=1}^{n} (H_{cr,i} - H_{mr,i})^{2}}{\sum_{i=1}^{n} H_{mr,i}^{2}}}$$
(4.121)

where  $H_{cr}$  is the computed representative wave height,  $H_{mr}$  is the measured representative wave height, and n is the total number of representative wave heights. It is expected that a good set of formulas should be able to predict well for all representative wave heights. Therefore, the average error ( $ER_{avg}$ ) from the four representative wave heights is used to examine the overall accuracy of the set of formulas.

The collected experimental data (shown in Table 4.15) are used to examine the existing formulas. From the known  $m_0$ , h, and m, the representative wave heights ( $H_m$ ,  $H_{rms}$ ,  $H_{1/3}$ , and  $H_{1/10}$ ) are computed from the formulas of LH52, F78, K96, BG00, and EHR06. The errors (ER and  $ER_{avg}$ ) of the existing formulas are shown in the first five rows of Table 4.16.

**Table 4.16** The errors (ER and  $ER_{avg}$ ) of the conversion formulas on estimating  $H_m$ ,  $H_{rms}$ ,  $H_{1/3}$ , and  $H_{1/10}$  for all data shown in Table 4.15.

Formulas		$ER_{avg}$			
	$H_{\scriptscriptstyle m}$	$H_{\it rms}$	$H_{1/3}$	$H_{\scriptscriptstyle 1/10}$	(%)
LH52	3.9	5.6	8.5	14.4	8.1
F78	3.8	2.9	3.7	7.5	4.5
K96	6.6	5.6	5.4	6.9	6.1
BG00	12.8	12.1	11.7	11.9	12.1
EHR06	6.8	5.6	5.1	6.3	6.0
MF78	3.6	2.9	3.2	4.0	3.4
Empirical	3.3	2.8	3.1	3.9	3.3

The results can be summarized as follows.

- a) Table 4.16 shows that the formulas of F78 give the best overall prediction. The overall accuracy of the existing formulas in descending order are F78, EHR06, K96, LH52, and BG00.
- b) The formulas of K96 and EHR06 give nearly the same accuracy, and give good overall prediction ( $ER_{avg} = 6.1$  and 6.0%, respectively), whereas the formulas of BG00 give significantly larger error than those of K96 and EHR06. However, Rattanapitikon (2010) showed that if  $H_{rms}$  is given, the formulas of K96, BG00, and EHR06 give very good predictions and have similar accuracy. Therefore, the fair overall prediction of BG00 ( $ER_{avg} = 12.1\%$ ) may be caused mainly by the formula for computing  $H_{rms}$  [Eq. (4.115)].
- c) The formulas of LH52, which are widely used, give good predictions at  $H_m$ ,  $H_{rms}$ , and  $H_{1/3}$ , but fair prediction at  $H_{1/10}$ . The errors tend to be larger for the larger representative wave heights. The errors of LH52 are considerably larger than those of F78, whereas the simplicity is equal. Therefore, the formulas of F78 are recommended to replace the widely used formulas of LH52.
- d) The formulas of F78 give very good predictions at  $H_m$ ,  $H_{rms}$ , and  $H_{1/3}$  (2.9  $\leq$  ER  $\leq$  3.8%). However, the error at  $H_{1/10}$  is equal to 7.5%, which is considerably

larger than those at  $H_m$ ,  $H_{rms}$ , and  $H_{1/3}$ . The cdf of F78 [Eq. (4.105)] should be improved for better accuracy at  $H_{1/10}$ .

As the cdf of F78 was developed based on deepwater conditions, some parameters in the cdf may not be the optimal values for shallow water conditions. Therefore, there is a possibility to improve its accuracy by reformulating some parameters in the cdf.

#### 4.5.4. Formulas modification

As the formulas of F78 give the best prediction, they are selected to be modified for better prediction. The cdf of F78 [Eq. (4.105)] is expected to be suitable for deepwater condition because it was developed based on deepwater wave data. When waves propagate in shallow water, the effect of wave breaking may become relevant, causing the wave height distribution to deviate from that of F78. Following the concept of Glukhovskiy (1966) and Klopman (1996), the effect of depth-limited breaking is taken into account by including a function of  $\sqrt{m_0}/h$  in the shape parameter of the cdf. The cdf of F78 can be written in general form as:

$$F(H) = 1 - \exp\left[-P\left(\frac{H}{C_1\sqrt{m_0}}\right)^S\right]$$
 (4.122)

in which

$$H_{rms} = C_1 \sqrt{m_0} \tag{4.123}$$

$$S = fu^{\frac{n}{2}} \left\{ \frac{\sqrt{m_0}}{h} \right\} \tag{4.124}$$

where P is the position parameter, S is the shape parameter,  $C_1$  is constant, and  $\int u^n \{x\}$  is a function of variable x. If S = 2.126,  $C_1 = 2.689$ , and P = 0.973, Eq. (4.122) will become the distribution of F78 [Eq. (4.105)].

From  $H_{rms} = \sqrt{\int_{0}^{\infty} H^2 f(H) dH}$ , the position parameter (P) can be expressed as:

$$P = \left\lceil \Gamma \left( \frac{2}{S} + 1 \right) \right\rceil^{S/2} \tag{4.125}$$

The average of the highest 1/N wave heights  $(H_{1/N})$  is determined from:

$$H_{1/N} = N \int_{H}^{\infty} Hf(H)dH = \frac{N}{P^{1/S}} \Gamma \left[ \frac{1}{S} + 1, \ln N \right] C_1 \sqrt{m_0}$$
 (4.126)

It can be seen that there are two independent parameters in Eq. (4.122), i.e.  $C_1$  and S. The main objective of this section is to determine the value of  $C_1$  and the formula of S.

# **4.5.4.1. Determination of** $C_1$ **and** S

As the experiment at Egmond covers a wide range of  $\sqrt{m_0}/h$ , it is used to calibrate and formulate  $C_1$  and S. The constant  $C_1$  can be determined from regression analysis between measured  $H_{rms}$  and  $\sqrt{m_0}$ . The required data for determining  $C_1$  are the measured data of  $H_{rms}$  and  $m_0$ . Based on a regression analysis between the measured  $H_{rms}$  and  $\sqrt{m_0}$ , the constant  $C_1$  is equal to 2.69 (with regression coefficient  $R^2 = 0.995$ ). Substituting  $C_1 = 2.69$  into Eq. (4.123), the formula for computing  $H_{rms}$  can be expressed as:

$$H_{rms} = 2.69\sqrt{m_0} \tag{4.127}$$

It can be seen that the value of  $C_1$  is the same as that of F78. This means that the value of  $C_1$  of F78 is already the optimal value.

The formula of the shape parameter (S) is determined from the graph which shows the relationship between measured S and  $\sqrt{m_0}/h$ . The data of  $m_0$  and h are available from the measurements. The measured value of S can be determined from the measured data of wave height distribution or representative wave heights of a wave record. In the present study, the measured S is determined from the measured representative wave heights because the measured wave height distribution is not available. The measured S can be determined from the ratio of representative wave heights as the following.

From Eq. (4.126), the ratio of representative wave heights  $(H_{1/10}/H_m, H_{1/10}/H_{1/3},$  and  $H_{1/3}/H_m)$  can be expressed as:

$$\frac{H_{1/10}}{H_m} = \frac{10\Gamma\left[\frac{1}{S} + 1, \ln 10\right]}{\Gamma\left[\frac{1}{S} + 1, \ln 1\right]}$$
(4.128)

$$\frac{H_{1/10}}{H_{1/3}} = \frac{10\Gamma\left[\frac{1}{S} + 1, \ln 10\right]}{3\Gamma\left[\frac{1}{S} + 1, \ln 3\right]}$$
(4.129)

$$\frac{H_{1/3}}{H_m} = \frac{3\Gamma\left[\frac{1}{S} + 1, \ln 3\right]}{\Gamma\left[\frac{1}{S} + 1, \ln 1\right]}$$
(4.130)

Equations (4.128) to (4.130) are used to determine the measured S from the measured  $H_m$ ,  $H_{1/3}$ , and  $H_{1/10}$  of a wave record. Equations (4.128) to (4.130) give three values of S for each wave record. The average value of the three S is used to represent the shape parameter (S) of the wave height distribution for the wave record.

Based on the measured data from Egmond site, the relationship between measured S and  $\sqrt{m_0}/h$  is shown in Fig. 4.4. When waves propagate in shallow water, their profiles become steeper and they eventually break. The higher waves tend to break at a greater distance from the shore. Closer to the shore, more and more waves are breaking, until almost all the waves break in the inner zone. Therefore, the zone in coastal region may be separated into 3 zones based on the fraction of breaking waves (total number of breaking

waves per total number of waves), i.e. offshore zone (where there is no wave breaking), outer surf zone (where the fraction of breaking waves increases as more and more waves are breaking), and inner surf zone (where almost all waves break).

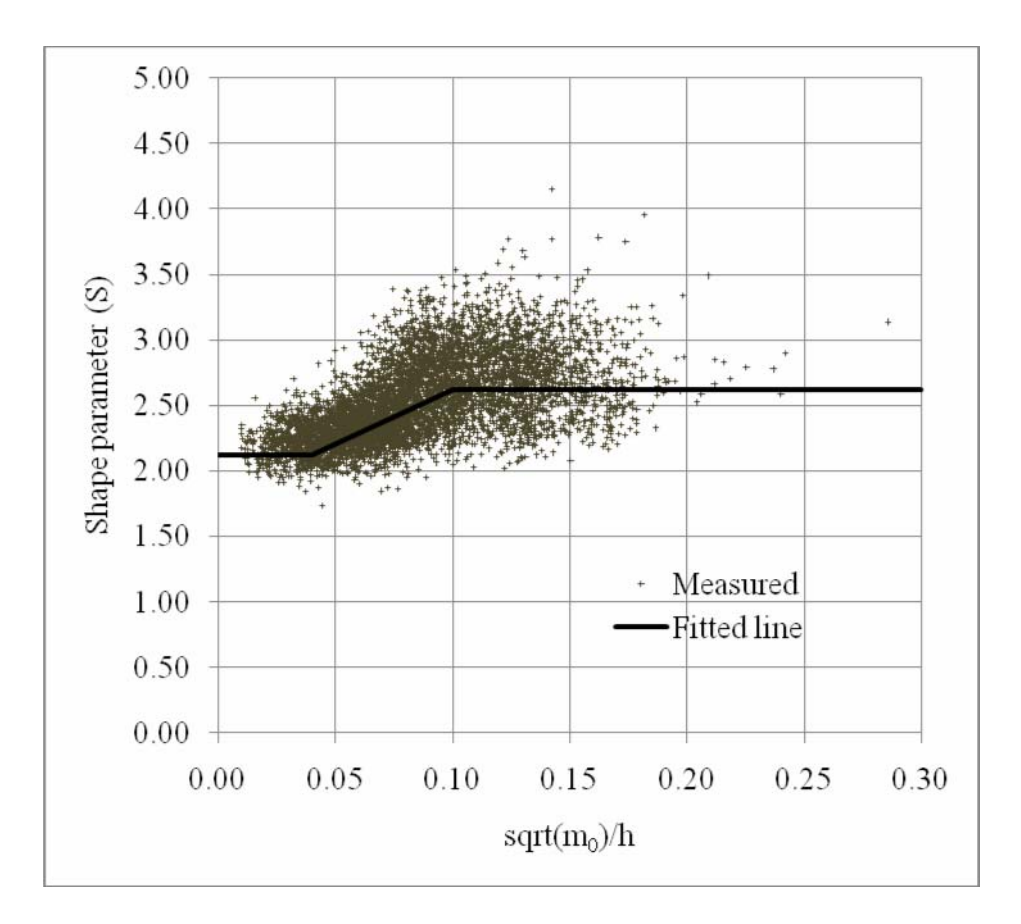


**Fig. 4.4** Relationship between measured S and  $\sqrt{m_0}/h$  (measured data from COAST3D project at Egmond).

It can be seen from Fig. 4.4 that the parameter S varies systematically across shore and the variation can be separated into three zones. The parameter S is almost constant in the first zone, then gradually increases in the second surf zone, and finally becomes almost constant again in the third zone. It is expected that wave breaking is the main factor to cause the change in S. The parameter S is constant in the first zone because there are no waves breaking in that zone (offshore zone). Once the higher waves break, the number of larger wave heights in a wave train is decreased due to wave breaking. This causes the pdf of wave heights to be narrower (and causes S larger) than that in the offshore zone. As more and more waves are breaking, the parameter S is gradually increased in the second zone until almost all waves break, then, the parameter S becomes constant in the third zone. Hence the three zones in Fig. 4.4 seem to correspond with the zones in coastal region. To simplify the calculation, the general form of S is expressed as:

$$S = \begin{cases} K_{1} & for \quad \frac{\sqrt{m_{0}}}{h} \leq x_{1} \\ K_{1} + \frac{(K_{2} - K_{1})}{(x_{2} - x_{1})} \left(\frac{\sqrt{m_{0}}}{h} - x_{1}\right) & for \quad x_{1} < \frac{\sqrt{m_{0}}}{h} < x_{2} \\ K_{2} & for \quad \frac{\sqrt{m_{0}}}{h} \geq x_{2} \end{cases}$$

$$(4.131)$$

where  $K_1$ ,  $K_2$ ,  $x_1$ , and  $x_2$  are constants which can be determined from formula calibration.

The approximated values of the constants  $K_1$ ,  $K_2$ ,  $x_1$ , and  $x_2$  are determined from visual fit of Fig. 4.4. These approximated values are used as the initial values in the calibration. Using the parameter S from Eq. (4.131) with the given constants ( $K_1$ ,  $K_2$ ,  $x_1$ , and  $x_2$ ) and  $C_1$  = 2.69, the representative wave heights ( $H_m$ ,  $H_{1/3}$ , and  $H_{1/10}$ ) are determined from Eq. (4.126). Then the errors ER and  $ER_{avg}$  are computed. The calibration of Eq. (4.131) is performed by gradually adjusting the constants  $K_1$ ,  $K_2$ ,  $K_3$ , and  $K_4$  until the error ( $ER_{avg}$ ) becomes minimum. After calibration, the formula of S can be expressed as:

$$S = \begin{cases} 2.12 & for \quad \frac{\sqrt{m_0}}{h} \le 0.04 \\ 2.12 + \frac{(2.62 - 2.12)}{(0.10 - 0.04)} \left(\frac{\sqrt{m_0}}{h} - 0.04\right) & for \quad 0.04 < \frac{\sqrt{m_0}}{h} < 0.10 \\ 2.62 & for \quad \frac{\sqrt{m_0}}{h} \ge 0.10 \end{cases}$$

$$(4.132)$$

The fitted line from Eq. (4.132) is shown as the solid line in Fig. 4.4.

The modified formulas are hereafter referred to as MF78. However, it should be noted that the *cdf* models of LH52, K96, and EHR06 can also be written in the same general form as that of Eq. (4.122). The modified formulas may also be considered as the modification of LH52, K96, and EHR06.

#### 4.5.4.2. Formulas examination

All collected experimental data (shown in Table 4.15) are used to examine the modified formulas (MF78). From the known  $\sqrt{m_0}$  and h, the representative wave heights  $H_{rms}$  and  $H_{1/N}$  are determined from Eqs. (4.127) and (4.126), respectively, in which the parameters S and P are determined from Eqs. (4.132) and (4.125), respectively. The errors (ER and  $ER_{avg}$ ) of MF78 on computing  $H_m$ ,  $H_{rms}$ ,  $H_{1/3}$ , and  $H_{1/10}$  are shown in the sixth row of Table 4.16. The results are summarized as follows:

- a) The average errors of MF78 for computing  $H_m$ ,  $H_{rms}$ ,  $H_{1/3}$ , and  $H_{1/10}$  are 3.6%, 2.9%, 3.2%, and 4.0%, respectively.
- b) Comparing with the formulas of F78, the accuracy of MF78 is improved slightly at  $H_m$ ,  $H_{rms}$ , and  $H_{1/3}$ , but improved significantly at  $H_{1/10}$ . As  $C_1$  of F78 and MF78 is

- the same value, the main contribution of the improvement is the shape parameter S [Eq. (4.132)].
- c) The formulas of MF78 are more complex than those of F78, but the accuracy is better, especially at  $H_{1/10}$ . It seems to be worthwhile to use MF78.

As the shape parameter S from Eq. (4.132) yields better estimation than that of F78 (S = 2.126), it may be used to indicate the limitation of F78. Equation (4.132) reveals some limitation of F78 as follows:

- a) It can be seen from Eq. (4.132) that the value of S in the offshore zone  $(\sqrt{m_0}/h \le 0.04)$  is nearly the same as that of F78. This shows that the formulas of F78 should be valid for either deepwater or offshore zone conditions. This also reveals the limitation of Eq. (4.132). The equation is limited for use in cases that the wave height distribution in deepwater (or in the offshore zone) is close to the distribution of F78 [Eq. (4.105)].
- b) In the surf zones ( $\sqrt{m_0}/h > 0.04$ ), the number of larger wave heights in a wave train is decreased due to wave breaking. This causes the pdf of wave heights to be narrower (larger S) than that in the offshore zone. The shape parameter of F78 (S=2.126) is smaller than that of MF78 [Eq. (4.132)]. This means that the parameter S of F78 tends to be underestimated and, consequently, gives overestimation of the number of large waves in the distribution. This seems to be the cause of the considerable error at  $H_{1/10}$  of F78 (ER=7.5%).

# 4.5.5. Empirical formulas

It can be seen from sections 4.5.1 and 4.5.4 that the representative wave heights can be determined from a given pdf (or cdf) of wave heights. For design purposes, it may not be necessary to know the pdf of wave heights; only a statistical-based representative wave height is required. Although the representative wave heights ( $H_m$ ,  $H_{rms}$ ,  $H_{1/3}$ , and  $H_{1/10}$ ) can be determined from the pdf of wave heights, it may not be convenient to do so. It is more convenient to determine  $H_m$ ,  $H_{rms}$ ,  $H_{1/3}$ , and  $H_{1/10}$  directly from empirical formulas. There seems to be no literature that proposes empirical formulas for estimating  $H_m$ ,  $H_{1/3}$ , and  $H_{1/10}$  from  $\sqrt{m_0}$ ; only that for estimating  $H_{rms}$  is available.

Rattanapitikon and Shibayama (2007) showed that if  $H_{rms}$  is given, the other representative wave heights can be determined from simple empirical formulas with very good accuracy. In addition, it can be seen from Eq. (4.127) that if  $\sqrt{m_0}$  is given,  $H_{rms}$  can be determined from a simple empirical formula. Therefore, the other representative wave heights should also be able to be computed by using simple empirical formulas. Hence the objective of this section is to develop the empirical formulas for computing  $H_m$ ,  $H_{rms}$ ,  $H_{1/3}$ , and  $H_{1/10}$ .

It can be seen from sections 4.5.1 and 4.5.4 that the general form of the existing formulas for computing the representative wave heights can be expressed as:

$$H_m = \beta_m \sqrt{m_0} \tag{4.133}$$

$$H_{rms} = \beta_{rms} \sqrt{m_0} \tag{4.134}$$

$$H_{1/3} = \beta_{1/3} \sqrt{m_0} \tag{4.135}$$

$$H_{1/10} = \beta_{1/10} \sqrt{m_0} \tag{4.136}$$

where  $\beta$  is the proportional coefficient of each relationship, and  $\beta_m$ ,  $\beta_{rms}$ ,  $\beta_{1/3}$ , and  $\beta_{1/10}$  are the proportional coefficients of  $H_m$ ,  $H_{rms}$ ,  $H_{1/3}$ , and  $H_{1/10}$ , respectively.

The representative wave heights ( $H_m$ ,  $H_{rms}$ ,  $H_{1/3}$ , and  $H_{1/10}$ ) can be determined from Eqs. (4.133) to (4.136), if the coefficients  $\beta$  are known. The main focus of this section is to develop empirical formulas for computing the coefficients  $\beta_m$ ,  $\beta_{rms}$ ,  $\beta_{1/3}$ , and  $\beta_{1/10}$ .

From the modified formulas, the parameter that affects the variation of  $\beta$  is the shape parameter S, and the parameter S depends on  $\sqrt{m_0}/h$ . Therefore, the parameter that affects the variation of  $\beta$  should be  $\sqrt{m_0}/h$ . Therefore, the variations of  $\beta$  can be determined from the graphs of  $\beta$  versus  $\sqrt{m_0}/h$ .

The measured data from Egmond site are used to derive the formulas of  $\beta$ . The required data for deriving the formulas are  $H_m$ ,  $H_{rms}$ ,  $H_{1/3}$ ,  $H_{1/10}$ ,  $m_0$ , and h. The coefficients  $\beta_m$ ,  $\beta_{rms}$ ,  $\beta_{1/3}$ , and  $\beta_{1/10}$  are determined from Eqs. (4.133) to (4.136).

An attempt is made to correlate the coefficients  $\beta_m$ ,  $\beta_{rms}$ ,  $\beta_{1/3}$ , and  $\beta_{1/10}$  with the dimensionless parameter  $\sqrt{m_0}/h$ . The relationships of  $\beta_m$ ,  $\beta_{rms}$ ,  $\beta_{1/3}$ , and  $\beta_{1/10}$  versus  $\sqrt{m_0}/h$  are shown in Fig. 4.5. It can be seen from Fig. 4.5 that the coefficients  $\beta_m$ ,  $\beta_{rms}$ ,  $\beta_{1/3}$ , and  $\beta_{1/10}$  vary systematically across shore, and the variations of the coefficients  $\beta_m$ ,  $\beta_{rms}$ ,  $\beta_{1/3}$ , and  $\beta_{1/10}$  are in similar fashion, and similar to the variation of S (see Fig. 4.4). Therefore, it is possible to write the curve fitting equations in a similar form as that of S [Eq. (4.132)] as:

$$\beta = \begin{cases} K_{3} & for \quad \frac{\sqrt{m_{0}}}{h} \leq 0.04 \\ K_{3} + \frac{(K_{4} - K_{3})}{(0.10 - 0.04)} \left(\frac{\sqrt{m_{0}}}{h} - 0.04\right) & for \quad 0.04 < \frac{\sqrt{m_{0}}}{h} < 0.10 \\ K_{4} & for \quad \frac{\sqrt{m_{0}}}{h} \geq 0.10 \end{cases}$$

$$(4.137)$$

where  $K_3$  and  $K_4$  are constants which can be determined from formula calibration.

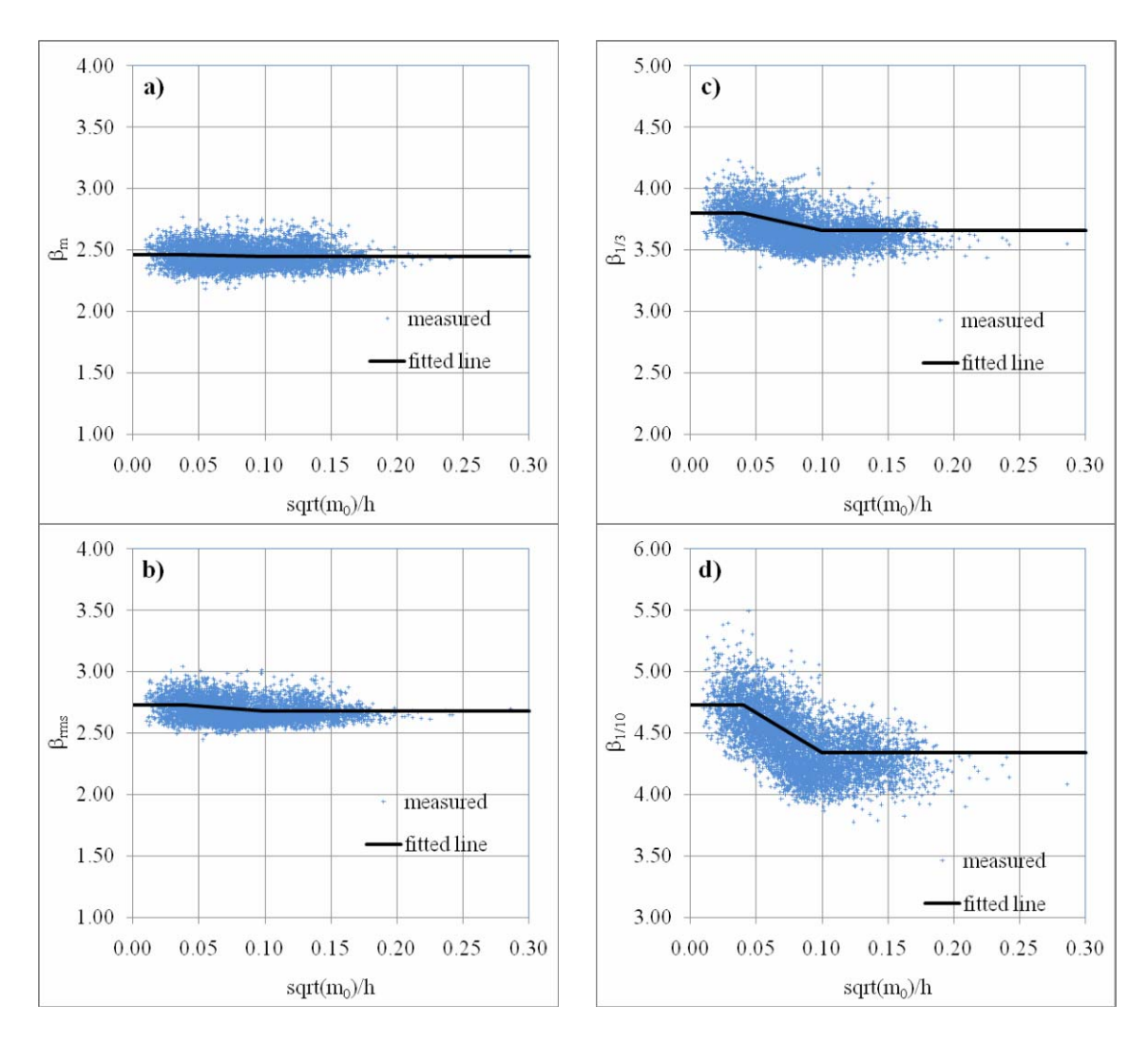


**Fig. 4.5** Relationships between  $\sqrt{m_0}/h$  versus a)  $\beta_m$ , b)  $\beta_{rms}$ , c)  $\beta_{1/3}$ , and d)  $\beta_{1/10}$  (measured data from COAST3D project at Egmond).

#### 4.5.5.1. Formula calibration

The measured data from Egmond site are used to calibrate the constants  $K_3$  and  $K_4$  in Eq. (4.137). The approximated values of the constants  $K_3$  and  $K_4$  for  $\beta_m$ ,  $\beta_{rms}$ ,  $\beta_{1/3}$ , and  $\beta_{1/10}$  are determined from visual fit of Fig. 4.5. These approximated values are used as the initial values in the calibration. Using the coefficients  $\beta$  from Eq. (4.137) with the given constants ( $K_3$  and  $K_4$ ), the corresponding representative wave heights ( $H_m$ ,  $H_{rms}$ ,  $H_{1/3}$ , and  $H_{1/10}$ ) are computed from Eqs. (4.133) to (4.136), respectively. Then the error (ER) of each representative wave height is computed from Eq. (4.121). The calibration of each formula is performed by gradually adjusting the constants  $K_3$  and  $K_4$  until the error (ER) becomes minimum. The best fitted constants ( $K_3$  and  $K_4$ ) for coefficients  $\beta_m$ ,  $\beta_{rms}$ ,  $\beta_{1/3}$ , and  $\beta_{1/10}$  are shown in Table 4.17. The fitted lines from Eq. (4.137) with the constants in Table 4.17 are shown as the solid lines in Fig. 4.5.

**Table 4.17** Calibrated constants  $K_3$  and  $K_4$  of the coefficients  $\beta$ .

Constants	$eta_{\scriptscriptstyle m}$	$eta_{\scriptscriptstyle rms}$	$oldsymbol{eta_{1/3}}$	$oldsymbol{eta_{1/10}}$
$K_3$	2.46	2.73	3.80	4.73
$K_4$	2.45	2.68	3.66	4.34

### 4.5.5.2. Examination of the empirical formulas

All collected data shown in Table 4.15 are used to verify the accuracy of the empirical formulas [Eqs. (4.133) to (4.136)]. Using the coefficients  $\beta$  from Eq. (4.137), the corresponding statistical-based wave heights ( $H_m$ ,  $H_{rms}$ ,  $H_{1/3}$ , and  $H_{1/10}$ ) are computed from Eqs. (4.133) to (4.136), respectively. The errors (ER and  $ER_{avg}$ ) of the empirical formulas on estimating  $H_m$ ,  $H_{rms}$ ,  $H_{1/3}$ , and  $H_{1/10}$  are shown in the last row of Table 4.16. The results are summarized as follows:

- a) The errors (ER) of the empirical formulas for computing  $H_m$ ,  $H_{rms}$ ,  $H_{1/3}$ , and  $H_{1/10}$  are 3.3%, 2.8%, 3.1%, and 3.9%, respectively. It can be seen from Table 4.16 that the empirical formulas give nearly the same accuracy as those of MF78. This shows that they can be used for computing the representative wave heights.
- b) The empirical formulas are slightly more complicated than those of F78, but simpler than those of MF78. Considering the accuracy and simplicity of all conversion formulas, the empirical formulas are recommended for the field conditions.

It should be noted that Eqs. (4.133) to (4.136) are empirical formulas. Their validity may be limited according to the range of experimental conditions that are employed in the calibration. The empirical formulas should be applicable for  $\sqrt{m_0}/h$  ranging between 0.003 and 0.286.

# V. CONCLUSIONS

The main purpose of the present study is to find out suitable wave models for computing common representative (i.e.  $H_m$ ,  $H_{rms}$ ,  $H_{1/3}$ ,  $H_{1/10}$ ,  $H_{max}$ , and  $H_{mo}$ ) based on three main approaches, i.e. empirical approach, representative wave approach, and conversion approach. A large amount of published experimental results covering a wide range of test conditions under irregular wave actions were used to verify the models. The study can be divided into 6 parts. The first part describes the transformation of representative wave heights based on empirical approach. The second part describes the development of wave models using representative wave approach. The third to sixth parts describes the transformation of representative wave heights based on the conversion approach. The following is the conclusions of each part.

- 1. The first part of this study was undertaken to develop empirical formulas for computing the representative wave heights. Laboratory data of unidirectional waves propagating on unbarred beaches, from small-scale and large-scale wave flumes, are used to verify the applicability of Goda formulas for computing the transformation of representative wave heights. The spectral peak period  $(T_p)$  is used in the calculations (instead of using  $T_{1/3}$  or  $T_{m-1,0}$ ) because it is the most commonly used parameter and typically reported for the irregular wave data. All wave parameters in the formulas ( $H_{rep,o}$ ,  $L_o$ ,  $K_s$ , and k) are calculated based on linear wave theory related to  $T_p$ . The verification results are presented in terms of root mean square relative error. The verification shows that the Goda formulas give very good predictions of  $H_{1/3}$  and  $H_{m0}$  but give fair prediction of  $H_{\mathrm{max}}$  . The Goda formulas are rewritten in the form of a general formula. The general form of Goda formulas is recalibrated and extended to compute other representative wave heights (i.e.  $H_m$ ,  $H_{rms}$ , and  $H_{1/10}$ ). After calibration, the accuracy of the general formula for computing  $H_{1/3}$ ,  $H_{\text{max}}$  and  $H_{\text{m0}}$  are improved significantly and the formula can be used for computing  $H_m$ ,  $H_{rms}$ , and  $H_{1/10}$ . The general formula gives very good predictions of  $H_m$ ,  $H_{rms}$ ,  $H_{1/3}$ ,  $H_{1/10}$ ,  $H_{max}$ , and  $H_{m0}$ . The overall errors of the general formula for computing  $H_m$ ,  $H_{rms}$ ,  $H_{1/3}$ ,  $H_{1/10}$ ,  $H_{max}$ , and  $H_{m0}$  are 7.5, 7.5, 7.4, 7.3, 8.8, and 5.9%, respectively.
- 2. The second part was carried out to investigate the possibility of using the wave representation method for computing the representative wave heights. The selected seven dissipation models of regular waves breaking were directly applied to the irregular waves, by using the representative wave heights, to investigate the applicability. The representative wave height transformation is computed from the energy flux conservation law. The breaking criterion of Miche (1994) was applied to compute the incipient breaker height or the starting point to include the energy dissipation into the energy flux conservation. A total of 1729 cases from 13 sources of published experimental results were used to calibrate and examine the models. The experiments cover a wide range of wave and bottom topography conditions, including small-scale, large-scale and field experiments. It was found that by using an appropriate dissipation model, the representative wave approach could be used to compute the representative wave heights transformation with very good predictions. This may lead to the conclusion that the concept of representative wave approach can be used for computing the irregular wave

height transformation. The greatest asset of the present model is its simplicity and ease of application, i.e. the representative wave heights transformation in the nearshore zone can be computed by using only one equation. This study is not meant to replace more complicated models; it is only intended to provide a simple estimation model for including into the cross-shore beach deformation model. As the present model is very simple, it may also serve as a reference model to test a more complicated model against.

- 3. The third part was undertaken to find out the suitable dissipation models, which can be used to compute  $H_{m0}$  for a wide range of experimental conditions. Fourteen existing dissipation models for computing the transformation of  $H_{rms}$  were applied to compute the transformation of  $H_{m0}$ . A total of 1,713 cases from 8 sources of published experimental results were used to examine the applicability of the models in predicting  $H_{\scriptscriptstyle m0}$  . The compiled experimental data cover a wide range of wave conditions  $(0.001 \le H_{m0.0}/L_0 \le 0.069)$ , including small-scale, large-scale and field experiments. The basic parameters used for determination of the accuracy of the models are the rms relative error  $(ER_g)$  of the three groups of experiment-scales and their average  $(ER_{avg})$ . The calibration of each model was conducted by varying the adjustable coefficients (K) in each model until the minimum error ( $ER_{avg}$ ), between the measured and computed wave height, is obtained. Using the calibrated coefficients, the errors ( $ER_g$  and  $ER_{avg}$ ) of the existing models were computed and compared. The comparison shows that the top two models are the models of JB07 and R07. The model of JB07 gives better overall accuracy than that of R07. The greater assets of R07 are its simplicity and it gives good predictions  $(ER_a < 10\%)$  for all experiment-scales. For better accuracy, the model of R07 was modified by changing the stable wave height formula in the model. Comparing with the existing models, the modified model (M1) is the simplest one but gives the best accuracy.
- 4. The fourth part was undertaken to find out the suitable dissipation models, which can be used to compute  $H_{rms}$  for a wide range of experimental conditions. The transformation of  $H_{rms}$  are computed from the energy flux conservation law. Fifteen existing dissipation models are selected to examine their applicability in computing  $H_{rms}$ . A total of 283 cases from 5 sources of published experimental results (including small-scale, large-scale and field experiments) were used to examine the applicability of the models. The verification results are presented in terms of average rms relative error of three experiment scales ( $ER_{avg}$ ). Because most of the existing models were developed without care on the difference between  $H_{rms}$ , the coefficients in the models may not be the optimal values for estimating  $H_{rms}$ . Therefore, coefficients in all models are recalibrated before examining the applicability of the existing models. The models developed based on representative wave concept trends to give better estimation those of parametric wave concept. The top four models that give very good prediction on  $H_{rms}$  are the models of BS85, RKS03, R07, and MD85 ( $8.8\% \le ER_{avg} \le 9.7\%$ ).
- 5. The fifth part was undertaken to find out the suitable conversion formulas for computing the representative wave heights ( $H_m$ ,  $H_{1/3}$ ,  $H_{1/10}$ , and  $H_{max}$ ) from the known common parameters obtained from the statistical-based wave model (i.e.  $H_{rms}$ , h, and  $T_p$ ). The conversion formulas from seven researchers (i.e. LH52, G66, K96, BG00, EHR06, RS07, and Y09) are selected to verify their applicability. The formulas of K96,

BG00, and EHR06 are modified by changing the breaker parameters. The formulas of Y09 are modified by reformulating the position and shape parameters (A and  $\kappa$ ) to assure the consistency of the distribution. A total of 17 sets of conversion formulas are considered in this study. The published experimental data from 10 sources (covering 2,619 cases) are used to calibrate and verify the formulas. The experiments cover small-scale, large-scale, and field experimental conditions. The verification results are presented in terms of overall average rms relative error of 3 experiment-scales and 4 representative wave heights ( $ER_{all}$ ). The constants in all formulas are recalibrated before comparing the accuracy of the formulas. The comparison shows that the formulas with breaker parameters give better accuracy than those without breaker parameters. The accuracy of all formulas with the breaker parameters is not much different and seems to be acceptable for the design of coastal and ocean structures. Considering accuracy and simplicity of the selected formulas, the formulas of RS07a seem to be the most suitable ones for computing the representative wave heights.

6. The last part was undertaken to find out suitable conversion formulas for estimating the statistical-based representative wave heights (i.e.  $H_m$ ,  $H_{rms}$ ,  $H_{1/3}$ , and  $H_{1/10}$ ) from the common parameters obtained from the spectral-based wave model (i.e.  $m_0$ and h). Conversion formulas can be derived from a given cdf (or pdf) of wave heights. Five existing *cdf* models were considered in this study, i.e. the models of LH52, F78, K96, BG00, and EHR06. Field data from COAST3D project (including 13,430 wave records) were used to examine the accuracy of the existing conversion formulas on estimating the representative wave heights. The data cover the wave conditions from deepwater to shallow water. The examination showed that the formulas of LH52, F78, K96, and EHR06 give good overall prediction, while the formulas of BG00 give fair overall prediction. Comparing among the existing formulas, the formulas of F78 give the best overall prediction. The formulas of F78 give very good predictions at  $H_{\rm m}$ ,  $H_{\rm rms}$ , and  $H_{\scriptscriptstyle{1/3}}$  , but give considerably larger error at  $H_{\scriptscriptstyle{1/10}}$  . The  $\it{cdf}$  of F78 was modified by reformulating the formula of shape parameter (S). The new shape parameter reveals that the distribution of F78 is valid in the offshore zone, but gives overestimation of the number of large waves in the surf zone. The modified formulas give better estimation than those of F78, especially for  $H_{1/10}$ . Simple empirical formulas were also proposed. The representative wave heights are expressed as a product of proportional coefficient ( $\beta$ ) and  $\sqrt{m_0}$  . The coefficient  $\beta$  is expressed as a step function of  $\sqrt{m_0}/h$  . The empirical formulas give nearly the same accuracy as those of modified formulas. Considering the accuracy and simplicity of all formulas, the empirical formulas are recommended for the field conditions.

# REFERENCES

- Abadie, S., Butel, R., Mauriet, S., Morichon, D. and Dupuis, H., 2006. Wave climate and longshore drift on the South Aquitaine coast. Continental Shelf Research 26, 1924-1939.
- Alsina, J.M. and Baldock T.E., 2007. Improved representation of breaking wave energy dissipation in parametric wave transformation models. Coastal Engineering 54, 765-769.
- Apotsos, A., Raubenheimer, B., Elgar, S. and Guza, R.T., 2008. Testing and calibrating parametric wave transformation models on natural beaches. Coastal Engineering 55, 224-235.
- Baldock, T.E., Holmes, P., Bunker, S. and Van Weert, P., 1998. Cross-shore hydrodynamics within an unsaturated surf zone. Coastal Engineering 34, 173-196.
- Battjes, J.A. and Groenendijk, H.W., 2000. Wave height distributions on shallow foreshores. Coastal Engineering 40, 161-182.
- Battjes, J.A. and Janssen, J.P.F.M., 1978. Energy loss and set-up due to breaking of random waves. In: Proc. 16th Conf. on Coastal Eng., ASCE, pp. 569-587.
- Battjes, J.A. and Stive M.J.F., 1985. Calibration and verification of a dissipation model for random breaking waves. J. Geophysical Research 90(C5), 9159-9167.
- Birkemeier, W.A., Donoghue, C., Long, C.E., Hathaway, K.K. and Baron C.F., 1997. The DELILAH Nearshore Experiment: Summary Data Report. Waterways Experiment Station, US Army Corps of Engineers.
- Bouws, E., Gunther, H., Rosenthal, W. and Vincent, C.L., 1985. Similarity of the wind wave spectrum in finite depth water. J. Geophysical Research 90 (C1), 975-986.
- Bruun, P., 1954. Coastal Erosion and Development of Beach Profiles. US Army Beach Erosion Board, Tech. Memorandum No. 44, US Army Corps of Engineers.
- Chawla, A., Haller, O. and Kirby, J.T., 1998. Spectral model for wave transformation and breaking over irregular bathymetry. J. Waterway, Port, Coastal and Ocean Engineering, ASCE 124(4), 189-198.
- Dally, W.R., 1990. Random breaking waves: A closed-form solution for planar beaches. Coastal Engineering 14, 233-263.
- Dally, W.R., 1992. Random breaking waves: Field verification of a wave-by-wave algorithm for engineering application. Coastal Engineering 16, 369-397.
- Dally, W.R., Dean, R.G. and Dalrymple, R.A., 1985. Wave height variation across beach of arbitrary profile. J. Geophysical Research 90(C6), 11917-11927.
- Deigaard, R., Justesen, P. and Fredsoe, J., 1991. Modelling of undertow by a one-equation turbulence model. Coastal Engineering 15, 431-458.
- Demerbilek, Z. and Vincent, L., 2006. Water wave mechanics (Part 2 Chapter 1). Coastal Engineering Manual, EM1110-2-1100. Coastal and Hydraulics Laboratory Engineering Research and Development Center, Waterways Experiment Station, US Army Corps of Engineers, pp. II-1-75.
- Dette, H.H, Peters, K. and Newe, J., 1998. MAST III SAFE Project: Data Documentation, Large Wave Flume Experiments '96/97. Report No. 825 and 830, Leichtweiss-Institute, Technical University Braunschweig.
- Elfrink, B., Hanes, D.M. and Ruessink, B.G., 2006. Parameterization and simulation of near bed orbital velocities under irregular waves in shallow water. Coastal Engineering 53, 915-927.
- Forristall, G.Z., 1978. On the statistical distribution of wave heights in storm. J. Geophysical Research 83, 2553-2558.

- Glukhovskiy, B.Kh., 1966. Investigation of sea wind waves. Leningrad, Gidrometeo-izdat (reference obtained from Bouws, E., 1979: Spectra of extreme wave conditions in the Southern North Sea considering the influence of water depth, In: Proc. of Sea Climatology Conference, Paris, pp. 51-71).
- Goda, Y., 1970. A synthesis of breaking indices. Transaction Japan Society of Civil Engineers 2, pp. 227-230.
- Goda, Y., 1974. Estimation of wave statistics from spectral information. In: Proc. Ocean Waves Measurement and Analysis Conference, ASCE, pp. 320-337.
- Goda, Y., 1975. Irregular wave deformation in the surf zone. Coastal Engineering in Japan, JSCE 18, 13-26.
- Goda, Y., 1979. A review on statistical interpretation of wave data. Report of Port and Harbour Research Institute 18, 5-32.
- Goda, Y., 2000. Random Seas and the Design of Maritime Structures. World Scientific Publishing Co. Pte. Ltd.
- Goda, Y., 2004. A 2-D random wave transformation model with gradation breaker index. Coastal Engineering Journal, JSCE 46, 1-38.
- Goda, Y., 2009. A performance test of nearshore wave height prediction with CLASH datasets. Coastal Engineering 56, 220-229.
- Goda, Y. and Kudaka, M., 2007. On the role of spectral width and shape parameters in control of individual wave height distribution. Coastal Engineering Journal 49, 311-335.
- Goodknight, R.C. and Russel, T.L., 1963. Investigation of the statistics of wave heights. J. Waterways and Harbors Division, ASCE 89(WW2), 29-55.
- Grasmeijer, B.T. and Ruessink, B.G., 2003. Modeling of waves and currents in the nearshore parametric vs. probabilistic approach. Coastal Engineering 49, 185-207.
- Grassa, J.M., 1990. Directional random waves propagation on beaches. In: Proc. 22nd Coastal Engineering Conf., ASCE, pp. 798-811.
- Groenendijk, H.W., 1998. Shallow Foreshore Wave Height Statistics, MSc. Thesis, Department of Civil Engineering, Delft University of Technology.
- Hamilton, D.G. and Ebersole, B.A., 2001. Establishing uniform longshore currents in a large-scale sediment transport facility. Coastal Engineering 42, 199-218.
- Hasselmann, K., Barnett, T.P., Bouws, E., Carlson, H., Cartwright, D.E., Enke, K., Ewing, J. A., Gienapp, H., Hasselmann, D.E., Kruseman, P., Meerburg, A., Muller, P., Olbers, D. J., Richter, K., Sell, W. and Walden, H., 1973. Measurements of windwave growth and swell decay during the Joint North Sea Wave Project (JONSWAP). Deutsche Hydrographische Zeitschrift A8(12), 1-95.
- Herbers, T.H.C., Elgar, S., Guza, R.T. and O'Reilly, W.C., 2006. Surface gravity waves and nearshore circulation. DUCK94 Experiment Data Server: SPUV Pressure Sensor Wave Height Data. Available online at: http://dksrv.usace.army.mi/jg/dk94dir.
- Horikawa, K. and Kuo, C.T., 1966. A study of wave transformation inside the surf zone. In: Proc. 10th Coastal Engineering Conf., ASCE, pp. 217-233.
- Hughes, S.A. and Borgman, L.E., 1987. Beta-Rayleigh distribution for shallow water wave heights. In: Proc. of the American Society of Civil Engineers Specialty Conference on Coastal Hydrodynamics, ASCE, 17-31.
- Hurue, M., 1990. Two-Dimensional Distribution of Undertow due to Irregular Waves. B.Eng. Thesis, Dept. of Civil Eng., Yokohama National University, Japan. (in Japanese)

- Isobe, M., 1987. A parabolic equation model for transformation of irregular waves due to refraction, diffraction and breaking. Coastal Engineering in Japan, JSCE 30(1), 33-47.
- Izumiya, T. and Horikawa, K., 1987. On the transformation of directional random wave under combined refraction and diffraction. Coastal Engineering in Japan, JSCE 30(1), 85-101.
- Janssen, T.T. and Battjes, J.A., 2007. A note on wave energy dissipation over steep beaches. Coastal Engineering 54, 711-716.
- Johnson, H.K., 2006. Wave modelling in the vicinity of submerged breakwaters. Coastal Engineering 53, 39-48.
- Katayama, H., 1991. Cross-shore Velocity Distribution due to Breaking of Irregular Waves on a Bar-Type Beach. B.Eng. Thesis, Department of Civil Engineering, Yokohama National University, Japan (in Japanese).
- Klopman, G., 1996. Extreme Wave Heights in Shallow Water, Report H2486. WL/Delft Hydraulics, The Netherlands.
- Kraus, N.C. and Smith, J.M., 1994. SUPERTANK Laboratory Data Collection Project. Technical Report CERC-94-3, Waterways Experiment Station, US Army Corps of Engineers.
- Kuriyama, Y. 1996. Model of wave height and fraction of breaking waves on a barred beach. In: Proc. 25th Coastal Engineering Conf., ASCE, pp. 247-259.
- Larson, M., 1995. Model for decay of random waves in surf zone. J. Waterway, Port, Coastal, and Ocean Engineering, ASCE 121 (1), 1-12.
- Long, C.E., 1991. Use of Theoretical Wave Height Distributions in Directional Seas. Technical Report CERC-91-6. Waterways Experiment Station, US Army Corps of Engineers.
- Longuet-Higgins, M.S., 1952. On the statistical distribution of the heights of sea waves. J. Marine Research 11(3), 245-266.
- Longuet-Higgins, M.S., 1980. On the distribution of the heights of sea waves: Some effects of nonlinearity and finite band width. J. Geophysical Research 85, 1519-1523.
- Mase, H. and Iwagaki, Y., 1982. Wave height distribution and wave grouping in surf zone. In: Proc. 18th Coastal Engineering Conf., ASCE, pp. 58-76.
- Mase, H. and Kirby, J.T., 1992. Hybrid frequency-domain KdV equation for random wave transformation. In: Proc. 23rd Coastal Engineering Conf., ASCE, pp. 474-487.
- Mase, H. and Kitano T., 2000. Spectrum-based prediction model for random wave transformation over arbitrary bottom topography. Coastal Engineering Journal, JSCE 42(1), 111-151.
- Mendez, F.J., Losada, I.J. and Medina, R., 2004. Transformation model of wave height distribution on planar beaches. Coastal Engineering 50, 97-115.
- Miche, R., 1944. Mouvements ondulatoires des mers en profondeur constante on decroissante. Ann. des Ponts et Chaussees, Ch.114, pp.131-164, 270-292, and 369-406.
- Mizuguchi, M., 1982. Individual wave analysis of irregular wave deformation in the nearshore zone. In: Proc. 18th Coastal Engineering Conf., ASCE, pp. 485-504.
- Mori, N. and Janssen, P., 2006. On kurtosis and occurrence probability of freak wave. J. Physical Oceanography 36, 1471-1483.
- Naess, A., 1985. On the distribution of crest-to-trough wave heights. Ocean Engineering 12, 221-234.

- Nairn, R.B., 1990. Prediction of cross-shore sediment transport and beach profile evolution. Ph.D. Thesis, Dept. of Civil Engineering, Imperial College, London.
- Oliveira, F.S.B.F., 2007. Numerical modeling of deformation of multi-directional random wave over a varying topography. Ocean Engineering 34, 337-342.
- Petrova, P.G. and Soares, C.G., 2011. Wave height distributions in bimodal sea states from offshore basins. Ocean Engineering 38, 658-672.
- Panchang, V.G., Pearce, B.R. and Briggs, M.J., 1990. Numerical simulation of irregular wave propagation over shoal. J. Waterway, Port, Coastal and Ocean Engineering, ASCE 116(3), 324-340.
- Rattanapitikon, W., 2007. Calibration and modification of energy dissipation models for irregular waves breaking. Ocean Engineering 34, 1592-1601.
- Rattanapitikon, W., 2008. Verification of significant wave representation method. Ocean Engineering 35, 1259-1270.
- Rattanapitikon, W., 2010. Verification of conversion formulas for computing representative wave heights. Ocean Engineering 37, 1554-1563.
- Rattanapitikon, W. and Sawanggun, S., 2008. Energy dissipation model for a parametric wave approach. Songklanakarin Journal of Science and Technology 30(3), 333-341.
- Rattanapitikon, W. and Shibayama T., 1998. Energy dissipation model for regular and irregular breaking waves. Coastal Engineering Journal, JSCE 40, 327-346.
- Rattanapitikon, W. and Shibayama, T., 2007. Estimation of shallow water representative wave heights. Coastal Engineering Journal, JSCE 49, 291-310.
- Rattanapitikon, W. and Shibayama, T., 2010. Energy dissipation model for computing transformation of spectral significant wave height. Coastal Engineering Journal, JSCE 52, 305-330.
- Rattanapitikon, W., Karunchintadit, R. and Shibayama, T., 2003. Irregular wave height transformation using representative wave approach. Coastal Engineering Journal, JSCE 45, 489-510.
- Risio, M.D., Lisi, I., Beltrami, G.M. and Girolamo, P.D., 2010. Physical modeling of the cross-shore short-term evolution of protected and unprotected beach nourishments. Ocean Engineering 37, 777-789.
- Roelvink, J.A. and Reniers, A.J.H.M., 1995. LIP 11D Delta Flume Experiments: A Data Set for Profile Model Validation. Report No. H 2130, Delft Hydraulics.
- Ruessink, B.G., 1999. COAST3D Data Report 2.5D Experiment, Egmond aan Zee. IMAU Report. Utrecht University.
- Ruessink, B.G., Walstra, D.J.R. and Southgate, H.N., 2003. Calibration and verification of a parametric wave model on barred beaches. Coastal Engineering 48, 139-149.
- Shuto, N., 1974. Nonlinear long waves in a channel of variable section. Coastal Engineering in Japan, JSCE 17, 1-12.
- Smith, E.R. and Kraus, N.C., 1990. Laboratory study on macro-features of wave breaking over bars and artificial reefs. Technical Report CERC-90-12, Waterways Experiment Station, US Army Corps of Engineers.
- Smith, J.M. and Seabergh, W.C., 2001. Wave Breaking on a Current at an Idealized Inlet with an Ebb Shoal. Report No. ERDC/CHL TR-01-7, Engineer Research and Development Center, US Army Corps of Engineers.
- Smith, J.M. and Vincent, C.L., 1992. Shoaling and decay of two wave trains on beach. J. Waterway, Port, Coastal, and Ocean Engineering, ASCE 118(5), 517-533.
- Soulsby, R.L., 1998. Coastal sediment transport: the COAST3D project. In: Proc. 26th Coastal Engineering Conf., ASCE, pp. 2548-2558.

- Southgate, H.N. and Nairn, R.B., 1993. Deterministic profile modelling of nearshore processes. Part 1. Waves and currents. Coastal Engineering 19, 27-56.
- Tayfun, A. and Fedele, F., 2007. Wave height distribution and nonlinear effects. Ocean Engineering 34, 1631-1649.
- Thompson, E.F. and Vincent, C.L., 1985. Significant wave height for shallow water design. J. Waterway, Port, Coastal and Ocean Engineering 111(5), 828-842.
- Thornton, E.B. and Guza, R.T., 1983. Transformation of wave height distribution. J. Geophysical Research 88(C10), 5925-5938.
- Thornton, E.B. and Guza, R.T., 1986. Surf zone longshore currents and random waves: field data and model. J. of Physical Oceanography 16, 1165-1178.
- Ting, F.C.K., 2001. Laboratory study of wave and turbulence velocity in broad-banded irregular wave surf zone. Coastal Engineering 43, 183-208.
- Ting, F.C.K., 2002. Laboratory study of wave and turbulence characteristics in narrow-banded irregular breaking waves. Coastal Engineering 46, 291-313.
- Van Rijn, L.C., Walstra, D.J.R., Grasmeijer, B., Sutherland, J., Pan, S. and Sierra, J.P., 2003. The predictability of cross-shore bed evolution of sandy beaches at the time scale of storms and seasons using process-based profile models. Coastal Engineering 47, 295-327.
- Vandever, J.P., Siegel, E.M., Brubaker, J.M. and Friedrichs, C.T., 2008. Influence of spectral width on wave height parameter estimates in coastal environments. J. Waterway, Port, Coastal, and Ocean Engineering 134(3), 187-194.
- Vink, A.S., 2001. Transformation of wave spectra across the surf zone. M.Sc. Thesis, Faculty of Civil Engineering and Geosciences, Delft University of Technology, The Netherlands.
- Whitehouse, R.J.S. and Sutherland, J., 2001. COAST3D Data Report 3D Experiment, Teignmouth, UK. HR Wallingford Report TR 119.
- You, Z.J., 2009. The statistical distribution of near bed wave orbital velocity in intermediate coastal water depth. Coastal Engineering 58, 844-852.

# **OUTPUTS**

# **International Journals:**

- 1) Rattanapitikon, W., 2010. Verification of conversion formulas for computing representative wave heights. Ocean Engineering 37, 1554-1563.
- 2) Rattanapitikon, W. and Shibayama, T., 2010. Energy dissipation model for computing transformation of spectral significant wave height. Coastal Engineering Journal, JSCE 52, 305-330.
- 3) Nuntakamol, P. and Rattanapitikon, W., 2011. Conversion formulas for estimating statistical-based representative wave heights from zeroth moment of wave spectrum based on field experiments. Ocean Engineering, **submitted**.

# **National Journals:**

1) Nuntakamol, P. and Rattanapitikon, W., 2011. Transformation of mean and highest one-tenth wave heights using representative wave approach. Kasetsart Journal: Natural Science, **submitted**.

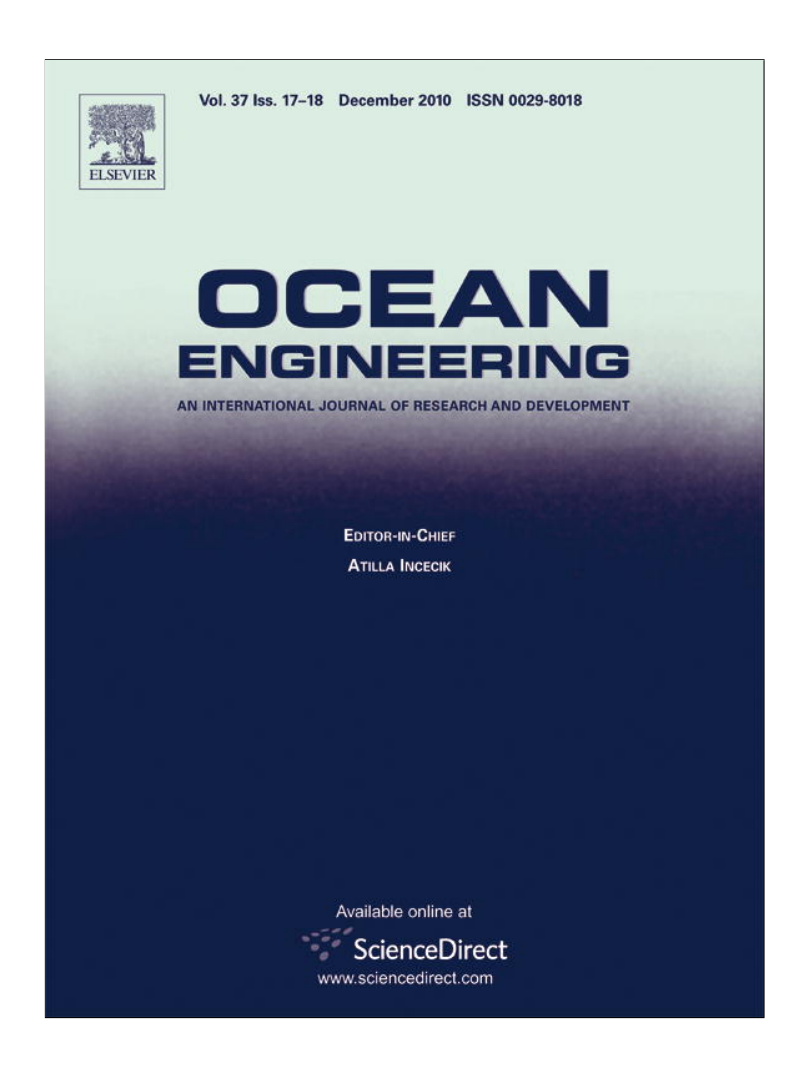
# **APPENDIX: PAPER REPRINTS**

# **A.1** Verification of conversion formulas for computing representative wave heights

Reprinted from:

Rattanapitikon, W., 2010. Verification of conversion formulas for computing representative wave heights. Ocean Engineering 37, 1554-1563.

Provided for non-commercial research and education use. Not for reproduction, distribution or commercial use.



This article appeared in a journal published by Elsevier. The attached copy is furnished to the author for internal non-commercial research and education use, including for instruction at the authors institution and sharing with colleagues.

Other uses, including reproduction and distribution, or selling or licensing copies, or posting to personal, institutional or third party websites are prohibited.

In most cases authors are permitted to post their version of the article (e.g. in Word or Tex form) to their personal website or institutional repository. Authors requiring further information regarding Elsevier's archiving and manuscript policies are encouraged to visit:

http://www.elsevier.com/copyright

# **Author's personal copy**

Ocean Engineering 37 (2010) 1554-1563



Contents lists available at ScienceDirect

# Ocean Engineering

journal homepage: www.elsevier.com/locate/oceaneng



# Verification of conversion formulas for computing representative wave heights

Winyu Rattanapitikon\*

Civil Engineering Program, Sirindhorn International Institute of Technology, Thammasat University, Pathum Thani 12121, Thailand

#### ARTICLE INFO

Article history: Received 18 January 2010 Accepted 26 September 2010 Editor-in-Chief: A.I. Incecik Available online 12 October 2010

Keywords:
Rayleigh distribution
Weibull distribution
Surf zone
Representative wave height
Conversion formula

#### ABSTRACT

This study is undertaken to find out suitable conversion formulas for computing representative wave heights (i.e. mean, significant, highest one-tenth, and maximum wave heights) from the known commonly used parameters (i.e. root mean square wave height, water depth, spectral peak period, and beach slope). Seventeen sets of conversion formulas (including existing and modified formulas) are recalibrated and their accuracy is compared. A large amount and wide range of experimental conditions from small-scale, large-scale, and field experiments (2619 cases collected from 10 sources) are used to calibrate and verify the conversion formulas. The examination shows that most of the selected formulas give very good predictions and have similar accuracy. The suitable formulas are recommended based on the consideration of accuracy and simplicity of the formulas.

© 2010 Elsevier Ltd. All rights reserved.

#### 1. Introduction

The representative wave heights [e.g. mean wave height  $(H_m)$ , root mean square wave height ( $H_{rms}$ ), significant wave height  $(H_{1/3})$ , highest one-tenth wave height  $(H_{1/10})$ , and maximum wave height  $(H_{max})$ ] are the essential required factors for the study of coastal processes and the design of coastal structures. The wave heights are usually available in deepwater but not available at the depths required in shallow water. The wave heights in shallow water can be determined from a wave transformation model or phase-resolving wave model. However, the output of many existing wave models (e.g. see Rattanapitikon, 2007) is the root mean square wave height  $(H_{rms})$ . Thus, it is necessary to know conversion formulas for converting from  $H_{rms}$  to other representative wave heights. The present study concentrates on the conversion formulas for converting from common parameters obtained from the wave models [i.e.  $H_{rms}$ , water depth (h), spectral peak period  $(T_p)$ , and beach slope (m)] to be other representative wave heights (i.e.  $H_m$ ,  $H_{1/3}$ ,  $H_{1/10}$ , and  $H_{max}$ ).

In deepwater, the probability density function (*pdf*) of measured wave heights from different oceans have been found to closely obey the Rayleigh distribution (Demerbilek and Vincent, 2006). Widely accepted conversion formulas are derived based on the assumption of the Rayleigh distribution of wave heights. The representative wave heights can all be converted one to another through the known proportional coefficients.

When waves propagate to shallow water, wave profiles steepen and eventually waves break. The higher waves tend to break at a greater distance from the shore. Closer to the shore, more and more waves are breaking, until in the inner surf zone almost all the waves break. Investigations of shallow-water wave records from several studies indicate the wave heights distribution deviates slightly from the Rayleigh distribution and the conversion formulas derived from the Rayleigh distribution are acceptable (e.g. Goodknight and Russell, 1963; Goda, 1974; Thornton and Guza, 1983). However, some researchers have pointed out that the wave heights deviate considerably from the Rayleigh distribution (e.g. Dally, 1990; Battjes and Groenendijk, 2000; Mendez et al., 2004); consequently, the conversion formulas derived from the Rayleigh distribution may not be valid in shallow water. It is expected that the deviation of wave heights from the Rayleigh distribution is mainly caused by the wave breaking.

Several conversion formulas have been proposed for computing the representative wave heights, e.g. the formulas of Longuet-Higgins (1952), Glukhovskiy (1966), Klopman (1996), Battjes and Groenendijk, (2000), and Rattanapitikon and Shibayama (2007). Most of them were developed based on an empirical or semi-empirical approach calibrated with experimental data. To make an empirical formula reliable, it has to be calibrated with a large amount and wide range of experimental conditions. However, most of the existing formulas were developed with limited experimental conditions. Therefore, their coefficients may not be the optimal values for a wide range of experimental conditions and their validity may be limited according to the range of experimental conditions that were employed in calibration or verification. It is not clear which formulas are suitable for

<sup>\*</sup>Tel.: +66 2564 3221; fax: +66 2986 9112. E-mail address: winvu@siit.tu.ac.th

Nomenclature	$H_{1/10} \  ilde{H}_{tr}$	highest one-tenth wave height normalized transitional wave height
A position parameter	$\tilde{H}_{x}$	normalized characteristic wave height
A <sub>s</sub> sediment scale parameter	$ ilde{H}_1$	normalized scale parameter no. 1
$C_i$ constant no. $i$	$ ilde{H}_2$	normalized scale parameter no. 2
erfc(x) complementary error function of variable x	$L_o$	deepwater wavelength related to the spectral peak
$E(H_{max})$ expected value of $H_{max}$		period
f(H) probability density function of wave height $(H)$	m	beach slope
$f_1(H_{max})$ probability density function of $H_{max}$	M	total number of individual waves identified by the
F(H) cumulative distribution function of wave height $(H)$		zero-crossing method
$F(H_{max})$ cumulative distribution function of H at $H=H_{max}$	$n_g$	total number of representative wave heights in each
$F_1(H_{max})$ cumulative distribution function of $H_{max}$		data group
h water depth	N	number of individual waves
$H_b$ breaker height	pdf	probability density function
<i>H<sub>cr</sub></i> computed representative wave height	P	probability of occurrence
$H_m$ mean wave height	$T_p$	spectral peak period
$H_{mr}$ measured representative wave height	$\Delta H_{mr}$	measurement error
$H_{max}$ maximum wave height	β	proportional coefficient
$H_N$ wave height with exceedance probability of $1/N$	$\gamma(a,x)$	lower incomplete Gamma function of variables a
$H_{rms}$ root mean square wave height		and x
$H_{tr}$ transitional wave height	$\Gamma(x)$	Gamma function of variable <i>x</i>
$H_1$ scale parameter no. 1	$\Gamma(a,x)$	upper incomplete Gamma function of variables a
H <sub>2</sub> scale parameter no. 2		and x
$H_{1/N}$ average of the highest $1/N$ wave heights	$\kappa$	shape parameter
$H_{1/3}$ significant wave height		

computing the representative wave heights from offshore to shoreline. No direct study has been made to describe clearly the accuracy of existing conversion formulas on the estimation of  $H_m$ ,  $H_{1/3}$ ,  $H_{1/10}$ , and  $H_{max}$  for a wide range of experimental conditions. This makes engineers and scientists hesitant in using those conversion formulas. The objective of this study is to find out the suitable conversion formulas that predict well for a wide range of experimental conditions.

This paper is divided into three main parts. The first part is a brief review of selected existing and modified formulas for computing the representative wave heights (i.e.  $H_m$ ,  $H_{1/3}$ ,  $H_{1/10}$ , and  $H_{max}$ ) from the known  $H_{rms}$ . The second part presents the collected data for verifying the conversion formulas. The third part describes the verification of the selected conversion formulas.

## 2. Selected conversion formulas

Two approaches have been used to derive the conversion formulas for computing representative wave heights. The first approach derives the formulas by curve fitting between the representative wave heights and the breaker height parameters. The second approach derives the formulas from the selected pdf of wave heights. Various conversion formulas have been proposed. some of which are expressed in terms of uncommon output parameters from most of the existing wave models (e.g. spectral bandwidth and wave nonlinearity parameters), e.g. the distributions of Naess (1985), Hughes and Borgman (1987), Mori and Janssen (2006), and Tayfun and Fedele (2007). Including more related parameters is expected to make the pdf more accurate. However, it may not be suitable to incorporate with most of the existing wave models because such parameters are not available from the wave models. Therefore, this study concentrates on only the formulas which are expressed in terms of common parameters obtained from the wave models, i.e.  $H_{rms}$ , h,  $T_p$ , and m. Brief reviews of selected existing and modified formulas for computing  $H_m$ ,  $H_{1/3}$ ,  $H_{1/10}$ , and  $H_{max}$  are presented below.

(a) Longuet-Higgins (1952), hereafter referred to as LH52, demonstrated that the Rayleigh distribution is applicable to the

wave heights in the sea. The validity of the distribution for deepwater waves has been confirmed by many researchers, even though the bandwidth may not always be narrow-banded (Demerbilek and Vincent, 2006). The cumulative distribution function (*cdf*) and the probability density function (*pdf*) of the Rayleigh distribution can be expressed as

$$F(H) = 1 - \exp\left[-\left(\frac{H}{H_{rms}}\right)^2\right],\tag{1}$$

$$f(H) = \frac{dF(H)}{dH} = \frac{2H}{H_{rms}^2} \exp\left[-\left(\frac{H}{H_{rms}}\right)^2\right],\tag{2}$$

where F(H) is the cumulative distribution function (cdf) of wave height (H), f(H) is the probability density function (pdf) of wave height (H), and  $H_{rms}$  is the root mean square (rms) wave height, which is defined as

$$H_{rms} = \sqrt{\frac{\sum H^2}{M}},\tag{3}$$

where M is the total number of individual waves identified by the zero-crossing method.

The conversion formulas are obtained by manipulation of the pdf of wave heights. The average of the highest 1/N wave heights  $(H_{1/N})$  is defined as

$$H_{1/N} = N \int_{H_N}^{\infty} Hf(H)dH, \tag{4}$$

where N is the number of individual waves, and  $H_N$  is the wave height with exceedance probability of 1/N which can be obtained from the cdf as

$$P(H > H_N) = \frac{1}{N} = 1 - F(H_N) = \exp\left[-\left(\frac{H_N}{H_{rms}}\right)^2\right].$$
 (5)

where P is the probability of occurrence. Manipulation of Eq. (5) yields,

$$H_N = (\ln N)^{1/2} H_{rms}. \tag{6}$$

Substituting f(H) from Eq. (2) and  $H_N$  from Eq. (6) into Eq. (4), and taking integration, the result is

$$H_{1/N} = \left[ \sqrt{\ln N} + \frac{N\sqrt{\pi}}{2} erfc(\sqrt{\ln N}) \right] H_{rms}, \tag{7}$$

where erfc(x) is the complementary error function of variable x. The representative wave heights (i.e.  $H_m$ ,  $H_{1/3}$ , and  $H_{1/10}$ ) can be determined by substituting N equal to 1, 3, and 10, respectively, into Eq. (7). The maximum wave height is affected by the total number of waves in a record (M) which varies from one sample to another. The probability distribution of  $H_{max}$  in general depends on the sample size and the parent distribution from which the sample was obtained. Longuet-Higgins (1952) proposed a cumulative distribution function of  $H_{max}$  by considering that the cumulative probability of  $H_{max}$  is equal to the total probability of all M waves being less than  $H_{max}$ . The result is

$$F_1(H_{max}) = [F(H_{max})]^M, \tag{8}$$

where  $F_1(H_{max})$  is the cumulative distribution function of  $H_{max}$ , and  $F(H_{max})$  is the cumulative distribution function of H at  $H=H_{max}$ . Eq. (8) is valid if  $H_{max}$  of all M waves are independently and identically distributed. Substituting Eq. (1) at  $H=H_{max}$  into Eq. (8), the cumulative distribution function of  $H_{max}$  is expressed as

$$F_1(H_{max}) = \left\{ 1 - \exp\left[ -\left(\frac{H_{max}}{H_{rms}}\right)^2 \right] \right\}^M. \tag{9}$$

The arithmetic mean (expected value) is usually used as an approximation of  $H_{max}$ . Based on Eq. (9), approximated formula for computing the arithmetic mean of  $H_{max}$  is expressed as

$$H_{max} = E(H_{max}) = \left[ \int_0^\infty H_{max} f_1(H_{max}) dH_{max} \right] \approx \left( \sqrt{\ln M} + \frac{0.5772}{2\sqrt{\ln M}} \right) H_{rms}, \tag{10}$$

where  $E(H_{max})$  is the expected value of  $H_{max}$ , and  $f_1(H_{max})$  is the pdf of  $H_{max}$ . From the known  $H_{rms}$  and M, the representative wave heights  $H_{1/N}$  are determined from Eq. (7) and  $H_{max}$  is determined from Eq. (10).

(b) Glukhovskiy (1966), hereafter referred to as G66, proposed a two parameter Weibull distribution to describe the wave height distribution in shallow water. The influence of depth-limited wave breaking is taken into account by including a function of  $H_m/h$  into the two parameters. However, the mean wave height  $(H_m)$  is not a common output from most existing wave models. Klopman (1996) suggested replacing  $H_m/h$  with  $0.7H_{rms}/h$ . The cdf and pdf of G66 can be written in terms of  $H_{rms}$  as

$$F(H) = 1 - \exp\left[-A\left(\frac{H}{H_{\text{true}}}\right)^{\kappa}\right],\tag{11}$$

$$f(H) = \frac{A\kappa H^{\kappa - 1}}{H_{rms}^{\kappa}} \exp\left[-A\left(\frac{H}{H_{rms}}\right)^{\kappa}\right],\tag{12}$$

where A and  $\kappa$  are the position and shape parameters, respectively, which can be determined from the following empirical formulas.

$$A = \left(1 + \frac{1}{\sqrt{2\pi}} \frac{C_2 H_{rms}}{h}\right)^{-1},\tag{13}$$

$$\kappa = \frac{C_1}{1 - C_2 H_{\text{rms}}/h},\tag{14}$$

where  $C_1$  and  $C_2$  are the constants. The proposed values of  $C_1$  and  $C_2$  are 2.0 and 0.7, respectively. It should be noted that when the ratio of  $H_{rms}/h$  gets small (deep water), then A approaches 1,  $\kappa$  approaches 2, and the G66 (Weibull) distribution reverts to Rayleigh. The wave height with exceedance probability of

 $1/N\ (H_N)$  and the average of the highest 1/N wave heights  $(H_{1/N})$  are obtained by manipulation of the probability function (similar procedure as that of LH52). The results are

$$H_N = \left(\frac{\ln N}{A}\right)^{1/\kappa} H_{rms},\tag{15}$$

$$H_{1/N} = \frac{N}{A^{1/\kappa}} \Gamma\left[\frac{1}{\kappa} + 1, \ln N\right] H_{rms},\tag{16}$$

where  $\Gamma(a,x)$  is the upper incomplete Gamma function of variables a and x. For computing the maximum wave height  $(H_{max})$ , following the same procedures as that of LH52, the cdf of  $H_{max}$  can be written as

$$F_1(H_{max}) = \left\{ 1 - \exp\left[ -A \left( \frac{H_{max}}{H_{rms}} \right)^{\kappa} \right] \right\}^M. \tag{17}$$

Based on Eq. (17), an approximated formula for computing the expected value of  $H_{max}$  is expressed as

$$H_{max} \approx \frac{1}{A^{1/\kappa}} \left( (\ln M)^{1/\kappa} + \frac{0.5772 (\ln M)^{1/\kappa - 1}}{\kappa} \right) H_{rms}. \tag{18}$$

From the known  $H_{rms}$ , h, and M, the representative wave heights  $H_{1/N}$  are determined from Eq. (16) and  $H_{max}$  is determined from Eq. (18), in which the parameters A and  $\kappa$  are determined from Eqs. (13) and (14), respectively. It was pointed out by Klopman (1996) that the distribution of G66 is not consistent, i.e. the first moment of the distribution is not equal to  $H_m$  (if the distribution is expressed in terms of  $H_m$ ) or the second moment of the distribution is not equal to  $H_{rms}^2$  (if the distribution is expressed in terms of  $H_{rms}$ ). However, the distribution of G66 has often been mentioned but it seems that no literature shows its applicability on estimating the representative wave heights. It may be worthwhile to examine its applicability on estimating the representative wave heights.

(c) Klopman (1996), hereafter referred to as K96, used the same probability function as that of G66 and consequently the same conversion formulas for computing  $H_{1/N}$  and  $H_{max}$  [Eqs. (16) and (18), respectively]. He modified the distribution of G66 by reformulating the position and shape parameters (A and  $\kappa$ ) to assure consistency of the distribution. The parameters A and  $\kappa$  of K96 are determined from the following formulas:

$$A = \left[\Gamma\left(\frac{2}{\kappa} + 1\right)\right]^{\kappa/2},\tag{19}$$

$$\kappa = \frac{C_3}{1 - C_4 H_{rms}/h},\tag{20}$$

where  $\Gamma(x)$  is the Gamma function of variable x, and  $C_3$  and  $C_4$  are the constants. The proposed values of  $C_3$  and  $C_4$  are 2.0 and 0.7, respectively. From the known  $H_{rms}$ , h, and M, the representative wave heights  $H_{1/N}$  can be determined from Eq. (16) and  $H_{max}$  can be determined from Eq. (18), in which the parameters A and K are determined from Eqs. (19) and (20), respectively.

(d) Battjes and Groenendijk (2000), hereafter referred to as BG00, proposed a composite Weibull wave height distribution to describe the wave height distribution on shallow foreshore. The distribution consists of a Weibull distribution with exponent of 2.0 for the lower wave heights and a Weibull with exponent of 3.6 for the higher wave heights. The two Weibull distributions are matched at the transitional wave height ( $H_{tr}$ ). The cumulative distribution function and the probability density function are

described as

$$F(H) = \begin{cases} 1 - \exp\left[-\left(\frac{H}{H_1}\right)^{C_5}\right] & \text{for } H < H_{tr} \\ 1 - \exp\left[-\left(\frac{H}{H_2}\right)^{C_6}\right] & \text{for } H \ge H_{tr} \end{cases}$$
(21)

$$f(H) = \begin{cases} \frac{C_5 H^{C_5 - 1}}{H_1^{C_5}} \exp\left[-\left(\frac{H}{H_1}\right)^{C_5}\right] & \text{for } H < H_{tr} \\ \frac{C_6 H^{C_6 - 1}}{H_2^{C_6}} \exp\left[-\left(\frac{H}{H_2}\right)^{C_6}\right] & \text{for } H \ge H_{tr} \end{cases}$$
(22)

where  $C_5$  and  $C_6$  are the constants,  $H_1$  and  $H_2$  are the scale parameters, and  $H_{tr}$  is the transitional wave height. The proposed values of  $C_5$  and  $C_6$  are 2.0 and 3.6, respectively. The transitional wave height ( $H_{tr}$ ) is determined from the following empirical formula:

$$H_{tr} = (0.35 + 5.8m)h,$$
 (23)

where m is the beach slope. At the transitional wave height, the wave height distribution abruptly changes its shape. This change in shape is ascribed to wave breaking. Therefore,  $H_{tr}$  can be considered as a kind of depth-limited breaking or breaker height  $(H_b)$ . For convenience in the calculation, all wave heights are normalized with  $H_{rms}$  as

$$\tilde{H}_{x} = \frac{H_{x}}{H_{rms}},\tag{24}$$

where  $\tilde{H}_x$  is the normalized characteristic wave height. The normalized transitional wave height  $(\tilde{H}_{tr})$  can be determined from

$$\tilde{H}_{tr} = \frac{C_7 H_{tr}}{H_{rms}},\tag{25}$$

where  $C_7$  is the constant. The proposed value of  $C_7$  is 1.0. The normalized scale parameters  $\tilde{H}_1$  and  $\tilde{H}_2$  are determined by solving the following 2 equations simultaneously:

$$\tilde{H}_2 = \tilde{H}_{tr} \left( \frac{\tilde{H}_1}{\tilde{H}_{tr}} \right)^{C_5/C_6}, \tag{26}$$

$$1 = \sqrt{\tilde{H}_1^2 \gamma \left[ \frac{2}{C_5} + 1, \left( \frac{\tilde{H}_{tr}}{\tilde{H}_1} \right)^{C_5} \right] + \tilde{H}_2^2 \Gamma \left[ \frac{2}{C_6} + 1, \left( \frac{\tilde{H}_{tr}}{\tilde{H}_2} \right)^{C_6} \right]}, \tag{27}$$

where  $\gamma(a,x)$  is the lower incomplete Gamma function of variables a and x. After manipulation of the probability function (for more detail, please see Groenendijk, 1998), the normalized  $H_N$  and  $H_{1/N}$  are expressed as

$$\tilde{H}_N = \frac{H_N}{H_{rms}} = \begin{cases} \tilde{H}_1[\ln N]^{1/C_5} & \text{for } \tilde{H}_N < \tilde{H}_{tr} \\ \tilde{H}_2[\ln N]^{1/C_6} & \text{for } \tilde{H}_N \ge \tilde{H}_{tr} \end{cases}, \tag{28}$$

$$\frac{H_{1/N}}{H_{rms}} = \begin{cases} N\tilde{H}_1 \left( \Gamma \left[ \frac{1}{C_5} + 1, \ln N \right] - \Gamma \left[ \frac{1}{C_5} + 1, \left( \frac{\tilde{H}_{tr}}{\tilde{H}_1} \right)^{C_5} \right] \right) + N\tilde{H}_2 \Gamma \left[ \frac{1}{C_6} + 1, \left( \frac{\tilde{H}_{tr}}{\tilde{H}_2} \right)^{C_6} \right] & \text{for} \quad \tilde{H}_N < \tilde{H}_{tr} \\ N\tilde{H}_2 \Gamma \left[ \frac{1}{C_6} + 1, \ln N \right] & \text{for} \quad \tilde{H}_N \ge \tilde{H}_{tr} \end{cases}$$

Unlike LH52, Battjes and Groenendijk (2000) did not use the probability function of  $H_{max}$  for computing  $H_{max}$ . They determined the highest wave height in a wave record of total number of waves M (or maximum wave height,  $H_{max}$ ) from the formula of  $H_N$  [Eq. (28)]. Substituting N=M into Eq. (28), the formula for computing the maximum wave height ( $H_{max}$ ) can be

expressed as

$$\tilde{H}_{M} = \frac{H_{max}}{H_{rms}} = \begin{cases} \tilde{H}_{1}[\ln M]^{1/C_{5}} & \text{for } \tilde{H}_{M} < \tilde{H}_{tr} \\ \tilde{H}_{2}[\ln M]^{1/C_{6}} & \text{for } \tilde{H}_{M} \ge \tilde{H}_{tr} \end{cases}$$
(30)

All conceivable normalized characteristic wave heights are a function of  $\tilde{H}_{tr}$  only. From the known  $H_{rms}$ , h, m, and M, the normalized transitional wave height ( $\tilde{H}_{tr}$ ) is determined from Eq. (25) and the normalized scale parameters  $\tilde{H}_1$  and  $\tilde{H}_2$  are determined from Eqs. (26) and (27) simultaneously. Once  $\tilde{H}_1$  and  $\tilde{H}_2$  have been determined,  $H_{1/N}$  can be determined from Eq. (29) and  $H_{max}$  can be determined from Eq. (30). It should be noted that the disadvantage of BG00 is the complexity of the formulas.

(e) Elfrink et al. (2006), hereafter referred to as EHR06, used the same probability function as that of G66 and K96 and, consequently, the same conversion formulas for computing  $H_{1/N}$  and  $H_{max}$  [Eqs. (16) and (18), respectively]. They modified the distribution of K96 by reformulating the shape parameter  $(\kappa)$ . The proposed formula for computing the parameter  $\kappa$  of EHR06 is expressed as

$$\kappa = C_8 \left[ \tanh \left( \frac{C_9 H_{rms}}{h} \right) - \left( \frac{C_9 H_{rms}}{h} \right)^2 \right]^2 + C_{10},$$
 (31)

where  $C_8$ – $C_{10}$  are the constants. The proposed values of  $C_8$ – $C_{10}$  are 15.5, 1.0, and 2.03, respectively. From the known  $H_{rms}$ , h, and M, the representative wave heights  $H_{1/N}$  are determined from Eq. (16) and  $H_{max}$  is determined from Eq. (18), in which the parameters A and  $\kappa$  are determined from Eqs. (19) and (31), respectively.

(f) Rattanapitikon and Shibayama (2007), hereafter referred to as RS07, modified the conversion formulas of LH52 by empirically incorporating the effect of wave breaking into the formulas. The proportional coefficients ( $\beta$ ) in the formulas of LH52 were fitted with three dimensionless parameters ( $H_{rms}/H_t$ ,  $H_{rms}/H_{tr}$ , and  $H_{rms}/H_b$ ); consequently, three conversion formulas (hereafter referred to as RS07a, RS07b, and RS07c, respectively) were proposed. The general formulas for computing  $H_{1/N}$  and  $H_{max}$  of RS07a–RS07c are expressed as

$$H_{1/N} = \beta_{1/N} H_{rms},$$
 (32)

$$H_{max} = \beta_{max} \left( \sqrt{\ln M} + \frac{0.5772}{2\sqrt{\ln M}} \right) H_{rms},\tag{33}$$

where  $\beta$  is the proportional coefficient, and subscripts 1/N and max represent the coefficients for  $H_{1/N}$  and  $H_{max}$ , respectively. The proportional coefficients  $\beta$  for RSO7a–RSO7c are determined from the following empirical formulas:

$$+1, \left(\frac{\tilde{H}_{tr}}{\tilde{H}_{2}}\right)^{C_{6}} \quad \text{for} \quad \tilde{H}_{N} < \tilde{H}_{tr}$$

$$\text{for} \quad \tilde{H}_{N} \ge \tilde{H}_{tr}$$

$$(29)$$

RS07a: 
$$\beta = \begin{cases} K_1 & \text{for } \frac{H_{rms}}{h} \le K_3 \\ K_1 + \frac{(K_2 - K_1)}{(K_4 - K_3)} \left(\frac{H_{rms}}{h} - K_3\right) & \text{for } K_3 < \frac{H_{rms}}{h} < K_4, \\ K_2 & \text{for } \frac{H_{rms}}{h} \ge K_4 \end{cases}$$
 (34)

W. Rattanapitikon / Ocean Engineering 37 (2010) 1554-1563

RS07b: 
$$\beta = \begin{cases} K_1 & \text{for } \frac{H_{rms}}{H_{tr}} \le K_5 \\ K_1 + \frac{(K_2 - K_1)}{(K_6 - K_5)} \left(\frac{H_{rms}}{H_{tr}} - K_5\right) & \text{for } K_5 < \frac{H_{rms}}{H_{tr}} < K_6, \\ K_2 & \text{for } \frac{H_{rms}}{H_{tr}} \ge K_6 \end{cases}$$

RS07c: 
$$\beta = \begin{cases} K_1 & \text{for } \frac{H_{rms}}{H_b} \le K_7 \\ K_1 + \frac{(K_2 - K_1)}{(K_8 - K_7)} \left( \frac{H_{rms}}{H_b} - K_7 \right) & \text{for } K_7 < \frac{H_{rms}}{H_b} < K_8, \\ K_2 & \text{for } \frac{H_{rms}}{H_b} \ge K_8 \end{cases}$$
(36)

where  $K_1$ – $K_8$  are the constants. The proposed values of  $K_1$ – $K_8$  for coefficients  $\beta$  are shown in the third to sixth columns of Table 1. The breaker height  $(H_b)$  is determined from the breaking criteria of Goda (1970) as

$$H_b = 0.1L_o \left\{ 1 - \exp\left[ -1.5 \frac{\pi h}{L_o} \left( 1 + 15m^{4/3} \right) \right] \right\}, \tag{37}$$

where  $L_o$  is the deepwater wavelength related to the spectral peak period  $(T_p)$ . The coefficient 0.1 is used according to Rattanapitikon and Shibayama (1998). From the known  $H_{rms}$ , h,  $T_p$ , m, and M, the representative wave heights  $H_{1/N}$  are determined from Eq. (32) and  $H_{max}$  is determined from Eq. (33), in which the coefficients  $\beta$  for RS07a, RS07b, and RS07c are determined from Eqs. (34)–(36), respectively.

(g) You (2009), hereafter referred to as Y09, proposed using modified Rayleigh and Weibull distributions to describe the distribution of wave orbital velocity amplitudes. As wave height and orbital velocity amplitude have a certain relationship, the distribution of the orbital velocity may also be applicable for describing the wave height distribution. The cumulative distribution functions of the modified Rayleigh distribution (hereafter referred to as Y09a) and the Weibull distribution (hereafter referred to as Y09b) can be rewritten in a general form as

$$F(H) = 1 - \exp\left[-A\left(\frac{H}{H_{rms}}\right)^{\kappa}\right]. \tag{38}$$

The cdf of Y09 [Eq. (38)] is the same as that of G66. The difference is the terms of parameters A and  $\kappa$  which are set to be constants as

Y09a: 
$$A = C_{11}$$
, (39)

**Table 1** Default and calibrated constants  $K_1$  to  $K_8$  of the coefficients  $\beta$  for RS07a–RS07c.

Formulas	Constants	Defau	Default constants			Calibi	ated co	onstant	s
		$\beta_1$	$\beta_{1/3}$	$\beta_{1/10}$	$\beta_{max}$	$\beta_1$	$\beta_{1/3}$	$\beta_{1/10}$	$\beta_{max}$
RS07a	$K_1$	0.87	1.43	1.81	0.97	0.89	1.41	1.75	1.00
	$K_2$	0.92	1.36	1.58	0.69	0.92	1.34	1.56	0.69
	$K_3$	0.10	0.10	0.10	0.10	0.06	0.06	0.06	0.06
	$K_4$	0.52	0.52	0.52	0.52	0.50	0.50	0.50	0.50
RS07b	$K_1$	0.87	1.43	1.81	0.97	0.89	1.41	1.75	1.00
	$K_2$	0.92	1.36	1.58	0.69	0.92	1.34	1.56	0.69
	$K_5$	0.25	0.25	0.25	0.25	0.15	0.15	0.15	0.15
	$K_6$	0.95	0.95	0.95	0.95	1.00	1.00	1.00	1.00
RS07c	$K_1$	0.87	1.43	1.81	0.97	0.89	1.41	1.75	1.0
	$K_2$	0.92	1.36	1.58	0.69	0.92	1.34	1.56	0.69
	$K_7$	0.43	0.43	0.43	0.43	0.25	0.25	0.25	0.25
	K <sub>8</sub>	1.00	1.00	1.00	1.00	1.00	1.00	1.00	1.00

$$\kappa = 2$$
, (40)

Y09b: 
$$A = 1$$
, (41)

$$\kappa = C_{12},\tag{42}$$

where  $C_{11}$  and  $C_{12}$  are the constants. The proposed values of  $C_{11}$  and  $C_{12}$  are 1.09 and 2.15, respectively. As the cdf of Y09 is the same as that of G66, the representative wave heights can be determined from the same equations as of G66. From the known  $H_{rms}$  and M, the representative wave heights  $H_{1/N}$  can be determined from Eq. (16) and  $H_{max}$  can be determined from Eq. (18), in which the parameters A and  $\kappa$  are determined from Eqs. (39) and (40) for Y09a and from Eqs. (41) and (42) for Y09b. It should be noted that the distributions of Y09 are not consistent. The second moment of the distributions are not equal to  $H_{rms}^2$ . However, You (2009) showed that the distributions give better accuracy than that of LH52. It may be worthwhile to examine their applicability on predicting the representative wave heights.

(h) As wave breaking may cause the wave height distribution to deviate from the Rayleigh distribution, the variable that may affect the distribution in the shallow water is the terms of depth-limited wave breaking or breaker height. There are three breaker parameters which were used by the previous researchers, i.e. h,  $H_{tr}$  [Eq. (23)], and  $H_b$  [Eq. (37)]. Using the suitable breaker parameters in the conversion formulas is expected to give better accuracy. The modification is carried out by changing the breaker parameters in the conversion formulas. Modified K96 formulas (hereafter referred to as MK96) are performed by changing the breaker parameters in the formula of  $\kappa$ . Replacing h in Eq. (20) by  $H_{tr}$  and  $H_b$ , respectively, the modified  $\kappa$  can be expressed as

MK96a: 
$$\kappa = \frac{C_{13}}{1 - C_{14}H_{rms}/H_{tr}},$$
 (43)

MK96b: 
$$\kappa = \frac{C_{15}}{1 - C_{16}H_{rms}/H_b}$$
, (44)

where  $C_{13}$ – $C_{16}$  are the constants which can be determined from formula calibration. The representative wave heights  $(H_{1/N})$  are determined from Eq. (16) and maximum wave height  $(H_{max})$  is determined from Eq. (18), in which the parameter A is determined from Eq. (19) and the parameters  $\kappa$  for MK96a and MK96b are determined from Eqs. (43) and (44), respectively.

(i) For similar reasons, modified BG00 formulas (hereafter referred to as MBG00) are performed by changing the breaker parameters in the formula of  $\tilde{H}_{tr}$ . Replacing  $H_{tr}$  in Eq. (25) by h and  $H_b$ , respectively, the modified  $\tilde{H}_{tr}$  can be expressed as

MBG00a: 
$$\tilde{H}_{tr} = \frac{C_{17}h}{H_{rms}}$$
, (45)

MBG00b: 
$$\tilde{H}_{tr} = \frac{C_{18}H_b}{H_{rms}},$$
 (46)

where  $C_{17}$  and  $C_{18}$  are the constants which can be determined from formula calibration. The representative wave heights  $H_{1/N}$  and  $H_{max}$  are determined from Eqs. (29) and (30), respectively, in which the parameters  $\tilde{H}_1$  and  $\tilde{H}_2$  are determined from Eqs. (26) and (27) simultaneously and  $\tilde{H}_{tr}$  for MBG00a and MBG00b are determined from Eqs. (45) and (46), respectively.

(j) As in item (h), modified EHR06 formulas (hereafter referred to as MEHR06) are performed by changing the breaker parameters in the formula of  $\kappa$ . Replacing h in Eq. (31) by  $H_{tr}$  and  $H_b$ , respectively, the modified  $\kappa$  can be expressed as

MEHR06a: 
$$\kappa = C_{19} \left[ \tanh \left( \frac{C_{20} H_{rms}}{H_{tr}} \right) - \left( \frac{C_{20} H_{rms}}{H_{tr}} \right)^2 \right]^2 + C_{21}, \quad (47)$$

MEHR06a: 
$$\kappa = C_{22} \left[ \tanh \left( \frac{C_{23} H_{rms}}{H_b} \right) - \left( \frac{C_{23} H_{rms}}{H_b} \right)^2 \right]^2 + C_{24},$$
 (48)

where  $C_{19}$ – $C_{24}$  are the constants which can be determined from formula calibration. The representative wave heights  $H_{1/N}$  are determined from Eq. (16) and  $H_{max}$  is determined from Eq. (18), in which the parameter A is determined from Eq. (19) and the parameters  $\kappa$  for MEHR06a and MEHR06b are determined from Eqs. (47) and (48), respectively.

(k) As the distribution of Y09 is not consistent, it should be modified for consistency. The modified Y09 is performed by reformulating the position and shape parameters (A and  $\kappa$ ). As the probability function of Y09 is the same as that of K96, the position parameter (A) can be determined from Eq. (19) while the shape parameter ( $\kappa$ ) is set to be a constant as

$$\kappa = C_{25},\tag{49}$$

where  $C_{25}$  is the constant which can be determined from formula calibration. The representative wave heights  $H_{1/N}$  can be determined from Eq. (16) and  $H_{max}$  can be determined from Eq. (18), in which the parameters A and  $\kappa$  are determined from Eqs. (19) and (49), respectively.

#### 3. Collected experimental data

The experimental data of representative wave heights (i.e.  $H_m$ ,  $H_{rms}$ ,  $H_{1/3}$ ,  $H_{1/10}$ , and  $H_{max}$ ) from 10 sources (covering 2619 cases and 19,776 wave records) have been collected for examination of the formulas. The data cover the wave heights in either the offshore zone or surf zone. The collected experiments are separated into 3 groups based on the experiment-scale, i.e. small-scale, large-scale, and field experiments. The small-scale experiments were conducted under fixed beach conditions whereas the large-scale and field experiments were carried out under movable (sandy) beach conditions. The experiments cover a variety of beach conditions and cover a range of deepwater rms wave steepness ( $H_{rmso}/L_0$ ) from 0.0002 to 0.059. A summary of the

collected laboratory data is given in Table 2. Some of the data sources are the same as those used by Rattanapitikon and Shibayama (2007). The additional data are from the LIP11D project (Roelvink and Reniers, 1995), SAFE project (Dette et al., 1998), Long (1991), and COAST3D project (Soulsby, 1998). A brief summary of the additional data is provided below.

LIP 11D Delta Flume Experiment (Roelvink and Reniers, 1995) was performed at Delft Hydraulics large-scale wave flume. A 175m-long sandy beach was constructed in a large wave tank of 233 m long, 5 m wide, and 7 m deep. The 2 major tests were performed, i.e., with dune (test no. 1A-1C) and without dune (test no. 2A-2C). Each major test consisted of several wave conditions. The duration of each wave condition lasted about 12–21 h. Initial beach profiles of the test no. 1A and 2A are equilibrium Dean-type beaches ( $h = A_s x^{2/3}$ , where  $A_s$  is the sediment scale parameter and xis the horizontal distance directed offshore). The beach profiles of other tests (test no. 1B, 1C, 2B, 2E, and 2C) were initiated using the final profile configuration of the previous test. Broad banded random waves, JONSWAP spectrum with spectral width parameter of 3.3, were generated. During the run, the sand bar feature grows and becomes more pronounced after some time. Ten fixed wave gages and one moveable wave gage were deployed in the flume to measure the wave transformation. Only the representative wave heights data from the moveable wave gage are available and are used in this study.

SAFE Project (Dette et al., 1998) was carried out to improve the methods of design and performance assessment of beach nourishment. The SAFE Project consisted of four activities, one of which was to perform experiments in a large-scale wave flume in Hannover, Germany. A 250-m-long sandy beach was constructed in a large wave tank of 300 m long, 5 m wide, and 7 m deep. The test program was divided into two major phases. The first phase (test no. A, B, C, and H) was intended to study the beach deformation of equilibrium profile with different beach slope changes. The equilibrium beach profile was adopted from Bruun's (1954) approach. In the second phase, the sediment transport behaviors of dunes with and without structural aid were investigated (test no. D, E, F, and G). The TMA spectral shape with

**Table 2** Collected experimental data.

Sources		Apparatus	Meas	ured wave heights	
Smith and Kraus (1990)		Small-scale	Н <sub>т</sub> , Н	$H_m$ , $H_{rms}$ , $H_{1/3}$ , $H_{max}$	
Ting (2001)	Small-scale	$H_m$ , $H$	$H_m$ , $H_{rms}$ , $H_{1/3}$ , $H_{1/10}$ , $H_{max}$		
Ting (2002)		Small-scale	$H_m$ , $H$	$_{rms}$ , $H_{1/3}$ , $H_{1/10}$ , $H_{max}$	
Kraus and Smith (1994): SUPERTANK project		Large-scale	$H_m$ , $H$	$_{rms}$ , $H_{1/3}$ , $H_{1/10}$ , $H_{max}$	
Roelvink and Reniers, (1995): LIP11D Project		Large-scale	$H_{rms}$ ,	$H_{1/3}, H_{1/10}, H_{max}$	
Dette et al. (1998): SAFE project		Large-scale	$H_{rms}$ ,	$H_{1/3}$ , $H_{1/10}$ , $H_{max}$	
Goodknight and Russell, (1963)		Field		rms, H <sub>1/3</sub> , H <sub>1/10</sub> , H <sub>max</sub>	
Long (1991)		Field		$_{rms}$ , $H_{1/3}$ , $H_{1/10}$ , $H_{max}$	
Ruessink (1999): COAST3D Project at Egmond	Field		$_{rms}$ , $H_{1/3}$ , $H_{1/10}$		
Whitehouse and Sutherland (2001): COAST3D Project at Teigmond		Field	$H_m$ , $H$	$T_{rms}$ , $H_{1/3}$ , $H_{1/10}$ , $H_{max}$	
Sources	No. of cases	No. of points	$M^{\mathrm{a}}$	$H_{rmso}/L_o$	
Smith and Kraus (1990)	12	96	500	0.021-0.059	
Ting (2001)	1	7	186-207	0.016	
Ting (2002)	1	7	154-162	0.015	
Kraus and Smith (1994): SUPERTANK project	128	2048	152-2046	0.001-0.046	
Roelvink and Reniers, (1995): LIP11D Project	87	170	461-892	0.001-0.029	
Dette et al. (1998): SAFE project	138	3557	182	0.001-0.020	
Goodknight and Russell (1963)	4	80	95-319	0.011-0.025	
Long (1991)	11	11	972-1693	0.002-0.024	
Ruessink (1999): COAST3D Project at Egmond	977	6480	-	0.002-0.030	
Whitehouse and Sutherland (2001): COAST3D Project at Teigmond	1260	7320	132–340	0.0002-0.028	
Total	2619	19,776	95-2046	0.0002-0.059	

<sup>&</sup>lt;sup>a</sup> For computing  $H_{max}$ .

spectral width parameter of 3.3 was used to design all irregular wave tests. A total of 27 wave gages was installed over a length of 175 m along one wall of the flume.

Long (1991) analyzed the measured data which were taken from the measurements archive of CERC's FRF in Duck, NC. Test data were time series from a Waverider buoy near 8-m-depth contour about 1 km offshore. Active depth-induced wave breaking happens at this depth only during extreme conditions. This depth is considered either to be intermediate or shallow for all wind waves of interest. Diversity of wave climate was established by selecting cases classified by energy level as well as broad and narrow energy spread in frequency. Eleven test cases were selected for analysis (from September 1986 to February 1987). The selected cases cover a sequence of measurements before, during, and after a large storm.

COAST3D project is a collaborative project co-funded by the European Commission's MAST-III program and national resources, running from October 1996 to March 2001 (Soulsby, 1998). The project was carried out to improve understanding of the coastal processes on non-uniform (3D) coasts. Two field experiments were performed at Egmond-aan-Zee (Ruessink, 1999) and at Teignmouth (Whitehouse and Sutherland, 2001). The data are available online at "http://www.hrwallingford.co.uk/projects/COAST3D/". A brief summary of the two sites is given below.

The Egmond site is located in the central part of the Dutch North Sea coast. The site was dominated by two well-developed shore-parallel bars intersected by rip channels. Two field experiments were executed, a pilot experiment in spring 1998 and main experiments (A and B) in autumn 1998. Contrary to the pilot campaign, the main experiment witnessed severe conditions. Large waves, strong wind, and water level rises due to storm surges were present, resulting in considerable morphologic change (e.g. bar movement, lowering of bar crests and the presence of rip channels). The experiments were divided into 3 cases, i.e. pre-storm (pilot experiment), storm (main-A experiment), and post storm (main-B experiment). A large variety of instruments, such as pressure sensors, wave buoys and current meters, were deployed at many stations in the study area. Only the stations which have the representative wave heights data are used in this study, i.e. stations 1a, 1b, 1c, 1d, 2, 7a, 7b, 7c, 7d, and 7e for pilot experiment; stations 1a, 1b, 1c, 1d, 2, 7a, 7b, and 7e for main-A experiment; and stations 1a, 1b, 1c, 1d, 2, 7b, 7d, and 7e for main-B experiment.

The Teigmond site is located on the south coast of Devon, UK. The wave climate was mainly characterized by small, short period wind-driven waves. The nature of the coastline was irregular and three-dimensional (3D), with a rocky headland, nearshore banks, and an estuary mouth all adjacent to the beach with its sea defenses (e.g. groins and seawalls). Two field experiments were executed, a pilot experiment (in March 1999) and a main experiment (during October to November 1999). A large variety of instruments, such as pressure sensors, wave buoys and current meters, was deployed at many stations in the study area. Only the stations which are not located close to the structures or river and have the representative wave heights data are used in this study, i.e. stations 15, 18, 22, and 25 for the pilot experiment and stations 3a, 4, 6, 9, 10, 15, 18, 25, 28, 32, and 33 for the main experiment.

## 4. Examination of existing conversion formulas

The objective of this section is to examine the applicability of the ten sets of existing conversion formulas (presented in Section 2) on estimating  $H_m$ ,  $H_{1/3}$ ,  $H_{1/10}$ , and  $H_{max}$  from the known  $H_{rms}$ . The measured representative wave heights from 10 sources

(covering 2619 cases) of published experimental results (shown in Table 2) are used to calibrate and verify the existing formulas. The basic parameter for measuring the accuracy of a formula is the rms relative error ( $ER_p$ ) which is defined as

$$ER_g = 100\sqrt{\frac{\sum_{i=1}^{n_g} (H_{cr,i} - H_{mr,i})^2}{\sum_{i=1}^{n_g} H_{mr,i}^2}},$$
 (50)

where  $H_{cr}$  is the computed representative wave height,  $H_{mr}$  is the measured representative wave height, and  $n_g$  is the total number of representative wave heights in each data group.

To measure a performance of a wave height transformation model, some researchers (e.g. Van Rijn et al., 2003; Grasmeijer and Ruessink, 2003) excluded the effect of measurement error by adding the measurement error  $(\Delta H_{mr})$  to the discrepancy term (i.e.  $|H_{cr}-H_{mr}|-\Delta H_{mr})$  in the equation for computing error of the model. The measurement error  $(\Delta H_{mr})$  may cause an effect on model comparison. However, the present study concentrates on conversion formulas, in which the computed representative wave height  $(H_{cr})$  is determined from the measured  $H_{rms}$ . Since the measured  $H_{rms}$  is determined from the same wave record as the measured representative wave heights  $(H_{mr})$ , the measurement error of  $H_{rms}$  and  $H_{mr}$  should be in the same proportion. Therefore, the measurement error may not affect the formula comparisons. Hence, the measurement error  $(\Delta H_{mr})$  is not included in Eq. (50).

The collected experiments are separated into three groups according to the experiment scale (i.e. small-scale, large-scale, and field experiments), and four representative wave heights (i.e.  $H_m$ .  $H_{1/3}$ ,  $H_{1/10}$ , and  $H_{max}$ ) are considered in this study. It is expected that a good formula should be able to predict well for all experiment-scales and all representative wave heights. Therefore, the average error from three experiment-scales ( $ER_{avg}$ ) is used to examine the accuracy of the formulas on estimating each representative wave height, and the overall average error from three experiment-scales and four representative wave heights ( $ER_{all}$ ) is used examine the overall accuracy of the formulas. The average error ( $ER_{avg}$ ) and overall average error ( $ER_{all}$ ) are defined as

$$ER_{avg} = \frac{\sum_{j=1}^{3} ER_{g,j}}{3},$$
 (51)

$$ER_{all} = \frac{\sum_{k=1}^{4} ER_{avg,k}}{4}.$$
 (52)

## 4.1. Examination of existing formulas using default constants

The examinations of the formulas of  $H_{1/N}$  and  $H_{max}$  are carried out by using the measured representative wave heights (i.e.  $H_{rms}$ ,  $H_m$ ,  $H_{1/3}$ ,  $H_{1/10}$ , and  $H_{max}$ ) shown in Table 2. From the measured  $H_{rms}$ , the other representative wave heights ( $H_m$ ,  $H_{1/3}$ , and  $H_{1/10}$ , and  $H_{max}$ ) are computed by using the formulas of  $H_{1/N}$  and  $H_{max}$ . Using the default constants  $(C_1-C_{12} \text{ and } K_1-K_8)$  in the computations, the errors ( $ER_{avg}$  and  $ER_{all}$ ) of existing formulas for computing  $H_m$ ,  $H_{1/3}$ ,  $H_{1/10}$ , and  $H_{max}$  are shown in Table 3. It can be seen from Table 3 that the formulas of G66, K96, RS07a, and RS07c give the same overall accuracy and give better prediction than the others. The overall accuracy of the formulas in descending order are the formulas of G66, K96, RS07a, RS07c, RS07b, BG00, EHR06, Y09b, Y09a, and LH53. Since most formulas were developed based on a limited range of experimental conditions, the constants in the formulas may not be the optimal values for a wide range of experimental conditions. Therefore, the errors in Table 3 should not be used to judge the applicability of the formulas. The constants in all formulas were recalibrated to minimize errors and the applicability of the formulas was then reassessed as shown in the following sections.

**Table 3** The errors ( $ER_{avg}$  and  $ER_{all}$ ) of the existing formulas on estimating  $H_m$ ,  $H_{1/3}$ ,  $H_{1/10}$ , and  $H_{max}$  from three experiment-scales (using default constants).

Formulas	Default constants	ERav	$ER_{avg}$		$ER_{all}$	
		$H_m$	$H_{1/3}$	$H_{1/10}$	H <sub>max</sub>	
LH52	=	3.2	5.0	11.8	24.8	11.2
G66	$C_1 = 2.0, C_2 = 0.7$	2.9	3.7	4.8	11.5	5.7
K96	$C_3 = 2.0, C_4 = 0.7$	3.3	3.4	4.6	11.7	5.7
BG00	$C_5 = 2.0$ , $C_6 = 3.6$ , $C_7 = 1.0$	2.7	3.7	6.4	11.6	6.1
EHR06	$C_8 = 15.5$ , $C_9 = 1.0$ , $C_{10} = 2.03$	3.1	3.9	5.5	15.2	6.9
RS07a	From Table 1	2.7	3.6	5.5	10.9	5.7
RS07b	From Table 1	2.7	3.6	5.3	12.0	5.9
RS07c	From Table 1	2.8	3.7	6.3	10.1	5.7
Y09a	$C_{11} = 1.09$	6.5	3.7	8.0	21.2	9.9
Y09b	$C_{12} = 2.15$	3.3	3.7	8.1	19.8	8.7

**Table 4** The average errors ( $ER_{avg}$  and  $ER_{all}$ ) of the selected formulas on estimating  $H_m$ ,  $H_{1/3}$ ,  $H_{1/10}$ , and  $H_{max}$  from three experiment-scales (using calibrated constants).

Formulas	Calibrated constants	ERav	ER <sub>avg</sub>		ER <sub>all</sub>	
		$H_m$	$H_{1/3}$	H <sub>1/10</sub>	H <sub>max</sub>	
LH52	=	3.2	5.0	11.8	24.6	11.1
G66	$C_1 = 2.0, C_2 = 0.64$	2.7	3.4	4.6	11.8	5.6
K96	$C_3 = 2.0, C_4 = 0.66$	3.2	3.2	4.5	11.8	5.7
BG00	$C_5 = 2.2$ , $C_6 = 3.3$ , $C_7 = 1.0$	2.6	3.3	4.9	11.9	5.7
EHR06	$C_8 = 31$ , $C_9 = 0.53$ , $C_{10} = 2.0$	3.2	3.2	4.7	11.2	5.6
RS07a	From Table 1	2.5	3.1	4.4	10.7	5.2
RS07b	From Table 1	2.4	3.2	4.5	12.0	5.5
RS07c	From Table 1	2.4	3.1	4.5	10.2	5.1
Y09a	$C_{11} = 1.12$	7.7	4.1	7.1	20.1	9.8
Y09b	$C_{12} = 2.41$	3.2	4.4	5.7	16.3	7.4
MK96a	$C_{13}$ =2.0, $C_{14}$ =0.32	3.1	3.4	4.6	12.8	5.9
MK96b	$C_{15}$ =2.0, $C_{16}$ =0.32	3.2	3.3	4.4	11.6	5.6
MBG00a	$C_5 = 2.2$ , $C_6 = 3.4$ , $C_{17} = 0.49$	2.7	3.1	5.1	10.7	5.4
MBG00b	$C_5 = 2.2$ , $C_6 = 3.5$ , $C_{18} = 1.1$	2.6	3.1	5.0	10.4	5.3
MEHR06a	$C_{19}$ =28, $C_{20}$ =0.27, $C_{21}$ =2.0	3.0	3.4	4.7	12.4	5.9
MEHR06b	$C_{22}$ =34, $C_{23}$ =0.23, $C_{24}$ =2.0	3.2	3.2	4.6	11.1	5.5
MY09	$C_{25}=2.6$	3.2	3.7	5.7	16.0	7.2

### 4.2. Calibration of selected formulas

The objective of this section is to calibrate the constants in the selected conversion formulas presented in Section 2 based on a large amount and wide range of experimental conditions. Most of measured data shown in Table 2 (except eight wave conditions from eight data sources) are used to calibrate the constants. The calibrations are conducted by gradually adjusting the constants until the minimum overall error ( $ER_{all}$ ) of the formulas is obtained. The optimum values of  $K_1$ – $K_8$  are shown in the last four columns of Table 1, while the optimum values of  $C_1$ – $C_{25}$  are shown in the second column of Table 4. Using the calibrated constants in the computations of  $H_m$ ,  $H_{1/3}$ ,  $H_{1/10}$ , and  $H_{max}$  for three experimental scales, the average errors ( $ER_{avg}$  and  $ER_{all}$ ) of the formulas are shown in Table 4, and the errors  $ER_g$  are shown in Table 5. The results can be summarized as follows:

- a) After calibrations, the constants in most existing formulas (except EHR06) have to be changed slightly. However, the use of calibrated constants in the formulas is expected to be more reliable than those of default constants because they are recalibrated with a larger amount and wider range of experimental conditions.
- b) The overall accuracy of the formulas in descending order are the formulas of RS07c, RS07a, MBG00b, MBG00a, RS07b, MEHR06b, EHR06, G66, MK96b, BG00, K96, MEHR06a, MK96a, MY09, Y09b, Y09a, and LH52. The formulas of RS07c give the best prediction ( $ER_{all}$ =5.1%), while the formulas of LH52 give the worst prediction ( $ER_{all}$ =11.1%). This shows that the distribution of wave heights deviates considerably from the Rayleigh distribution. However, the use of LH52 seems to be acceptable for computing  $H_m$  and  $H_{1/3}$ .
- c) It can be seen from Table 5 that the formulas of LH52, Y09a, Y09b, and MY09 give poor predictions ( $ER_g > 20\%$ ) on estimating  $H_{max}$  for small-scale experiments. Only the formula of LH52 gives poor prediction on estimating  $H_{max}$  for large-scale experiments.
- d) The selected formulas can be separated into two groups, i.e. with breaker parameters (the formulas of G66, K96, BG00, EHR06, RS07a, RS07b, RS07c, MK96a, MK96b, MBG00a, MBG00b, MEHR06a, and MEHR06b), and without breaker parameters (the formulas of LH52, Y09a, Y09b, and MY09). As expected, the formulas with breaker parameters give better accuracy than those without breaker parameters. The overall

**Table 5** The errors ( $ER_g$ ) of the selected formulas on estimating  $H_m$ ,  $H_{1/3}$ ,  $H_{1/10}$ , and  $H_{max}$  for small-scale, large-scale, and field experiments (using calibrated constants).

Formulas	Formulas Small-scale				Large-s	cale			Field			
	$H_m$	H <sub>1/3</sub>	$H_{1/10}$	H <sub>max</sub>	$H_m$	$H_{1/3}$	$H_{1/10}$	H <sub>max</sub>	$H_m$	$H_{1/3}$	H <sub>1/10</sub>	H <sub>max</sub>
LH52	4.5	7.9	15.3	43.2	2.3	3.7	10.8	20.7	2.9	3.4	9.4	9.9
G66	2.3	3.7	4.3	16.2	3.9	3.8	5.2	9.8	2.1	2.7	4.1	9.5
K96	2.8	3.7	4.3	16.2	4.4	3.5	5.2	9.9	2.3	2.5	4.1	9.5
BG00	2.4	4.6	4.9	12.6	3.3	2.5	5.1	10.0	2.2	2.7	4.7	13.0
EHR06	2.6	3.4	4.6	14.8	4.4	3.6	5.1	9.3	2.5	2.7	4.4	9.5
RS07a	2.2	4.1	4.1	11.9	3.1	3.0	5.1	10.0	2.0	2.3	4.0	10.1
RS07b	2.3	4.3	4.3	14.1	2.9	2.9	4.9	9.7	2.0	2.4	4.2	12.2
RS07c	2.2	4.1	4.3	10.4	3.0	2.9	5.0	9.6	2.0	2.4	4.1	10.7
Y09a	9.5	3.8	9.3	35.5	5.8	4.8	6.8	16.1	7.9	3.7	5.2	8.8
Y09b	4.4	3.7	5.3	22.9	2.3	5.2	6.4	12.8	2.9	4.2	5.3	13.2
MK96a	2.5	3.8	4.4	18.3	3.9	3.4	4.9	9.6	2.7	3.0	4.4	10.4
MK96b	2.7	3.6	4.1	14.8	4.5	3.5	5.1	9.8	2.5	2.7	4.2	10.2
MBG00a	2.4	4.2	5.1	10.5	3.6	2.6	5.3	10.4	2.0	2.4	4.8	11.2
MBG00b	2.3	4.3	4.9	9.3	3.4	2.5	5.1	10.3	2.0	2.5	4.8	11.7
MEHR06a	2.4	3.6	4.6	17.6	3.8	3.4	4.8	9.1	2.8	3.1	4.6	10.6
MEHR06b	2.6	3.4	4.4	14.1	4.4	3.5	5.0	9.3	2.6	2.8	4.4	10.0
MY09	2.0	4.3	5.5	20.9	5.0	4.0	6.4	12.9	2.6	2.8	5.2	14.1

W. Rattanapitikon / Ocean Engineering 37 (2010) 1554-1563

**Table 6**Selected experimental data for verifying the selected formulas.

Sources	Case no.	No of points	$M^{a}$	H <sub>rmso</sub> /L <sub>o</sub>
Smith and Kraus (1990)	R2000	8	500	0.059
Kraus and Smith (1994): SUPERTANK project	A0509A	16	354-376	0.043
Roelvink and Reniers, (1995): LIP11D Project	1A0203	2	828-891	0.018
Dette et al. (1998): SAFE project	06129601	21	182	0.007
Goodknight and Russell, (1963)	Audrey	14	95-319	0.011-0.021
Long (1991)	140986a	1	1693	0.003
Ruessink (1999): COAST3D Project at Egmond	05064	9	-	0.006
Whitehouse and Sutherland (2001): COAST3D Project at Teigmond	12500	1	-	0.0003
Total		72	95-1693	0.0003-0.059

<sup>&</sup>lt;sup>a</sup> For computing  $H_{max}$ .

errors ( $ER_{all}$ ) of the formulas with breaker parameters are in the range 5.1–5.9% while the others are in the range 7.2–11.1%. This means that the effect of wave breaking is significant and the formulas with breaker parameters are superior.

- e) Comparing among the formulas with breaker parameters, it can be seen from Tables 4 and 5 that no formula gives significantly better results than the others.
- f) The accuracy of all formulas with the breaker parameters is very good  $(5.1 \le ER_{all} \le 5.9)$  and seems to be acceptable for the design of coastal structures. It should be noted that, in practical work, the representative wave heights are determined from the selected conversion formulas based on the output  $(H_{rms})$  from the selected wave model. As the average errors of some existing wave models on predicting  $H_{rms}$  are in the range 8.1-11.4% (Rattanapitikon, 2007), the errors of predicting other representative wave heights should be larger than those shown in Tables 4 and 5.
- g) Considering the complexity of the formulas with breaker parameters, the formulas of RS07a are the simplest ones while the formulas of MBG00b are the most complex ones. Considering accuracy and simplicity of the all formulas, the formulas of R07a seem to be the most attractive ones for general applications.

# 4.3. Verification of selected formulas

Eight wave conditions from eight sources (which have more than one case each) are used to verify the conversion formulas. The first case from each data source is selected for verifying the formulas. The experimental conditions of the selected data are shown in Table 6. Using the calibrated constants in the computations of  $H_m$ ,  $H_{1/3}$ ,  $H_{1/10}$ , and  $H_{max}$  for three experiment-scales, the average errors ( $ER_{avg}$  and  $ER_{all}$ ) of the formulas are shown in Table 7. The results can be summarized as follows:

- a) The overall accuracy of the formulas in descending order are the formulas of MBG00b, RS07c, MBG00a, RS07a, MEHR06b, EHR06, G66, BG00, MK96b, K96, MEHR06a, RS07b, MK96a, MY09, Y09b, Y09a, and LH52. The formulas of MBG00b give the best prediction ( $ER_{all} = 5.2\%$ ), while the formulas of LH52 give the worst prediction ( $ER_{all} = 10.2\%$ ).
- b) The errors in the verification are slightly different from that in the calibration. This is because the number of data that were used in the calibration and verification are different. However, the results of verification are overall similar to that of calibration, i.e. the use of LH52 is acceptable for computing  $H_m$  and  $H_{1/3}$ ; the effect of wave breaking is significant and the formulas with breaker parameters are superior; and the formulas with breaker parameters give very good predictions and have similar accuracy.

**Table 7** Verification results of the selected formulas on estimating  $H_m$ ,  $H_{1/3}$ ,  $H_{1/10}$ , and  $H_{max}$  from three experiment-scales (using calibrated constants).

Formulas	Calibrated constants	$ER_{avg}$		ER <sub>all</sub>		
		$H_m$	$H_{1/3}$	$H_{1/10}$	H <sub>max</sub>	
LH52	-	3.1	4.2	6.8	26.7	10.2
G66	$C_1 = 2.0, C_2 = 0.64$	2.7	3.4	6.3	13.7	6.5
K96	$C_3 = 2.0, C_4 = 0.66$	3.1	3.3	6.2	13.7	6.6
BG00	$C_5 = 2.2$ , $C_6 = 3.3$ , $C_7 = 1.0$	2.5	3.2	6.1	14.2	6.5
EHR06	$C_8 = 31$ , $C_9 = 0.53$ , $C_{10} = 2.0$	3.2	3.3	6.1	12.9	6.4
RS07a	From Table 1	2.4	3.4	6.6	12.7	6.3
RS07b	From Table 1	2.6	3.6	7.2	14.8	7.0
RS07c	From Table 1	2.6	3.4	6.8	10.0	5.7
Y09a	$C_{11} = 1.12$	7.0	5.2	6.6	21.6	10.1
Y09b	$C_{12} = 2.41$	3.1	5.5	8.9	16.8	8.6
MK96a	$C_{13} = 2.0$ , $C_{14} = 0.32$	3.1	3.6	6.8	14.9	7.1
MK96b	$C_{15} = 2.0$ , $C_{16} = 0.32$	3.7	3.5	6.9	12.0	6.5
MBG00a	$C_5 = 2.2$ , $C_6 = 3.4$ , $C_{17} = 0.49$	2.3	3.0	5.2	12.4	5.7
MBG00b	$C_5 = 2.2$ , $C_6 = 3.5$ , $C_{18} = 1.1$	2.5	2.8	5.3	10.4	5.2
MEHR06a	$C_{19}$ =28, $C_{20}$ =0.27, $C_{21}$ =2.0	3.1	3.6	6.8	14.6	7.0
MEHR06b	$C_{22}$ =34, $C_{23}$ =0.23, $C_{24}$ =2.0	3.8	3.5	6.7	11.2	6.3
MY09	$C_{25} = 2.6$	4.0	4.6	8.7	16.4	8.4

#### 5. Conclusions

This study is undertaken to find out the suitable conversion formulas, which can be used to compute the representative wave heights ( $H_m$ ,  $H_{1/3}$ ,  $H_{1/10}$ , and  $H_{max}$ ) from the common parameters obtained from the wave model. The conversion formulas from seven researchers (i.e. LH52, G66, K96, BG00, EHR06, RS07, and Y09) are selected to verify their applicability. The formulas of K96, BG00, and EHR06 are modified by changing the breaker parameters. The formulas of Y09 are modified by reformulating the position and shape parameters (A and  $\kappa$ ) to assure the consistency of the distribution. A total of 17 sets of conversion formulas are considered in this study. The published experimental data from 10 sources (covering 2619 cases) are used to calibrate and verify the formulas. The experiments cover small-scale, largescale, and field experimental conditions. The verification results are presented in terms of overall average rms relative error of 3 experiment-scales and 4 representative wave heights (ER<sub>all</sub>). The constants in all formulas are recalibrated before comparing the accuracy of the formulas. The comparison shows that the formulas with breaker parameters give better accuracy than those without breaker parameters. The accuracy of all formulas with the breaker parameters is not much different and seems to be acceptable for the design of coastal and ocean structures. Considering accuracy and simplicity of the selected formulas, the formulas of RS07a seem to be the most suitable ones for computing the representative wave heights.

#### Acknowledgements

This research was sponsored by the Thailand Research Fund. Thanks and sincere appreciation are expressed to the researchers names listed in Table 2 for publishing the valuable data.

#### References

- Battjes, J.A., Groenendijk, H.W., 2000. Wave height distributions on shallow foreshores. Coastal Engineering 40, 161-182.
- Bruun, P., 1954, Coastal Erosion and Development of Beach Profiles, US Army Beach Erosion Board, Tech. Memorandum No. 44, US Army Corps of Engineers. Dally, W.R., 1990. Random breaking waves: a closed-form solution for planar beaches. Coastal Engineering 14, 233–263.
- Demerbilek, Z., Vincent, L., 2006. Water wave mechanics (Part 2—Chapter 1). Coastal Engineering Manual, EM1110-2-1100. Coastal and Hydraulics Laboratory—Engineering Research and Development Center, WES, US Army Corps of Engineers, pp. II-1-75.
- Dette, H.H., Peters, K., Newe, J., 1998. MAST III—SAFE Project: Data Documentation, Large Wave Flume Experiments '96/97, Report No. 825 and 830. Leichtweiss-Institute, Technical University Braunschweig.
- Elfrink, B., Hanes, D.M., Ruessink, B.G., 2006. Parameterization and simulation of near bed orbital velocities under irregular waves in shallow water. Coastal Engineering 53, 915-927.
- Glukhovskiy, B.Kh., 1996. Investigation of sea wind waves. Leningrad, Gidrometeoizdat (reference obtained from Bouws, E., 1979. Spectra of extreme wave conditions in the Southern North Sea considering the influence of water depth. In: Proceedings of the Sea Climatology Conference, Paris, pp. 51-71).
- Grasmeijer, B.T., Ruessink, B.G., 2003. Modeling of waves and currents in the nearshore parametric vs. probabilistic approach. Coastal Engineering 49, 185–207.
- Goda, Y., 1970. A synthesis of breaking indices. Transaction Japan Society of Civil Engineers 2, 227-230.
- Goda, Y., 1974. Estimation of wave statistics from spectral information. In: Proceedings of the Ocean Waves Measurement and Analysis Conference, ASCE, pp. 320-337
- Goodknight, R.C., Russell, T.L., 1963. Investigation of the statistics of wave heights. Journal of Waterways and Harbors Division, ASCE 89 (WW2), 29-55
- Groenendijk, H.W., 1998. Shallow Foreshore Wave Height Statistics, M.Sc. Thesis, Department of Civil Engineering, Delft University of Technology.
- Hughes, S.A., Borgman, L.E., 1987. Beta-Rayleigh distribution for shallow water wave heights. In: Proceedings of the American Society of Civil Engineers Specialty Conference on Coastal Hydrodynamics, ASCE, pp. 17-31.
- Klopman, G., 1996. Extreme Wave Heights in Shallow Water, Report H2486. WL/Delft Hydraulics, The Netherlands.

- Kraus, N.C., Smith, J.M., 1994. SUPERTANK Laboratory Data Collection Project, Technical Report CERC-94-3. WES, US Army Corps of Engineers, pp. 55-73.
- Long, C.E., 1991. Use of Theoretical Wave Height Distributions in Directional Seas, Technical Report CERC-91-6. WES, US Army Corps of Engineers
- Longuet-Higgins, M.S., 1952. On the statistical distribution of the heights of sea waves. Journal of Marine Research 11 (3), 245–266. Mendez, F.J., Losada, I.J., Medina, R., 2004. Transformation model of wave height
- distribution on planar beaches. Coastal Engineering 50, 97-115.
- Mori, N., Janssen, P., 2006. On kurtosis and occurrence probability of freak wave. Journal of Physical Oceanography 36, 1471-1483.
- Naess, A., 1985. On the distribution of crest-to-trough wave heights. Ocean Engineering 12, 221-234.
- Rattanapitikon, W., Shibayama, T., 1998. Energy dissipation model for regular and irregular breaking waves. Coastal Engineering Journal, JSCE 40 (4), 327-346.
- Rattanapitikon, W., 2007. Calibration and modification of energy dissipation models for irregular waves breaking. Ocean Engineering 34, 1592-1601.
- Rattanapitikon, W., Shibayama, T., 2007. Estimation of shallow water representative wave heights. Coastal Engineering Journal, JSCE 49 (3), 291–310.
- Roelvink, J.A., Reniers A.J.H.M., 1995. LIP 11D Delta Flume Experiments: A Data Set for Profile Model Validation, Report No. H 2130. Delft Hydraulics, The Netherlands.
- Ruessink, B.G., 1999. COAST3D Data Report—2.5D Experiment, Egmond aan Zee, IMAU Report. Utrecht University.
- Smith, E.R., Kraus, N.C., 1990. Laboratory Study on Macro-Features of Wave Breaking over Bars and Artificial Reefs, Technical Report CERC-90-12. WES, US Army Corps of Engineers.
- Soulsby, R.L., 1998. Coastal sediment transport: the COAST3D project. In: Proceedings of the 26th Coastal Engineering Conference, ASCE, pp. 2548–2558.
- Tayfun, A., Fedele, F., 2007. Wave height distribution and nonlinear effects. Ocean Engineering 34, 1631-1649.
- Thornton, E.B., Guza, R.T., 1983. Transformation of wave height distribution.
- Journal of Geophysical Research 88 (C10), 5925-5938.
  Ting, F.C.K., 2001. Laboratory study of wave and turbulence velocity in broadbanded irregular wave surf zone. Coastal Engineering 43, 183-208.
- Ting, F.C.K., 2002. Laboratory study of wave and turbulence characteristics in narrow-banded irregular breaking waves. Coastal Engineering 46, 291–313.
- Van Rijn, L.C., Walstra, D.J.R., Grasmeijer, B., Sutherland, J., Pan, S., Sierra, J.P., 2003. The predictability of cross-shore bed evolution of sandy beaches at the time scale of storms and seasons using process-based profile models. Coastal Engineering 47, 295-327.
- Whitehouse, R.J.S., Sutherland, J., 2001. COAST3D Data Report-3D Experiment, Teignmouth, UK. HR Wallingford Report TR 119.
- You, Z.J., 2009. The statistical distribution of nearbed wave orbital velocity in intermediate coastal water depth. Coastal Engineering 58, 844-852.





Coastal Engineering Journal, Vol. 52, No. 4 (2010) 305–330 © World Scientific Publishing Company and Japan Society of Civil Engineers DOI: 10.1142/S0578563410002191

# ENERGY DISSIPATION MODEL FOR COMPUTING TRANSFORMATION OF SPECTRAL SIGNIFICANT WAVE HEIGHT

#### WINYU RATTANAPITIKON

Civil Engineering Program, Sirindhorn International Institute of Technology, Thammasat University, Pathumthani 12121, Thailand winyu@siit.tu.ac.th

#### TOMOYA SHIBAYAMA

Department of Civil and Environmental Engineering, Waseda University, Ookubo, Shinjuku-ku, Tokyo 169-8555, Japan shibayama@waseda.jp

> Received 15 July 2009 Revised 11 August 2010

The objective of this study is to propose the most suitable dissipation model for computing the transformation of spectral significant wave height  $(H_{m0})$ . A wide range of experimental conditions, covering small-scale, large-scale, and field experiments, were used to examine the models. Fourteen existing dissipation models, for computing root-mean-square wave heights  $(H_{rms})$ , were applied to compute  $H_{m0}$ . The coefficients of the models were recalibrated and the accuracy of the models was compared. It appears that the model of Janssen and Battjes [2007] with new coefficients gives the best overall prediction. The simple model proposed in the present paper was modified by changing the formula of stable wave height in the dissipation model. Comparing with the existing models, the modified model is the simplest one but gives better accuracy than those of existing models.

Keywords: Irregular wave model; spectral significant wave height; energy dissipation; wave height transformation.

#### 1. Introduction

Representative wave heights are the essential required factors for many coastal engineering applications such as the design of coastal structures and the study of beach deformations. Among various representative wave heights, the significant wave

height  $(H_s)$  is most frequently used in the field of coastal engineering [Goda, 2000]. There are two main methods to describe the significant wave height, i.e. statistical analysis (or individual wave analysis) and spectral analysis. The statistical-based significant wave height  $(H_{1/3})$  is defined as the average height of the highest one-third of the individual waves in a record, while the spectral significant wave height  $(H_{m0})$  is defined as four times of square root of zero moment of wave spectrum  $(H_{m0} = 4.0\sqrt{m_0})$ . These two definitions of significant wave height are equal if the wave height distribution obeys a Rayleigh distribution.

In deepwater, the measured wave heights from different oceans have been found to closely conform to the Rayleigh distribution [Demerbilek and Vincent, 2006]. The relationship  $H_{1/3} = H_{m0} = 4.0\sqrt{m_0}$  can be derived based on the assumption of a Rayleigh distribution. The relationship has been confirmed by many wave observation data taken throughout the world [Goda, 2000]. However, the proportional constants are smaller than those derived from the Rayleigh distribution, e.g. the ratio  $H_{1/3}/\sqrt{m_0}$  is approximately 3.8 instead of 4.0 [Goda, 1979]. When waves propagate in shallow water, their profiles steepen and they eventually break. The process of wave breaking becomes relevant in shallow water, causing the wave height distribution to deviate from the Rayleigh distribution. Several researchers stated that the wave height distribution deviated considerably from the Rayleigh distribution [e.g. Klopman, 1996; Battjes and Groenendijk, 2000; Mendez et al., 2004]. This causes the statistical based wave height to differ from the corresponding spectral based wave height.

The two significant wave heights are both important, and neither one alone is sufficient for successful application of wave height for engineering problems [Goda, 1974]. While some formulas in the coastal works are appropriate for  $H_{1/3}$ , others may be more appropriate for  $H_{m0}$ . The spectral wave heights  $(H_{m0})$  should be used in those applications where the effect of average wave energy is more important than the individual waves.

The wave heights are usually available in deepwater (from measurements or wave hindcasts) but not available at the required depths in shallow water. The wave height at desired depth can be determined from a wave model. During the past few decades, many wave models have been proposed but most of them are for computing the root-mean-square wave heights  $(H_{rms})$ , not for  $H_{m0}$ . However, measured ocean wave records are often analyzed spectrally by the instrument package and expressed in terms of  $H_{m0}$ . Similarly, modern wave hindcasts are often expressed in terms of  $H_{m0}$ . It seems to be convenient for engineers to have a wave height transformation model for computing the transformation of  $H_{m0}$  directly. Therefore, the present study concentrates on a wave height transformation model for computing the transformation model for computing the transformation model for computing

In the present study, the transformation of  $H_{m0}$  is computed from the energy flux conservation equation. The main difficulty of modeling the wave height transformation is how to formulate the rate of dissipation due to wave breaking. Various

dissipation models have been proposed by many researchers but most of them were proposed for computing  $H_{rms}$ . Therefore, the existing dissipation models have to be converted to be expressed in terms of  $H_{m0}$  before applying to compute the transformation of  $H_{m0}$ . Similar to the significant wave height, the root-mean-square wave height  $(H_{rms})$  can be classified according to its definition based on statistical-based root-mean-square wave height  $(H_{rms})$  and spectral-based root-mean-square wave height  $(H_{rms})$ . If an energy dissipation model is proposed in terms of  $H_{rms}$ , it seems to be difficult to convert the model to be expressed in terms of  $H_{m0}$ . However, if an energy dissipation model is proposed in terms of  $H_{rms}$ , it can be converted to be expressed in terms of  $H_{m0}$  easily (because  $H_{m0} = \sqrt{2}H_{rms}$ ). Unfortunately, most existing models were developed without regard for the difference between  $H_{rms}$  and  $H_{rms}$ . Moreover, it is not clear which model is the most suitable one for computing  $H_{m0}$ . The main objectives of this study are to apply the existing dissipation models of  $H_{rms}$  to compute the transformation of  $H_{m0}$  and to find out the most suitable model for computing  $H_{m0}$ .

# 2. Compiled Experimental Data

Experimental data on  $H_{m0}$  transformation from 8 sources, including 1,713 cases, have been compiled to examine the models. A summary of the compiled experimental data is given in Table 1. The experiments cover a wide range of wave and beach conditions, including small- and large-scale laboratory and field experiments. The experiments of Smith and Vincent [1992], Hamilton and Ebersole [2001], and Smith and Seabergh [2001] were performed under fixed bed conditions, while the others were performed under moveable bed (sandy beach) conditions. Only the data in the nearshore zone (excluding swash zone) are considered in this study. The data cover a range of deepwater wave steepness  $(H_{m0,0}/L_0)$  from 0.001 to 0.069. A brief summary of the compiled data is provided below.

Sources	No. of cases	No. of data points	Apparatus	Deepwater wave steepness $(H_{m0,0}/L_0)$
Smith and Vincent [1992]	4	36	small-scale	0.032 – 0.064
Hamilton and Ebersole [2001]	1	10	small-scale	0.023
Smith and Seabergh [2001]	15	180	small-scale	0.007 – 0.069
SUPERTANK project	128	2,047	large-scale	0.002 – 0.064
LIP IID project	95	923	large-scale	0.005 – 0.039
SAFE project	138	3,557	large-scale	0.009 – 0.021
DELILAH project	745	5,049	field	0.001 – 0.036
DUCK94 project	587	6,104	field	0.001 – 0.041
Total	1,713	17,906		0.001 – 0.069

Table 1. Summary of compiled experimental data.

The experiment of Smith and Vincent [1992] was conducted to investigate shoaling and decay of multiple wave trains using a small wave flume of 45.7 m long, 0.45 m wide, and 0.9 m deep. The bottom of the flume is smooth concrete and rises at a slope of 1:30 from the middle of the flume. Twelve double-peaked spectra were generated by superimposing two spectra of the TMA type [Bouws et al., 1985] with a spectral width parameter of 20. The cases include two double-peak wave period combinations  $(T_p = 2.5 \,\mathrm{s}/1.25 \,\mathrm{s}$  and  $2.5 \,\mathrm{s}/1.75 \,\mathrm{s})$  with two total wave heights  $(H_{m0} = 15.2 \,\mathrm{cm}$  and 9.2 cm). The four most energetic cases (i.e. cases 1, 3, 7, and 9) and the dominant peak periods were used in the present study. Water surface elevations were measured at nine cross-shore locations using electrical-resistance gages. The significant wave heights were determined from water surface elevations in the frequency band 0.1 to 2.5 Hz.

The experiment of Hamilton and Ebersole [2001] was conducted to establish uniform longshore currents in a wave basin, which has dimensions of 30 m cross-shore, 50 m longshore, and 1.4 m deep. A concrete beach with 1/30 slope has a cross-shore dimension of 21 m and a longshore dimension of 31 m. The irregular waves were developed from the TMA spectrum [Bouws et al., 1985], with a significant wave height of 0.21 m, spectral peak period of 2.5 s, direction 10°, and spectral width parameter of 3.3. Water surface elevations were measured at ten cross-shore locations using capacitance-type wave gages and four other wave gages were fixed in the longshore direction near the wave generators. The significant wave heights were analyzed based on a lower cut-off frequency of 0.2 Hz.

The experiment of Smith and Seabergh [2001] was conducted to study the effect of ebb current on wave shoaling and breaking in an idealized inlet. The experiment was performed in a wave basin, which has dimensions of 99 m long, 46 m wide, and 0.6 m deep. The physical model included an offshore equilibrium slope, an elliptical ebb shoal located seaward of the inlet, rubble jetties, and a flat entrance channel. The tests were performed under the conditions of regular and irregular waves and with and without currents. Only irregular waves with no current conditions (in total 15 cases) are considered in this study. The irregular waves were developed from the TMA spectrum [Bouws et al., 1985], with significant wave heights from 0.018 to 0.079 m, wave periods from 0.7 to 1.7 s, spectral width parameter of 3.3, and incident wave direction perpendicular to the shore. Water surface elevations were measured at eleven cross-shore locations using capacitance-type gages. The significant wave heights were analyzed over the entire collected water surface elevations.

The SUPERTANK laboratory data collection project [Kraus and Smith, 1994] was conducted to investigate cross-shore hydrodynamic and sediment transport processes from August 5 to September 13, 1992 at Oregon State University, Corvallis, Oregon, USA. A 76-m-long sandy beach was constructed in a large wave tank of 104 m long, 3.7 m wide, and 4.6 m deep. Wave conditions included both regular and irregular waves. In all, 20 major tests were performed, and each major test consisted of several cases. Most of the tests (14 major tests) were performed under the

irregular wave actions. The wave conditions were designed to balance the need for repetition of wave conditions to move the beach profile toward equilibrium and development of a variety of conditions for hydrodynamic studies. The TMA spectral shape [Bouws et al., 1985] was used to design all irregular wave tests. The compiled experiments for irregular waves included 128 cases of wave and beach conditions, covering incident significant wave heights from 0.2 to 1.0 m, spectral peak periods from 3.0 to 10.0 s, and spectral width parameter between 3.3 (broad-banded) and 100 (narrow-banded). Sixteen resistance-type gages were used to measure water surface elevations across shore. A 10-Hz, fifth-order anti-aliasing Bessel filter was applied to eliminate noise and avoid aliasing. The wave spectral analysis was performed on total, low-pass, and high-pass signals. The data from the total signals were used in this study.

LIP 11D Delta Flume Experiment [Roelvink and Reniers, 1995] was performed at Delft Hydraulics large-scale wave flume. A 175-m-long sandy beach was constructed in a large wave tank of 233 m long, 5 m wide and 7 m deep. The two major tests were performed, i.e. with dune (test no. 1A-1C) and without dune (test no. 2A-2C). Each major test consisted of several wave conditions. The duration of each wave condition lasted about 12–21 hr. Initial beach profiles of tests no. 1A and 2A are equilibrium Dean-type beaches. The beach profiles of other tests (test no. 1B, 1C, 2B, 2E, and 2C) were initiated using the final profile configuration of the previous test. Broad banded random waves, JONSWAP spectrum [Hasselmann et al., 1973] with spectral width parameter of 3.3, were generated. During the run, the sand bar feature grows and becomes more pronounced after some time. Ten fixed wave gages were deployed in the flume to measure water surface elevations. To avoid aliasing, each signal was filtered by analog filter at 5 Hz before analyzing. The compiled experiments included 95 cases of wave and beach conditions, covering incident significant wave heights from 0.6 to 1.4 m, spectral peak periods from 5 to 8 s, and water level from 4.1 to 4.6 m.

The SAFE Project [Dette  $et\ al.$ , 1998] was carried out to improve the methods of design and performance assessment of beach nourishment. The SAFE Project consisted of four activities, one of which was to perform experiments in a large-scale wave flume in Hannover, Germany. A 250-m-long sandy beach was constructed in a large wave tank of 300 m long, 5 m wide and 7 m deep. The test program was divided into two major phases. The first phase (cases A, B, C, and H) was aimed to study the beach deformation of equilibrium profile with different beach slope changes. The equilibrium beach profile was adopted from Bruun's [1954] approach. In the second phase, the sediment transport behaviors of dunes with and without structural aid were investigated (cases D, E, F, and G). The TMA spectral shape [Bouws  $et\ al.$ , 1985] was used to design all irregular wave tests. The tests were performed under normal wave conditions and storm wave conditions. A total of 27 wave gages was installed over a length of 175 m along one wall of the flume. The records from all gages were checked for plausibility before analysis. The compiled experiments

included 138 cases of wave and beach conditions, covering incident significant wave heights from 0.65 to  $1.20\,\mathrm{m}$ , mean wave period of  $5.5\,\mathrm{s}$ , and water level from 4.0 to  $5.0\,\mathrm{m}$ .

DELILAH Project [Birkemeier et al., 1997] was conducted on the barred beach in Duck, North Carolina, USA in October 1990. The objective of the project is to improve fundamental understanding and modeling of surf zone physics. The experiment emphasized surf zone hydrodynamics in the presence of a changing barred bathymetry. Nine pressure gauges were installed to measure the nearshore wave heights across-shore and one of them was in the swash zone. Tidal elevations were measured at the FRF pier. The significant wave heights were determined from water surface elevations in the frequency band 0.04–0.4 Hz. The measured wave heights are available at http://dksrv.usace.army.mi/jg/del90dir. The data of wave heights and water depths measured during Oct 2-21, 1990 are available. The wave heights and water depths data are available at approximately every 34 min. A total of 776 sets of measured wave heights and water depths are available on the data server. A data set that has only a few points of measurements is not suitable to use for verifying the models. A total of 745 data sets are considered in this study. The incident waves (at the most offshore-ward position) cover the range of significant wave height from 0.4 to 0.7 m, wave period from 3.4 to 13.5 s, and direction from  $-36^{\circ}$  to  $2^{\circ}$  (counter-clockwise from shore normal).

DUCK94 Project [Herbers et al., 2006] was conducted on the barred beach in Duck, North Carolina, USA during Aug—Oct 1994. The project objective is the same as that of DELILAH. The experiment emphasized surf zone hydrodynamics, sediment transport and morphological evolution. Thirteen pressure gauges were installed to measure the nearshore wave heights across-shore and one of them was in the swash zone. Tidal elevations were measured at the FRF pier. The significant wave heights were determined from water surface elevations in the frequency band 0.05–0.25 Hz. The measured wave heights, and water depths are available at http://dksrv.usace.army.mi/jg/dk94dir. The wave heights and water depths at every 3h that were measured during Aug 15–Oct 31, 1994 are used in the present study. Excluding the data sets that have only a few points of measurements, a total of 587 data sets are considered in the present study. The incident waves (at the most offshore-ward position) cover the range of significant wave height from 0.2 to 2.6 m, wave period from 4.4 to 11.4 s, and direction from -56° to 71° (counter-clockwise from shore normal).

# 3. Model Development

When waves propagate to the nearshore zone, wave profiles steepen and eventually waves break. Once the waves start to break, a part of wave energy is transformed into turbulence and heat, and wave height decreases towards the shore. In the present study, wave height transformation is computed from the energy flux conservation

equation. It is

$$\frac{\partial (Ec_g \cos \theta)}{\partial x} = -D_B \tag{1}$$

where E is the wave energy density,  $c_g$  is the group velocity,  $\theta$  is the mean wave angle, x is the distance in cross shore direction, and  $D_B$  is the energy dissipation rate due to wave breaking which is zero outside the surf zone. The energy dissipation rate due to bottom friction is neglected. In the present study, all variables are based on the linear wave theory and the Snell's law is employed to describe wave refraction as

$$\frac{\sin \theta}{c} = \text{constant} \tag{2}$$

where c is the phase velocity.

For the spectral analysis, the moments of a wave spectrum are important in characterizing the spectrum and useful in relating the spectral description of waves to the significant wave height. The representative value of the total wave energy is the zero moment of wave spectrum  $(m_0)$ , which can be obtained by integrating the wave spectrum (S(f)) in the full range of frequency (f). The integral is, by definition of the wave spectrum, equal to the variance of the surface elevation [Goda, 2000]. Therefore, the zero moment of the spectrum  $(m_0)$  can be expressed as

$$m_0 = \int_0^\infty S(f)df = \frac{1}{t_n} \int_0^{t_n} \eta^2 dt$$
 (3)

where  $\eta$  is the water surface elevation, t is time, and  $t_n$  is the total time of the wave record.

The zero moment  $(m_0)$  can be related to the significant wave height by considering the total energy density of a wave record. From linear wave theory, the total energy density is twice the potential energy density, which can be written in terms of the surface elevation as

$$E = 2E_p = \frac{2}{t_p} \int_0^{t_n} \frac{\rho g \eta^2}{2} dt = \rho g m_0 \tag{4}$$

where  $E_p$  is the potential energy density,  $\rho$  is the water density, and g is the acceleration due to gravity.

As the spectral significant wave height  $(H_{m0})$  is defined as  $H_{m0} = 4\sqrt{m_0}$ , the total energy density of a wave record [Eq. (4)] can be written in terms of  $H_{m0}$  as

$$E = \frac{1}{16} \rho g H_{m0}^2 \tag{5}$$

Substituting Eq. (5) into Eq. (1), the governing equation for computing the transformation of  $H_{m0}$  can be written as

$$\frac{\rho g}{16} \frac{\partial (H_{m0}^2 c_g \cos \theta)}{\partial x} = -D_B \tag{6}$$

The transformation of  $H_{m0}$  can be computed from the energy flux balance equation [Eq. (6)] by substituting the formula of the energy dissipation rate  $(D_B)$  and numerically integrating from offshore to shoreline. In the offshore zone, the energy dissipation rate is set to zero. The difficulty of the energy flux conservation approach is how to formulate the energy dissipation rate caused by the breaking waves. Various dissipation models have been proposed but most of them were proposed in terms of  $H_{rms}$ . The selected existing dissipation models are described in the following subsection.

# 3.1. Existing energy dissipation models

## 3.1.1. Model overview

The first attempt at examination is to collect the existing dissipation models for computing  $H_{rms}$ . Because of the complexity of the wave breaking mechanism, most of the energy dissipation models were developed based on the empirical or semi-empirical approach calibrated with the measured data. Brief reviews of some selected existing dissipation models are described below.

(a) Battjes and Janssen [1978], hereafter referred to as BJ78, proposed to compute  $D_B$  by multiplying the fraction of irregular breaking waves  $(Q_b)$  by the energy dissipation of a single broken wave. The energy dissipation of a broken wave is described by the bore analogy and assuming that all broken waves have a height equal to breaking wave height  $(H_b)$ . The model was proposed as

$$D_B = K_1 Q_b \frac{\rho g H_b^2}{4T_p} \tag{7}$$

where  $T_p$  is the spectral peak period and  $K_1$  is the adjustable coefficient. The proposed value of  $K_1$  is 1.0. The fraction of breaking waves  $(Q_b)$  was derived based on the assumption that the probability density function (pdf) of wave heights could be modeled with a Rayleigh distribution truncated at the breaking wave height  $(H_b)$  and all broken waves have a height equal to the breaking wave height. The result is

$$\frac{1 - Q_b}{-\ln Q_b} = \left(\frac{H_{rms}}{H_b}\right)^2 \tag{8}$$

in which the breaking wave height  $(H_b)$  is determined from the formula of Miche [1944] with additional coefficient 0.91 as

$$H_b = K_2 L \tanh(0.91 \ kh) \tag{9}$$

where L is the wavelength related to  $T_p$ , k is the wave number, h is the mean water depth,  $K_2$  is the adjustable coefficient. The proposed value of  $K_2$  is 0.14. The  $D_B$  model of BJ78 has been used successfully in many applications

Constants	Values
$a_0$	0.2317072
$a_1$	-3.6095814
$a_2$	22.5948312
$a_3$	-72.5367918
$a_4$	126.8704405
$a_5$	-120.5676384
$a_6$	60.7419815
$a_7$	-12.7250603

Table 2. Values of constants  $a_0$  to  $a_7$  for computing  $Q_b$ .

[e.g. Abadie et al., 2006; Johnson, 2006; and Oliveira, 2007]. As Eq. (8) is an implicit equation, it has to be solved for  $Q_b$  by an iteration technique, or by a 1-D look-up table [Southgate and Nairn, 1993]. It can be also determined from the polynomial equation as

$$Q_b = \sum_{n=0}^{7} a_n \left(\frac{H_{rms}}{H_b}\right)^n \tag{10}$$

where  $a_n$  is the constant of nth term. A multiple regression analysis is used to determine the constants  $a_0$  to  $a_7$ . The correlation coefficient  $(R^2)$  of Eq. (10) is very close to 1 (0.99999999). The values of constants  $a_0$  to  $a_7$  are shown in Table 2. Equation (10) is applicable for  $0.25 < H_{rms}/H_b < 1.0$ . For  $H_{rms}/H_b \le 0.25$ , the value of  $Q_b$  is very small and can be set at zero. The value of  $Q_b$  is set to be 1.0 when  $H_{rms}/H_b \ge 1.0$ . As Eqs. (8) and (10) give almost identical results  $(R^2 = 0.999999999)$ , for convenience, Eq. (10) is used in this study.

(b) Thornton and Guza [1983], hereafter referred to as TG83, proposed to compute  $D_B$  by integrating from 0 to  $\infty$  the product of the dissipation for a single broken wave and the pdf of the breaking wave height. The energy dissipation of a single broken wave is described by their bore model which is slightly different from the bore model of BJ78. The pdf of breaking wave height is expressed as a weighting of the Rayleigh distribution. By introducing two forms of the weighting, two models of  $D_B$  were proposed. After calibrating with small-scale experimental data, the models were proposed to be model 1 (hereafter referred to as TG83a):

$$D_B = K_3 \frac{3\sqrt{\pi}}{4} \left(\frac{H_{rms}}{H_b h}\right)^4 \frac{\rho g H_{rms}^3}{4T_p h} \tag{11}$$

in which

$$H_b = K_4 h \tag{12}$$

model 2 (hereafter referred to as TG83b):

$$D_B = K_5 \frac{3\sqrt{\pi}}{4} \left(\frac{H_{rms}}{H_b}\right)^2 \left\{1 - \frac{1}{[1 + (H_{rms}/H_b)^2]^{2.5}}\right\} \frac{\rho g H_{rms}^3}{4T_p h}$$
(13)

in which

$$H_b = K_6 h \tag{14}$$

where  $K_3$  to  $K_6$  are the adjustable coefficients. The proposed values of  $K_3$  to  $K_6$  are 0.51, 0.42, 0.51, and 0.42, respectively.

(c) Battjes and Stive [1985], hereafter referred to as BS85, used the same energy dissipation model as that of BJ78.

$$D_B = K_7 Q_b \frac{\rho g H_b^2}{4T_p} \tag{15}$$

where  $K_7$  is the adjustable coefficient. The proposed value of  $K_7$  is 1.0. They modified the model of BJ78 by recalibrating the additional coefficient in the breaker height formula [Eq. (9)]. The coefficient was related to the deepwater wave steepness  $(H_{rms,0}/L_0)$ . After calibration with small-scale and field experiments, the breaker height formula was modified to be

$$H_b = K_8 L \tanh \left\{ \left[ 0.57 + 0.45 \tanh \left( 33 \frac{H_{rms,0}}{L_0} \right) \right] kh \right\}$$
 (16)

where  $H_{rms,0}$  is the deepwater root-mean-square wave height,  $L_0$  is the deepwater wavelength, and  $K_8$  is the adjustable coefficient. The proposed value of  $K_8$  is 0.14. Hence, the model of BS85 is similar to that of BJ78 except for the formula of  $H_b$ .

(d) Southgate and Nairn [1993], hereafter referred to as SN93, modified the model of BJ78 by changing the expression of energy dissipation of a breaker height from the bore model of BJ78 to be the bore model of TG83 as

$$D_B = K_9 Q_b \frac{\rho g H_b^3}{4T_p h} \tag{17}$$

where  $K_9$  is the adjustable coefficient. The proposed value of  $K_9$  is 1.0. The fraction of breaking waves  $Q_b$  is determined from Eq. (8). The breaker height  $(H_b)$  is determined from the formula of Nairn [1990] as

$$H_b = K_{10}h \left[ 0.39 + 0.56 \tanh \left( 33 \frac{H_{rms,0}}{L_0} \right) \right]$$
 (18)

where  $K_{10}$  is the adjustable coefficient. The proposed value of  $K_{10}$  is 1.0. Hence, the model of SN93 is similar to that of BJ78 except for the formulas of energy dissipation of a single breaker height and  $H_b$ .

(e) Baldock et al. [1998], hereafter referred to as BHV98, proposed to compute  $D_B$  by integrating from  $H_b$  to  $\infty$  the product of the energy dissipation for a broken wave and the pdf of wave heights. The energy dissipation of a broken wave is described by the bore model of BJ78. The pdf of wave heights inside the surf zone was assumed to be the Rayleigh distribution. The result is

$$D_{B} = \begin{cases} K_{11} \exp\left[-\left(\frac{H_{b}}{H_{rms}}\right)^{2}\right] \frac{\rho g(H_{b}^{2} + H_{rms}^{2})}{4T_{p}} & \text{for } H_{rms} < H_{b} \\ K_{11} \exp[-1] \frac{2\rho g H_{b}^{2}}{4T_{p}} & \text{for } H_{rms} \ge H_{b} \end{cases}$$
(19)

where  $K_{11}$  is the adjustable coefficient. The proposed value of  $K_{11}$  is 1.0. The breaker height  $(H_b)$  is determined from the formula of Nairn [1990] as

$$H_b = K_{12}h \left[ 0.39 + 0.56 \tanh \left( 33 \frac{H_{rms,0}}{L_0} \right) \right]$$
 (20)

where  $K_{12}$  is the adjustable coefficient. The proposed value of  $K_{12}$  is 1.0.

(f) Rattanapitikon and Shibayama [1998], hereafter referred to as RS98, modified the model of BJ78 by changing the expression of energy dissipation of a single broken wave from the bore concept to the stable energy concept as

$$D_B = K_{13} Q_b \frac{c\rho g}{8h} \left[ H_{rms}^2 - \left( h \exp\left( -0.58 - 2.0 \frac{h}{\sqrt{LH_{rms}}} \right) \right)^2 \right]$$
 (21)

where  $K_{13}$  is the adjustable coefficient and the fraction of breaking wave  $(Q_b)$  is computed from Eq. (8). The proposed value of  $K_{13}$  is 0.10. The breaking wave height  $(H_b)$  is computed by using the breaking criteria of Goda [1970] as

$$H_b = K_{14}L_o \left\{ 1 - \exp\left[ -1.5 \frac{\pi h}{L_o} (1 + 15m^{4/3}) \right] \right\}$$
 (22)

where m is the average bottom slope and  $K_{14}$  is the adjustable coefficient. The proposed value of  $K_{14}$  is 0.10.

(g) Ruessink et al. [2003], hereafter referred to as RWS03, used the same energy dissipation model as that of BHV98 [Eq. (19)] but a different breaker height formula. The breaker height formula of BJ78 [Eq. (9)] is modified by relating the additional coefficient with the terms kh. After calibration with field experiments, the model was proposed to be

$$D_{B} = \begin{cases} K_{15} \exp\left[-\left(\frac{H_{b}}{H_{rms}}\right)^{2}\right] \frac{\rho g(H_{b}^{2} + H_{rms}^{2})}{4T_{p}} & \text{for } H_{rms} < H_{b} \\ K_{15} \exp[-1] \frac{2\rho g H_{b}^{2}}{4T_{p}} & \text{for } H_{rms} \ge H_{b} \end{cases}$$
(23)

in which

$$H_b = K_{16}L \tanh[(0.86kh + 0.33)kh] \tag{24}$$

where  $K_{15}$  and  $K_{16}$  are the adjustable coefficients. The proposed values of  $K_{15}$  and  $K_{16}$  are 1.0 and 0.14, respectively.

(h) Rattanapitikon et al. [2003], hereafter referred to as RKS03, developed an energy dissipation model based on the representative wave approach. They applied the dissipation model for regular waves for computing the energy dissipation of irregular waves. It was found that the stable energy concept of Dally et al. (1985) can be used to describe the energy dissipation of irregular wave breaking. After calibration with laboratory and field experiments, the model was proposed to be

$$D_B = K_{17} \frac{\rho g c_g}{8h} [H_{rms}^2 - (0.42H_b)^2]$$
 (25)

where  $K_{17}$  is the adjustable coefficient. The proposed value of  $K_{17}$  is 0.12. The value of  $D_B$  is set to be zero when  $H_{rms} \leq 0.42H_b$  and the breaker height  $(H_b)$  is computed by using the breaking criteria of Miche [1944] as

$$H_b = K_{18}L \tanh(kh) \tag{26}$$

where  $K_{18}$  is the adjustable coefficient. The proposed value of  $K_{18}$  is 0.14.

(i) Rattanapitikon [2007], hereafter referred to as R07, modified six existing models by changing the breaker height formulas in the dissipation models. A total of 42 possible models were considered in the study. Considering accuracy, variance of errors, and simplicity of the possible models, the following model was recommended

$$D_B = K_{19} \frac{\rho g c_g}{8h} [H_{rms}^2 - (0.47H_b)^2]$$
 (27)

where  $K_{19}$  is the adjustable coefficient. The proposed value of  $K_{19}$  is 0.07. The value of  $D_B$  is set to be zero when  $H_{rms} \leq 0.47H_b$  and the breaker height  $(H_b)$  is computed by modifying the breaking criteria of BJ78 as

$$H_b = K_{20}L \tanh(0.68kh)$$
 (28)

where  $K_{20}$  is the adjustable coefficient. The proposed value of  $K_{20}$  is 0.14. Hence, the model of R07 is similar to that of RKS03 except for the formula of  $H_b$ .

(j) Alsina and Baldock [2007], hereafter referred to as AB07, modified the model of BHV98 by changing the energy dissipation of a broken wave from the bore model of BJ78 to be the bore model of TG83. The correction is introduced to prevent a shoreline singularity that can develop in shallow water. They proposed

an alternative dissipation model as

$$D_B = K_{21} \frac{\rho g H_{rms}^3}{4T_p h} \left\{ \left[ \left( \frac{H_b}{H_{rms}} \right)^3 + \frac{3}{2} \frac{H_b}{H_{rms}} \right] \exp \left[ -\left( \frac{H_b}{H_{rms}} \right)^2 \right] + \frac{3}{4} \sqrt{\pi} \left[ 1 - erf \left( \frac{H_b}{H_{rms}} \right) \right] \right\}$$

$$(29)$$

where erf is the error function and  $K_{21}$  is the adjustable coefficient. The proposed value of  $K_{21}$  is 1.0. The breaking wave height  $(H_b)$  is determined from the formula of BS85 as

$$H_b = K_{22}L \tanh \left\{ \left[ 0.57 + 0.45 \tanh \left( 33 \frac{H_{rms,0}}{L_0} \right) \right] kh \right\}$$
 (30)

where  $K_{22}$  is the adjustable coefficient. The proposed value of  $K_{22}$  is 0.14.

(k) Janssen and Battjes [2007], hereafter referred to as JB07, derived the same dissipation model as that of AB07 (independently of the study of AB07). The main difference between JB07 and AB07 is the breaker height formula. Their dissipation model can be summarized as

$$D_B = K_{23} \frac{\rho g H_{rms}^3}{4T_p h} \left\{ \left[ \left( \frac{H_b}{H_{rms}} \right)^3 + \frac{3}{2} \frac{H_b}{H_{rms}} \right] \exp \left[ -\left( \frac{H_b}{H_{rms}} \right)^2 \right] + \frac{3}{4} \sqrt{\pi} \left[ 1 - erf \left( \frac{H_b}{H_{rms}} \right) \right] \right\}$$

$$(31)$$

where  $K_{23}$  is the adjustable coefficient. The proposed value of  $K_{23}$  is 1.0. The breaking wave height  $(H_b)$  is determined from the formula of Nairn [1990] as

$$H_b = K_{24}h \left[ 0.39 + 0.56 \tanh \left( 33 \frac{H_{rms,0}}{L_0} \right) \right]$$
 (32)

where  $K_{24}$  is the adjustable coefficient. The proposed value of  $K_{24}$  is 1.0.

(1) Rattanapitikon and Sawanggun [2008], hereafter referred to as RS08, modified the model of BJ78 by changing the expression of fraction of breaking waves. In contrast to the common derivation, the fraction of breaking waves was not derived from the assumed pdf of wave heights, but derived directly from the measured wave heights. After calibration, the model can be expressed as

$$D_B = K_{25} \frac{\rho g H_b^2}{4T} \left[ 2.096 \left( \frac{H_{rms}}{H_b} \right)^2 - 1.601 \left( \frac{H_{rms}}{H_b} \right) + 0.293 \right] \text{ for } \frac{H_{rms}}{H_b} > 0.46$$
(33)

where  $K_{25}$  is the adjustable coefficient. The proposed value of  $K_{25}$  is 1.0. The value of  $D_B$  is set to be zero when  $H_{rms}/H_b \leq 0.46$  and the breaking wave height  $(H_b)$  is determined from the formula of BS85 as

$$H_b = K_{26}L \tanh \left\{ \left[ 0.57 + 0.45 \tanh \left( 33 \frac{H_{rms,0}}{L_0} \right) \right] kh \right\}$$
 (34)

where  $K_{26}$  is the adjustable coefficient. The proposed value of  $K_{26}$  is 0.14.

(m) Apotsos et al. [2008], hereafter referred to as AREG08, modified six existing dissipation models by recalibrating the coefficient in the breaker height formulas incorporated in the dissipation models. The coefficient was related to the deepwater wave height  $(H_{rms,0})$ . The comparison showed that the model TG83b [Eq. (13)] with new breaker height formula gives the smallest error. The modified model was proposed to be

$$D_B = K_{27} \frac{3\sqrt{\pi}}{4} \left(\frac{H_{rms}}{H_b}\right)^2 \left\{1 - \frac{1}{[1 + (H_{rms}/H_b)^2]^{2.5}}\right\} \frac{\rho g H_{rms}^3}{4T_p h}$$
(35)

$$H_b = K_{28}[0.18 + 0.40 \tanh(0.9H_{rms,0})]h \tag{36}$$

where  $K_{27}$  and  $K_{28}$  are the adjustable coefficients. The proposed values of  $K_{27}$  and  $K_{28}$  are 1.0 and 1.0, respectively.

## 3.1.2. Model analysis

The development of the existing dissipation models may be classified into two approaches, i.e. parametric wave approach and stable energy approach. The parametric wave approach seeks to reduce the computational effort by describing the energy dissipation rate in terms of time-averaged parameter. Its description is reduced to a single representative wave height, period, and direction. As this approach relies on the macroscopic features of breaking waves and predicts only the transformation of root-mean-square (rms) wave height, it is suitable when a detail wave height distribution is not needed. The approach assumes that the Rayleigh pdf (or modified Rayleigh pdf) is valid in the surf zone. The average rate of energy dissipation is described by integrating the product of energy dissipation of a single broken wave and the probability of occurrence of breaking waves. Most of the selected models (except RKS03 and R07) were developed based on this approach. The models were developed based on the work of BJ78. The significant differences of those models are the assumption on probability of occurrence of breaking waves, the formulation of energy dissipation of a single broken wave, and the breaker height formula. The models may be grouped into three groups based on the assumed probability of occurrence of breaking waves. The first group (BJ78, BS85, SN93, RS98, and RS08) describes the pdf of wave heights in the surf zone through a sharp cutoff Rayleigh distribution, truncated at a breaker height  $(H_b)$  at which all waves are assumed to break and have heights equal to the breaker height. The second group (TG83a, TG83b, and AREG08) describes the probability of occurrence of breaking waves through a weighted Rayleigh distribution. The third group (BHV98, RWS03, AB07, and JB07) describes the pdf of wave heights in the surf zone through a complete Rayleigh distribution and the wave heights which are greater than a breaker height  $(H_b)$  are considered as broken waves.

The stable energy concept was introduced by Dally et al. [1985] for computing the energy dissipation rate due to regular wave breaking. The model was developed based on the measured breaking wave height on the horizontal bed. When a breaking wave enters an area with a horizontal bed, the breaking continues (the wave height decreases) until some stable wave height is attained. The development of the stable energy concept was based on an observation of stable wave height on horizontal slopes. Dally et al. [1985] assumed that the energy dissipation rate was proportional to the difference between the local energy flux per unit depth and the stable energy flux per unit depth. The energy dissipation will be zero if the wave height is less than the stable wave height. The model seems to be widely used for computing regular wave height transformation. For irregular waves, RKS03 and R07 showed that the stable energy concept is applicable for computing the transformation of  $H_{rms}$ . The approach has the merits of easy understanding, simple application and it is not necessary to assume the shape of the pdf of wave heights. The stable wave heights of the RKS03 and R07 were proposed in terms of breaker heights. The model of RKS03 used the breaker height formula of Miche [1944], while the model of R07 used the breaker height formula of BJ78. It is known that the process of wave breaking in shallow water is influenced by the incident wave steepness and bottom slope. However, the effect of beach slope is not included in the stable energy models. The effect of beach slope may be included in the models by changing the breaker height formula from Miche [1944] or BJ78 to be the other breaker height formula which includes the effect of beach slope.

These two approaches rely on the macroscopic features of breaking waves and predict only the transformation of  $H_{rms}$ . The two approaches have different advantages and disadvantages. The advantage of the stable energy approach is that it is able to stop wave breaking over bar-trough or step profiles, while the parametric wave approach gives a continuous dissipation due to wave breaking. However, the parametric approach may not give much error in predicting wave height in the trough region because the values of  $H_{rms}/H_b$  and  $Q_b$  are very small in the trough. The prediction may not be locally precise in the trough region, but generally patterns of wave transformation were reported adequately [Battjes and Janssen, 1978]. The advantage of the parametric wave approach is that it is able to compute a fraction of wave breaking (which is useful for computing undertow and suspended sediment concentration), while the fraction of wave breaking cannot be determined from the stable energy approach.

# 3.2. Model adaptation

As the existing dissipation models (shown in Sec. 3.1) were proposed in terms of  $H_{rms}$ , the models have to be converted to be expressed in terms  $H_{m0}$  before applying to compute  $H_{m0}$ . By assuming that  $H_{m0} = \sqrt{2}H_{rms}$ , the existing dissipation models are applied for computing the transformation of  $H_{m0}$  by substituting  $H_{rms} = H_{m0}/\sqrt{2}$  into the models (shown in Sec. 3.1). Then the wave height transformation models can be constructed by substituting the dissipation models into the energy flux balance equation [Eq. (6)]. Nevertheless, it is not clear which dissipation model is the most suitable one for computing  $H_{m0}$ . Therefore, all of them were used to examine their applicability on simulating  $H_{m0}$ .

## 4. Model Examination

The objective of this section is to examine the applicability of the fourteen existing dissipation models in simulating  $H_{m0}$ . The measured  $H_{m0}$  from the compiled experiments (shown in Table 1) are used to examine the accuracy of existing models. The transformation of  $H_{m0}$  is computed by numerical integration of the energy flux balance equation [Eq. (6)] with the existing energy dissipation models. A backward finite difference scheme is used to solve the energy flux balance equation [Eq. (6)]. The basic parameter for determination of the overall accuracy of a model is the average root-mean-square relative error  $(ER_{avg})$ , which is defined as

$$ER_{avg} = \frac{\sum_{j=1}^{tn} ER_{gj}}{tn} \tag{37}$$

where  $ER_{gj}$  is the root-mean-square relative error of the data group j (the group number), and tn is the total number of groups. The small value of  $ER_{avg}$  indicates good overall accuracy of the model. The root-mean-square relative error of the data group  $(ER_q)$  is defined as

$$ER_g = 100\sqrt{\frac{\sum_{i=1}^{n_g} (H_{ci} - H_{mi})^2}{\sum_{i=1}^{n_g} H_{mi}^2}}$$
 (38)

where i is the wave height number,  $H_{ci}$  is the computed wave height of number i,  $H_{mi}$  is the measured wave height of number i, and ng is the total number of measured wave heights in each data group.

The compiled experiments are separated into three groups according to the experiment scale, i.e. small-scale, large-scale and field experiments. It is expected that a good model should be able to predict well for the three groups of different scale. As the present study concentrates on only the transformation of wave height (excluding wave set-up), the measured mean water depth is used in the computation. However, the measured wave set-up is not available for the field data. The water depth including tidal change is used for the field experiments.

			•			
Models	$D_B$ formulas	Default coefficients		$ER_g$		$ER_{avg}$
			Small-scale	Large-scale	Field	
BJ78	Eq. (7)	$K_1 = 1.0, K_2 = 0.14$	9.7	10.5	17.7	12.6
TG83a	Eq. (11)	$K_3 = 0.51, K_4 = 0.42$	13.1	16.1	11.2	13.4
TG83b	Eq. (13)	$K_5 = 0.51, K_6 = 0.42$	11.6	8.1	11.3	10.3
BS85	Eq. (15)	$K_7 = 1.0, K_8 = 0.14$	8.3	6.7	10.2	8.4
SN93	Eq. (17)	$K_9 = 1.0, K_{10} = 1.0$	9.6	9.4	14.5	11.1
BHV98	Eq. (19)	$K_{11} = 1.0, K_{12} = 1.0$	7.9	6.5	13.5	9.3
RS98	Eq. (21)	$K_{13} = 0.10, K_{14} = 0.10$	12.4	7.1	10.1	9.9
RWS03	Eq. (23)	$K_{15} = 1.0, K_{16} = 0.14$	10.8	7.8	10.0	9.5
RKS03	Eq. (25)	$K_{17} = 0.12, K_{18} = 0.14$	8.9	8.6	12.9	10.1
R07	Eq. (27)	$K_{19} = 0.07, K_{20} = 0.14$	7.5	7.2	9.3	8.0
AB07	Eq. (29)	$K_{21} = 1.0, K_{22} = 0.14$	7.8	7.1	10.5	8.5
JB07	Eq. (31)	$K_{23} = 1.0, K_{24} = 1.0$	8.8	7.2	11.1	9.0
RS08	Eq. (33)	$K_{25} = 1.0, K_{26} = 0.14$	7.9	6.7	10.5	8.3
AREG08	Eq. (35)	$K_{27} = 1.0, K_{28} = 1.0$	10.3	9.1	12.8	10.7

Table 3. The errors  $ER_g$  and  $ER_{avg}$  of each dissipation model for three groups of experiment-scales by using the default coefficients (measured data from Table 1).

Using the default coefficients  $(K_1-K_{28})$  in the computations, the errors  $(ER_g$  and  $ER_{avg})$  of each dissipation model on predicting  $H_{m0}$  for three groups of experiment-scales have been computed and are shown in Table 3.

It can be seen from Table 3 that the models of R07, RS08, BS85, and AB07give similar overall accuracy (8.0  $\leq ER_{avq} \leq$  8.5) and give better accuracy than the others. For computing beach deformation, a wave model has to be run many times to account the frequent updating of beach profile. The error from the wave model may be accumulated from time to time. Therefore, for computing the beach deformation, the error of the wave model should be kept as small as possible. Hence, the best model should be selected for incorporating the beach deformation model. It can be seen from Table 3 that there is only one model (model of R07) that gives good predictions for the three groups of experiment-scales. Moreover, the model R07 also gives the best overall prediction ( $ER_{avg} = 8.0$ ). However, because some dissipation models were developed with limited experimental conditions and it is not clear whether the models were developed for statistical-based or spectral-based wave heights, the coefficients in each model may not be the optimal values for computing  $H_{m0}$ . Therefore, the errors in Table 3 should not be used to judge the applicability of the existing models. The coefficients in all models should be recalibrated before comparing the applicability of the models.

Each model is calibrated by determining the optimal values of coefficients K which yield the minimum  $ER_{avg}$ . In order to determine the universal coefficients

Models	$D_B$ formulas Calibrated coefficients		$ER_g$		$ER_{avg}$	
			Small-scale	Large-scale	Field	
BJ78	Eq. (7)	$K_1 = 0.92, K_2 = 0.12$	13.1	7.9	12.7	11.2
TG83a	Eq. (11)	$K_3 = 0.52, K_4 = 0.45$	11.0	15.9	12.4	13.1
TG83b	Eq. (13)	$K_5 = 0.42, K_6 = 0.41$	10.5	7.9	12.2	10.2
BS85	Eq. (15)	$K_7 = 0.75, K_8 = 0.13$	7.6	6.1	10.4	8.0
SN93	Eq. (17)	$K_9 = 1.4, K_{10} = 0.95$	7.5	7.1	11.5	8.7
BHV98	Eq. (19)	$K_{11} = 0.88, K_{12} = 0.97$	7.7	6.5	13.3	9.2
RS98	Eq. (21)	$K_{13} = 0.10, K_{14} = 0.10$	12.4	7.1	10.1	9.9
RWS03	Eq. (23)	$K_{15} = 1.0, K_{16} = 0.15$	9.1	7.9	10.3	9.1
RKS03	Eq. (25)	$K_{17} = 0.07, K_{18} = 0.11$	9.3	7.2	9.5	8.7
R07	Eq. (27)	$K_{19} = 0.07, K_{20} = 0.14$	7.5	7.2	9.3	8.0
AB07	Eq. (29)	$K_{21} = 0.86, K_{22} = 0.13$	7.8	6.4	10.2	8.1
JB07	Eq. (31)	$K_{23} = 0.70, K_{24} = 0.83$	6.9	5.8	10.8	7.8
RS08	Eq. (33)	$K_{25} = 0.75, K_{26} = 0.13$	7.6	6.2	10.4	8.1
AREG08	Eq. (35)	$K_{27} = 0.80, K_{28} = 0.90$	10.7	8.6	12.2	10.5
M1	Eq. (42)	$K_{29} = 0.27$	6.7	7.2	9.2	7.7
M2	Eq. (43)	$K_{30} = 0.75$	24.2	8.6	13.7	15.5

Table 4. The errors  $ER_g$  and  $ER_{avg}$  of each dissipation model for three groups of experiment-scales by using the calibrated coefficients (measured data from Table 1).

K, all compiled experimental data are used to calibrate the models. Using default coefficients K, wave height transformation for all experiments have been computed and then the average error  $(ER_{avg})$  of the model has been computed from the measured and computed wave heights. The computations are repeated for various choices of coefficients K, until the minimum error  $(ER_{avg})$  is obtained.

The calibrated coefficients  $K_1$  to  $K_{28}$  are summarized in the third column of Table 4. Using the calibrated coefficients  $(K_1 - K_{28})$  in the computations, the errors  $(ER_g \text{ and } ER_{avg})$  of each dissipation model on predicting  $H_{m0}$  for three groups of experiment-scales have been computed and are shown in Table 4. The results can be summarized as follows:

- (a) The error  $(ER_g)$  of the calibrated models is in the range of 5.8 to 15.9%. The model of JB07 gives the best predictions for small-scale and large-scale experiments, while the model of R07 gives the best prediction for field experiments.
- (b) Considering overall accuracy  $(ER_{avg})$  of the models, the overall accuracies of the models in descending order are JB07, R07, BS85, RS08, AB07, RKS03, SN93, RWS03, BHV98, RS98, TG83b, AREG08, BJ78, and TG83a. The first five of which give similar accuracy  $(7.8 \le ER_{avg} \le 8.1)$  and give better accuracy than the others. The accuracy of the five models seems to be sufficient for the design of coastal structures. As the model of JB07 gives the best overall

prediction ( $ER_{avg} = 7.8$ ), it seems to be the most suitable one for incorporating the beach deformation model. Since the model of JB07 was developed based on a full Rayleigh distribution of wave heights (which is the individual wave analysis or statistical analysis), the model should be appropriate for computing the statistical-based wave heights. Moreover, several researchers [e.g. Klopman, 1996; Battjes and Groenendijk, 2000; Mendez et al., 2004] showed that the Rayleigh distribution is not valid in the surf zone. Surprisingly, the model of JB07 gives the best overall prediction.

- (c) The main difference among the models of TG83a, TG83b, AREG08, AB07, and JB07 is the distribution function of breaking wave heights. As the models of AB07 and JB07 are significantly better than those of TG83a, TG83b and AREG08, it is expected that the key step change and improvement in the parametric models was the adoption of a Rayleight pdf for all waves as proposed by Baldock  $et\ al.\ [1998]$ .
- (d) The main difference among the models of BHV98, RWS03, AB07, and JB07 is the energy dissipation of a single broken wave, i.e. BHV98 and RWS03 used the bore model of BJ78, while AB07 and JB07 used the bore model of TG83. The results show that the bore model of TG83 is more suitable to incorporate in the models.
- (e) Comparing among the models developed based on the parametric wave approach (BJ78, TG83a, TG83b, BS85, SN93, BHV98, RS98, RWS03, AB07, JB07, RS08, and AREG08), the model JB07 gives the best overall prediction. The significant differences of those models are the assumption on probability of occurrence of breaking waves, the formulation of energy dissipation of a single broken wave, and the breaker height formula. This indicates that the combination which is proposed by JB07 is the most suitable one for computing the transformation of  $H_{m0}$ .
- (f) Comparing between the models developed based on the stable energy approach (RKS03 and R07), the model R07 gives the better overall prediction than the other. This indicates that the breaker height formula used by R07 is more suitable than the other.
- (g) Either parametric wave approach or stable energy approach can be used to compute the transformation of  $H_{m0}$ . The best model for parametric wave approach is JB07, while the best model for stable energy approach is R07.
- (h) Although the model of JB07 gives the best overall prediction, it does not give good predictions for all experiment-scales. The model gives good predictions for small-scale and large-scale experiments but gives fair prediction for field experiments. Another model, which may be used to incorporate in the beach deformation model, is the model of R07. The model gives the second best overall prediction ( $ER_{avg} = 8.0$ ) and gives good predictions for all experiment-scales. Moreover, the model of R07 is much simpler than that of JB07.

#### 5. Model Modification

Because of the simplicity and good predictions for all experiment-scales of R07's model, the model was selected to modify for better accuracy. The model of R07 can be written in general form as

$$D_B = 0.07 \frac{\rho g c_g}{8h} \left[ 0.5 H_{m0}^2 - H_{st}^2 \right] \tag{39}$$

where  $H_{st}$  is the stable wave height. The model of R07 was developed based on the stable energy wave concept. The concept was firstly introduced by Dally  $et\ al.$  [1985] for computing energy dissipation of regular wave breaking. The energy dissipation is assumed to be proportional to the difference between the local energy flux and the stable energy flux. Based on a wide range of experimental conditions, Rattanapitikon  $et\ al.$  [2003] showed that the following stable wave height formulas could also be used for computing the energy dissipation of regular wave breaking.

(a) Dally et al. [1985]:

$$H_{st} = 0.4h \tag{40}$$

(b) Rattanapitikon and Shibayama [1998]:

$$H_{st} = h \exp\left(-0.36 - 1.25 \frac{h}{\sqrt{LH}}\right) \tag{41}$$

It is expected that the accuracy of the R07's model [Eq. (39)] could be improved by using the suitable  $H_{st}$  formula, and the formula for regular wave breaking may be applicable for irregular wave breaking. In this section, an attempt has been made to modify the model of R07 by changing the terms of stable wave height. Substituting Eqs. (40) and (41) into Eq. (39), the two modified energy dissipation models for computing  $H_{m0}$  (hereafter referred to as M1 and M2, respectively) can be expressed as

M1: 
$$D_B = 0.07 \frac{\rho g c_g}{8h} \left[ 0.5 H_{m0}^2 - (K_{29}h)^2 \right]$$
 (42)

$$M2: \quad D_B = 0.07 \frac{\rho g c_g}{8h} \left[ 0.5 H_{m0}^2 - \left( K_{30} h \exp\left( -0.36 - 1.25 \frac{2^{1/4} h}{\sqrt{L H_{m0}}} \right) \right)^2 \right]$$
(43)

where  $K_{29}-K_{30}$  are the adjustable coefficients.

The calibration of the two modified dissipation models is performed by using the measured data shown in Table 1. The calibrations are conducted by gradually adjusting the coefficients until the minimum error ( $ER_{avg}$  of each model is obtained. The calibrated coefficients of M1 and M2 and the errors ( $ER_g$  and  $ER_{avg}$  for three groups of experiment-scales are shown in the last two rows of Table 4. The results can be summarized as follows:

- (a) Comparing between the two modified models, the model M1 is much better than the model M2. The model M2 gives too much errors and it should not be used for computing  $H_{m0}$ .
- (b) Comparing among the models developed based on the stable energy approach (RKS03, R07, M1, and M2), the model M1 gives the best overall prediction. This indicates that the stable wave height formula of Dally *et al.* [1985] is the most suitable one for computing the transformation of  $H_{m0}$ .
- (c) Comparing with the existing models, the model M1 is the simplest model. Because of the simplicity of M1, it is expected that this model will give less accuracy than the others. Surprisingly, the result shows that the simplest model gives the best overall prediction. It should be noted that the stable wave height in the model M1 is proportional to the breaker height formula of TG83 [Eq. (12)]. Attempts have been made to modify the model M1 by using other breaker height formulas [Eqs. (9), (16), (18), (22), (24), and (36)]. However, it was found that no model gives better prediction than that of M1.
- (d) Comparing between the best existing model (JB07) and the model M1, the model M1 gives slightly better overall prediction than that of JB07. The model of M1 gives the best predictions for small-scale and field experiments, while the model of JB07 gives the best prediction for large-scale experiments. Moreover, the model M1 gives good predictions for all experiment-scales while the model JB07 does not. Considering the complexity of the models, the model M1 is much simpler than that of JB07. As the simple model gives slightly better accuracy than the more complicated model, it may not necessary to use the complicated model to compute the transformation of  $H_{m0}$ .
- (e) In the present study, the most suitable model is selected based on accuracy and simplicity of the models. Considering the accuracy of the models, the models M1, JB07, R07, BS85, RS08, and AB07 give nearly the same accuracy (7.7  $\leq ER_{avg} \leq 8.1$ ) and give better accuracy than the others. Considering the simplicity of the 6 models, the formula of model M1 is the simplest one. Therefore, the model M1 is judged to be the most suitable model. Substituting the calibrated coefficients into the model M1, the recommended model can be written as

$$\frac{\rho g}{16} \frac{\partial (H_{m0}^2 c_g \cos \theta)}{\partial x} = -0.07 \frac{\rho g c_g}{8h} \left[ 0.5 H_{m0}^2 - (0.27h)^2 \right]$$
(44)

The greatest asset of the model M1 is its simplicity and ease of application, i.e. the transformation of  $H_{m0}$  from offshore to shoreline can be computed by using only one equation [Eq. (44)]. The model can be converted to compute the transformation of spectral-based root-mean-square wave height  $(H_{rmsE})$  by substituting  $H_{m0} = \sqrt{2}H_{rmsE}$  into Eq. (44). The result is

$$\frac{\rho g}{8} \frac{\partial (H_{rmsE}^2 c_g \cos \theta)}{\partial x} = -0.07 \frac{\rho g c_g}{8h} \left[ H_{rmsE}^2 - (0.27h)^2 \right]$$
 (45)

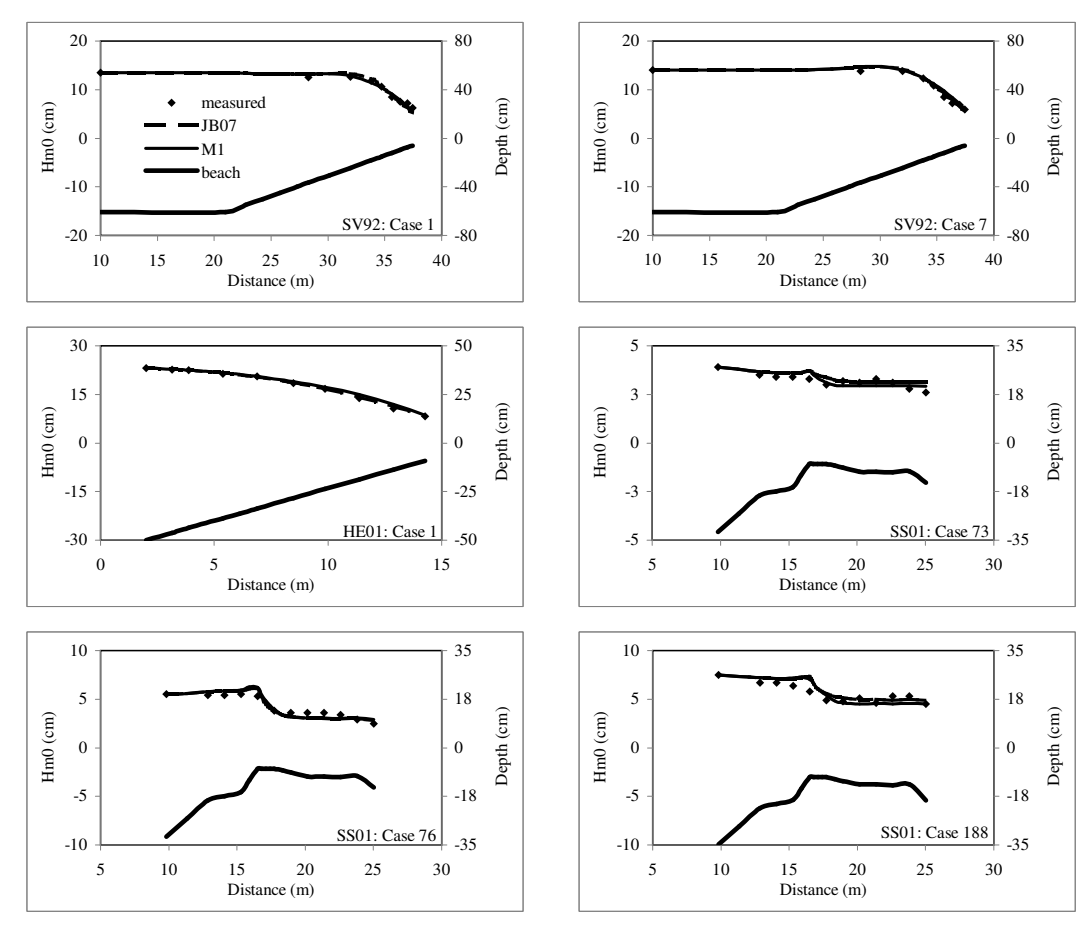


Fig. 1. Examples of measured and computed  $H_{m0}$  transformation from models JB07 and M1 (measured data from small-scale experiments).

To gain an impression of overall performance of the best model of the two approaches, the results of JB07 and M1 are plotted against the measured data. Examples of computed  $H_{m0}$  transformation across-shore are shown in Figs. 1–3. Case numbers in Figs. 1–3 are kept to be the same as the originals. Overall, it can be seen that the two models are quite realistic in simulation of the  $H_{m0}$  and have similar accuracy. Because the  $H_{m0}$  is computed by a simple expression of energy flux conservation, the models are limited to use on open coasts away from river mouths and coastal structures. As the swash processes are not included in the models, the models are limited to use in the nearshore zone (excluding swash zone). Furthermore, the major disadvantage of the models is that they do not provide any detail on the behavior of individual waves. For example, all waves are assumed to refract based on the mean wave angle, which is not realistic in the case of broad-banded spectra. The effect of directional spread on wave refraction is presented in the book of Goda [2000]. For more accuracy, it is essential to follow individual wave transformation.

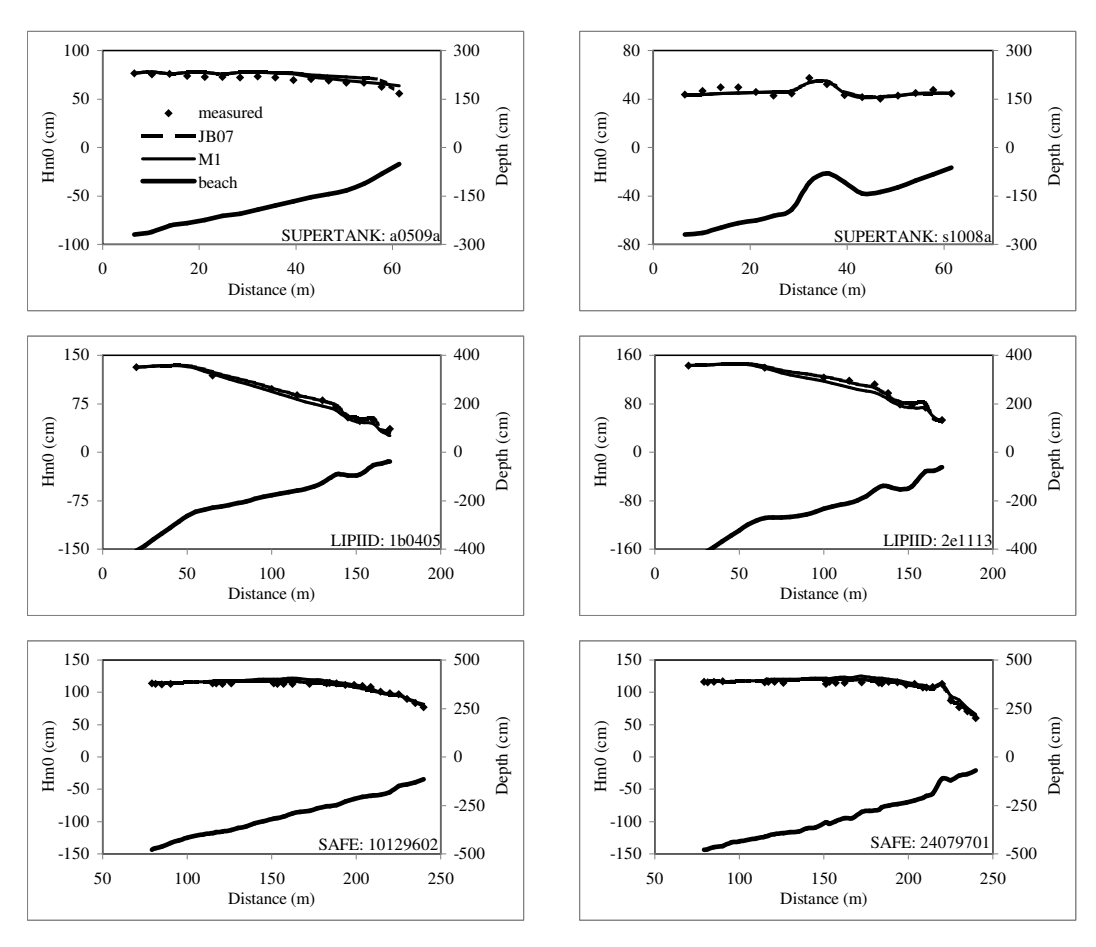


Fig. 2. Examples of measured and computed  $H_{m0}$  transformation from models JB07 and M1 (measured data from large-scale experiments).

#### 6. Conclusions

Fourteen existing dissipation models for computing the transformation of  $H_{rms}$  were applied to compute the transformation of  $H_{m0}$ . A total of 1,713 cases from 8 sources of published experimental results were used to examine the applicability of the models in predicting  $H_{m0}$ . The compiled experimental data cover a wide range of wave conditions  $(0.001 \le H_{m0,0}/L_0 \le 0.069)$ , including small-scale, large-scale and field experiments. The basic parameters used for determination of the accuracy of the models are the rms relative error  $(ER_g)$  of the three groups of experiment-scales and their average  $(ER_{avg})$ . The calibration of each model was conducted by varying the adjustable coefficients (K) in each model until the minimum error  $(ER_{avg})$ , between the measured and computed wave height, is obtained. Using the calibrated coefficients, the errors  $(ER_g$  and  $ER_{avg})$  of the existing models were computed and compared. The comparison shows that the top two models are the models of JB07 and R07. The model of JB07 gives better overall accuracy than that of R07. The

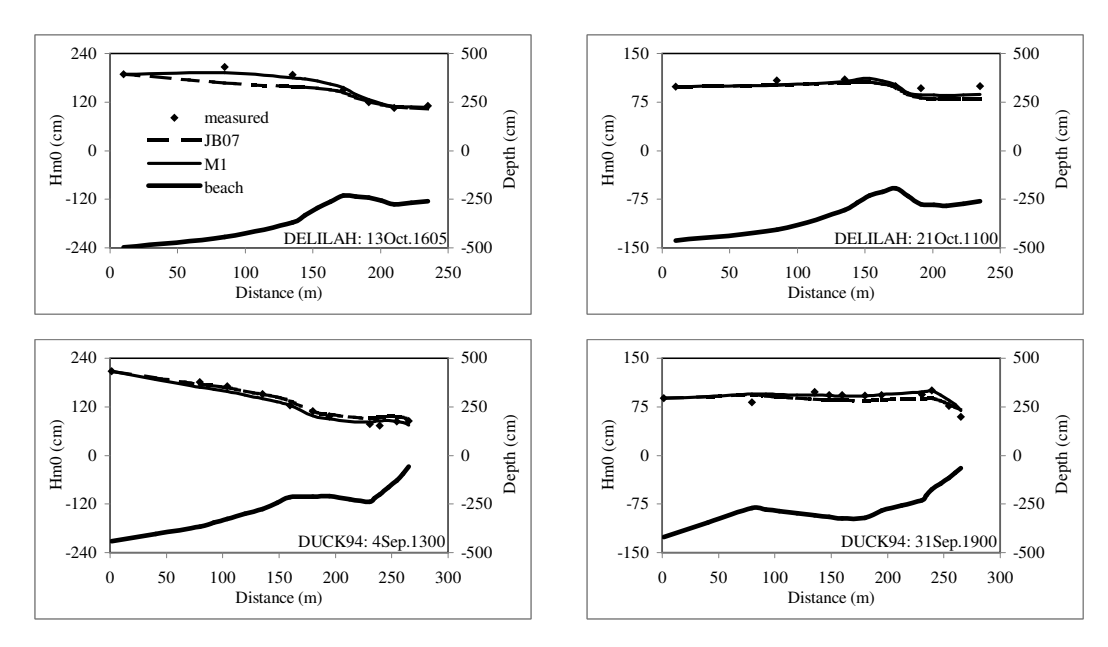


Fig. 3. Examples of measured and computed  $H_{m0}$  transformation from models JB07 and M1 (measured data from field experiments).

greater assets of R07 are its simplicity and it gives good predictions ( $ER_g < 10$ ) for all experiment-scales. For better accuracy, the model of R07 was modified by changing the stable wave height formula in the model. Comparing with the existing models, the modified model (M1) is the simplest one but gives the best accuracy.

## Acknowledgements

This research was sponsored by the Thailand Research Fund. The data collection of the DELILAH and DUCK94 projects were funded by the US Office of Naval Research and the US National Science Foundation. Thanks and sincere appreciation are expressed to the researchers names listed in Table 1 for publishing the valuable data.

## References

Abadie, S., Butel, R., Mauriet, S., Morichon, D. & Dupuis, H. [2006] "Wave climate and longshore drift on the South Aquitaine coast," *Continental Shelf Research* 26, 1924–1939.

Alsina, J. M. & Baldock, T. E. [2007] "Improved representation of breaking wave energy dissipation in parametric wave transformation models," *Coastal Engineering* **54**, 765–769.

Apotsos, A., Raubenheimer, B., Elgar, S. & Guza, R. T. [2008] "Testing and calibrating parametric wave transformation models on natural beaches," *Coastal Engineering* **55**, 224–235.

Baldock, T. E., Holmes, P., Bunker, S. & Van Weert, P. [1998] "Cross-shore hydrodynamics within an unsaturated surf zone," *Coastal Engineering* **34**, 173–196.

Battjes, J. A. & Janssen, J. P. F. M. [1978] "Energy loss and set-up due to breaking of random waves," in *Proc. 16th Coastal Engineering Conference*, ASCE, pp. 569–587.

- Battjes, J. A. & Stive, M. J. F. [1985] "Calibration and verification of a dissipation model for random breaking waves," *J. Geophysical Research* **90**(C5), 9159–9167.
- Battjes, J. A. & Groenendijk, H. W. [2000] "Wave height distributions on shallow foreshores," Coastal Engineering 40, 161–182.
- Bouws, E., Gunther, H., Rosenthal, W. & Vincent, C. L. [1985] "Similarity of the wind wave spectrum in finite depth water," J. Geophysical Research 90(C1), 975–986.
- Birkemeier, W. A., Donoghue, C., Long, C. E., Hathaway, K. K. & Baron C. F. [1997] The DELILAH Nearshore Experiment: Summary Data Report. Waterways Experiment Station, US Army Corps of Engineers.
- Bruun, P. [1954] Coastal Erosion and Development of Beach Profiles. US Army Beach Erosion Board, Tech. Memorandum No. 44, US Army Corps of Engineers.
- Dally, W. R., Dean, R. G. & Dalrymple, R. A. [1985] "Wave height variation across beach of arbitrary profile," *J. Geophysical Research* **90**(C6), 11917–11927.
- Demerbilek, Z. & Vincent, L. [2008] "Water wave mechanics," Coastal Engineering Manual, EM1110-2-1100. Coastal and Hydraulics Laboratory Engineering Research and Development Center, WES, U.S. Army Corps of Engineers, p. II-1-75.
- Dette, H. H, Peters, K. & Newe, J. [1998] MAST III SAFE Project: Data Documentation, Large Wave Flume Experiments '96/97. Report No. 825 and 830, Leichtweiss-Institute, Technical University Braunschweig.
- Goda, Y. [1970] "A synthesis of breaking indices," Transaction Japan Society of Civil Engineers, Part 2, pp. 227–230.
- Goda, Y. [1974] "Estimation of wave statistics from spectral information," in *Proc. Ocean Waves Measurement and Analysis Conference*, ASCE, pp. 320–337.
- Goda, Y. [1979] "A review on statistical interpretation of wave data," Report of Port and Harbour Research Institute 18, 5–32.
- Goda, Y. [2000] Random Seas and the Design of Maritime Structures (World Scientific Publishing Co. Pte. Ltd., Singapore).
- Goda, Y. [2009] "A performance test of nearshore wave height prediction with CLASH datasets," Coastal Engineering 56, 220–229.
- Hamilton, D. G. & Ebersole, B. A. [2001] "Establishing uniform longshore currents in a large-scale sediment transport facility," *Coastal Engineering* **42**, 199–218.
- Hasselmann, K., Barnett, T. P., Bouws, E., Carlson, H., Cartwright, D. E., Enke, K., Ewing, J. A., Gienapp, H., Hasselmann, D. E., Kruseman, P., Meerburg, A., Müller, P., Olbers, D. J., Richter, K., Sell, W. & Walden, H. [1973] "Measurements of wind-wave growth and swell decay during the Joint North Sea Wave Project (JONSWAP)," Deutsche Hydrographische Zeitschrift A 8(12), 1–95.
- Herbers, T. H. C., Elgar, S., Guza, R. T. & O'Reilly, W. C. [2006] Surface gravity waves and nearshore circulation. DUCK94 Experiment Data Server: SPUV Pressure Sensor Wave Height Data. Available online at: http://dksrv.usace.army.mi/jg/dk94dir.
- Janssen, T. T. & Battjes, J. A. [2007] "A note on wave energy dissipation over steep beaches," Coastal Engineering 54, 711–716.
- Johnson, H. K. [2006] "Wave modelling in the vicinity of submerged breakwaters," Coastal Engineering 53, 39-48.
- Klopman, G. [1996] "Extreme Wave Heights in Shallow Water," Report H2486. WL/Delft Hydraulics, The Netherlands.
- Kraus, N. C. & Smith, J. M. [1994] SUPERTANK Laboratory Data Collection Project. Technical Report CERC-94-3, Waterways Experiment Station, US Army Corps of Engineers, Vols. 1–2.
- Mendez, F.J., Losada, I.J. & Medina, R. [2004] "Transformation model of wave height distribution on planar beaches," *Coastal Engineering* **50**, 97–115.
- Miche, R. [1944] "Mouvements ondulatoires des mers en profondeur constante on decroissante," in *Ann. des Ponts et Chaussees*, Ch. 114, pp. 131–164, 270–292, and 369–406.
- Nairn, R. B. [1990] Prediction of Cross-shore Sediment Transport and Beach Profile Evolution. Ph.D. thesis, Department of Civil Eng., Imperial College, London.

- Oliveira, F. S. B. F. [2007] "Numerical modeling of deformation of multi-directional random wave over a varying topography," *Ocean Engineering* **34**, 337–342.
- Rattanapitikon, W. & Shibayama, T. [1998] "Energy dissipation model for regular and irregular breaking waves," Coastal Engineering Journal 40, 327–346.
- Rattanapitikon, W., Karunchintadit, R. & Shibayama, T. [2003] "Irregular wave height transformation using representative wave approach," *Coastal Engineering Journal* 45, 489–510.
- Rattanapitikon, W. [2007] "Calibration and modification of energy dissipation models for irregular waves breaking," Ocean Engineering 34, 1592–1601.
- Rattanapitikon, W. & Sawanggun, S. [2008] "Energy dissipation model for a parametric wave approach," Songklanakarin Journal of Science and Technology 30(3), 333–341.
- Roelvink, J. A. & Reniers A. J. H. M. [1995] LIP 11D Delta Flume Experiments: A Data Set for Profile Model Validation. Report No. H 2130, Delft Hydraulics.
- Ruessink, B. G., Walstra, D. J. R. & Southgate, H. N. [2003] "Calibration and verification of a parametric wave model on barred beaches," *Coastal Engineering* 48, 139–149.
- Smith, M. K. & Vincent, C. L. [1992] "Shoaling and decay of two wave trains on beach," *Journal of Waterway, Port, Coastal, and Ocean Engineering* 118(5), 517–533.
- Smith, J. M. & Seabergh, W. C. [2001] Wave Breaking on a Current at an Idealized Inlet with an Ebb Shoal. Report No. ERDC/CHL TR-01-7, Engineer Research and Development Center, US Army Corps of Engineers.
- Southgate, H. N. & Nairn, R. B. [1993] "Deterministic profile modelling of nearshore processes, Part 1: Waves and currents," Coastal Engineering 19, 27–56.
- Thompson, E. F. & Vincent, C. L. [1985] "Significant wave height for shallow water design," *Journal of Waterway, Port, Coastal and Ocean Engineering* **111**(5), 828–842.
- Thornton, E. B. & Guza, R. T. [1983] "Transformation of wave height distribution," J. Geophysical Research 88(C10), 5925–5938.